De Novo Designed Molecules Based on Non-covalent Interactions: Design, Synthesis and Structural Studies

A THESIS SUBMITTED TO THE

UNIVERSITY OF PUNE

FOR THE DEGREE OF

DOCTOR OF PHILOSOPHY

(IN CHEMISTRY)

BY

PRANJAL KUMAR BARUAH

ORGANIC CHEMISTRY SYNTHESIS DIVISION

NATIONAL CHEMICAL LABORATORY

PUNE 411008

INDIA

JUNE 2007

DECLARATION

I hereby declare that the thesis entitled "***De Novo* Designed Molecules Based on Non-covalent Interactions: Design, Synthesis and Structural Studies**", submitted for the Degree of Doctor of Philosophy in Chemistry to the University of Pune, has not been submitted by me to any other university or institution. This work has been carried out at the Organic Chemistry Synthesis Division, National Chemical Laboratory, Pune under the supervision of Dr. G. J. Sanjayan (Research guide).

Date:
Organic Chemistry Synthesis Division
National Chemical Laboratory
Pune-411008

Pranjal Kumar Baruah
(Research student)

Dr G. J. Sanjayan
Organic Chemistry Synthesis Division

Tel: +91-20-25902082
Fax: +91-20-25902624
e-mail: gj.sanjayan@ncl.res.in

National Chemical Laboratory
Dr Homi Bhabha Road
Pune – 411 008, INDIA

CERTIFICATE

Certified that the work incorporated in the thesis, "***De Novo* Designed Molecules Based on Non-covalent Interactions: Design, Synthesis and Structural Studies**", submitted by **Mr. Pranjal Kumar Baruah**, for the degree of **Doctor of Philosophy**, was carried out by the candidate under my supervision in Organic Chemistry Synthesis Division, National Chemical Laboratory, Pune, India. Materials obtained from other sources have been duly acknowledged in the thesis.

Date:

Place: Pune

Dr. G. J. Sanjayan
(Research Guide)

Dedicated
To
My Family

Acknowledgements

It gives me an immense pleasure to express my deep sense of gratitude towards my research guide ***Dr. G. J. Sanjayan*** *for all the advice, guidance, support and encouragement during every stage of this work. He made me realize the importance of doing quality research, in a better way at crucial stage of my career. He taught me each and every aspect of research, from working table to formulation of ideas to presentation of results. I thank him for giving me enough freedom and giving his valuable suggestions whenever needed. Although this eulogy is insufficient, I preserve an everlasting gratitude for him.*

I sincerely thank Dr. P. R. Rajamohanan and Dr. S. Ravidranathan for their help in 2D NMR analysis.

I thank Dr. Rajesh Gonnade for his help in getting the single X-ray structures.

I thank Professor H.-J. Hoffmann, Germany for his help in ab initio studies of my oligomers. I also thank Professor Judith Howard, U. K.for variable temperature X-ray studies.

My special thanks to Mrs. Kavitha, NMR division; for her help in carrying out the dilution and titration experiments. Without her help this work would have been delayed by two to three months.

I take this opportunity to thank my teachers Professor I. Haq and P. K. Gogoi, Dibrugarh University, and Dr. G. Bez NEHU for their encouragement and motivation during my M. Sc.

I am also thankful to Mrs. Shantakumari for mass analysis, Mrs. Renu for TEM analysis, Mr. Gaikwad for SEM analysis, Dr. Pankaj Poddar for AFM analysis.

I would like to thank my labmates Panchami, Amol, Srinivas, Sridevi, Arup, Kale, Pinak, Nilesh, Arif, Divya, Gouripriya, Leena, Ramesh, Ashly for maintaining a cheerful atmosphere in the lab. I thank Kapil, Prakash, Sathyanarayana, Manish, Marivel, Sunil, Seetha, Amit for friendly atmosphere in my previous lab.

No word will be sufficient to express my thanks to my friends Diganta, Sanjib and Kalita during this long stay in NCL. I thank Sanjib for being with me starting from my M. Sc. I am quite lucky to have a friend like Diganta who was always there with me and helped me whenever it is needed; be it personal or research related.I thank Pranjal Kalita for helping me at various stages in this period.

I thank Sashanka, Jadabda, Manashda, Senapatida, Khirud, Lakshi, Ankur, Rahul, Getali, Siddhartha, Ananta, Mukul, Satish, Suvarna, Nagesh, Sreadha, Baag, Kishan, Ramesh, Sushil, Nagendra, Alok, Baisakhi for extending their friendly support.

I have no words to express my gratitude to my family. Being the youngest one in my family and staying so far from home makes one home sick at times; but they are quite supportive during my Ph. D. period. It was my sister and brother who has always helped me during my studies and in taking right decisions at crucial stages of my life. I am also thankful to my niece because whenever I got frustrated it was talking with her which made me relaxed.

I take this opportunity to thank each and every person who have helped and supported me throughout my education period.

I thank library staff for providing excellent facility both in terms of reference books as well as journals.

I thank director NCL, for allowing me to work in this premier institute, providing the excellent infrastructure.

I thank CSIR, New Delhi, for the financial support.

Pranjal Kumar Baruah

CONTENTS

Abbreviations

Ac	Acetyl
Ac_2O	Acetic anhydride
$CDCl_3$	Deuterated chloroform
D_2O	Deuterium oxide
EtOAc	Ethyl acetate
TEA/Et_3N	Triethylamine
m.p.	Melting point
TMEDA	Tetramethylethylenediamine
THF	Tetrahydrofuran
TMS	Trimethylsilyl
$CHCl_3$	Chloroform
DMF	Dimethylforamamide
CH_2Cl_2	Methylene chloride
MeOH	Methanol
TPP	Triphenylphosphine (PPh_3)
TFA	Trifluoroacetic acid
IBCF	Isobutyl chloroformate
***t*-BuOK**	Potassium tertiary butoxide
MALDI-TOF	Matrix Assisted Laser Desorption Ionization Time of Flight
ESI-MS	Electrospray Ionization Mass Spectroscopy
NMR	Nuclear magnetic resonace
HMBC	Hetero multiple bond correlation
COSY	Corelated spectroscopy
NOESY	Nuclear Overhauser enhancement Spectroscopy
HSQC	Hetronuclear single quantum coherence
Ala	Alanine
Aib	α–Aminoisobutyric acid
$SOCl_2$	Thionyl chloride
H-Bond	Hydrogen bond
TLC	Thin Layer Chromatography
Pd/C	Palladium 10% on activated carbon
DCC	Dicyclohexylcarbodiimide
DCU	Dicyclohexyl urea
DIPEA/DIEA	Diisopropylethylamine
DMAP	4',4'-Dimethylaminopyridine
HBTU	2-(1H-Benzotriazole-1-yl)-1,1, 3,3-tetramethyluronum hexafluorophosphate
HOBt	1-Hydroxybenzotriazole
Pro	Proline
Py	Pyridine
***t*-Boc**	*tert*-Butyloxycarbonyl
Cbz	Carboxybenzyl
DMSO	Dimethyl sulfoxide
NaOEt	Sodium ethoxide
TEM	Transmission Electron Microscope

ABSTRACT

Chapter I describes the design, synthesis and structural investigation of hydrogen bond-mediated highly stable molecular duplexes, and further related studies.

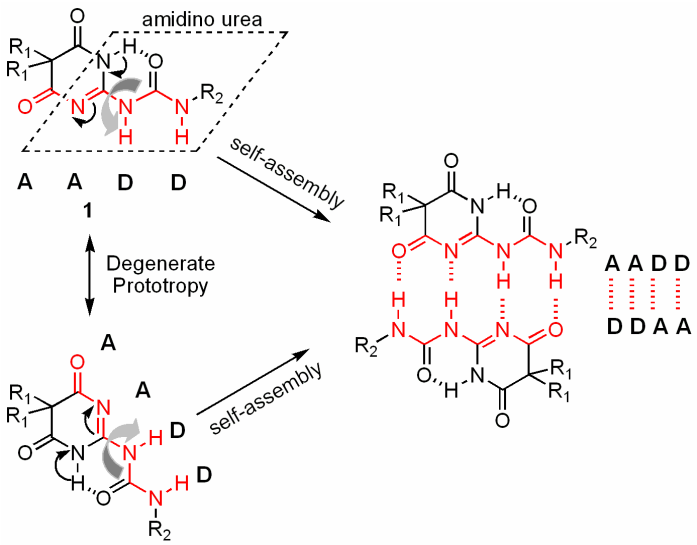

The self-assembling systems described herein have been shown to form strong molecular duplexes, as evident from ESI-Mass, X-ray analysis, and extensive NMR studies. It is noteworthy that these self-assembling systems, exhibiting "degenerate porototropy can be readily accessed in three steps. This chapter also describes the attempts made towards synthesis of more stable hydrogen bonded molecular duplexes.

Chapter 2 describes the design, synthesis and structural investigations of novel foldamers (conformationally ordered synthetic oligomers) derived from α-amino acid and aromatic amino acid conjugates.

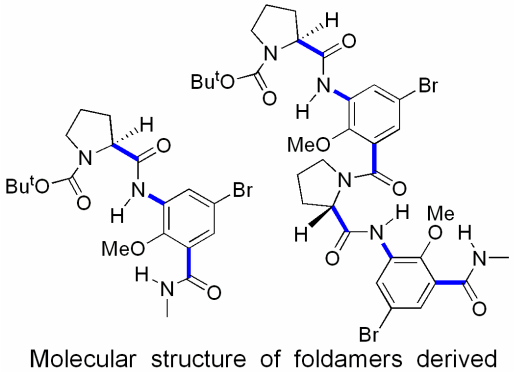

Molecular structure of foldamers derived from proline (Pro) and 3-amino-5-bromo-2-methoxy benzoic acid (Amb) as alternating subunits that form stable γ-turn conformation. *Note: the conformational restriction imposed by the Pro and Amb residues is highlighted in blue bold bonds.*

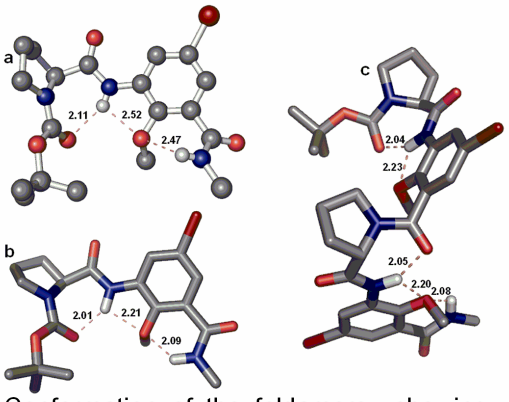

Conformation of the foldamers showing bifurcated H-bond stabilized γ-turn motifs. (a) single crystal X-ray structure of dipeptide. (b) conformation of dipeptide at the HF/6-31G* level of ab initio MO theory. (c) conformation of tetrapeptide at the HF/6-31G* level of ab initio MO theory.

It also describes the design, synthesis and structural studies of novel hybrid foldamers based on Aib-Amb motif.

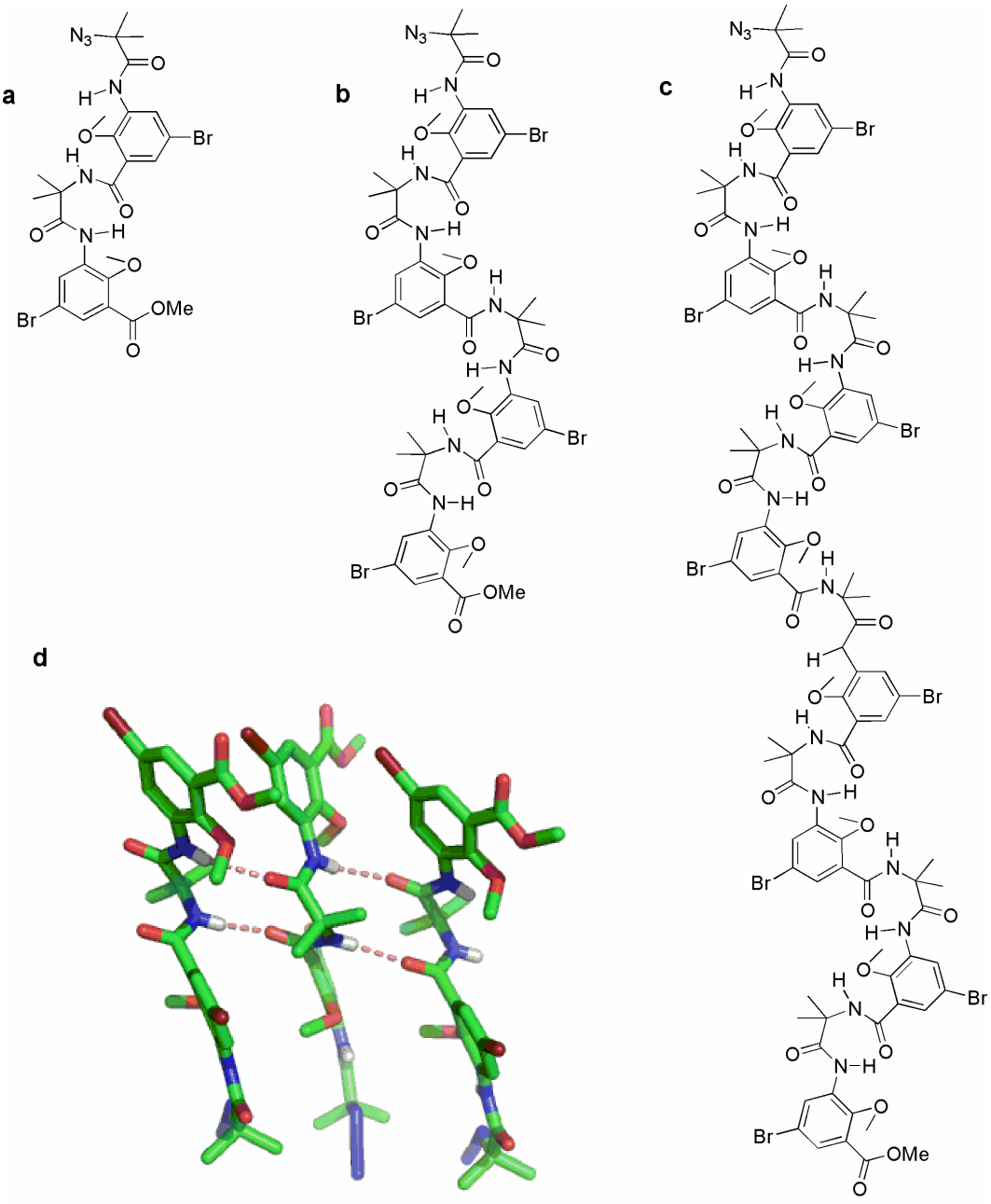

Molecular structure and crystal structure showing self-assembly of *Aib-Amb* derived foldamers.
(a), (b), and (c) molecular structures of tetra-, octa- and hexadeca- peptides, respectively.
(d) crystal structure showing self-assembly of tetrameric foldamer.

Chapter 3 describes the design, synthesis and structural studies of a new class of aromatic oligoamide foldamers based on binaphthol (BINOL) monomers. Series of oligomers with differing chirality of the individual BINOL building blocks and mixed sequences of alternate BINOL and pyridyl building blocks have been synthesized and structurally characterized. It is shown that oligomers consisting of only three building blocks of the same class, which differ in chirality due to restricted rotation, provide a great number of highly ordered structures with remarkable shape diversity and structural architecture.

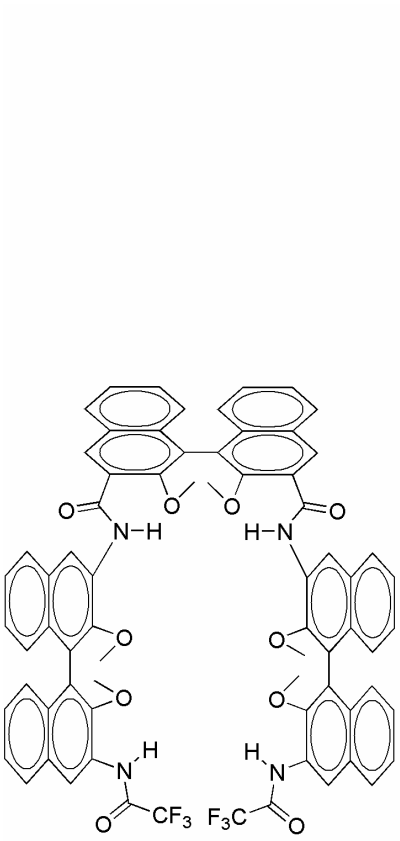

1

1a [R][R][R] **1b [S][S][S]**

1c [S][R][S] **1d [R][S][R]**

BINOL-based aromatic foldamers 1a-d synthesized in this study. These oligomers containing three BINOL building blocks differ in the positioning of the BINOL enantiomers [R] and [S].

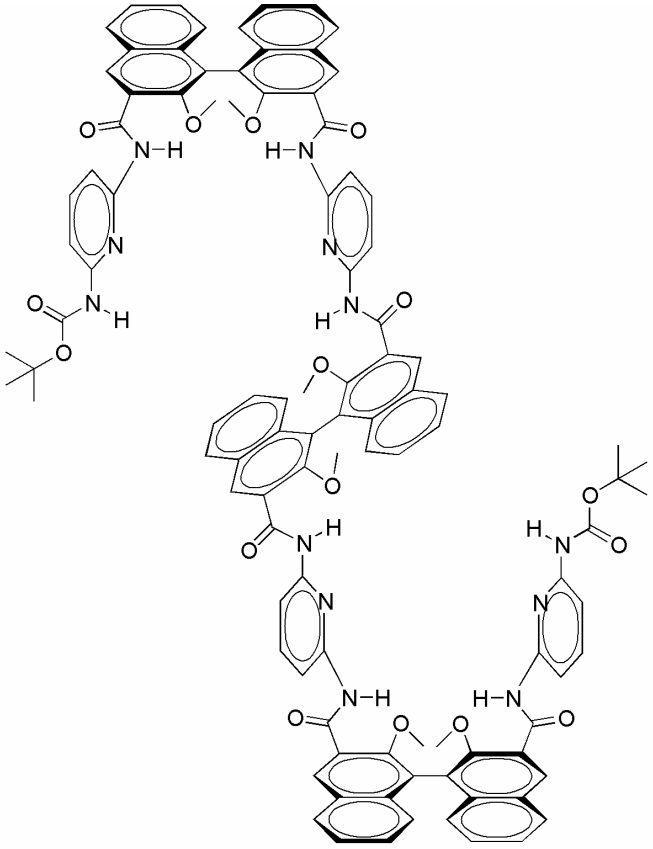

2

2a [S][S][S] **2b [S][R][S]**

BINOL-pyridine-based hybrid foldamer structures 2a and 2b synthesized in this study. These oligomers containing three BINOL building blocks differ in the positioning of the BINOL enantiomers [R] and [S].

List of publications:

1.*Self-assembly with degenerate prototropy*: **Baruah, P. K.**; Gonnade, R.; Phalgune, U. D.; Sanjayan, G. J. *J. Org. Chem*. **2005**, *70*, 6461-6467.

2. *The solid-state behaviour of 4,6-dioxo-5,5-diethylenepyrimidine-2-isobutylurea*: Spencer, E. C.; Howard, J. A. K.; **Baruah, P. K.**; Sanjayan, G. J. *CrystEngComm* **2006**, *8*, 468–472.

3. *Enforcing Periodic Secondary Structures in Hybrid Peptides: A Novel Hybrid Foldamer Containing Periodic γ-Turn Motifs*: **Baruah, P. K.**; Sreedevi, N. K.; Gonnade, R.; Ravindranathan, S.; Damodaran, K.; Hofmann, H.-J.; Sanjayan, G. J. *J. Org. Chem*. **2007**, *72*, 636-639.

4. *BINOL-Based Foldamers - Access to Oligomers with Diverse Structural Architectures*; **Baruah, P. K.**; Gonnade, R.; Rajamohanan, P. R.; Hofmann, H.-J.; Sanjayan, G. J. *J. Org. Chem.* **2007**, *in press*.

5. *Aib-rich Sheet-Forming Abiotic Foldamers*: **Baruah, P. K.**; Sreedevi, N. K.; Majumdar, B.; Pasricha, R.; Poddar, P.; Ravindranathan, S.; Sanjayan, G. J. *communicated*.

6. *Tetrazole-based novel hydrogen bonding motifs*: **Baruah, P. K.**; Gonnade, R.; Sanjayan, G. J. *Manuscript under preparation*.

CHAPTER I

Self Assembly with Degenerate Prototropy

-Science is always wrong. It never solves a problem without creating ten more.

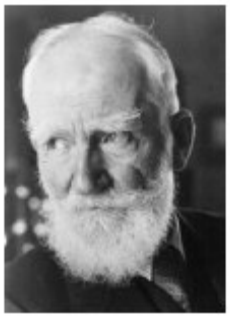

by George Bernard Shaw
Born: 26th July 1856, Ireland.
Death: 2nd November 1950

1.1 Introduction

There has been a tremendous development in the field of molecular chemistry for more than 175 years, since the synthesis of urea by *Friedrich Wohler*[1] in 1828. It is a fact of mere imagination what complex structures one can attain by the making and, or breaking of covalent bonds between atoms in a controlled and precise manner. Organic synthesis has since then grew rapidly and masterfully, leading to brilliant achievements. It has been a long way from *Wohler's* urea to the synthesis of Vitamin B_{12} by *Robert Woodward*[2]and *Albert Eschenmoser*[3] assisted by hundred or so collaborators!

Molecular chemistry, thus, has established its power over the covalent bond. Beyond molecular chemistry there lies the field S*upramolecular Chemistry*, whose goal is to gain control over the intermolecular interaction. The concept and the term of supramolecular chemistry were introduced in 1978 by Jean Marie Lehn.[4,5] So it can be said in words, ''just as there is a field of *molecular chemistry* based on covalent bonds, there is a field of *supramolecular chemistry*, the chemistry of molecular assemblies and of the intermolecular interactions''.

Supramolecular chemistry can be broadly classified into two broad areas: (1) *supermolecules*, well-defined, discrete oligomeric species that result from intermolecular association of a few components (a receptor and its substrate(s)) following a built in 'Aufbau' scheme based on the principles of molecular recognition; (2) *supramolecular assemblies*, polymolecular entities that result from the spontaneous association of a large unidentified number of components into a specific phase having more or less well-defined microscopic characteristics depending on its nature (such as films, membranes, micelles, mesomorphic phase, solid state structures, etc.). It thus covers the rational, coherent approach to molecular associations, from smallest, the dimer to the largest, the organized phase, and to their designed manipulation.

1.1.1 Self- Assembly: Programmed Supramolecular Systems

Self-assembly has become a subject of great interest to chemists stimulated by nature's ability to perfectly control the aggregates in solution.[6] Currently there is intense interest

in constructing nanostructures through the self-assembly of both biological and synthetic systems.[7] In nature, the cooperative action of numerous non-covalent forces leads to highly specific molecular recognition events. On the other hand, the preparation of nanostructures with even the best present-day synthetic methods still presents one of the most daunting challenges. Molecular recognition finds explicit application in the field of supramolecular chemistry as a means of controlling the evolution of supramolecular species and devices as they build up from their components and operate through *self-process*. The control of organization; self-organisation at the molecular level is a field of major interest in molecular design and engineering, which may be expected to become a subject of increasing activity.[8]

Supramolecular chemistry has relied on more or less rigidly organized, synthetically built up molecular receptors for effecting molecular recognition, catalysis, transport processes, etc. Beyond *preorganization* based on covalent bonding, lies the design of systems undergoing self-organization (systems capable of spontaneously generating well-defined supramolecular architectures from its components under a given set of condition). Self assembly can give rise to various sets of diverse structures such as double[9] and triple helical[10] metal complexes.

1.1.2 Self assembly of organic molecules through hydrogen bonding

To build up a supramolecular architecture, it requires two or more hydrogen bonding subunits whose disposition determines the final structure. When two subunits are incorporated into a single group, it will then possess two recognition faces and may be termed as *Janus* molecule, double faced H-bonding recognition units. If the faces are same or different the units are *homotopic* or *heterotopic*; when they are complimentary, the unit is self-complimentary and may be termed as *plerotopic*. Each recognition may have one, two, three, four, etc. hydrogen bonding donor (**D**) or acceptor (**A**) centers. The stability and selectivity of the association depend on the nature and position of these centers.[11] For example tridentate groups of barbituric acid and 2, 4, 6-triaminopyrimidine

types may associate either as crinckled tape[12] or as a supramolecular macrocycle, a rosette[13] (figure 1).

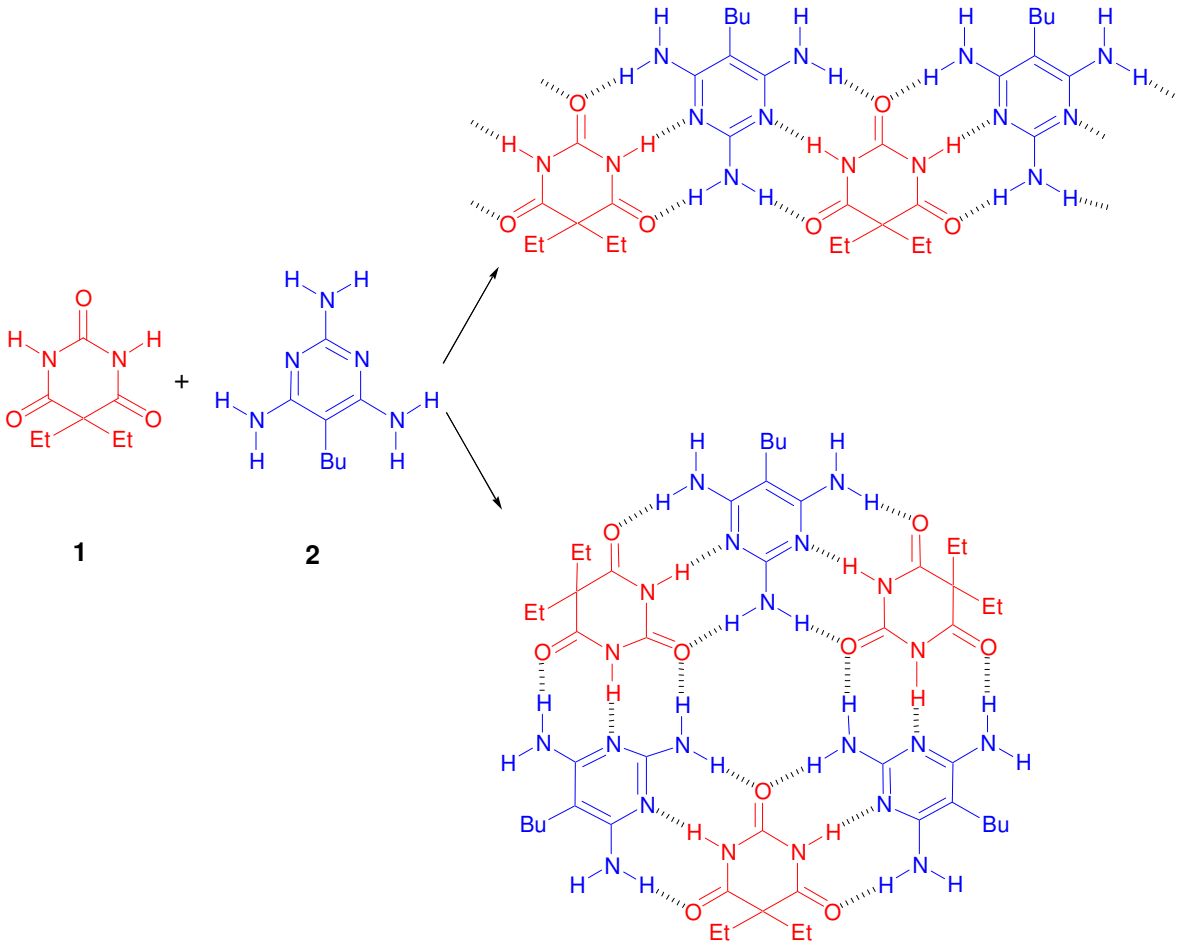

Figure 1: Supramolecular assembly of barbituric acid and 2, 4, 6-triaminopyrimidine.

1.2 Design, Synthesis and Structural Studies of highly stable molecular duplexes devoid of prototropy

Over the past decade, development of novel "designed molecules"; molecules designed to serve specific purpose or programmed to attain specific structural/conformational

features, have achieved new dimensions as would be evident from the recent literature.[14,15] It is anticipated that use of specific non-covalent interactions to modulate the dimensions and chemical properties of novel organic molecules would eventually pave the way for designing new materials, electronic devices, drug candidates and drug delivery systems for use in the atom-size realm of nanotechnology. Kaifer et al. has shown the utilization of electrochemical (redox) conversions to modulate the strength of host-guest interactions.[16] Issac et al. has shown the molecular recognition properties of the Cucurbit[n]uril family which shows excellent binding properties towards various guest molecules.[17]

The breadth of knowledge acquired in this area over the years has been overwhelming. The pioneering work of Whitesides[18] and others[19-21] in the area of hydrogen-bonding-driven molecular self-assembly has yielded a plethora of novel designed structural architectures, having potential utility in the area ranging from medicinal chemistry to material science. Lehn's group[22] has developed several highly interesting molecular constructs with pre-defined structural features through metal coordination with variously substituted bipyridyl ligands. Hamilton et al.[23] developed complexes based on the 2-aminopyridinecarboxylic acid system. By combining multiple hydrogen bonds, Zimmerman,[24] Lehn,[25] and Mascal[26] described the creation of cyclic self-assembling structures. In addition, Reinhoudt et al.[27] and de Mendoza et al.[28] have shown the assembly of calix[4]arene derivatives. Ghadiri et al.[29] designed dimeric structures with eight hydrogen bonds using modified cyclic peptides. Extremely stable dimers based on guanine were reported recently by Sessler et al.[30] Rebek et al.[31] designed concave molecules that assembled into structures reminiscent of tennis balls. Diavis et al. showed *N*-Carbamoyl squaramides, form hydrogen-bonded dimers in solution and in non-polar organic solvents.[32] A novel metal-organic anion receptor containing urea functionalized *iso*quinoline ligands that exhibits remarkably strong binding of sulfate by completely encapsulating the anion in a "cone" conformation in both solution and the solid state, has been reported.[33]

Due to their strength, directionality, and specificity, arrays of multiple hydrogen bonds are useful building blocks for the construction of complex structures. These properties are expected to be particularly pronounced in large arrays of hydrogen bonds. Such arrays indeed form very stable complexes as have been shown for receptors for urea,[34] guanines,[35] for self-assembled receptors.[36] However, the use of these arrays is limited by the synthetic efforts required for their preparation.

Recently Meijer et al.[37] and Zimmermann et al.[38] have reported highly stable self assembling molecular duplexes with quadruple hydrogen bond. These systems are quite stable in non polar solvents and the dimerisation constant is of the order of 10^6 M^{-1} in $CDCl_3$. The stability of these hydrogen bonding motifs are governed by the primary hydrogen bonding interactions as well as secondary electrostatic repulsive and attractive interactions. The stability of hydrogen bonding molecular duplexes can be further enhanced by ionic interactions as was shown by Schmuck et. al.[19] They find application in various disciplines like- in the nucleation and stabilization of beta sheets as reported by Bing Gong.[39]

Although natural duplex, DNA can act as a template in directing the reaction, but self assembling entities have more advantage due to ready availability in large quantities, much lower molecular weights, and compatibility with a wide variety of organic solvents compared to the former. The number of complimentary and self complimentary duplexes can be calculated by the following equations.[40]

$$N = 2^{n-2} + 2^{(n-3)/2} \quad \text{When n = odd number} \qquad \textbf{1.1}$$

$$N = 2^{n-2} + 2^{(n-2)/2} \quad \text{When n = even number} \qquad \textbf{1.2}$$

Where, N: no of duplexes

n: no of hydrogen bonding sites

1st term -No of complimentary duplexes

2nd term - No of self-complimentary duplexes

The possible types of self-complimentary and complimentary arrays with their dimerisation constant are as shown in (figure 2).[41]

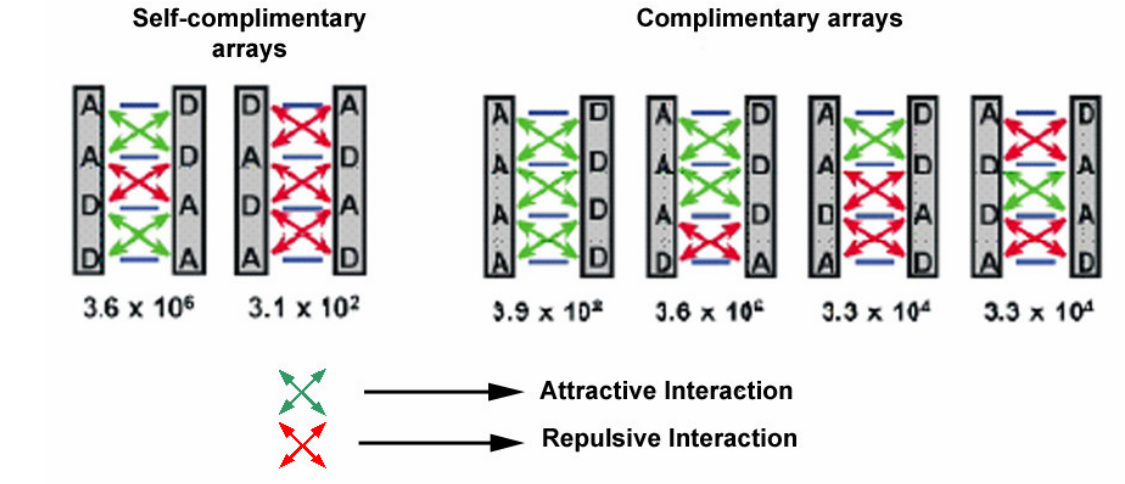

Figure 2: complimentary and self-complimentary arrangements in a quadruple H-bonded system.

In view of the partial positive charges on H atom and partial negative charges on N and O atoms, four of the secondary interactions are attractive and two are repulsive for DDAA dimer, while all six interactions are repulsive for ADAD dimer. The net of two stabilizing interactions each and six destabilizing interactions can account for the stronger and much weaker binding for DDAA and ADAD dimers, respectively.

In order to account for the role of secondary interactions in the stability of H-bonded complexes, Schneider[42] proposed an empirical equation for nucleobases and synthetic host-guest complexes mediated by H-bonding in chloroform. As has been seen in the equation **1.3**, analysis of 64 association constants for 58 different complexes led to only one increment for the primary H-bonding interactions (-7.9kJ/mol each) and one for the secondary interactions (±2.9 kJ/mol each) in terms of free energy, irrespective of whether they are attractive or repulsive. The difference between the calculated and experimental free energy is only ±1.8 kJ mol^{-1}.

$$\Delta G = -7.9 \times m \pm 2.9 \times n \text{ (kJ/mol)} \qquad \textbf{1.3}$$

m: number of H-bonds(PI, primary interactions)

n: number of secondary interactions (+ for repulsive and –for attractive interactions).

The table **1-1**[24, 37a, 38a, 43-45] shown below summarizes the relationship between ΔG (kcal/mol) and association constants in K_{dimer} (M^{-1}), $\Delta G = RT\ln(K_{dimer})$.

The above mentioned empirical equation is entirely based on N-H···N and N-H···O=C-H bonds so that the actual values for other types of H-bonds may not be the same as those empirically anticipated, which is directly indicated by DADA arrays.[37a] Another factor, preorganization of complex geometry induced by intramolecular H-bond, which would increase the stability of H-bonded complexes, is not taken into account in the above equation.

***Table 1.1*:** Calculated *vs* Experimental values for heterocyclic complexes.

Arrays	PI	Secondary interactions			K_{dimer} (M^{-1})	
	H-Bonds	Repulsive	Attractive	Net	Predicted	Exp.
DA·AD	2	-2	0	-2	60	10^1
DD·AA	2	0	2	2	3.6×10^3	10^3
DAD·ADA	3	-4	0	-4	1.3×10^2	10^2
DDA·AAD	3	-2	2	0	1.4×10^4	10^4
DDD·AAA	3	0	4	4	1.5×10^6	10^5
DADA·ADAD	4	-6	0	6	3.1×10^2	10^1- 10^5
DDAA·AADD	4	-2	4	2	3.6×10^6	10^6
DDDD·AAAA	4	0	6	6	3.9×10^8	?

Recently various groups have designed and synthesised self-assembling molecular duplexes (complimentary and self complimentary) with multiple hydrogen bonding donor and acceptor sites. Some of the self-assembling H-bonded molecular duplexes reported in the literature are as shown below in (figure 3).

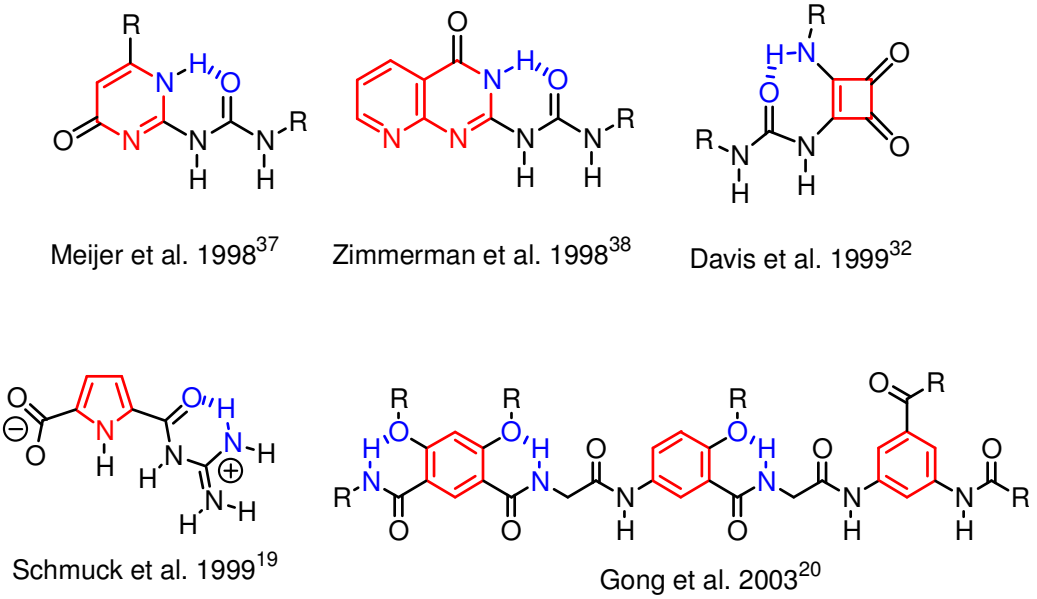

Figure 3: Selected examples of self-assembling motifs.

Although the generality of the quadruple hydrogen bonding molecular duplexes developed by Meijer and Zimmerman have attracted considerable attention from scientific community, they suffer from the problem of prototropy (due to prototropy, Zimmerman's pyrido-pyrimidinone-based self-assembling system exists in as many as four protamers (figure 4), and Meijer's ureidopyrimidinone has been shown to display mainly two types of protamer formation (figure 5), depending upon the substitution pattern on the heterocyclic ring). Prototropy is a major type of tautomerism observed in heterocycles due to proton shift. Therefore supramolecular polymers derived from such prototropy-prone heterocycle-based self-assembling modules can exist in multiple prototropic forms, rendering their structural investigation tricky.[46]

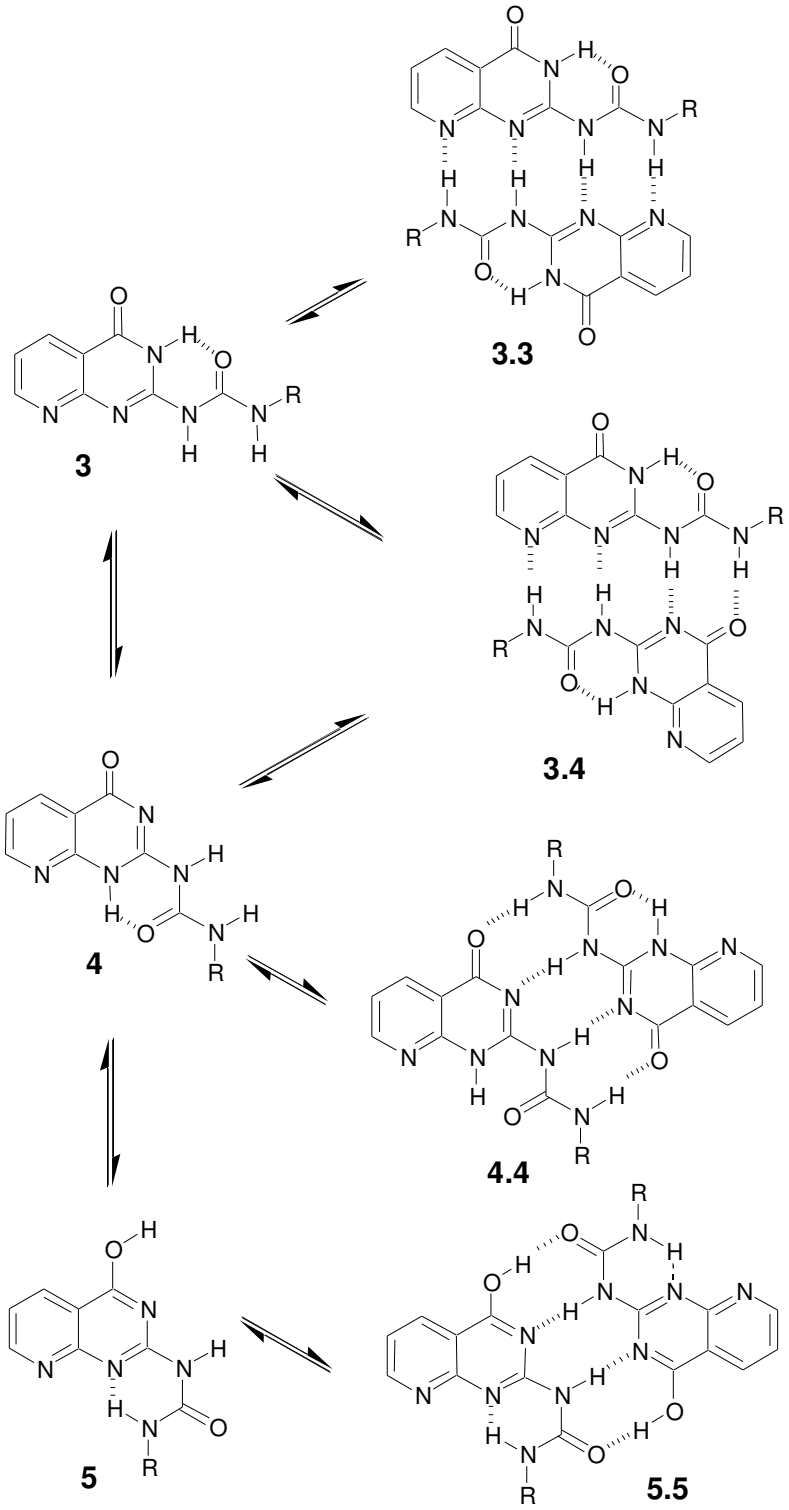

Figure 4: Multiple protamer formation in Zimmermann's pyrido-pyrimidinone-based self-assembling system.

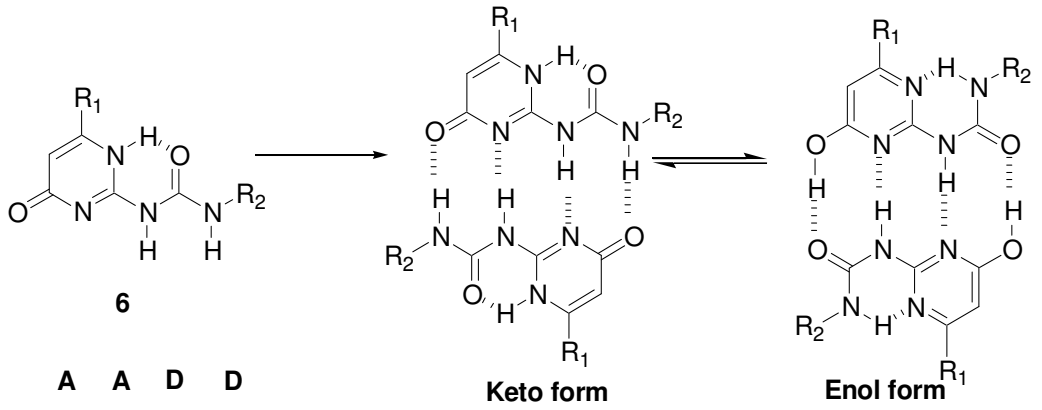

Figure 5: Multiple protamer formation in Meijer's ureidopyrimidinone based self-assembling system.

1.2.1 Objective

Our major interest in this area was to develop a self-assembling system free of prototropy related problems, as narrated earlier. For this reason we have chosen the principle of degenerate prtotropy that has been observed in heterocyles such as imidazole for a long time. As a proof-of-principle, the utility of degenerate prototropy is demonstrated herein by developing heterocycle-based AADD-type self-assembling modules that exist as single set of protameric pair (duplex) both in solution and solid state. The strategy disclosed herein has the potential for significantly augmenting the "tool-box" of the modern day supramolecular chemist, as well as providing a novel approach to the field of rational design using the concept of degenerate prototropy.

1.2.2 Design Principles

Prototropy is a major type of phenomenon observed in heterocycles resulting in various tautomeric forms. Degenerate prototropy, also known as degenerate tautomerism, is a phenomenon by which annular prototropic shift regenerates the same structure due to the chemical equivalence of the protamers.[47] One of the simplest systems that exhibit degenerate prototropy is imidazole wherein both the protamers, formed by 1,3-annular prototropic shift, are rendered equivalent, by prototropic degeneracy (figure 6).

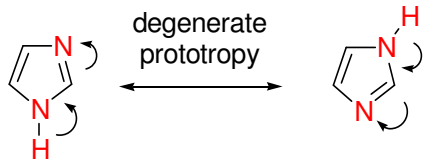

Figure 6: Degenerate prototropy in imidazole

Though a number of systems have been shown to exhibit this fascinating phenomenon,[48] its utility as a nifty concept in the rational design of novel systems largely remains unexplored. In order to tackle the multiple protamer formations in heterocycle-based AADD type self-assembling systems, the following systems were designed (figure 7).

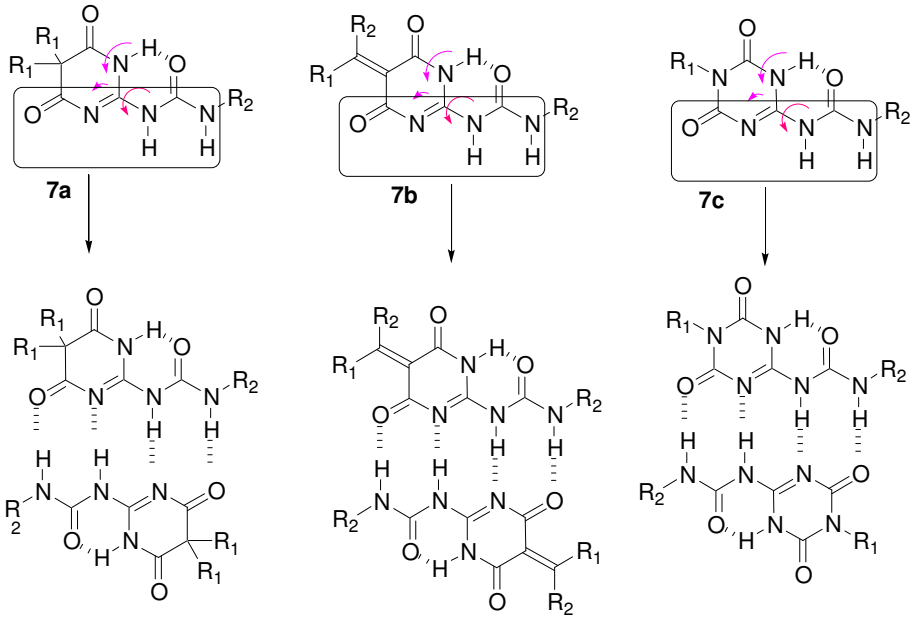

Figure 7: Identifying the possible systems with degenerate prototropy.

Among the above three possible systems we chose **7a** due to it's anticipated ease of synthesis and because of the possibility that due to α,α-dialkyl substitution, such compounds might crystallize easily.[49] Hydrogen-bonded self-assembling systems usually show poor tendency to crystallize under ordinary conditions presumably due to their inefficient packing in crystalline lattices.[50] This has prompted researchers to utilize drastic conditions to crystallize self-assembling organic systems, using high pressure and

temperature,[51] a condition routinely used for crystallizing quartz, zeolites, and inorganic open-frame structures.[52]

As discussed earlier the design principles were based on the observation that 1,3 annular prototropic shift in heterocycles such as imidazole, results in prototropic degeneracy due

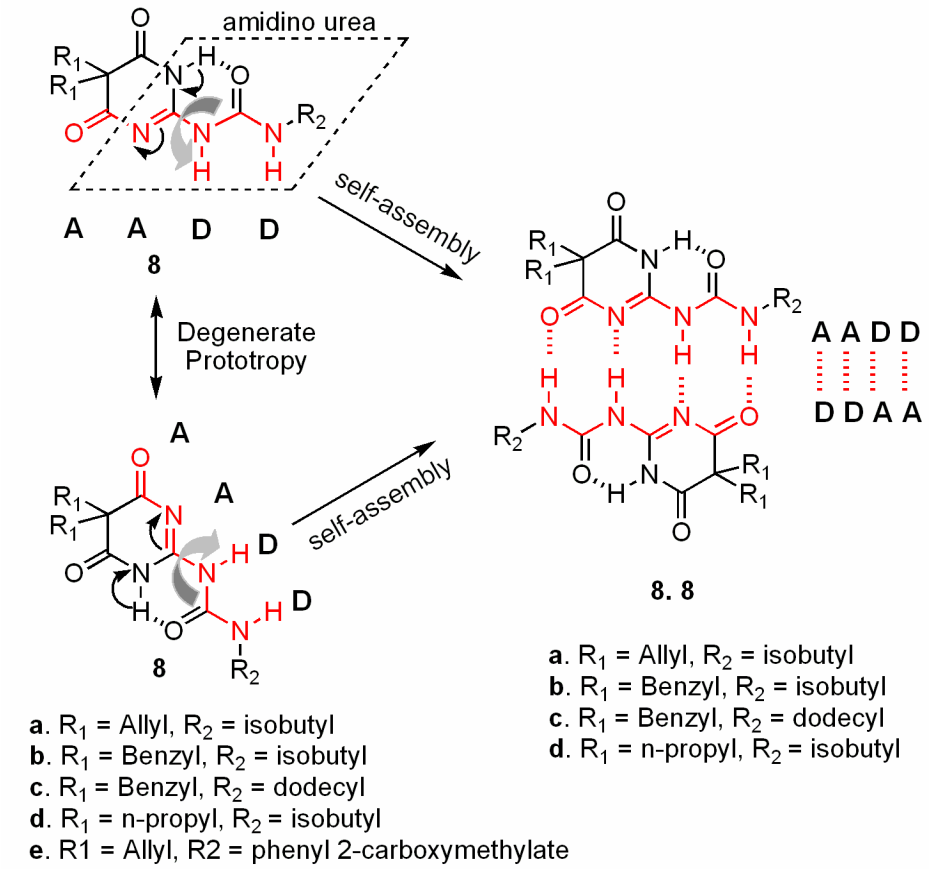

Figure 8: Degenerate prototropy in **8**. Block arrows indicate rotation (180^0) of urea moiety about the bond connecting the heterocycle.

to the chemical equivalence of the protamers. It was anticipated that acylation of the amidino urea moiety with a symmetrical bis-acyl unit, as in **8**, should provide the molecule sufficient room for degenerate prototropy. In the urea construct **8**, the amidino urea moiety is tethered to an α,α-disubstituted malonyl unit such that annular 1,3

prototropic shift, accompanied by the 180^0 rotation of the urea moiety[53] about the bond connecting the heterocyclic ring, would result in prototropic degeneracy, since the protamers would be, in all respects, equivalent (figure 8). Thus, the dimerization of **8** can be expected to lead to only a single set of hydrogen bonded duplex. Structural studies, vide infra, indeed showed that **8** forms only a single set of molecular duplex **8.8**, both in solution and solid state.

1.2.3 Synthesis

The synthesis of the ureidopyrimidinone moiety **8** can be achieved by the following two ways. Diethyl malonate can be condensed with guanidine hydrochloride and the condensed product can be subjected to reaction with isocyanates. This resulting product can be finally alkylated using alkyl halides. But alkylation of the active methylene $-CH_2$ in the heterocyclic ring in the presence of other acidic protons (-NHs) could eventually lead to mixture of products. Therefore we chose the second route involving alkylation of the diethyl malonate, condensation with guaninidine and further reaction with various isocyanates, which should be free of above mentioned problems.

1.2.3.1 Identifying the best method for preparation

Strategy-I

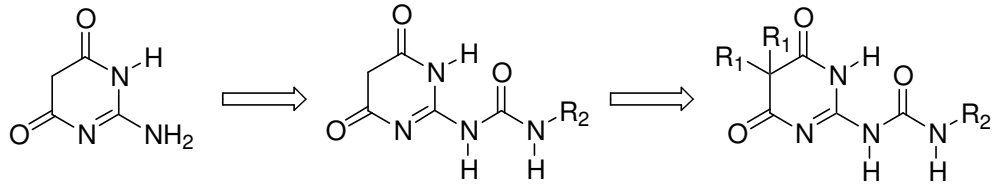

Strategy-II

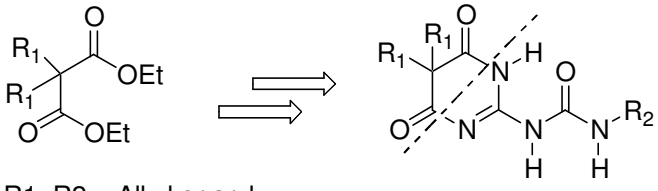

R1, R2 = Alkyl or aryl

Scheme 1:

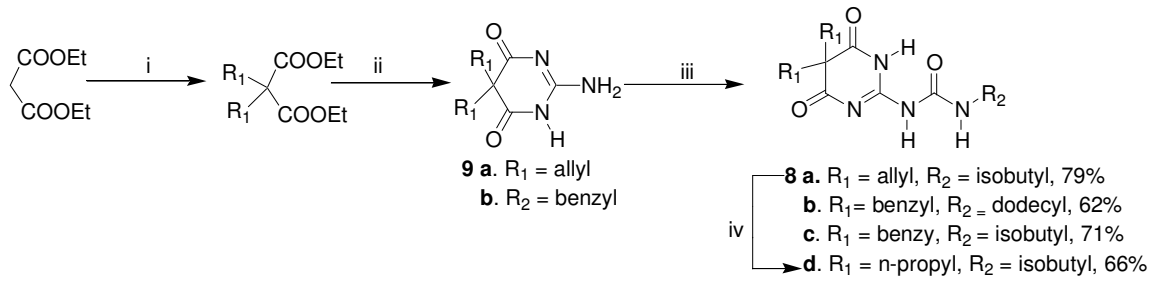

Reagents and conditions: (i) R_1Cl, KOH, DMSO; (ii) NaOEt, guanidine hydrochloride, ethanol, reflux, 4 h; (iii) R_2NCO, pyridine, 80-90 ^{0}C, 2 h; (iv) H_2, Pd-C (10%).

The synthesis of **8** starts with alkylation of diethyl malonate (scheme 1). Use of various alkyl iodides using bases like t-BuOK, NaH, NaOEt always gave a mixture of products including mono, di alkylated as well as decarboxylated product. It has been reported that using KOH as a base and DMSO as a solvent various substrates having acidic protons can be alkylated[54] with very high yields and without the formation of mixture of products. Alkylation of diethyl malonate with benzyl and allyl chloride under this condition furnished the dialkylated product in very good yield (95%). 2-amino-5,5-disubstituted-1H-pyrimidine-4,6-diones **9**, were easily prepared by condensation of α,α-dialkyl malonates and free guanidine.[55] The 2-amino-5,5-disubstituted-1H-pyrimidine-4,6-diones **9** were further subjected to reaction with various isocyanates, prepared *in situ* by reaction of amines with triphosgene; to furnish the self-assembling systems **8**. **8d** was obtained by hydrogenation of **8a** with Pd-C (10%).

1.2.4 Results and discussion

Contrary to its precursors, **8** was highly soluble in nonpolar organic solvents including petroleum ether (>>100 mM in petroleum ether) at ambient temperature. This observation suggests that the polar groups (NHs) are strongly masked by hydrogen bonding. In other words the molecule forms strong dimer preventing formation of

polymeric aggregates.[56] ^{1}H and ^{13}C NMR (500 and 125 MHz, respectively) spectra of **8a** in $CDCl_3$ show single set of well-resolved signals (figure 9).

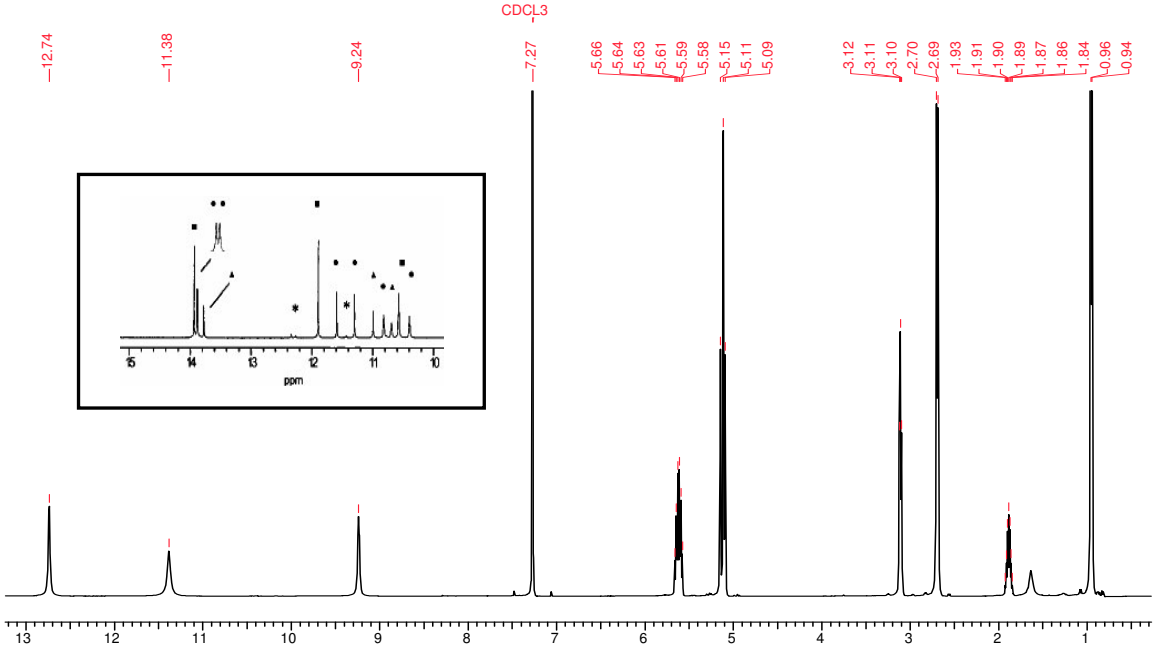

Figure 9: ^{1}H (500 MHz) NMR spectra of **8a** in $CDCl_3$ showing single set of well resolved signals. (In the inset is shown the NH signals of Zimmerman's self assembling system in tolune-d_8 at $-30^{0}C$. *Note*: Signals corresponding to all sets of protameric duplexes are clearly visible as compared to only one set of signal in our system.)

The significant downfield NH chemical shifts were indicative of strong hydrogen bonding interactions in solution. Both the urea NH signals of **8a**, appearing at 9.24 and 11.38 ppm, showed concentration-dependent changes in their chemical shifts, supporting their role in forming intermolecular hydrogen bonding. The NH group (12.74 ppm) involved in the formation of the intramolecular S(6) ring[57] that pre-fixes the linear AADD hydrogen bonding array, showed insignificant concentration-dependant shift. The NH protons were assigned by 2D COSY as well as by dilution experiment.

1.2.5 NMR Dilution Studies

The dimerization constant K_{dim} for **8a** was measured by ^{1}H NMR dilution method using the following equation[58]

$$\delta_{obs} = \delta_{mono} + \frac{1 + 4K_{\dim}C - (1 + 8K_{\dim}C)^{1/2}}{4K_{\dim}C}(\delta_{\dim er} - \delta_{obs}) \qquad \textbf{1.4}$$

^{1}H NMR binding studies,[58a] in the concentration range of 100 – 0.5 mM range, gave the dimerization constant (K_{dim}) 1.2 x 10^4 M^{-1} for **8a** in $CDCl_3$. Dimerization of **8a** was studied in a mixture of $CDCl_3$ with 5% DMSO-d_6 which is a strong hydrogen bond acceptor solvent. The dimerization constant obtained for our system is relatively low when compared to the dimerization constant (K_{dim}) of Meijer's **AADD** type ureidopyrimidinones containing a heterocyclic aromatic unit which is in *keto-enol* tautomeric equilibrium.[37a] The relatively low K_{dim} of our system is presumably due to the absence of π-electron density in the heterocyclic ring that could have positively contributed to the duplex stability as in ureidopyrimidinones.[59] The table showing the chemical shift with concentration in 100% $CDCl_3$ and in 5% DMSO-D_6 in $CDCl_3$ is as shown below (Table 1.2).

***Table 1.2*:** Variation of chemical shift of the NH's with concentration in (a) 100% $CDCl_3$ and (b) 5% DMSO in $CDCl_3$.

100% $CDCl_3$			**5% DMSO in $CDCl_3$**		
Concentration [mM]	δ (NH-3) [ppm]	δ (NH-2) [ppm]	Concentration [mM]	δ (NH-3) [ppm]	δ (NH-2) [ppm]
100	9.24	11.38	200	9.03	11.35
80	9.23	11.37	150	8.99	11.34
60	9.22	11.36	100	8.94	11.32
50	9.21	11.35	80	8.89	11.31
25	9.17	11.31	50	8.79	11.27
15	9.14	11.28	10	8.34	11.11
10	9.09	11.23	5	7.97	10.98
6	9.07	11.18	1	7.20	10.70
4	8.99	11.12	0.5	6.88	10.59
2	8.86	11.00			
0.5	8.60	10.71			

Graph showing Concentration *vs* Chemical shift

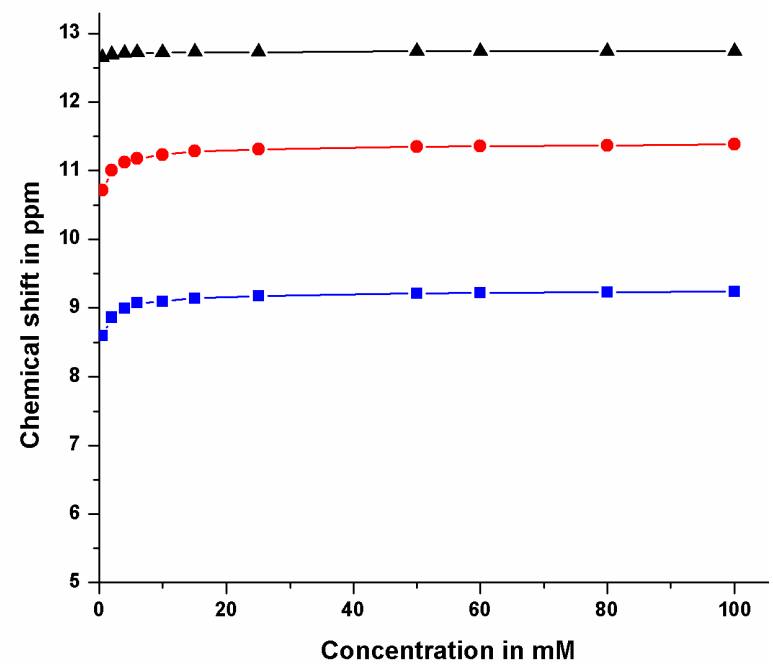

Figure 10: A plot of the variation of chemical shifts for NH signals of **8a** in $CDCl_3$ with concentration.

δ_{mono} was obtained by both extrapolating the curve to 0 concentration (figure 11) and also by nonlinear curve fitting (figure 12), as given below.

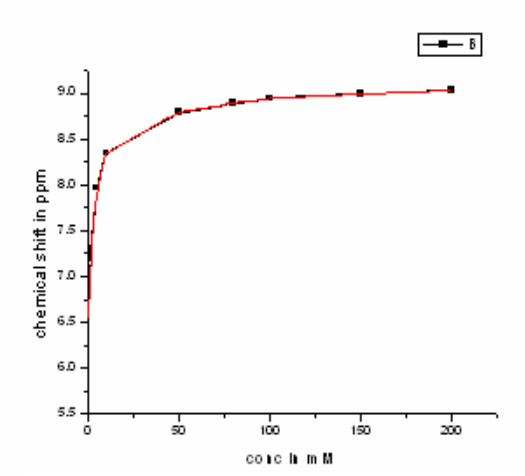

***Figure 11*:** Extrapolation curve method

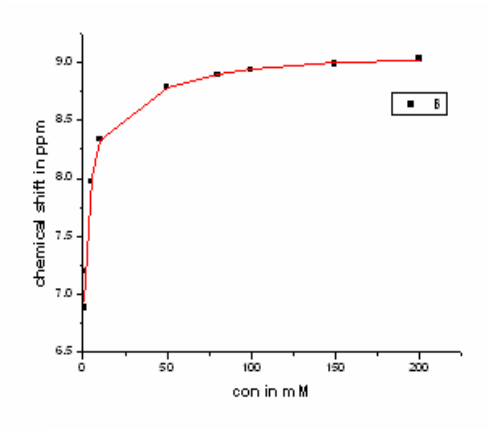

***Figure 12*:** Non-linear curve fitting Procedure

δ_{mono} obtained for **NH3** by *extrapolation to zero concentration* is **6.56 ppm** and by *non-linear curve fitting* is **6.69 ppm**. The function used for the nonlinear curve fitting procedure is 'Expass' and the equation is: **y = y0 + A1*(1 - exp(-x/t1)) + A2*(1 - exp(-x/t2)).** In neat DMSO-d6, the δ value obtained for **NH2** is **11.36 ppm** which is higher than the **δ 10.71 ppm** in 0.5mm $CDCl_3$. This unusual down field shift may be due to the interaction between solvent (DMSO) and NHs of the compound. Though the same trend is not observed for **NH3,** we feel that since the DMSO interaction with NHs is prominent, it may not be a good idea to take into account the δ_{mono} obtained for NHs in DMSO.

δ_{dimer} = 9.29 ppm (the value obtained by extrapolating the curve to 200mM in $CDCl_3$)

1.2.6 Evidence of dimer formation by ESI mass spectroscopy

MADLI and ESI spectrometry have led the way in protein and peptide detection and sequencing, DNA sequencing, protein folding, in vitro drug analysis, and drug discovery. In MALDI, the sample is co-crystallized at fairly high dilution with a chemical matrix (roughly 100 to one or higher). The matrix is sublimated by a laser pulse and carries the analyte molecules into the gas phase. The ionization event occurs with several mechanisms. The transfer of noncovalently bound complexes into the gas phase is possible with soft ionization techniques, and therefore the determination of the complex's stoichiometry and sometimes mode and energy of interaction. Ganem et al. were the first to describe the use of a soft ionization method, ion spray mass spectrometry, for the identification of noncovalent host–guest interactions.[60] ESI is the predominant method used for mass spectrometric investigation of noncovalent complexes, with MALDI mass spectrometry applied much less frequently. It is normally a greater challenge to apply MALDI–MS to noncovalent complexes, because the generally weak interaction forces have to survive both the sample crystallization as well as the laser desorption/ionization event. MALDI is therefore believed to be somewhat less "soft" than ESI.

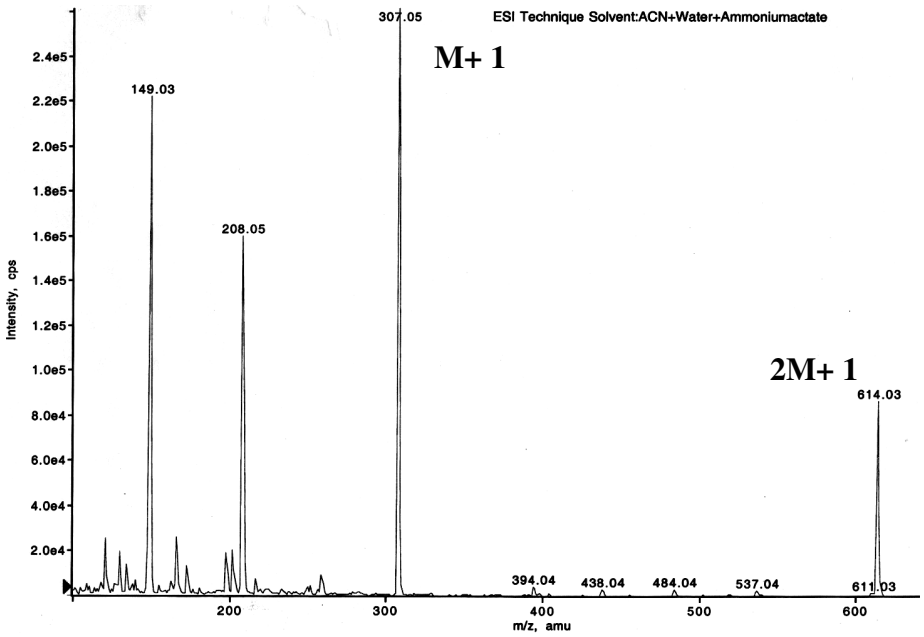

Figure 13: ESI Mass spectrum of **8a**.

ESI mass spectrometry is an effective tool in investigating the formation of hydrogen-bonded molecular self-assemblies. In addition to the molecular ion peaks (M +1) ascribable due to the monomers **8**, the ESI spectrum (figure 13) showed sizable peaks (30% compared to the monomer peak) corresponding to the dimers **8.8** (2M +1). This observation strongly suggests that **8** undergoes strong molecular duplex formation.

1.2.7 Evidence of dimer formation in solid state

Hydrogen-bonded self-assembling systems usually show poor tendency to crystallize under ordinary conditions presumably due to their inefficient packing in crystalline lattices. An interesting property associated with our self-assembling systems is their remarkably high propensity to easily crystallize into large crystals under ambient conditions, presumably as a consequence of the intrinsic nature of rigid α,α-dialkylated systems to efficiently pack into crystalline lattices.[49] The solid-state structures of **8a-c** were determined by single crystal X-ray diffraction[61] (figure 14).

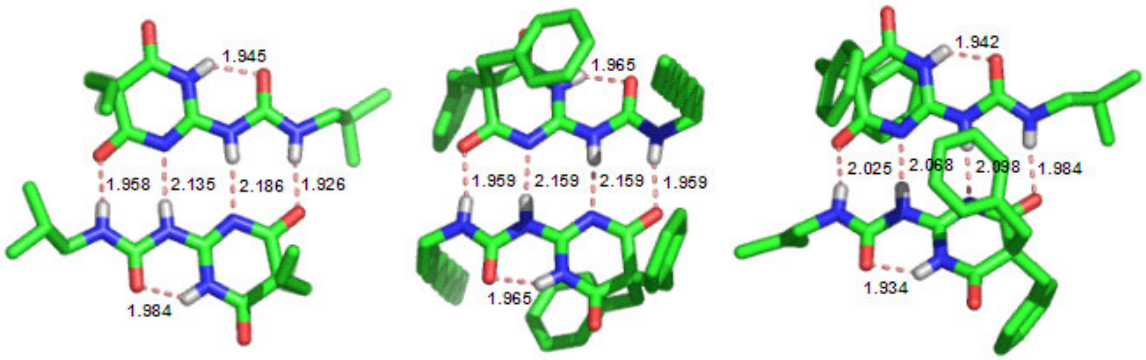

Figure 14: Single crystal X-ray structures of dimers **8.8a** (left), **8.8b** (middle) and **8.8c** (right). Hydrogen bonding is highlighted in dashes (salmon colored), above which hydrogen bond distances (NH···N and NH···O) are displayed in Å. All hydrogens, other than at the hydrogen bonding sites, have been deleted for clarity. This figure was made using PyMOL.[63]

Comparison of the X-ray structures of **8a-c** revealed the following facts. All three compounds, irrespective of the nature of substituents, form centrosymmetric dimers **8.8** in the solid state, maintaining similar hydrogen bonding codes.[37a] The dimers are held together by four C(4) type[57] intermolecular hydrogen bonds between self-complimentary AADD type linear hydrogen-bonding arrays. The urea functionality is in a trans-trans geometry, as expected, and an intramolecular S(6) type[57] hydrogen bond bridges the pyrimidine N-H to the urea carbonyl group that preorganizes the AADD array of hydrogen bonding sites. In all the cases, the AADD array deviates slightly from linearity, the outer N-H···O hydrogen bonds being somewhat shorter than the inner N-H···N hydrogen bonds.

Interestingly, the dimer **8.8a** forms self-assembled infinite chains of helical nature (figure 15) through a relatively weaker bifurcated intermolecular hydrogen bonding

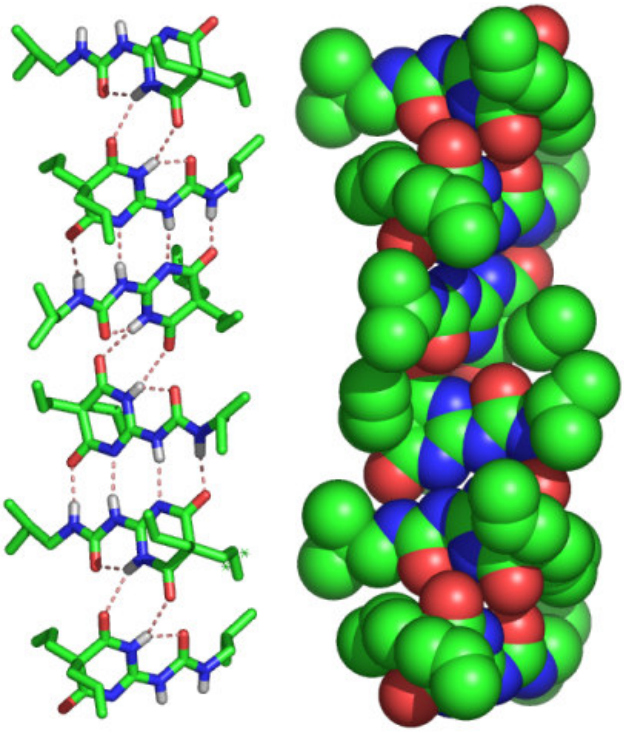

Figure 15: Further self-assembly of **8.8a**, capped stick (left) and sphere (right) representations, showing infinite chains of helical nature. All hydrogens have been deleted for clarity in the sphere representation. This figure was made using PyMOL.[63]

involving the pyrimidine ring N-H and the remaining carbonyl group of another molecule forming 12-membered ring hydrogen-bonded network, although similar arrangement is not observed in **8.8b** and **8.8c**. The bifurcated hydrogen bonds in the extended self-assembled net work of **8.8a** are relatively weaker as the D-H···A distances are longer [d(H···O) = 2.464 and 2.526 Å]. Although a highly symmetrical hydrogen bonding pattern is maintained in **8b**, similar trend is absent in **8a** and **8c**. Notably, in **8.8c**, the hydrogen bonding arrays are considerably forced out of plane presumably due to the steric clash between benzyl and isobutyl substituents, though such an interaction does not prevent dimer formation.

1.2.9 Effect of electronic hindrance in duplex formation

Substituents are known to play a crucial role in dictating the mode of association of self-assembling systems, either through steric hindrance[7a] or through hyper conjugation effects.[62] Whitesides et al. have cleverly made use of steric hindrance as a major driving force in specifically obtaining cyclic rosette, tape or crinkled tape self-assembled structures using the melamine-cyanuric acid self-assembling motifs.[7a] In an effort to evaluate the influence of electronic hindrance in duplex formation, we designed and synthesized the self-complimentary motif **8e**, having an o-carboxymethyl phenyl substituent tethered to the urea moiety.

Scheme 2:

10 **11** **8 e** R1= allyl

Reagents and conditions: (i) $SOCl_2$, isopropanol; (ii) triphosgene, Et_3N, DCM; (iii) **9a**, pyridine, reflux.

Anthranilic acid was first esterified using thionyl chloride in isopropanol, followed by conversion to the corresponding isocyanate by reacting with triphosgene and triethylamine (scheme 2). 2-amino-5,5-diallyl-1H-pyrimidine-4,6-dione was further subjected to reaction with isocyanate prepared *in situ* by reaction of isopropyl 2-aminobenzoate with triphosgene.

8e was highly soluble in nonpolar organic solvents suggesting that the protons were solvent shielded. Observation of 2M+ peak in the ESI mass spectrum also strongly suggested the dimer formation. In stark contrast to such findings, surprisingly, the duplex formation through quadruple intermolecular hydrogen bonding could not be observed in the solid state as unambiguously confirmed by single crystal X-ray studies. Instead of

dimerization, **8e** formed an extended sheet-like structure through intermolecular hydrogen bonding (figure 16).

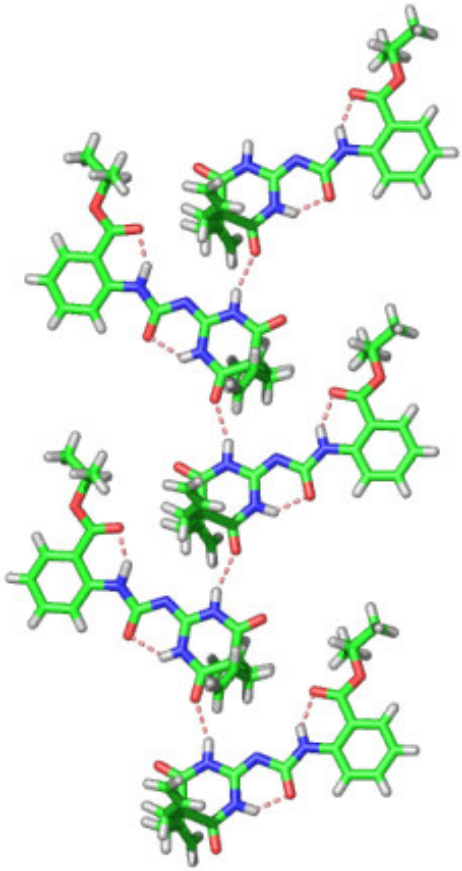

***Figure 16*:** Single crystal X-ray structure of **8e** showing self-assembly, through intermolecular hydrogen bonding, forming one-dimensional sheet-like network. This figure was made using PyMOL.[63]

Analysis of the single crystal structure of **8e** revealed the presence of two intramolecular hydrogen-bonding with in the molecule. Interestingly, unlike in **8a-c**, the AADD type hydrogen-bonding linear array is non-existent in **8e**. The non-formation of duplex **8.8e** is presumably due to the unfavorable electronic repulsion that would have been resulted by the close proximity of the anthranilic acid carbonyls and the heterocyclic carbonyls in the duplex **8.8e**.

1.3 Polymorphism in 8a

Polymorphism, a phenomenon of existence of a compound in different crystalline forms, is one of the contemporary areas of solid-state studies as an interdisciplinary subject embracing all major sections of science (biology, chemistry, physics, etc.).[64] The phenomenon of polymorphism is not limited to molecular compounds, but indeed, it was recognized long ago in elements as 'allotropy'. For example, carbon with different structural forms differentiated by the bonding between the atoms, exist in different forms known as graphite, diamond and fullerenes is a famous representative example. The importance of polymorphism is now well appreciated both in the context of fundamental aspects of structural features as well as in terms of its impact on the preparation and formulation of specialty chemicals, pharmaceuticals, explosives, dyes, pigments, flavors, agrochemicals, etc.[65-66] The phenomenon has gained paramount importance especially in pharmaceutical industry, because of the relevance of a particular form in formulations and bioavailabilty. Polymorphs, exhibiting diverse packing arrangements, due to different arrangement and/or conformation, might differ significantly in their physico-chemical properties such as solubility, stability, change in free energy, melting point, density, etc. Hence, preparation of particular polymorph of an active substrate has become utmost important consideration in the synthesis of pharma compounds to ensure that the same form/modification is always being produced consistently and reproducibly.

In order to study the solid state behavior of our self assembling molecular duplexes we have done the variable temperature X-ray studies on **8a**. Two polymorphic forms of **8a** have been identified, and these are denoted as the α and γ forms. The α form undergoes a phase transition at 250–255 K during which the sample converts to the β form, the crystals twin during this phase transition. Both the α and γ forms undergo a destructive phase transition, the onset of which is at approximately 165 K. Again, the phase transition is accompanied by the appearance of twinning in the crystal. The actual temperature at which the crystals crumble is strongly dependent on the cooling rate. At a cooling rate of 120 K min^{-1} a crystal of the α form disintegrated at 150–160 K. An

attempt to 'ease' a crystal through the transition by reducing the cooling rate to 0.5 K min^{-1} failed with the crystal crumbling at 132(2) K.

The asymmetric unit of the α form comprises a single molecule of **8a**. Crystals that are of the α form at room temperature, display the β form between ~250 K and the onset of the second phase transition at ~160 K. A total of four **8a** molecules are present in the asymmetric unit of the β form (figure 18). A conventional polymorphic relationship exists between the γ form of **8a** and the α and β forms.

In the solid-state structure of the α form the **8a** molecules are organized into dimer units as shown in (figure 17) by the two **8a** molecules with grey and orange carbon backbones. The crystal structure of the α form is stabilized by an intricate network of strong hydrogen bonds (figure 17). The dimer demonstrates an AADD quadruple hydrogen bond array. Crystals that are of the α form at room temperature, display the β form between ~250 K and the onset of the second phase transition at ~160 K. A total of four **8a** molecules are present in the asymmetric unit of the β form (figure 18). As might be expected, there are no significant differences (i.e. a difference notably greater then twice the estimated standard deviation) in the **8a** bond lengths between the α and β forms, or between the symmetry independent molecules within the asymmetric unit of β form. A conventional polymorphic relationship exists between the γ form of **8a** and the α and β forms. Three **8a** molecules are present in the asymmetric unit of the γ form. As in the case of the other two forms, within the crystal structure of the γ form the molecules are organized into dimer units (figure 19), although intriguingly, these dimer units are not further organized into chains; instead the dimers are present as discrete entities, a feature that noticeably distinguishes the γ form from the α and β forms.

The hydrogen bonding pattern of the α, β and γ form are as shown below:

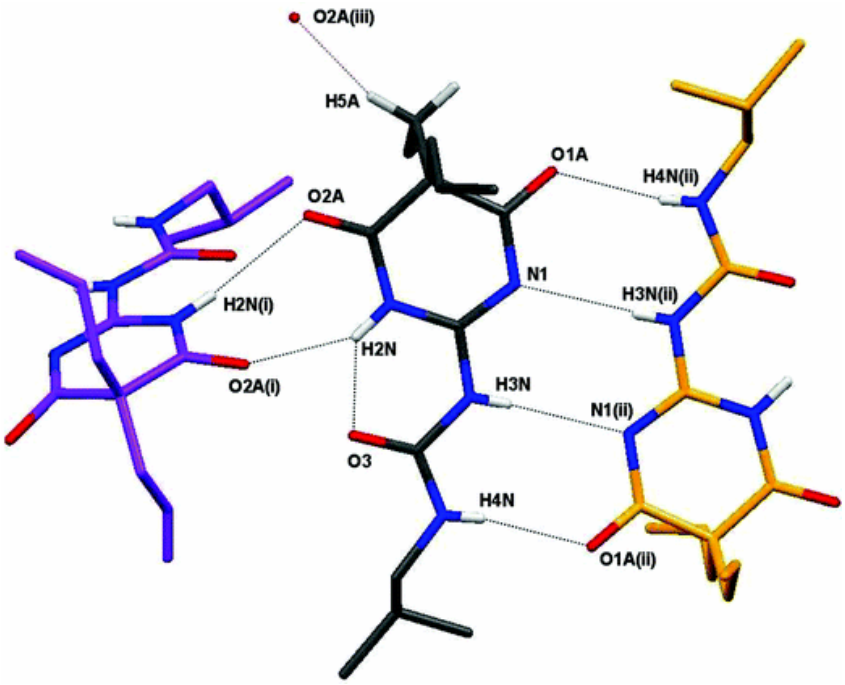

Figure 17: Hydrogen bonds present in the crystal structure of the α form of **8a** (shown by dashed lines).

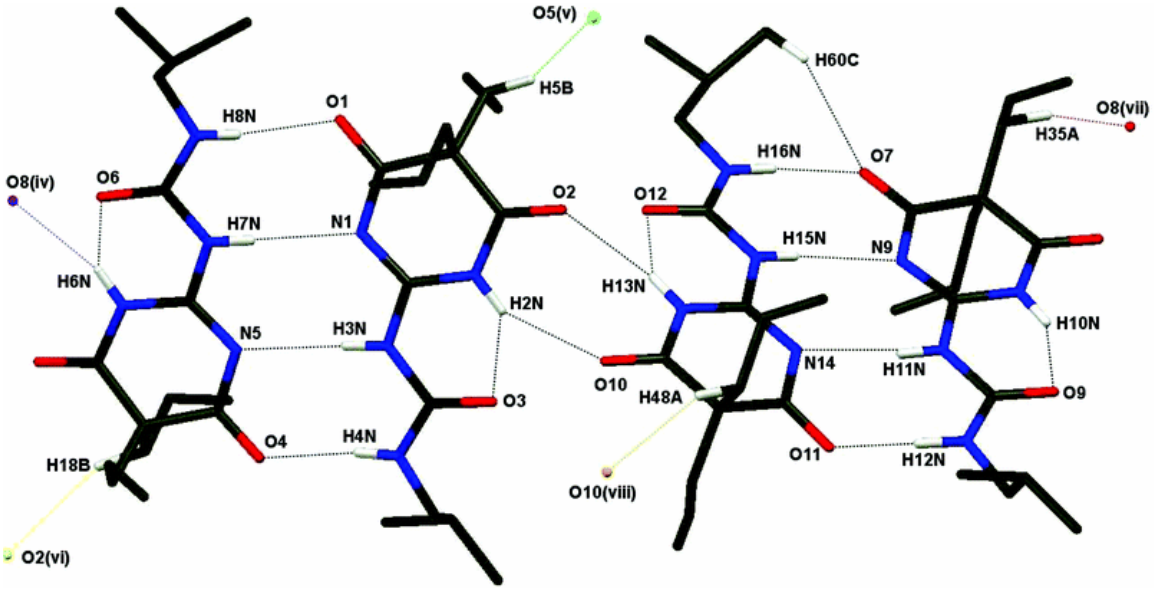

Figure 18: The asymmetric unit of the β form of **8a**. For clarity only one component of the disordered groups are displayed. Hydrogen bonds are shown by dashed lines.

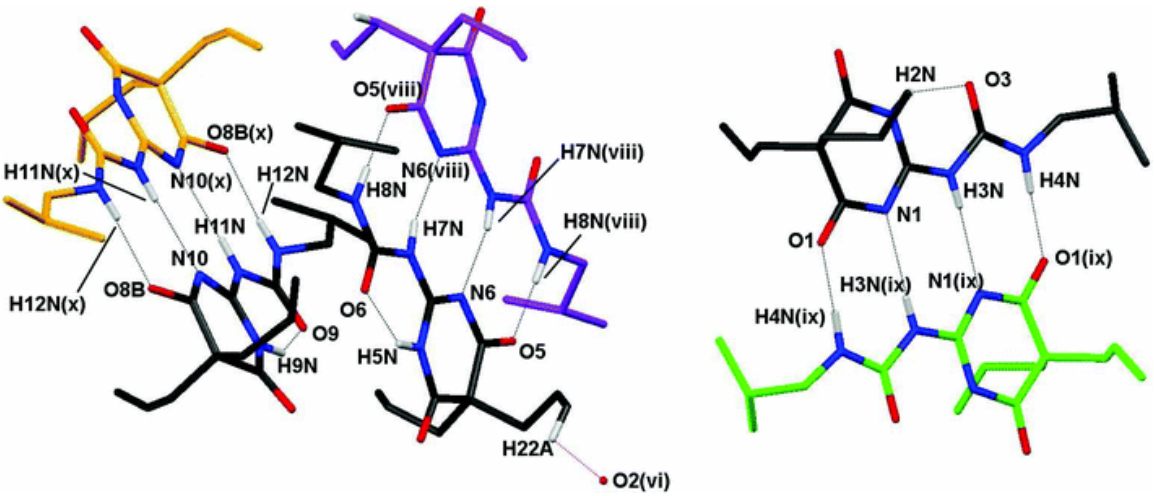

Figure 19: Hydrogen bonds present in the γ form of **8a** (shown as dashed lines). The **8a** molecules with green, purple and orange carbon backbones are symmetry equivalent molecules.

1.4 Attempted Modulation of H-bonding strength

The value for the dimerization constant of our system **8a** is relatively low when compared to the dimerization constant (K_{dim}) of Meijer's AADD type ureidopyrimidinones containing a heterocyclic aromatic unit which is in keto-enol tautomeric equilibrium (see, reference 34a). The relatively low K_{dim} of our self-assembling system is presumably due to the absence of π-electron density in the heterocyclic ring that could have positively contributed to the duplex stability as in ureidopyrimidinones.[67]

Investigations of the effect of the substituents at the 6-position (R_1) (figure 20) of Meijer's self-assembling system revealed that electron-withdrawing groups such as p-nitrophenyl- or trifluoro- and R_2 = n-$C_{18}H_{37}$, n -C_4H_9 favored the pyrimidin- 4-ol form in chloroform as well as in toluene, and the monomeric tautomer (**A**) in DMSO-d_6. However, when R_1 was the aryl electron donating moiety C_6H_2- $(OC_{13}H_{27})_3$ (and R_2 = n-C_4H_9), the 4[1H]-pyrimidinone form (**B**) predominated (87:13 B/C) in $CDCl_3$. The presence of alkyl groups at R_1 (e.g., Me and R_2 = n-C_4H_9) led to an even stronger preference for tautomer in keto form (>99%) in $CDCl_3$.

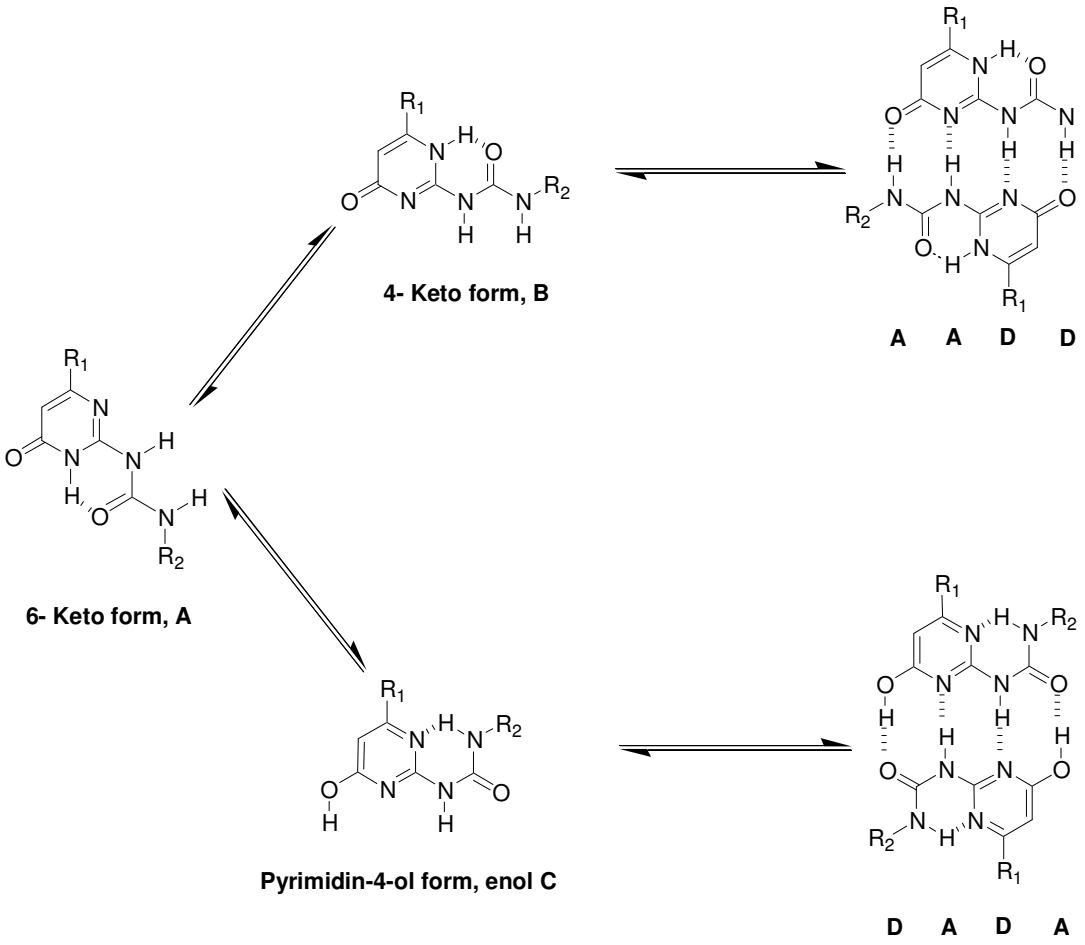

***Figure 20*:** Tautomerism in Meijer's ureidopyrimidinone system.

In order to increase the stability and hence the dimerization constant of our system, the acidity of the NHs involved should be increased. It has long been known that the NHs of the thiourea moiety are more acidic than the corresponding urea moiety. This phenomenon is explained by assuming that the higher acidity of the thiourea hydrogens dominates the weaker hydrogen bond accepting ability of sulfur as compared to oxygen.[68] We anticipated that substitution of the oxygen atom in the urea moiety in our self-assembling system by sulphur should increase the stability of the resulting molecular duplex.

1.4.1 Synthesis

The urea oxygen can be substituted by sulphur by various reagents such as P_2S_5, Lawesson reagent, etc. Reaction of **8a** with P_2S_5/ Lawesson reagent led to intractable mixture of products in different solvents and reaction conditions (scheme 4). An alternate route by reacting **9a** with phenyl and isobutyl isothiocyanate did not give any tangible result (scheme 3).

Scheme 3:

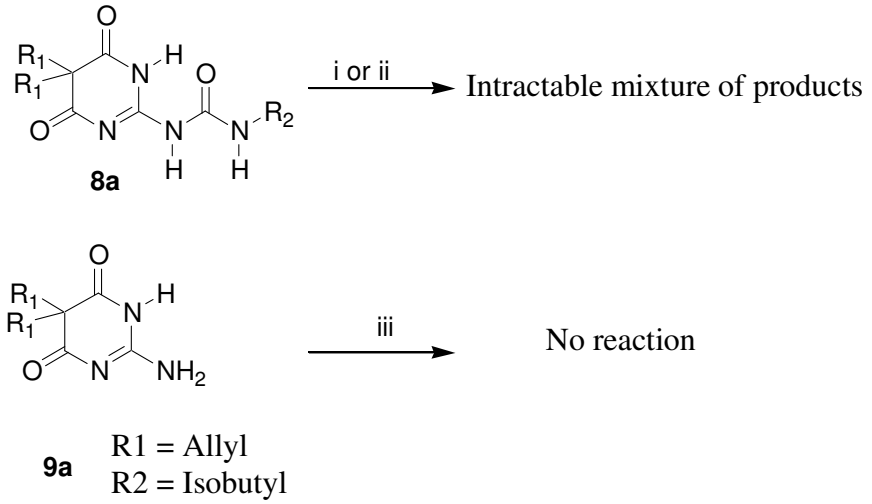

Reagents and conditions: (i) P_2S_5 (ii) Lawesson reagent (iii) Phenyl or isobutyl isothiocyanate, t-BuOK, DMF, Heat.

In the context of peptidomimetic chemistry, it has long been recognized that the tetrazole moiety can serve as a surrogate for terminal carboxylic acid residues,[69] as well as for cis amide bonds.[70] Since tetrazole ring is highly electron withdrawing, the acidity of the tetrazole NH is almost comparable with that of carboxylic acid. Hence it was expected that the tetrazole moiety could be introduced in our self assembling unit and the resulting molecule would have high dimerization constant, due to the increased acidity of the tetrazole NH. We attempted several schemes but none of them afforded a tangible result.

Scheme 4:

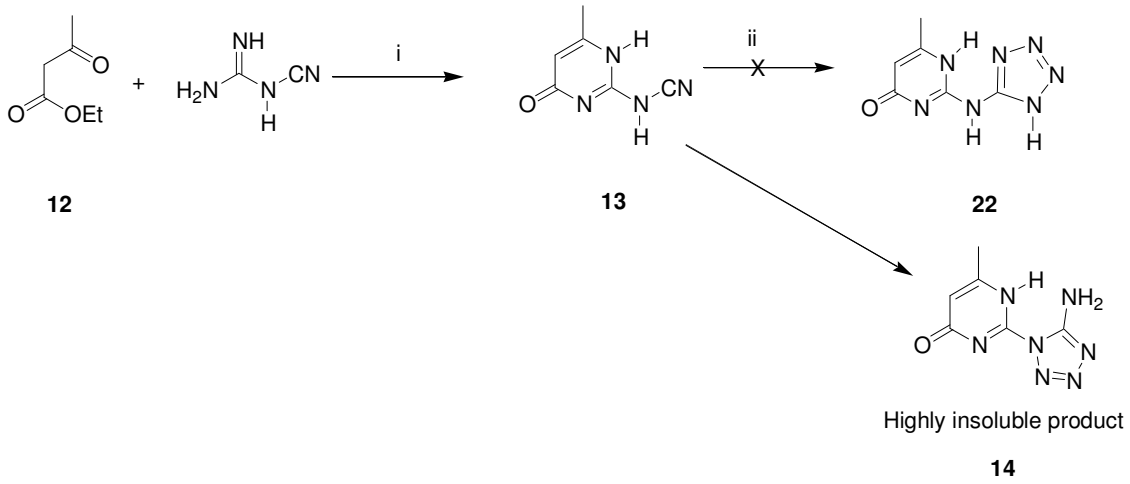

Reagents and conditions: (i) NaOEt, reflux; (ii) NaN_3, $ZnBr_2$, isopropanol, 80 ^{0}C.

Ethyl acetoacetate was condensed with dicyandiamide to afford **13** which was further reacted with sodium azide (scheme 4) in presence on zinc bromide[71] to furnish a highly insoluble product (even in DMSO-d_6). The high insolubility property suggests that the product is a regioisomer **14**; which could be expected to undergo extensive aggregation since the labile protons are solvent exposed. From the solubility property and mass spectrum, we propose that the product is **14**, rather than **22.**

In another strategy, N-benzyl 5-bromotetrazole **18** obtained from benzylamine in three steps,[72] was allowed to react with **9a** under basic condition (t-BuOK, NaOEt) but no product has been obtained (scheme 5). Since the corresponding fluoro analogue of **18** could be expected to be more reactive than the bromo compound, we tried to exchange the bromine by fluorine in DMSO and DMF but no halogen exchange was observed.

Scheme 5:

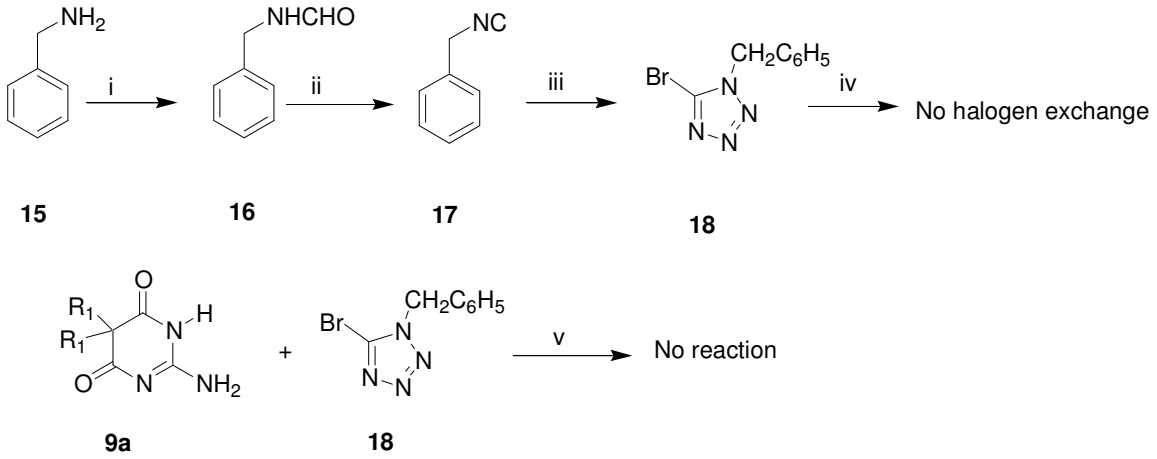

Reagents and conditions: (i) $HCOOC_2H_5$; (ii) $(Cl_3CO)_3CO$, Et_3N; (iii) NBS, NaN_3, $CHCl_3$, H_2O; (iv) KF, DMSO or DMF, heat; (v) **9a**, DMF/DMSO, heat.

It has been reported in the literature that 5-guanidinotetrazole[73] **21** can be prepared by condensation of cyanamide **19** with 5-aminotetrazole **20** in neutral medium. We anticipated that **21** when condensed with dialkyl malonates or with beta-keto esters would give various self-assembling modules having AADD array of hydrogen bonding code (scheme 6).

Scheme 6:

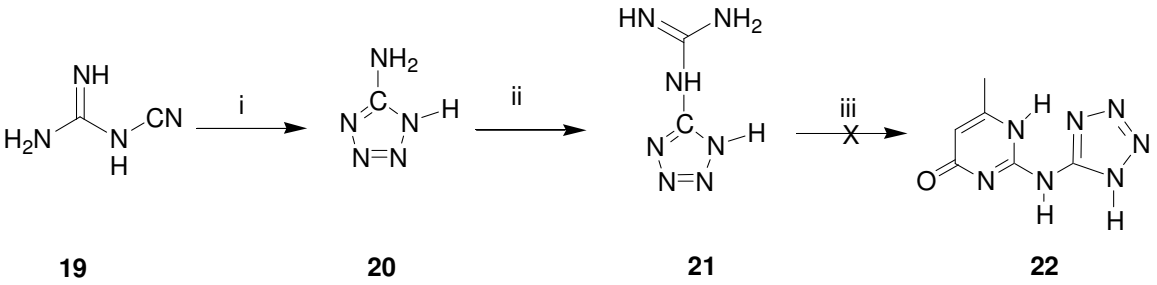

Reagents and conditions: (i) NaN_3, Conc. HCl, H_2O, reflux; (ii) NH_2CN, H_2O, heat; (iii) NaOEt, Ethylacetoacetate, heat.

According to this strategy 5-guanidinotetrazole **21** was allowed to react with ethyl acetoacetate, under various conditions. However the formation of **22** could not be achieved.

Since the intermediate **21** used in this reaction may not tolerate drastic condition, as above we attempted a milder reaction condition. Accordingly, α,α-dibenzyl malonic diacid chloride[75] was allowed to react with **21** in presence of DIEA (scheme 7).

Scheme 7:

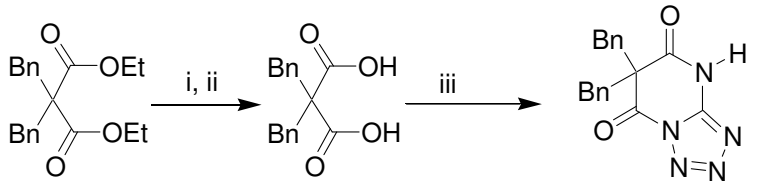

Reagents and conditions: (i) NaOH, heat (ii) Dil. HCl (iii) (a) Oxalyl chloride; (b) **21**, DIEA.

However characterization data (NMR, X-ray, mass) showed that the product formed was, surprisingly **23** and not **22**. It should be noted that **23** was also formed when 5-amino tetrazole **20** was reacted with α,α-dibenzyl malonic diacid chloride, under similar conditions (scheme 7).

1.4.2 Results and discussion

Structural investigations (*vide infra*) confirmed that the product was actually **23** and not **22**. This observation suggests that **21** is actually not guanidine-substituted tetrazole, as claimed in the literature; but simply an addition complex of cyanamide and 5-amino tetrazole **20**.

ESI mass spectrometry is an effective tool in investigating the formation of hydrogen-bonded molecular self assemblies. In addition to the molecular ion peak (MH^+) ascribable

due to the monomer **23**, the ESI spectrum showed a peak corresponding to the dimer **23.23** (M_2H^+).

Investigation of the NMR spectrum of the molecule in $CDCl_3$ showed a strongly deshielded peak at 10.62 for the NH participating in the dimer formation. The significant downfield shift is due to the hydrogen bonding between the oxygen of the carbonyl and the tetrazole NH, coupled with the strong electron withdrawing effect of the tetrazole ring. The strength of the dimer could not be measured by NMR dilution method due to the broadness of the NH signal which merges with the baseline at lower concentration.

1.4.3 Self-assembly in soild state

The X-ray structure of the molecule shows that it forms dimer in the solid state (figure 21). The eight-membered ring hydrogen-bonded network, formed by the self-assembly of the duplexe, is characterized by the graph set $R_2^2(8)$.[57] The DH···A distance is found to be 1.88 Å and the DH···A angle is 174.78. The dimer is nearly plannar, which is essential for the formation of strong hydrogen bonding interaction.

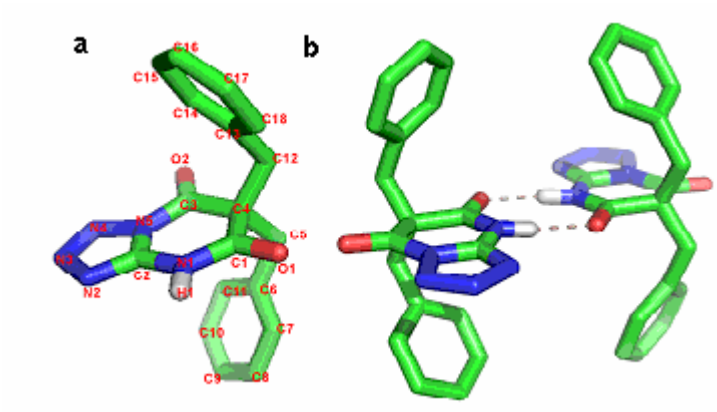

Figure 21: (a) Single crystal X-ray structure of **23** with labeled atoms. (b) Single crystal X-ray structures of dimer **23**.**23**. Hydrogens except the ones participating in hydrogen bonding interactions are ommited for clarity.

The dimers further self assemble through C-H···N interaction between N4 nitrogen of the tetrazozole ring of one dimer unit with one of the hydrogens of benzyl CH_2- group [d(H···N) = 2.73 Å] of another dimer unit to form a zig-zag structure (figure 22).

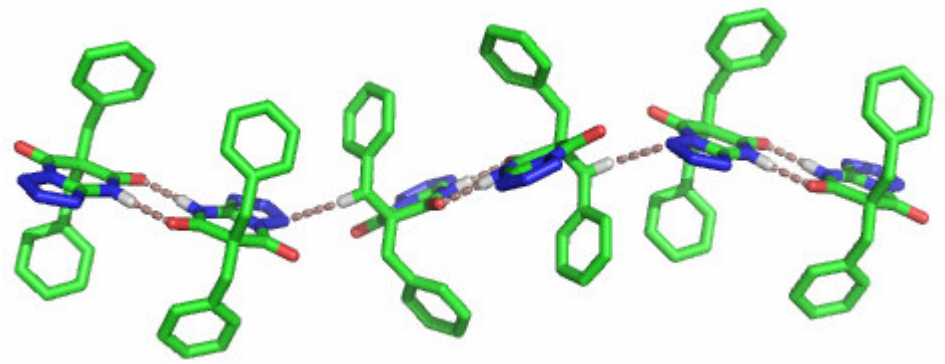

Figure 22: Single crystal X-ray structure of **23** showing self-assembly, through intermolecular C-H···N interaction, forming zig-zag structure.

Further, the ensemble forms layered structure in three-dimension which are held together by C-H···N and C-H···π interactions (figure 23).

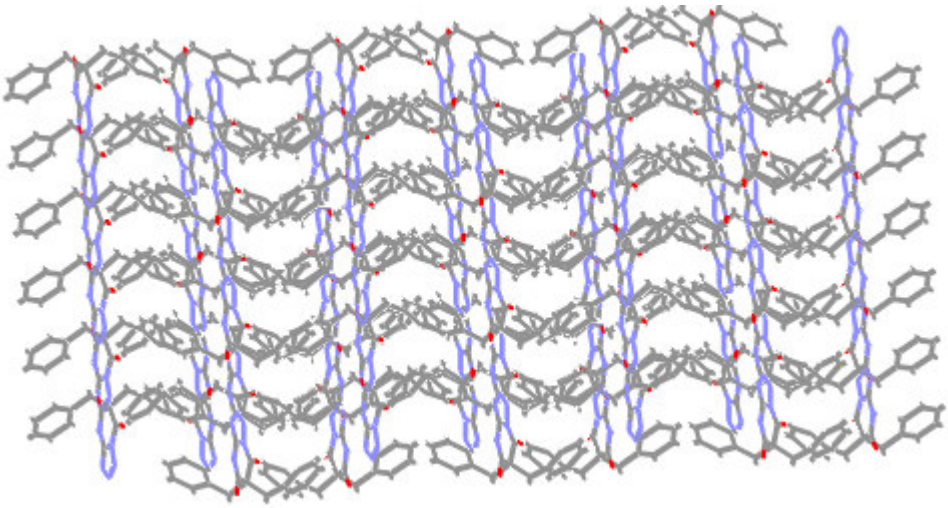

Figure 23: Three dimensional layered structure formed by **23** through C-H···N and C-H···π interactions.

1.5 Conclusion

In conclusion we have been successful with our rational approach for addressing the prototropy related problems in heterocycle-based self-assembling systems by the use of degenerate prototropy. As a proof of principle, we demonstrated herein the utility of degenerate prototropy in designing heterocycle-based AADD type self-assembling constructs free of multiple protamers. Our unique design strategy has allowed for an added dimension in the self-assembled H-bonded molecular duplexes reported herein, drawing a stark distinction between itself and previously known systems having similar hydrogen bonding codes.[37-38] Their ready synthetic accessibility coupled with the novel property of degenerate prototropy and the great ease of crystal formation would make these novel self-assembling molecules promising candidates for many proposed applications. Kaifer et al.[74] has already shown that these self assembling molecules can be used for making electronic devices.

Further three distinct forms of **8a** have been characterized crystallographically, and their individual structures analysed. It is interesting to note that the quadruple AADD hydrogen array persists in all the three polymorphic forms of **8a** and in both temperature dependent phases (α and β forms). This observation further highlights the stability of the AADD dimer unit. Additionally, this study suggests that polymorphism in quadruple hydrogen bonded self assembled should not be a barrier to their use in the development of new supramolecular architectures because, due to its exceptional stability, these systems are always expected to from strong dimer.

1.6 Experimental Section

Single Crystal X-ray Crystallographic Studies

The X-ray data of **8a-c**, and **8e** were collected on a SMART APEX CCD diffractometer with omega and phi scan mode, $\lambda_{MoK\alpha}$ = 0.71073 Å at T = 133(2) K. All the data were corrected for Lorentzian, polarization and absorption effects using SAINT and SADABS programs. The crystal structure of **8a-c,e** were solved by direct method using SHELXS-97 and the refinement was performed by full matrix least squares of F^2 using SHELXL-97 (G. M. Sheldrick, SHELX-97 program for crystal structure solution and refinement, University of Göttingen, Germany, **1997**). Hydrogen atoms were included in the refinement as per the riding model.

Crystal data for **8a** ($C_{15}H_{22}N_4O_3$): M = 306.37, crystal dimensions 0.75 x 0.65 x 0.25 mm^3, Triclinic, space group P-1, a = 13.5798(18), b = 14.1602(19), c = 17.503(2) Å, α = 91.381(2)°, β = 94.924(2)°, γ = 98.849(2)°, V = 3311.0(8) $Å^3$, Z = 8; ρ_{calcd} = 1.229 gcm^{-3}, μ (Mo-K_α) = 0.087 mm^{-1}, *F(000)* = 1312, $2\theta_{max}$ = 50.00°, 31720 reflections collected, 11607 unique, 9602 observed ($I > 2\sigma(I)$) reflections, 827 refined parameters, R value 0.0440, $wR2$ = 0.1146 (all data R = 0.0537, $wR2$ = 0.1216), S = 1.051, minimum and maximum transmission 0.9373 and 0.9785 respectively, maximum and minimum residual electron densities +0.427 and –0.306 e $Å^{-3}$.

Crystal data for **8b** ($C_{31}H_{42}N_4O_3$): M = 518.69, crystal dimensions 0.94 x 0.09 x 0.03 mm^3, Triclinic, space group P-1, a = 6.467(4), b = 13.910(8), c = 16.488(10) Å, α = 90.717(11)°, β = 91.918(11)°, γ = 95.011(11)°, V = 1476.6(15) $Å^3$, Z = 2; ρ_{calcd} = 1.167 gcm^{-3}, μ (Mo-K_α) = 0.076 mm^{-1}, *F(000)* = 560, $2\theta_{max}$ = 50.00°, 10631 reflections collected, 5176 unique, 2703 observed ($I > 2\sigma(I)$) reflections, 344 refined parameters, R value 0.0553, $wR2$ = 0.0992 (all data R = 0.1255, $wR2$ = 0.1202), S = 0.939, minimum and maximum transmission 0.9323 and 0.9977 respectively, maximum and minimum residual electron densities +0.152 and –0.154 e $Å^{-3}$.

Crystal data for **8c** ($C_{23}H_{26}N_4O_3$): M = 406.48, Crystal dimensions 0.70 x 0.68 x 0.13 mm^3, monoclinic, space group $P2_1/n$, a = 23.675(3), b = 18.479(3), c = 30.427(4) Å, β = 100.690(3)°; V = 13081(3) $Å^3$; Z = 24; ρ_{calcd} = 1.238 gcm^{-3}, μ (Mo-K_α) = 0.084 mm^{-1},

F(000) = 5184, $2\theta_{max}$ = 50.00°, 64574 reflections collected, 22995 unique, 14350 observed ($I > 2\sigma(I)$) reflections, 1685 refined parameters, *R* value 0.0647, *wR*2 = 0.1495 (all data *R* = 0.1109, *wR*2 = 0.1693), S = 1.014, minimum and maximum transmission 0.9437 and 0.9892 respectively, maximum and minimum residual electron densities +0.725 and –0.420 e $Å^{-3}$.

Crystal data for **8e** ($C_{21}H_{24}N_4O_5$): *M* = 412.44, crystal dimensions 0.67 x 0.41 x 0.29 mm^3, Triclinic, space group *P*-1, *a* = 12.065(9), *b* = 13.786(10), *c* = 14.428(10) Å, α = 98.58(3)°, β = 108.43(2)°, γ = 100.28(2)°, *V* = 2185(3) $Å^3$, *Z* = 4; ρ_{calcd} = 1.254 gcm^{-3}, μ (Mo-K_α) = 0.091 mm^{-1}, *F(000)* = 872, $2\theta_{max}$ = 50.00°, 10384 reflections collected, 6921 unique, 4800 observed ($I > 2\sigma(I)$) reflections, 569 refined parameters, *R* value 0.0762, *wR*2 = 0.2161 (all data *R* = 0.1031, *wR*2 = 0.2461), S = 1.044, minimum and maximum transmission 0.9416 and 0.9741 respectively, maximum and minimum residual electron densities +0.553 and –0.298 e $Å^{-3}$.

Crystal data for **23**: $C_{18}H_{15}N_5O_2$, M= 333.35, crystal size, 0.41 x 0.10 x 0.04 mm^3, T = 297(2) K, crystal system, orthorhombic, space group *Pbca*; *a* = 8.6247(13), *b* = 16.777(3), *c* = 22.950(4) Å, v = *3320.8(9)* $Å^3$, *Z* = 8, *F*(000) = 1392, *d* calc [$g\ cm^{-3}$] = 1.334, μ [mm^{-1}] = 0.091, absorption correction, multi-scan, T_{min} = 0.9633; T_{max} = 0.9965; 15340 reflection collected, 2932 unique reflections, 1813 observed reflections, 286 refined parameters, R_1 [$I>2\sigma(I)$] = 0.0515, WR_2 = 0.1041 (all data *R* = 0.1005, *wR*2 = 0.1217), goodness of fit, 1.008, $\Delta\rho_{max}$, $\Delta\rho_{min}$ (e $Å^{-3}$)= 0.187, -0.235.

Experimental Procedures

5,5-Diallyl-2-amino-1H-pyrimidine-4,6-dione 9a: Sodium metal (4.66 g, 202.6 mmol, 3.04 equiv.) was dissolved carefully in absolute ethanol (56 mL). To the above solution was added α,α-diallyl-malonic acid diethyl ester (16 g, 66.6 mmol, 1 equiv.) followed by the addition of guanidine hydrochloride (10.83 g, 113.3 mmol, 1.7 equiv.). The reaction mixture was refluxed for 4 hours, cooled and filtered through celite. The filtrate was acidified with aq. acetic acid and the precipitated amino pyrimidine was filtered, washed

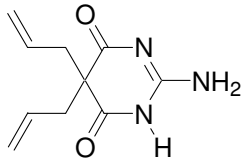

9a

with water and dried. The product was purified by crystallization from aq. DMSO (10.5 g, 76%). mp > 260^0C; IR (Nujol) ν (cm^{-1}): 3238, 3193, 2947, 2923, 2854, 1730, 1695, 1649, 1485, 1390; ^{1}H NMR (Na salt) (300 MHz, D_2O): δ 5.49-5.35 (m, 2H), 4.91 (t, 4H, *J* = 8.7 Hz), 2.43 (d, 4H, *J* = 6.4 Hz); ^{13}C NMR (Na salt) (75 MHz, D_2O): δ 200.8, 182.9, 145.8, 131.3, 68.1, 55.3; ESI Mass: 208.05 (M+1); Anal. Calcd. for $C_{10}H_{13}N_3O_2$: C, 57.96; H, 6.32; N, 20.28. Found: C, 57.67; H, 6.53; N, 20.11.

2-Amino-5,5-dibenzyl-1H-pyrimidine-4,6-dione 9b: Following the similar procedure for the synthesis of **9a** and using α,α-dibenzyl-malonic acid diethyl ester (15.02 g, 44.1 mmol), **9b** was synthesized which was purified by crystallization from aq. DMSO (8.7g, 64%). mp > 260^0C; IR (Nujol) ν (cm^{-1}): 3240, 3197, 2923, 2854, 1689, 1454, 1384; ^{1}H NMR (500 MHz, DMSO-d_6): δ 10.44 (s, 1H), 7.21-7.02 (m, 12H), 3.18 (s, 4H); ^{13}C NMR (125 MHz, DMSO-d_6): δ 177.1, 157.2, 136.4, 129.5, 128.2, 126.9, 59.0, 44.5; ESI Mass: 308.04 (M+1); Anal. Calcd. for $C_{18}H_{17}N_3O_2$: C, 70.34; H, 5.58; N, 13.67. Found: C, 69.97; H, 5.74; N, 13.69.

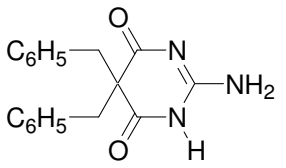

9b

1-(5,5-Diallyl-4,6-dioxo-1,4,5,6-tetrahydro-pyrimidin-2-yl)-3-isobutyl-urea 8a: To a stirred solution of dry dichloromethane (10 mL) at 0^0C, containing triphosgene (2.71 g, 9.1 mmol, 0.63 equiv.) was added a mixture of isobutyl amine (2.61 mL, 26.1 mmol, 1.8 equiv.) and N-ethyldiisopropyl amine (9.81 mL, 57.3 mmol, 3.96 equiv.) dissolved in dry DCM (5 mL) drop wise. After stirring for 10 min. at 0^0C, dry pyridine (40 mL) was added to the above reaction mixture, followed by the addition of 5,5-diallyl-2-amino-1H-pyrimidine-4,6-dione (3.0 g, 14.5 mmol, 1 equiv.). The reaction mixture was heated on an oil bath held at 90-100^0C for 2 hours. After cooling, the reaction mixture was filtered off, and the solvents were removed under vacuum. The residue was dissolved in ethyl acetate and was washed with water and brine. The organic layer was dried with anhydrous sodium sulfate, and concentrated under reduced pressure. The crude product was purified by column chromatography (5% ethyl acetate/pet. ether) on silica gel to give 3.52g (79%) of **8a** as colorless crystalline solid which could be further easily crystallized from petroleum ether (60-80^0 C) to give large crystals. mp 121^0C; IR ($CHCl_3$) ν (cm^{-1}): 3232, 3076, 3026, 2964, 1706, 1614,

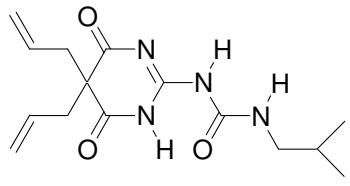

8a

1571, 1529, 1245; ^{1}H NMR (500 MHz, $CDCl_3$): δ 12.74 (s, 1H), 11.38 (s, 1H), 9.24 (s, 1H), 5.66-5.58 (m, 2H), 5.11 (t, 4H, *J* = 13.6 Hz), 3.11 (t, 2H, *J* = 6.2 Hz), 2.70 (d, 4H, *J* = 7.4 Hz), 1.8 (sept, 1H, *J* = 6.7 Hz), 0.95 (d, 6H, *J* = 6.6 Hz); ^{13}C NMR (125 MHz, $CDCl_3$): δ 182.7, 171.8, 158.3, 155.5, 131.0, 120.4, 58.5, 47.8, 42.8, 28.3, 20.1; ESI Mass: 307.05 (M+1), 614.03 (2M+1); Anal. Calcd. for $C_{15}H_{22}N_4O_3$: C, 58.81; H, 7.24; N, 18.29. Found: C, 58.53; H, 7.45; N, 18.18.

1-(5,5-Dibenzyl-4,6-dioxo-1,4,5,6-tetrahydro-pyrimidin-2-yl)-3-dodecyl-urea 8b:

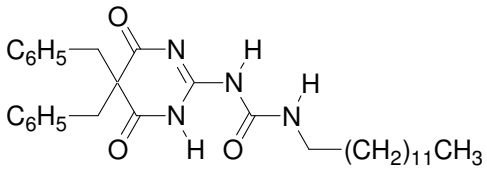

8b

Following the similar procedure for the synthesis of **8a** and using 2-amino-5,5-dibenzyl 1H-pyrimidine-4,6-dione (1.1 g, 3.6 mmol), **8b** was synthesized (1.19 g, 62%), which was easily crystallized from pet. ether into large crystals. mp 72-73^{0}C; IR ($CHCl_3$) ν (cm^{-1}): 3230, 3020, 2927, 2854, 1703, 1612, 1569, 1529, 1245, 1215; ^{1}H NMR (500 MHz, $CDCl_3$): δ 12.28 (s, 1H), 10.52 (s, 1H), 8.94 (s, 1H), 7.23-7.08 (m, 10H), 3.36 (q, 4H, *J* = 13, 11.5 Hz), 3.23 (q, 2H, *J*= 6.9, 5.4 Hz), 1.61 (q, 2H, *J* = 6.9 Hz), 1.38-1.25 (b, 18H), 0.88 (t, 3H, *J* = 6.9 Hz); ^{13}C NMR (125 MHz, $CDCl_3$): δ 182.0, 171.8, 157.2, 155.2, 135.1, 129.6, 128.4, 127.4, 62.1, 45.1, 40.3, 31.9, 29.6, 29.4, 29.3, 29.2, 27.0, 22.6, 14.0; ESI Mass: 520.03 (M+1), 1038.02 (2M+1); Anal. Calcd. for $C_{31}H_{42}N_4O_3$: C, 71.78; H, 8.16; N, 10.80. Found: C, 71.88; H, 8.35; N, 10.83.

1-(5,5-Dibenzyl-4,6-dioxo-1,4,5,6-tetrahydro-pyrimidin-2-yl)-3-isobutyl-urea 8c:

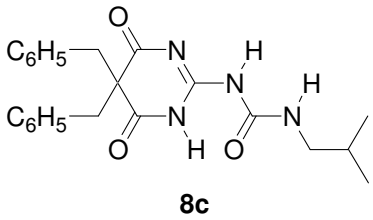

8c

Following the similar procedure for the synthesis of **8a** and using 2-amino-5,5-dibenzyl-1H-pyrimidine-4,6-dione (2.0 g, 6.5 mmol), **8c** was synthesized (1.9 g, 72%), which could be further easily crystallized from DCM-pet. ether to give large crystals. mp 157-158 ^{0}C; IR ($CHCl_3$) ν (cm^{-1}): 3230, 3062, 3031, 2962, 1706, 1612, 1571, 1529, 1244; ^{1}H NMR (500 MHz, $CDCl_3$): δ 12.32 (s, 1H), 10.50 (s, 1H), 9.02 (s, 1H), 7.23-7.08 (m, 10H), 3.36 (q, 4H, *J* = 13.0, 14.5 Hz), 3.07 (t, 2H, *J* = 6.1 Hz), 1.91 (sept., 1H, *J* = 6.5 Hz), 1.00 (d, 6H, *J* = 6.9 Hz); ^{13}C NMR (125 MHz, $CDCl_3$): δ 181.9, 171.7, 157.2, 155.4, 135.1, 129.6, 128.4, 127.3, 62.1, 47.7, 45.0, 28.4, 20.1; ESI Mass: 407.05 (M+1), 814.05 (2M+1); Anal. Calcd. for $C_{23}H_{26}N_4O_3$: C, 67.96; H, 6.45; N, 13.78. Found: C, 67.85; H, 6.57; N, 13.61.

1-(4,6-Dioxo-5,5-di-n-propyl-1,4,5,6-tetrahydro-pyrimidin-2-yl)-3-isobutyl-urea 8d:

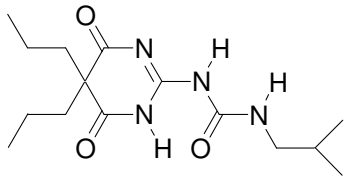

8d

1-(5,5-Diallyl-4,6-dioxo-1,4,5,6-tetrahydro-pyrimidin-2-yl)-3-isobutyl-urea **8a** (300 mg, 1.0 mmol) was subjected to hydrogenation with 10% Pd/C (60 mg) under balloon atmosphere for 12 hours. Purification by recrystallization from pet. ether afforded needle shaped crystals of **8d** (203 mg, 67%). mp 161^{0}C ; IR ($CHCl_3$) ν (cm^{-1}): 3232, 3062, 3026, 2964, 1706, 1614, 1571, 1529, 1463, 1245; ^{1}H NMR (500 MHz, $CDCl_3$): δ 12.71 (s, 1H), 11.51 (s, 1H), 9.17 (s, 1H), 3.11 (t, 2H, *J* = 6.2 Hz), 1.97-1.83 (m, 5H), 1.28-1.15 (m, 4H), 0.93 (d, 6H, *J* = 6.6 Hz), 0.86 (t, 6H, *J* =7.3 Hz); ^{13}C NMR (125 MHz, $CDCl_3$): δ 183.8, 173.1, 158.0, 155.8, 58.4, 47.6, 41.8, 28.2, 20.0, 18.6, 14.0; ESI Mass: 311.05 (M+1), 622.03 (2M+1); Anal. Calcd. for $C_{15}H_{26}N_4O_3$: C, 58.04; H, 8.44; N, 18.05. Found: C, 58.37; H, 8.16; N, 17.82.

2-[3-(5,5-Diallyl-4,6-dioxo-1,4,5,6-tetrahydro-pyrimidin-2-yl)-ureido]-benzoic acid isopropyl ester 8e: Following the similar procedure for the synthesis of **8a** and using 2-amino-5,5-diallyl-1H-pyrimidine-4,6-dione (0.5 g, 2.4 mmol), **8e** was synthesized (0.8 g, 80%), which could be further easily crystallized from DCM-pet. ether to give large crystals. mp 140-141^{0}C (DCM-pet. ether); IR ($CHCl_3$) ν (cm^{-1}): 3265, 3083, 3020, 2981, 1730, 1689, 1652, 1585, 1512, 1442, 1377, 1255; ^{1}H NMR (500 MHz, $CDCl_3$): δ 12.06 (s, 1H), 11.09 (s, 1H), 8.18 (b, 1H), 8.56 (d, 1H, *J* = 8.45 Hz), 8.03 (d, 1H, *J* = 7.65 Hz), 7.54 (t, 1H, *J* = 8.03 Hz), 7.08 (t, 1H, *J* = 7.65 Hz), 5.70-5.63 (m, 2H), 5.28-5.14 (m, 5H), 2.75 (d, 2H, *J* = 7.65 Hz), 1.39 (d, 6H, *J* = 6.12 Hz); ^{13}C NMR (75 MHz, $CDCl_3$): δ 171.6, 169.7, 167.1, 160.3, 149.7, 141.0, 133.9, 130.7, 130.4, 122.1, 120.9, 119.4, 115.7, 68.8, 57.8, 42.1, 21.7; ESI Mass: 413.3 (M+1), 825.6 (2M+1); Anal. Calcd. for $C_{21}H_{24}N_4O_5$: C, 61.16; H, 5.87; N, 13.58. Found: C, 61.22; H, 5.84; N, 13.55.

8e

1-Benzyl-5-bromo-1H-tetrazole: To a solution of N-bromosuccinimide (1.14 g, 6.4 mmol, 1 equiv.) in chloroform (20 mL) at 0^{0}C was added a solution of sodium azide (0.42 g, 6.4 mmol, 1equiv.) in water (5 mL). To this reaction mixture at 0^{0}C was added tetrabutylammonium bromide (0.05

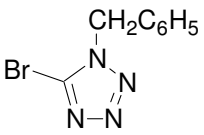

18

g) and stirred for 5 min. A solution of benzyl isocyanide (0.75 g, 6.4 mmol, 1 equiv.), **17** in chloroform (5 mL) was added at one portion. The reaction mixture was stirred at 0^0C for 45 min. and then allowed to become ambient. The organic layer was separated, washed with water (2 x 200ml) and dried over Na_2SO_4. The crude product was purified by column chromatography on silica gel to give (0.6 g, 39.2 %) of reddish brown solid.

6,6-Dibenzyl-4H-tetrazolo[1,5-a]pyrimidine-5,7-dione 23: Dibenzyl diethylmalonate and dibenzyl malonic acid was synthesized according to the literature procedure.[54, 75]

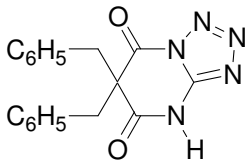

23

Dibenzyl malonic acid (2.85 g, 10 mmol, 1 equiv.) was dissolved in dry DCM (10 mL). Oxalyl chloride (3.5 mL, 40 mmol, 4 equiv.) was added at 0^0C and a drop of DMF in catalytic amount. The reaction mixture was stirred at RT for 2 hrs. The solvent was stripped off under reduced pressure. To the solution of **21** (1.27 g, 10 mmol, 1 equiv.) in dry DMF (5 mL) and DIEPA (5.2 mL, 30 mmol, 3 equiv.) at -20^0C was added the diacid chloride in dry DMF (5 mL). After addition the reaction mixture was allowed to warm to room temperature and stirred at RT for 4 hrs. The reaction mixture was poured in water and added acetic acid (10-15 drops). 1N HCl was added slowly until the reaction mixture was acidic and extracted with ethyl acetate. The combined DCM layer was washed with water and brine. The organic layer was dried over anhydrous sodium sulphate, and purified by column chromatography over silica gel (1.95 g, 81.5%) to afford white solid.

IR ($CHCl_3$) ν (cm^{-1}): 3373.3, 3020.3, 1772.5, 1701.1, 1498.6, 1490.9, 1456,2, 1363.6, 1299.93; ^{1}H NMR (300 MHz, $CDCl_3$): δ 10.71 (bs, 1H), 7.12 (m, 10 H), 3.60 (s, 4H); ^{13}C NMR (75 MHz, $CDCl_3$): δ 169.5, 163.1, 150.0, 133.2, 129.2, 128.9, 128.1, 63.5, 45.2; ESI Mass: 334.2 (M+1), 356.1 (M+Na), 667.3 (2M+1), 689.24 (2M+Na), 705.2 (2M+K); Anal. Calcd. for $C_{18}H_{15}N_5O_2$: C, 64.86; H, 4.54; N, 21.01. Found: C, 64.89; H, 4.63; N, 20.87.

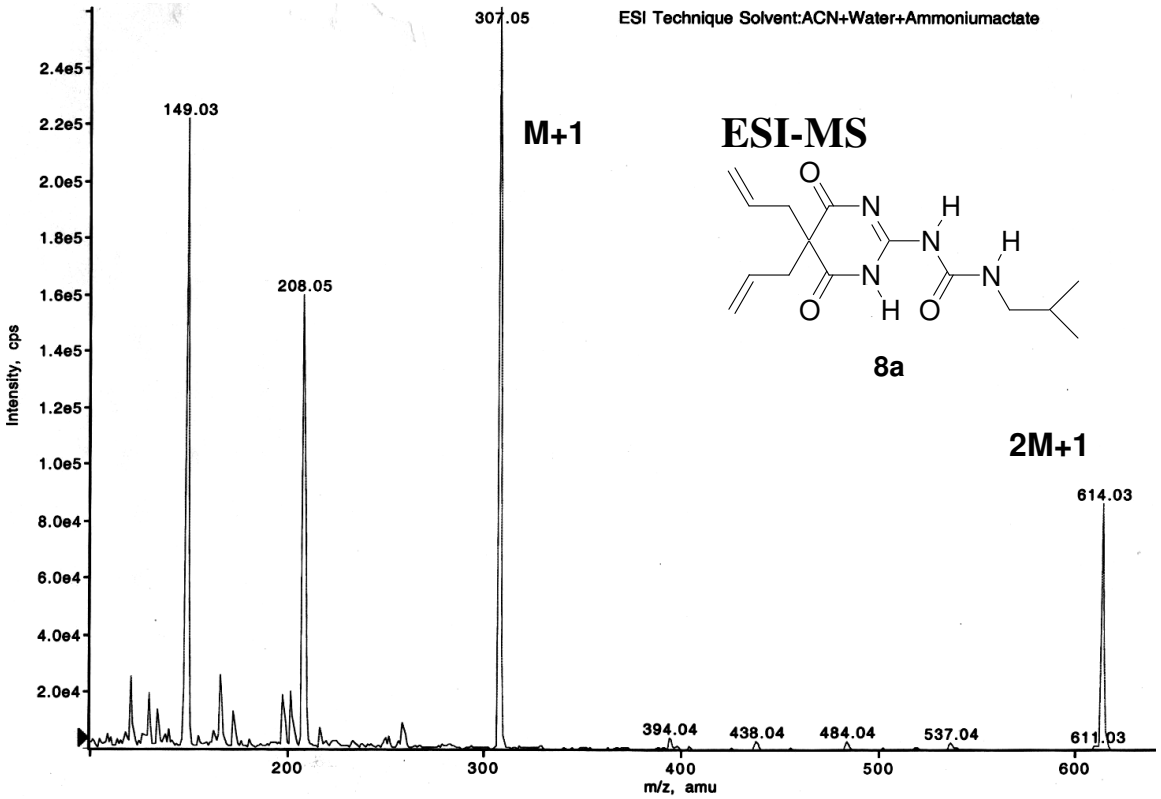
ESI Technique Solvent:ACN+Water+Ammoniumactate
307.05
149.03
208.05
M+1
ESI-MS
8a
2M+1
614.03
394.04
438.04
484.04
537.04
611.03
Intensity, cps
m/z, amu

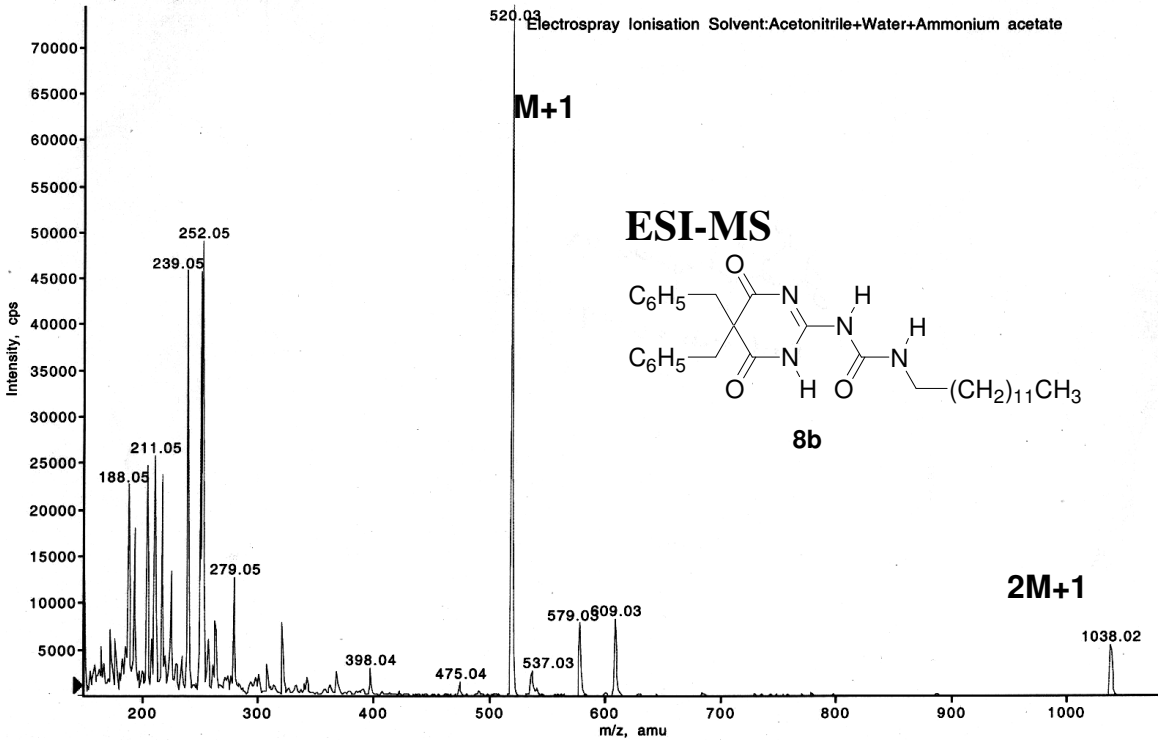
Electrospray Ionisation Solvent:Acetonitrile+Water+Ammonium acetate
520.03
M+1
ESI-MS
8b
2M+1
252.05
239.05
211.05
188.05
279.05
398.04
475.04
537.03
579.03
609.03
1038.02
Intensity, cps
m/z, amu

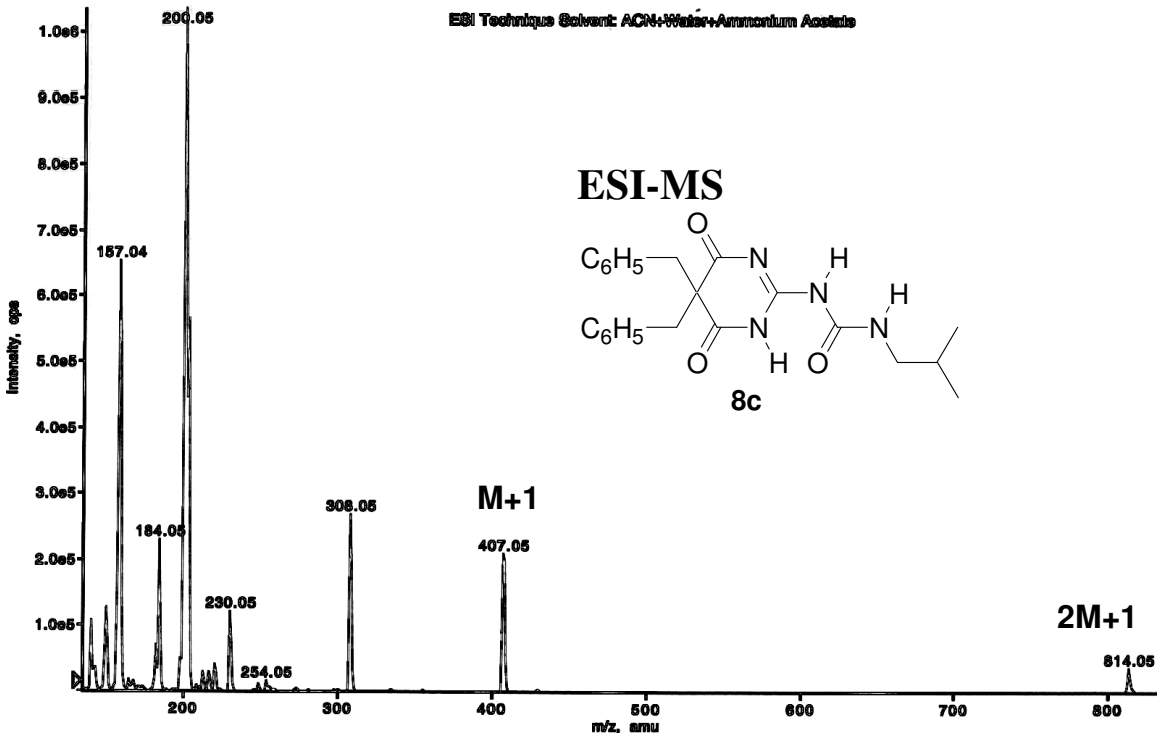
ESI Technique Solvent: ACN+Water+Ammonium Acetate
200.05
157.04
184.05
230.05
254.05
306.05
407.05
814.05
M+1
2M+1
Intensity, cps
m/z, amu
ESI-MS
8c

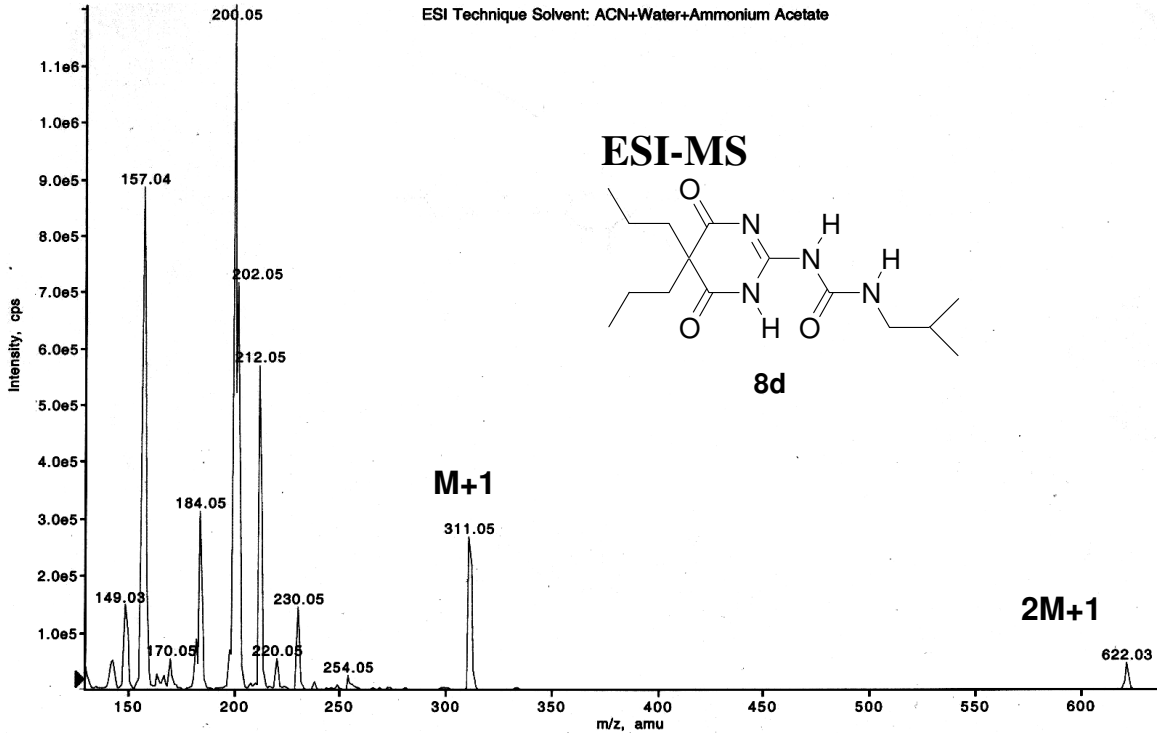
ESI Technique Solvent: ACN+Water+Ammonium Acetate
200.05
157.04
202.05
212.05
184.05
311.05
149.03
230.05
170.05
220.05
254.05
622.03
M+1
2M+1
Intensity, cps
m/z, amu
ESI-MS
8d

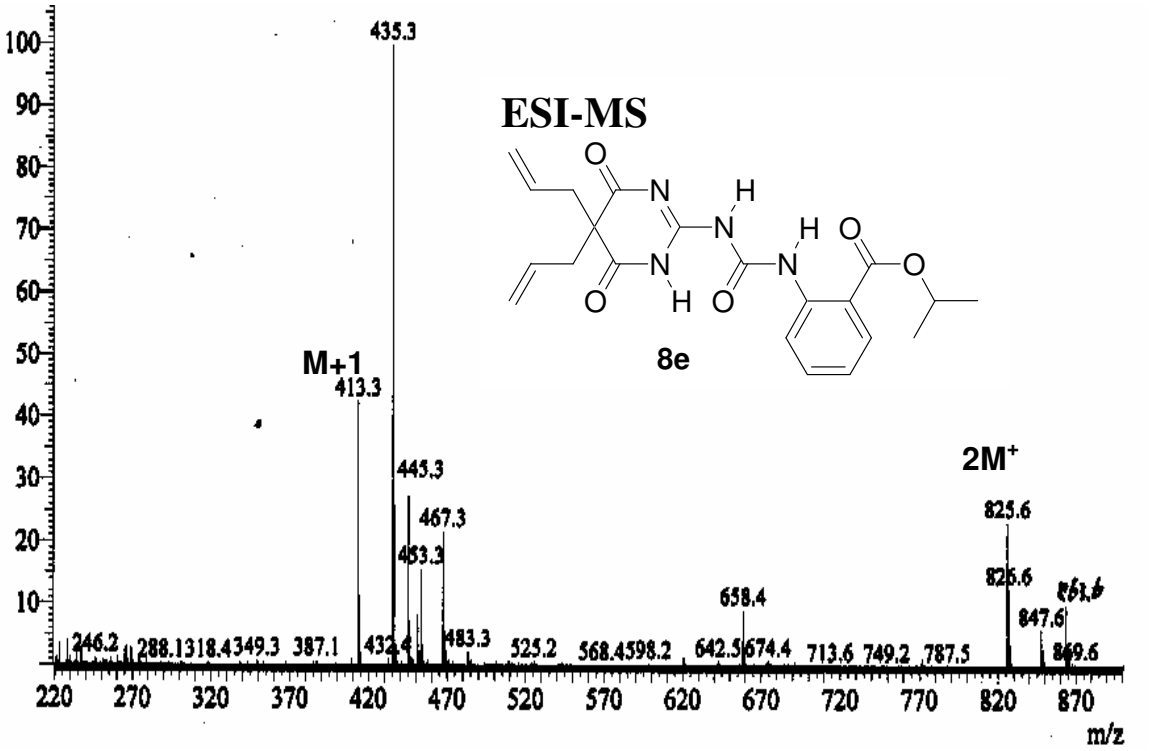
ESI-MS
8e
M+1
2M+
435.3
413.3
445.3
467.3
453.3
825.6
826.6
658.4
847.6
246.2
288.1
318.4
349.3
387.1
432.4
483.3
525.2
568.4
598.2
642.5
674.4
713.6
749.2
787.5
869.6
m/z

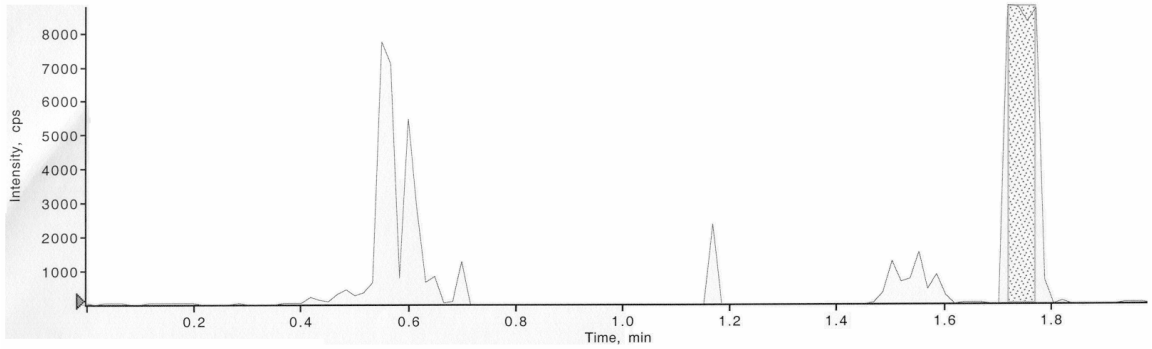
Intensity, cps
Time, min

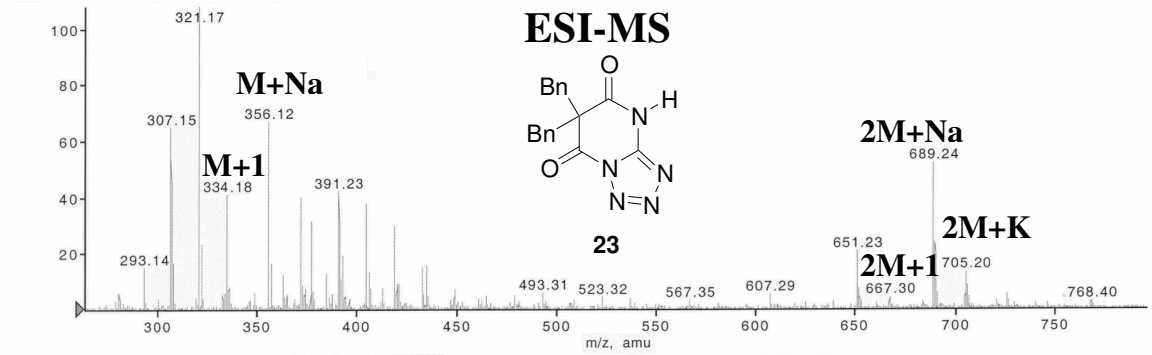
ESI-MS
M+Na
M+1
2M+Na
2M+K
2M+1
23
m/z, amu

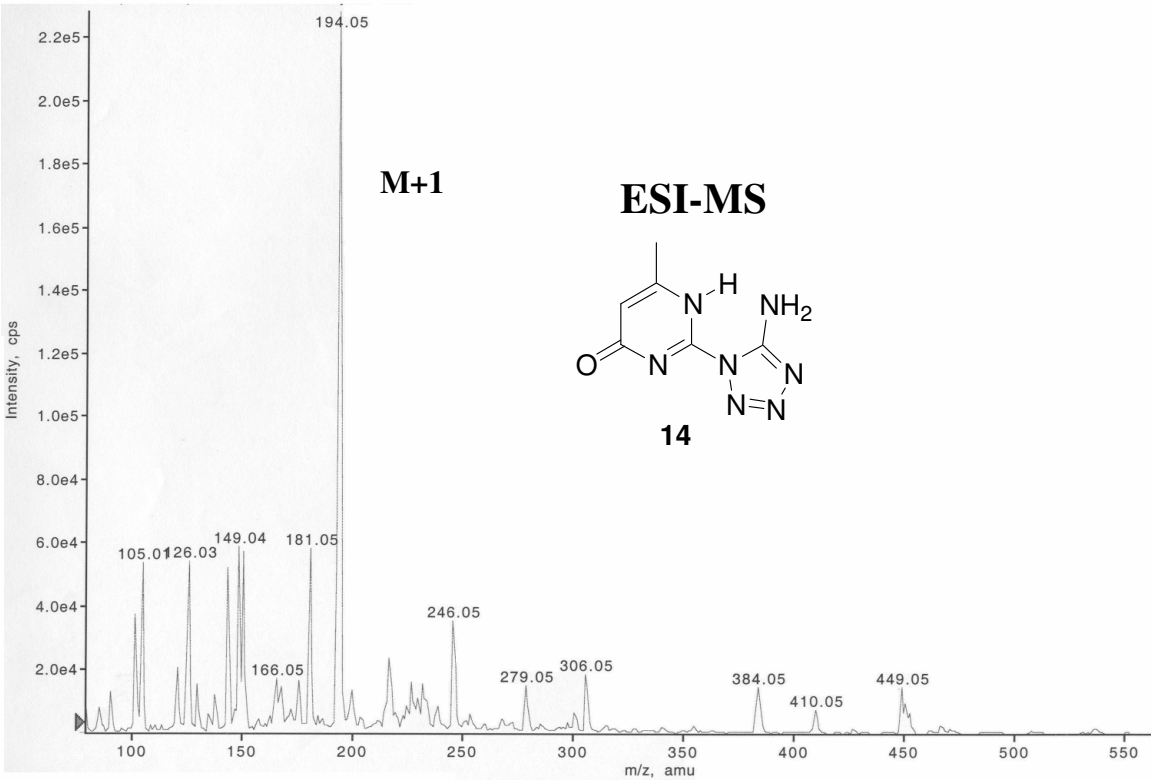
M+1
ESI-MS
14
Intensity, cps
m/z, amu

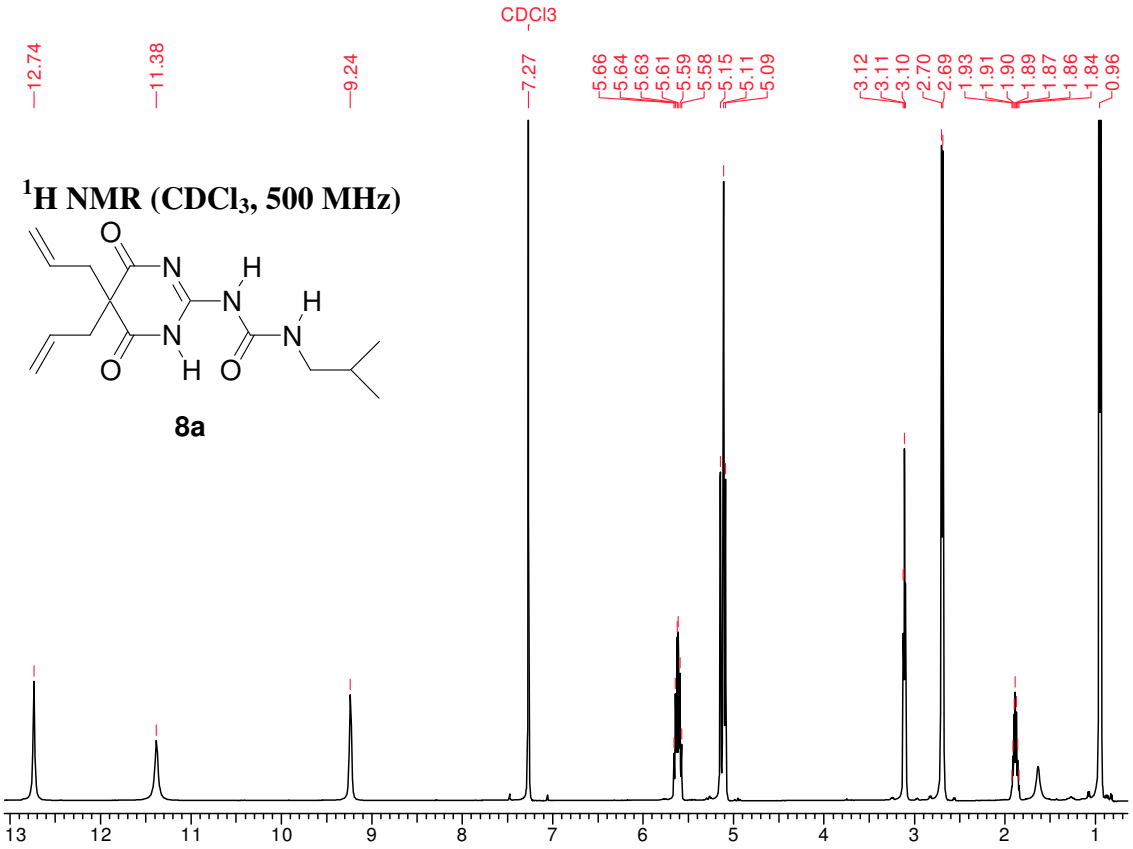

^{1}H NMR ($CDCl_3$, 500 MHz)

8a

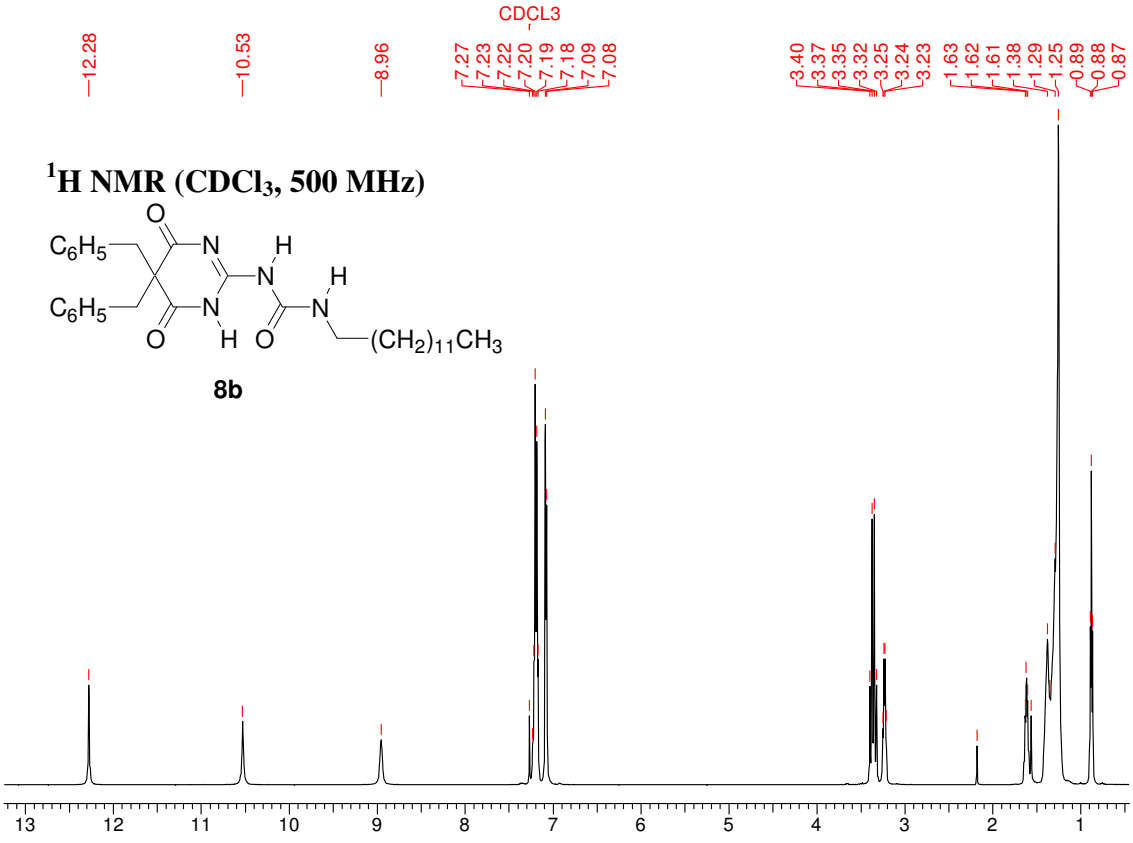

^{1}H NMR ($CDCl_3$, 500 MHz)

8b

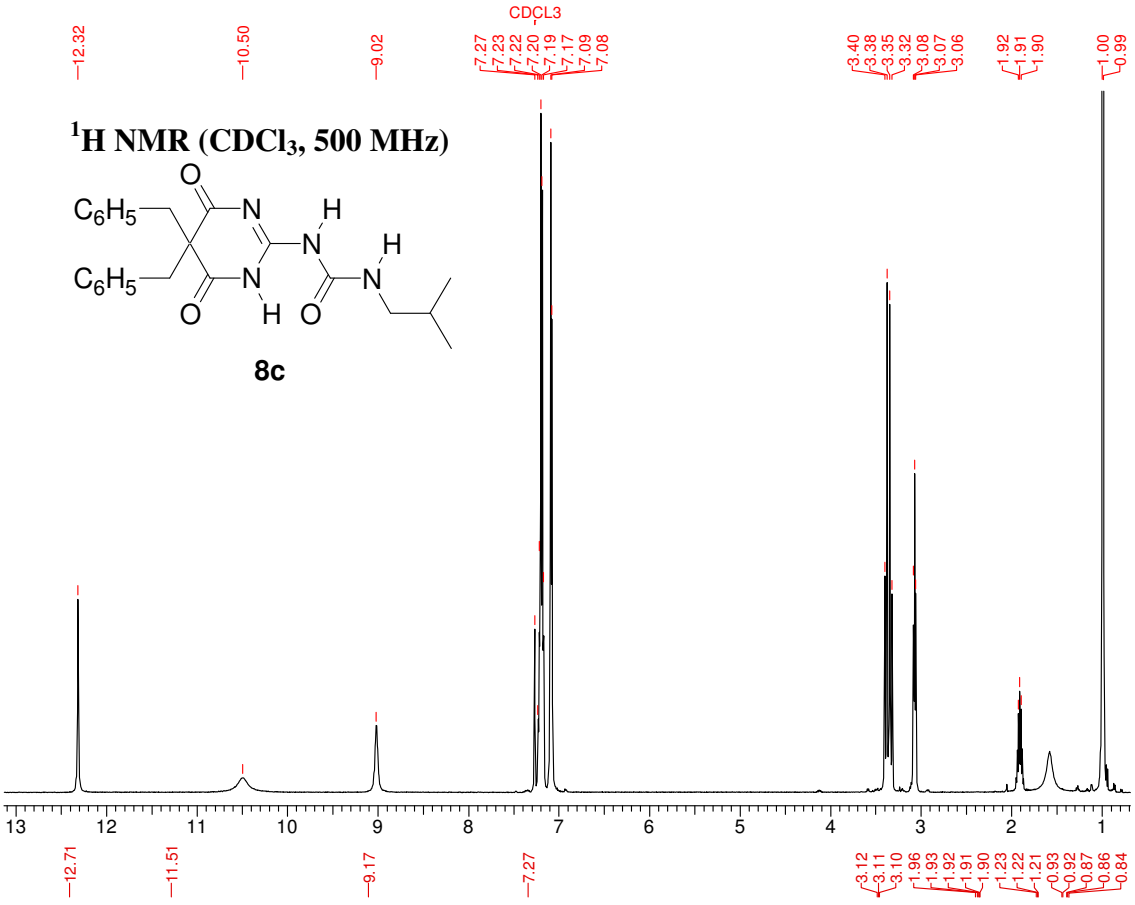

^{1}H NMR ($CDCl_3$, 500 MHz)

8c

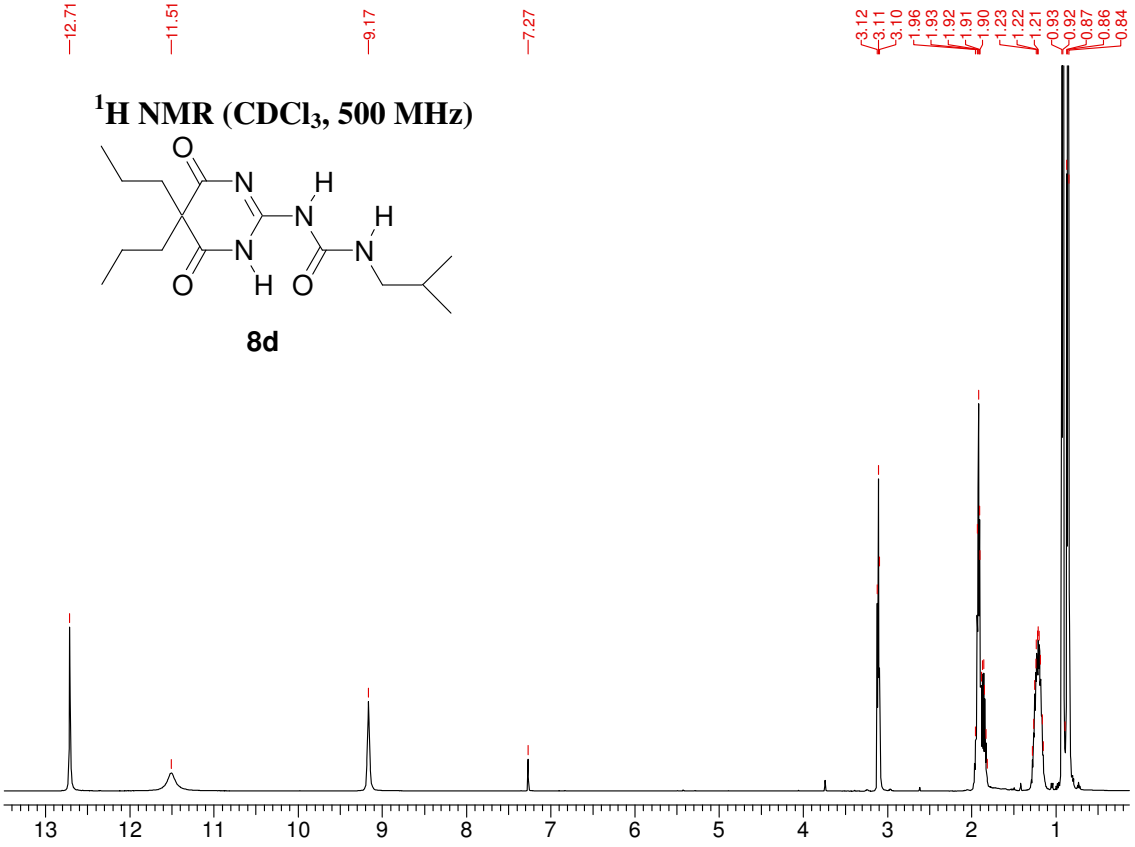

^{1}H NMR ($CDCl_3$, 500 MHz)

8d

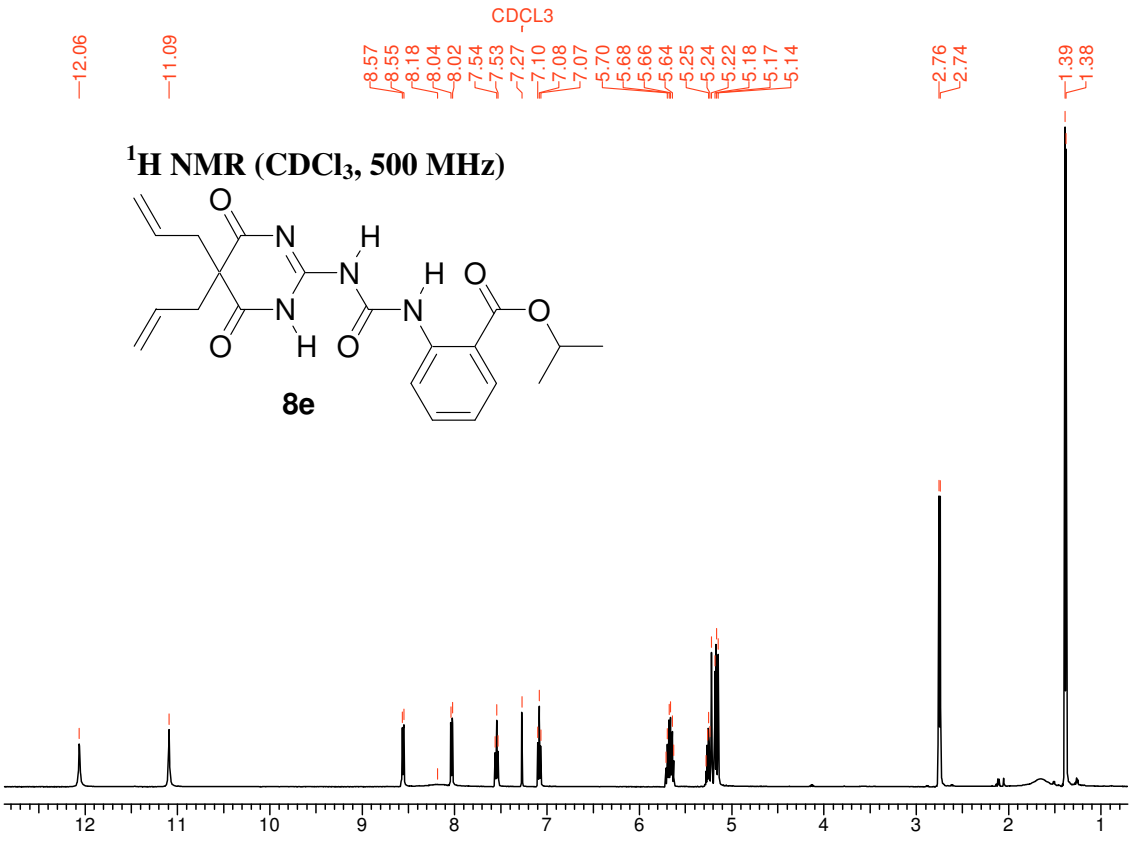

^{1}H NMR ($CDCl_3$, 500 MHz)

8e

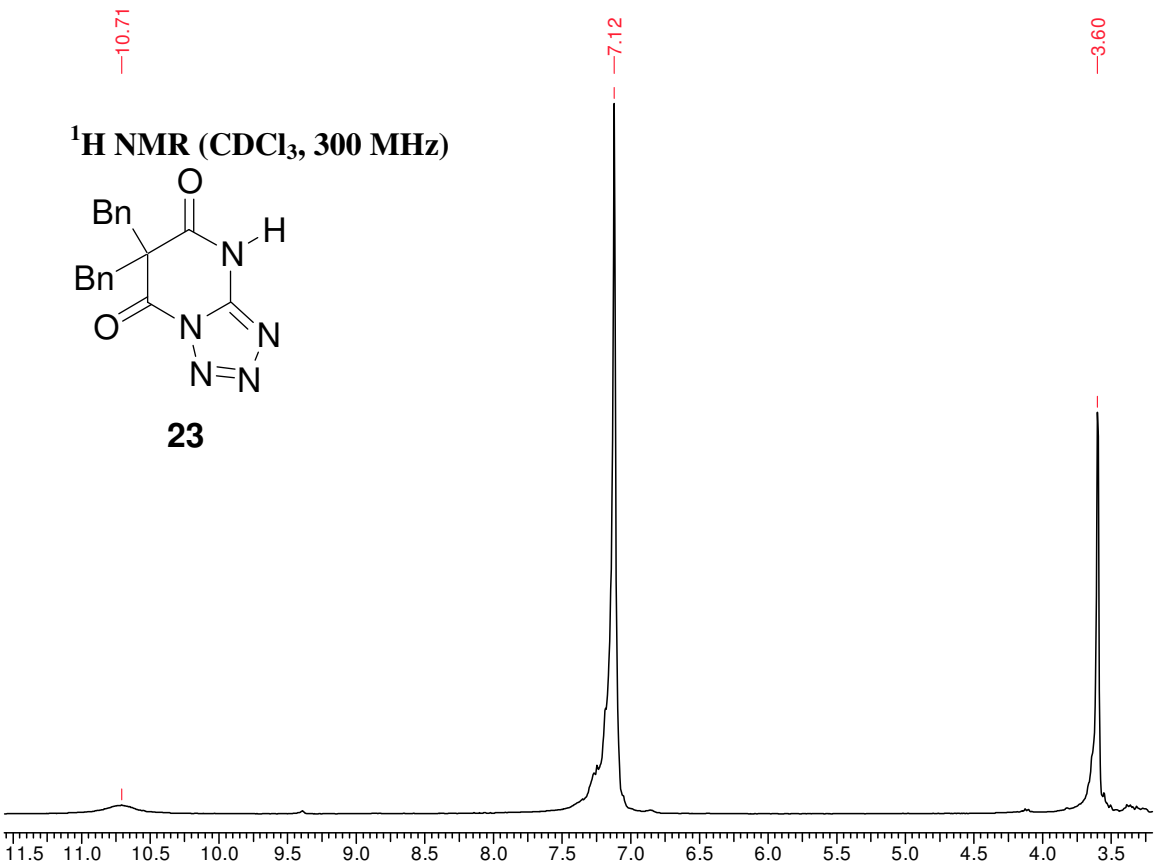

^{1}H NMR ($CDCl_3$, 300 MHz)

23

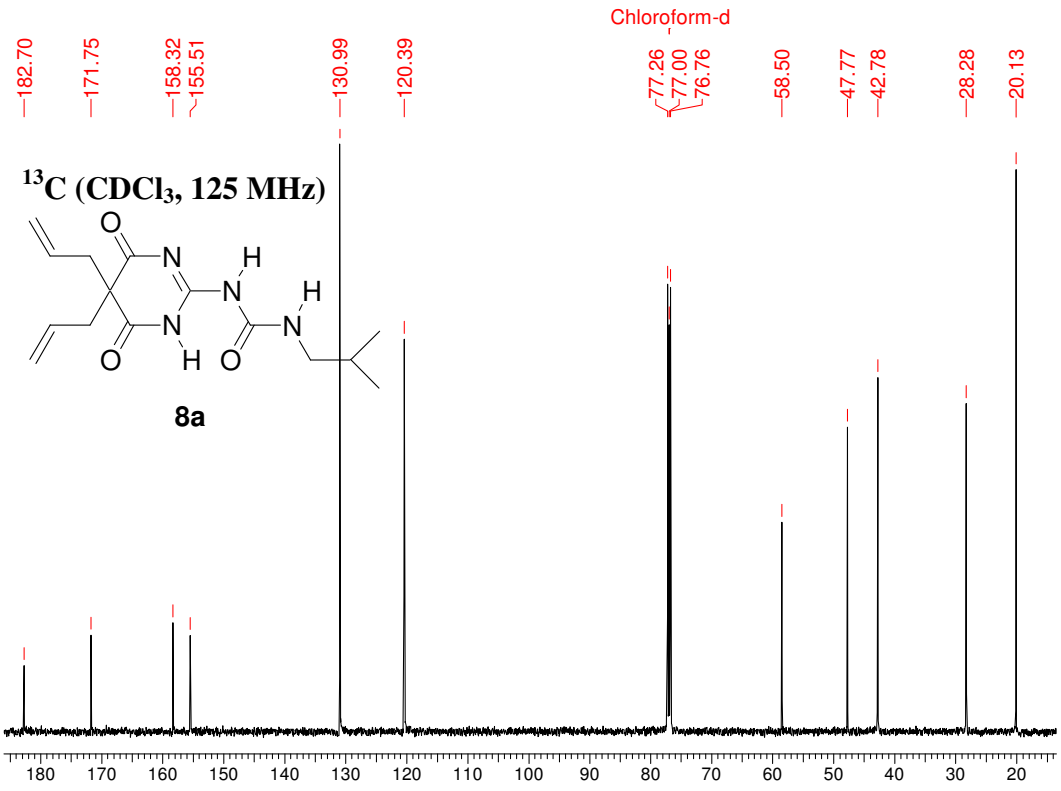
Chloroform-d
182.70
171.75
158.32
155.51
130.99
120.39
77.26
77.00
76.76
58.50
47.77
42.78
28.28
20.13
13C (CDCl3, 125 MHz)
8a

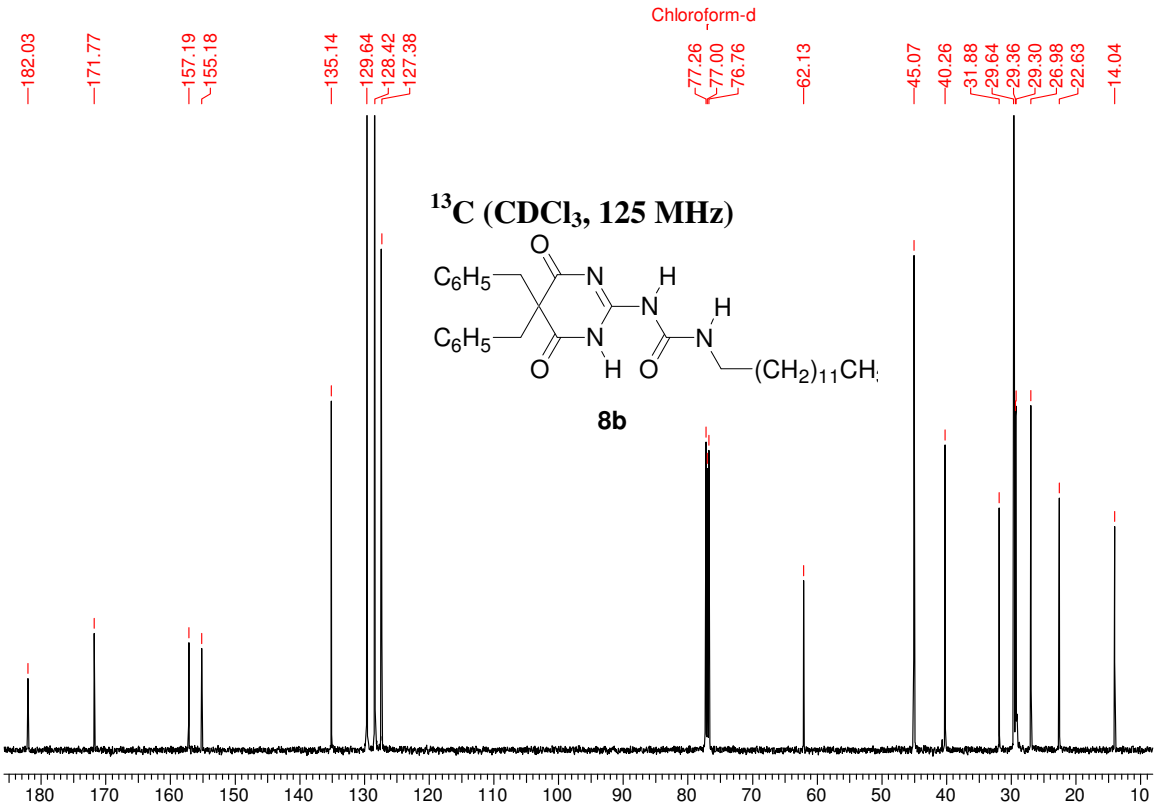
Chloroform-d
182.03
171.77
157.19
155.18
135.14
129.64
128.42
127.38
77.26
77.00
76.76
62.13
45.07
40.26
31.88
29.64
29.36
29.30
26.98
22.63
14.04
13C (CDCl3, 125 MHz)
8b

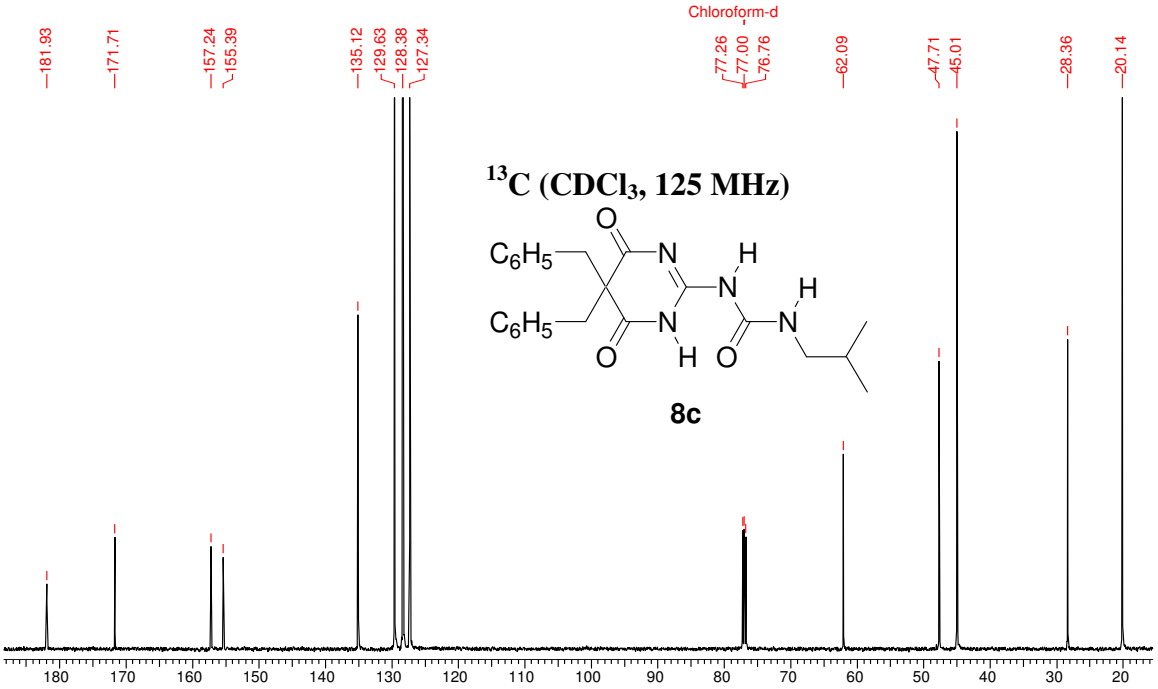

^{13}C ($CDCl_3$, 125 MHz)

8c

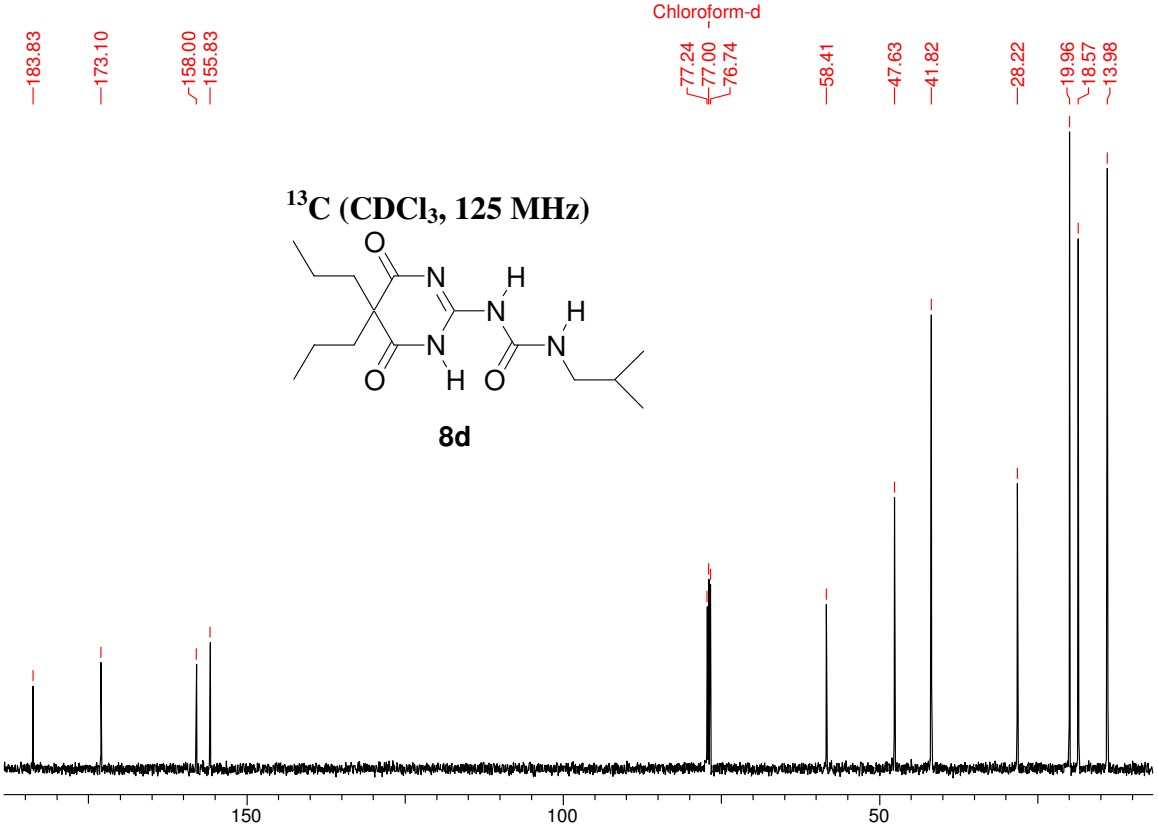

^{13}C ($CDCl_3$, 125 MHz)

8d

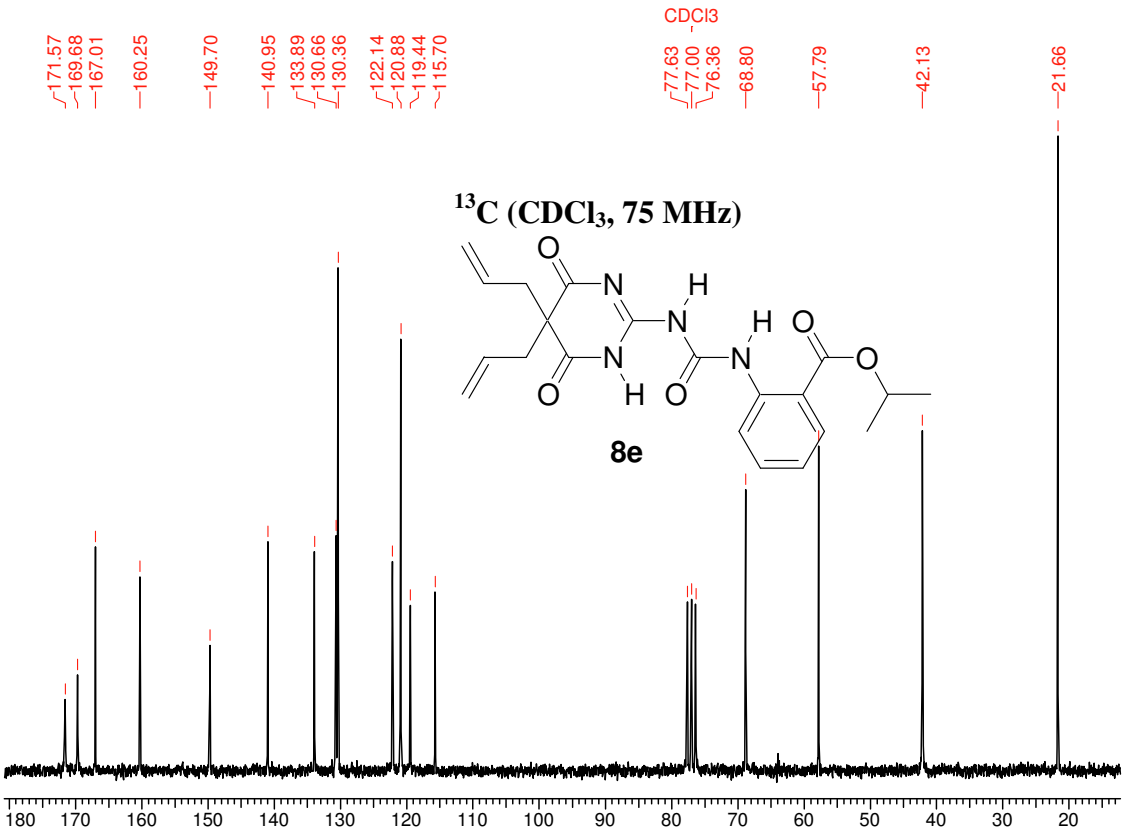
171.57
169.68
167.01
160.25
149.70
140.95
133.89
130.66
130.36
122.14
120.88
119.44
115.70
CDCl3
77.63
77.00
76.36
68.80
57.79
42.13
21.66
13C (CDCl3, 75 MHz)
8e
180 170 160 150 140 130 120 110 100 90 80 70 60 50 40 30 20

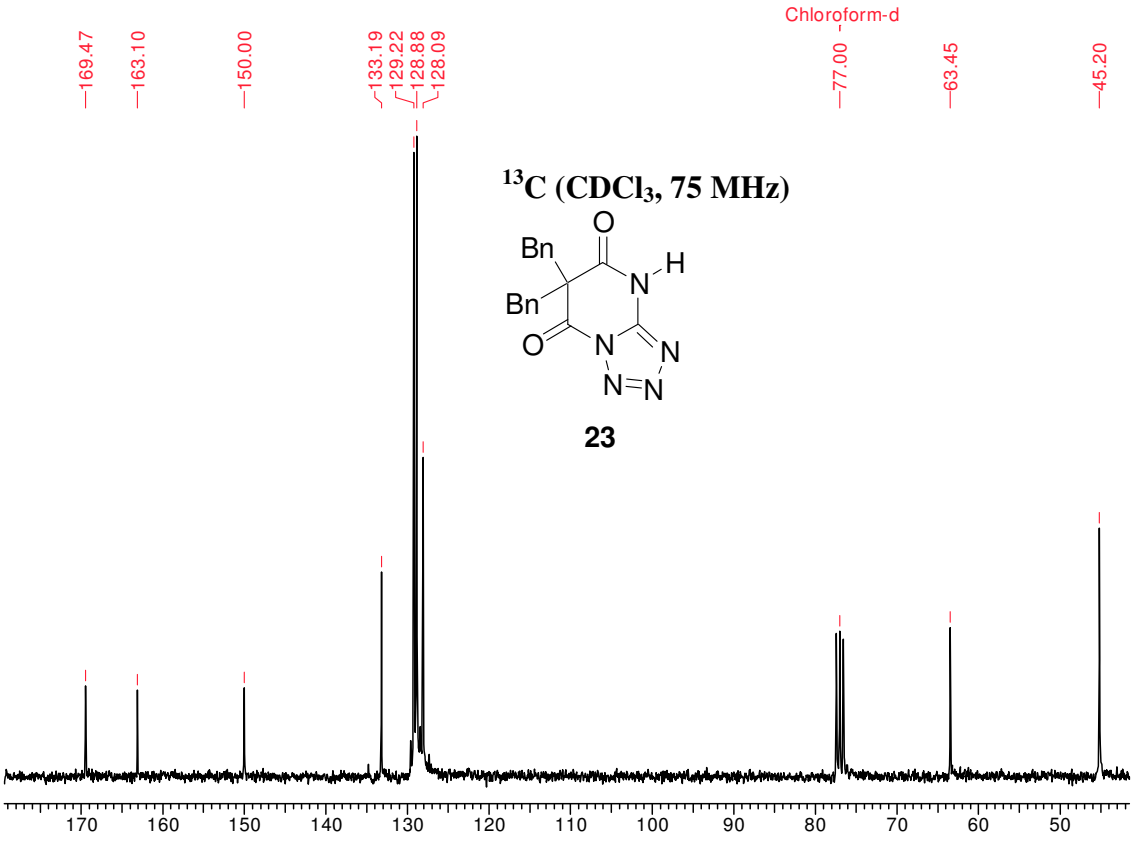
169.47
163.10
150.00
133.19
129.22
128.88
128.09
Chloroform-d
77.00
63.45
45.20
13C (CDCl3, 75 MHz)
Bn
Bn
23
170 160 150 140 130 120 110 100 90 80 70 60 50

2D COSY Spectrum of 8a:

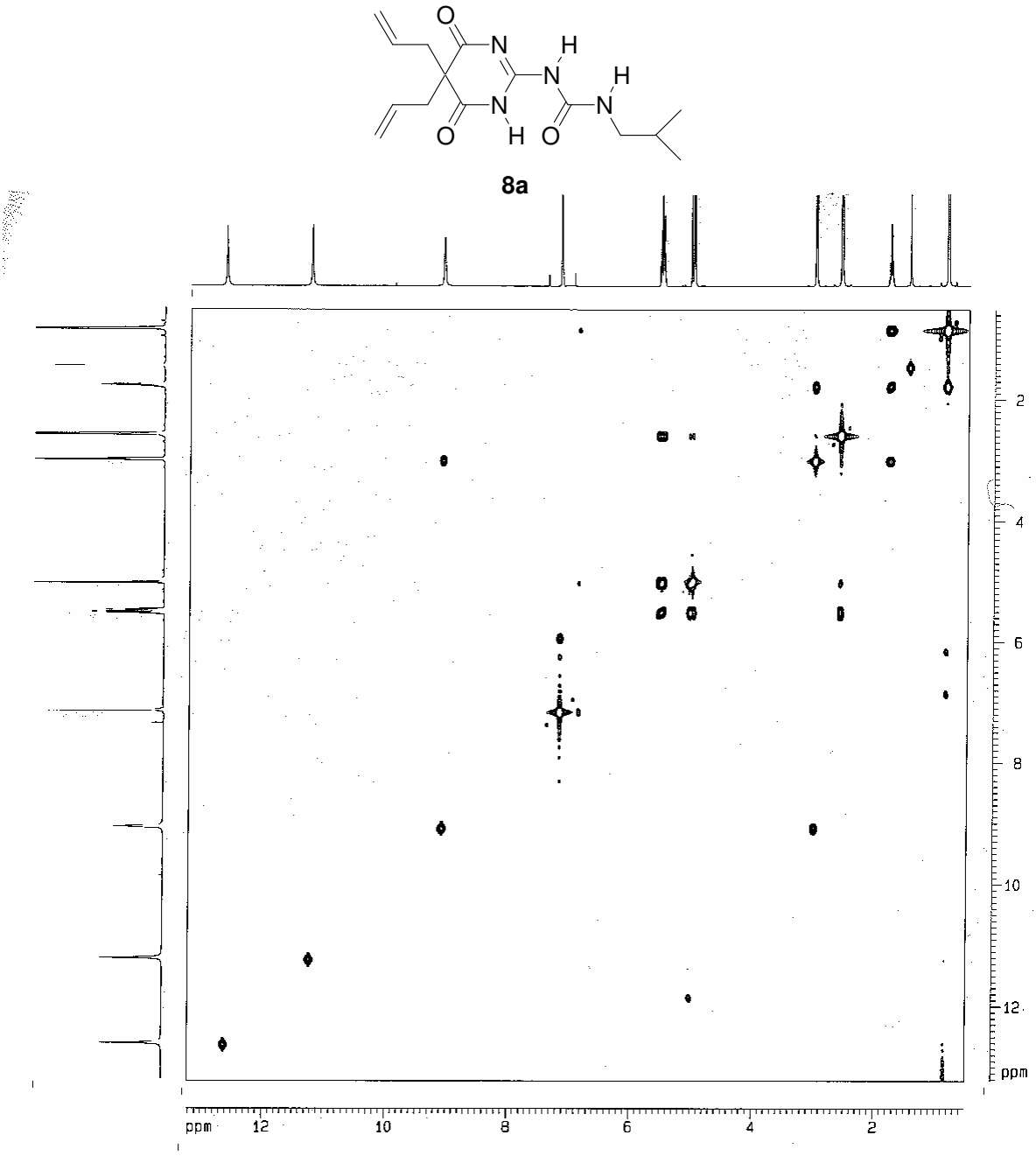

1.7 References and notes

(1) Wohler, F. *Poggendrofs Ann. Physik* **1828**, *12*, 253.

(2) Woodward, R. B. *Pure Appl. Chem.* **1968**, *17*, 519.

(3) Eschenmoser, A. *Quart. Rev.* **1970**, *24*, 366; *Chem. Soc. Rev.* **1976**, *5*, 377; *Nova Acta Leopoldina* **1982**, *55*, 5.

(4) Lehn, J.-M. *Pure Appl. Chem.* **1978**, *50*, 871.

(5) Lehn, J.-M. *Supramolecular Chemistry: Concepts and* Perspectives; VCH: Weinheim, **1995**.

(6) For reviews, see: (a) Lawrence, D. S.; Jiang, T.; Levett, M. *Chem. Rev.* **1995**, *95*, 2229; (b) Philip, D.; Stoddart, J. F. *Angew. Chem. Int. Ed.* **1996**, *35*, 1154.

(7) For reviews, see: (a) Whitesides, G. M.; Simanek, E. E.; Mathias, J. P.; Seto, C. T.; Chin, D. N.; Mammen, M.; Gordon, D. M. *Acc. Chem. Res.* **1995**, *28*, 37; (b) Conn, M. M; Rebek, J. Jr. *Chem. Rev.* **1997**, *97*, 1647; (c) de Mandoza, J. *Chem. Eur. J.* **1998**, *4*, 1373.

(8) Lehn, J.-M. *Angew. Chem. Int. Ed.* **1988**, *27*, 89.

(9) Lehn, J.-M.; Regault, A. *Angew. Chem. Int. Ed.* **1988**, *27*, 1095.

(10) Traunger, J. W.; Baird, E. E.; Dervan, P. B. *Nature* **1996**, *382*, 559.

(11) Parnata, J.; Wierschke, S. G.; Jorgenson, W. L. *J. Am. Chem. Soc.* **1991**, *113*, 2810.

(12) (a) Lehn, J.-M.; Mascal, M.; Decain, A.; Fischer, J. *Chem. Commun.* **1990**, 479; (b) MacDonald, J. C.; Whitesides, G. M. *Chem. Rev.* **1994**, *94*, 2383.

(13) Zerkowski, J. A.; Seto, C. T. *J. Am. Chem. Soc.* **1992**, *114*, 5473.

(14) For an excellent recent review, see: (a) Peczuh, M. W.; Hamilton, A. D. *Chem. Rev*. **2000**, *100*, 2479; (b) Stigers, K. D.; Soth, M. J.; Novick, J. S. *Curr Opin. Chem. Biol.* **1999**, 714.

(15) (a) Thomas, B.; Mathias, D.; Helen, S. E.; Alex, V. Z. *Angew. Chem. Int. Ed*. **2001**, *40*, 2848; (b) Kolomiets, E.; Berl, V.; Odriozola, I.; Stadler, A. M.; Kyritsakas, N.; Lehn, J.-M. *Chem. Commun.*, **2003**, 2868; (c) Fenniri, H.; Deng, B. L.; Ribbe, A. E. *J. Am. Chem. Soc.* **2002,** *124*, 11064.

(16) (a) Isnin, R.; Salam, C.; Kaifer, A. E. *J. Org. Chem.* **1991**, *56*, 35; (b) Isnin, R., Kaifer, A. E. *J. Am. Chem. Soc.* **1991**, *113*, 8188; (c) Mirzoian, A.; Kaifer, A. E. *Chem.*

Eur. J. **1997**, *3*, 1052; (d) Kaifer, A. E. Acc. Chem. Res. **1999,** *32*, 62; (e) Moon, K.; Grindstaff, J.; Sobransingh, D.; Kaifer, A. E. *Angew. Chem. Int. Ed.* **2004**, *43*, 5496; (f) Ling, Y.; Wang, W.; Kaifer, A. E. *Chem. Commun.* **2007**, 610.

(17) (a) Witt, D.; Lagona, J.; Damkaci, F.; Fettinger, J. C.; Isaacs, L. *Org. Lett.* **2000**, *2*, 755; (b) Liu, S.; Ruspic, C.; Mukhopadhyay, P.; Chakrabarti, S.; Zavalij, P. Y.; Isaacs, L. *J. Am. Chem. Soc.* **2005**, *127*, 15959; (c) Huang, W.-H.; Liu, S.; Zavalij, P. Y.; Isaacs, L. *J. Am. Chem. Soc.* **2006**, *128*, 14744; (d) Lagona, J.; Wagner, B. D.; Isaacs, L. *J. Org. Chem.* **2006**, *71*, 1181.

(18) Simanek, E. E.; Mammen, M.; Gordon, D. M.; Chin, D.; Mathias, J. P.; Seto, C. T.; Whitesides, G. M. *Tetrahedron* **1995**, *51*, 607.

(19) Schmuck, C.; Wienand, W. *J. Am. Chem. Soc*. **2003**, *125*, 452.

(20) (a) Zeng, H.; Yang, X.; Brown, A. L.; Martinovic, S.; Smith, R. D.; Gong, B. *Chem. Commun.* **2003**, 1556; (b) Martinovic, X. S.; Smith, R. D.; Gong, B. *J. Am. Chem. Soc*. **2003**, *125*, 9932; (c) Zhao, X.; Wang, X.-Z.; Jiang, X.-K.; Chen, Y.-Q.; Li, Z.-T.; Chen, G.-J. *J. Am. Chem. Soc.* **2003**, *125*, 15128.

(21) Sijbesma, R. P.; Beijer, F. H.; Brunsveld, L.; Folmer, B. J. B.; Hirschberg, J. H. K.; Lange, R. F. M.; Lowe, J. K. L.; Meijer, E. W. *Science* **1997**, *278*, 1601.

(22) Marquis, A.; Kintzinger, J.-P.; Graff, R.; Baxter, P. N. W.; Lehn, J.-M. *Angew. Chem. Int. Ed*. **2002**, *41*, 2760.

(23) Yang, J.; Fan, E.; Geib, S. J.; Hamilton, A. D. *J. Am. Chem. Soc.* **1993**, *115*, 5314.

(24) Kolotuchin, S. V.; Zimmerman, S. C. *J. Am. Chem. Soc.* **1998**, *120*, 9092.

(25) Marsh, A.; Silvestri, M.; Lehn, J.-M. *Chem. Commun.* **1996**, 1527.

(26) Mascal, M.; Hext, N. M.; Warmuth, R.; Moore, M. H.; Turkenburg, J. P. *Angew. Chem. Int. Ed.* **1996**, *35*, 2204.

(27) Vreekamp, R. H.; van Duynhoven, J. P. M.; Hubert, M.; Verboom, W.; Reinhoudt, D. N. *Angew. Chem. Int. Ed.* **1996**, *35*, 1215.

(28) Gonza´lez, J. J.; Prados, P.; de Mendoza, J. *Angew. Chem. Int. Ed.* **1999**, *38*, 525.

(29) (a) Ghadiri, M. R.; Kobayashi, K.; Granja, J. R.; Chadha, R. K.; McRee, D. E. *Angew. Chem. Int. Ed.* **1995**, *34*, 93; (b) Kobayashi, K.; Granja, J. R.; Ghadiri, M. R. *Angew. Chem. Int. Ed.* **1995**, *34*, 95.

(30) Sessler, J. L.; Wang, R. *Angew. Chem. Int. Ed*. **1998**, *37*, 1726.

(31) (a) Szabo, T.; Hilmersson, G.; Rebek, J. Jr. *J. Am. Chem. Soc.* **1998**, *120*, 6193; (b) Rebek, J. Jr. *Acc. Chem. Res.* **1999**, *33*, 278.

(32) Davis, A. P.; Draper, S. M.; Dunnea, G.; Ashtonb, P. *Chem. Commun.* **1999**, 2265.

(33) Bondy, C. R.; Gale, P. A.; Loeb, S. J. *J. Am. Chem. Soc.* **2004**, *126*, 5030.

(34) Bell, T. W.; Liu, J. *J. Am. Chem. Soc.* **1988**, *110*, 3673.

(35) Bell, T. W.; Hou, Z.; Zimmerman, S. C.; Thiesen, P. A. *Angew. Chem. Int. Ed.* **1995**, *34*, 2163.

(36) Wyler, R.; de Mendoza, J.; Rebek, J. Jr. *Angew. Chem. Int. Ed.* **1993**, *32*, 1699.

(37) (a) Beijer, F. H.; Sijbesma, R. P.; Kooijman, H.; Spek, A. L.; Meijer, E. W. *J. Am. Chem. Soc.* **1998,** *120*, 6761; (b) Ligthart, G. B. W. L.; Ohkawa, H.; Sijbesma, R. P.; Meijer, E. W. *J. Am. Chem. Soc.* **2005**, *127*, 810 and references cited therein.

(38) (a) Corbin, P. S.; Zimmerman, S. C. *J. Am. Chem. Soc.* **1998,** *120,* 9710; (b) Corbin, P. S.; Lawless, L. J.; Li, Z.; Ma, Y.; Witmer, M. J.; Zimmerman, S. C. *PNAs* **2002**, *99*, 5099.

(39) Zeng, H.; Yang, X.; Flowers, R. A.; Gong, B. *J. Am. Chem. Soc.* **2002**, *124*, 2903.

(40) Zeng, H.; Miller, R. S.; Flowers, R. A.; Gong, B. *J. Am. Chem. Soc.* **2000,** *122*, 2635.

(41) Sijbesma, R. P.; Meijer, E. W. *Chem. Commun.* **2003**, 5.

(42) Sartorius, J.; Schneider, H.-J. *Chem. Eur. J.* **1996**, *2*, 1446.

(43) (a) Beijer, F. H.; Kooijman, H; Speck, A. L.; Sijbesma, R. P.; Meijer, E. W. Angew. Chem. Int. Ed. **1998**, *37*, 75; (b) Folmer, B. J. B.; Sijbesma, R. P.; Kooijman, H; Speck, A. L.; Meijer, E. W. *J. Am. Chem. Soc.* **1999**, *121*, 9001.

(44) (a) Murray, T. J.; Zimmerman, S. C. *J. Am. Chem. Soc.* **1992**, *114*, 4010; (b) Fenlon, E. E; Murray, T. J.; Zimmerman, S. C. *J. Org.Chem.*. **1993**, *58*, 6625; (c) Zimmerman, S. C.; Murray, T. J. *Tetrahedron Lett.* **1994**, *35*, 4077.

(45) (a) Pranata, J.; Wierschke, S. G.; Jorgensen, W. L. *J. Am. Chem. Soc.* **1991**, *113*, 2810; (b) Jorgensen, W. L.; Pranata, J. *J. Am. Chem. Soc.* **1990**, *112*, 2008.

(46) The tautomeric rearrangement of supramolecular polymers having ureidopyrimidinone self-assembling modules had been investigated by 1H DQ NMR spectroscopy under fast MAS conditions, see: Schnell, I.; Langer, B.; Sontjens, S. H. M.;

Sijbesma, R. P.; van Genderen, M. H. P.; Spiess, H. W; *Phys. Chem. Chem. Phys.* **2002**, *4*, 3750.

(47) Elguero, J.; Marzin, C.; Katritzky, A. R.; Linda, P. *The Tautomerism of Heterocycles: Advances in Heterocyclic Chemistry*, Academic press, New York**, 1976**.

(48) (a) Komber, H.; Limbach, H. H.; Boehme, F.; Kunert, C. *J. Am. Chem. Soc.*, **2002**, *124*, 11955; (b) Maki, J.; Klika, K. D.; Sjoholm, R.; Kronberg, L. *J. Chem. Soc. Perkin Trans 1*, **2001**, 1216; (c) Thoburn, J. D.; Luettke, W.; Benedict, C.; Limbach, H. H.; *J. Am. Chem. Soc*., **1996**, *118*, 12459; (d) Helaja, J.; Montforts, F. P.; Kilpelaeinen, I.; Hynninen, P. H. *J. Org. Chem*., **1999**, *64*, 432.

(49) Karle, I. L. *Acta Crystallogr*, *Sect. B* **1992**, *48*, 341.

(50) Atwood, J. L.; Davies, J. E. D.; MacNicol, D. D.; Vogtle, F. *Comprehensive Supramolecular Chemistry,* Eds., Pergamon Press, Oxford, **1996**, *Vol. 9*, pp 671.

(51) Ranganathan, A.; Pedireddi, V. R.; Rao, C. N. R. *J. Am. Chem. Soc*. **1999**, *121*, 1752.

(52) Rao, C. N. R. *Chemical Approaches to the Synthesis of Inorganic Materials*; John Wiley: New York, **1993**.

(53) Amide bond prefers *trans* geometry, see: Katrizky, A. R.; Ghiviriga, I. *J. Chem. Soc. Perkin Trans*. *2*, **1995**, 1651.

(54) Johnstone, R. A. W.; Tuli, D.; Rose, M. E. *J. Chem. Res. Synop.* **1980**, *9*, 283.

(55) Lehn, J.–M.; Mascal, M.; DeCian, A.; Fischer, J. *J. Chem. Soc. Perkin Trans. 2*, **1992**, 461.

(56) (a) Mathias, J. P.; Simanek, E. E.; Whitesides, G. M. *J. Am. Chem. Soc.* **1994**, *116*, 4326; (b) Simard, M.; Su, D.; Wuest, J. D. *J. Am. Chem. Soc*. **1991***, 113*, 4696.

(57) Etter, M. C. *Acc. Chem. Res.* **1990**, *23*, 120.

(58) (a) Wilcox, C. S. *In frontiers in supramolecular chemistry and photo chemisty* **1990**, pp 123; (b) Schumk, C.; Wienand, W. *J. Am. Chem. Soc*. **2003**, *125*, 452.

(59) Lafitte, V. G. H.; Aliev, A. E.; Hailes, H. C.; Bala, K, Golding, P. *J. Org. Chem.* **2005**, *70*, 2701.

(60) Ganem, B.; Li, Y.T.; Henion, J. T. J. *Am. Chem. Soc.* **1991**, *113,* 6294.

(61) The crystal structure of **1a-c,** and **1e** were solved by direct method using SHELXS-97 and the refinement was performed by full matrix least squares of F2 using SHELXL-

97 (Sheldrick, G. M. SHELX-97 program for crystal structure solution and refinement, University of Göttingen, Germany, **1997**). Hydrogen atoms were included in the refinement as per the riding model.

(62) Substituents can influence the mode of hydrogen bonding (hydrogen-bonding codes) in dimer formation; see reference 37a.

(63) Delano, W. L.; **2004**, *The PyMOL Molecular Graphics System*; http://www.pymol.org.

(64) (a) Bernstein, J. *Polymorphism in Molecular Crystals*; Oxford University Press: New York, **2002**; (b) McCrone W. C. in *Physics and Chemistry of the Organic Solid State, Vol. II* (Eds: Fox, D.; Labes, M. M.; Weissberger A.), Interscience, New York, **1965**, pp. 725; (c) Byrn, S. R. *Solid State Chemistry of Drugs*, Academic Press: New York, **1992**; (d) Brittain, H. G. *Polymorphism in Pharmaceutical Solids*; Marcel Dekker Inc.: New York, **1999**; (e) Threlfall, T. L. *Analyst* **1995**, *120*, 2435; (f) Dunitz, J. D.; Bernstein, J. *Acc. Chem. Res*. **1995**, *28*, 193; (g) Davey, R. J. *Chem. Commun*. **2003**, 1463.

(65) (a) McMahon, J. A.; Zaworotko, M. J.; Remenar, J. F. *Chem. Commun*. **2004**, 278; (b) Remenar, J. F.; Morissette, S. L.; Peterson, M. L.; Moulton, B.; MacPhee, J. M.; Guzman, H. R.; Almarsson, O. *J. Am. Chem. Soc*. **2003**, *125*, 8456; (c) Special Issue: *Org. Proc. Res. Dev*. **2003**, *7*, 957.

(66) (a) Vishweshwar, P.; McMahon, J. A.; Bis, J. A.; Zaworotko, M. J. *J. Pharm. Sci.* **2006**, *95*, 499; (b) Thallapally, P. K.; Jetti, R. K. R.; Katz, A. K.; Carrell, H. L.; Singh, K.; Lahiri, K.; Kotha, S.; Boese, R.; Desiraju, G. R. *Angew. Chem. Int. Ed.* **2004**, *43*, 1149; (c) Special Issue: *Polymorphism in Crystals, Cryst. Growth Des*. **2003**, *3*, 867; (d) Almarsson, O.; Zaworotko, M. J. *Chem. Commun*. **2004**, 1889.

(67) For a related example, see: Lafitte, V. G. H.; Aliev, A. E.; Hailes, H. C.; Bala, K.; Golding, P. *J. Org. Chem.* **2005**, *70*, 2701.

(68) (a) Scheerder, J.; Engbersen, J. F. J.; Alessandro, C.; Ungaro, R.; Reinhoudt, D. N. *J. Org. Chem.* **1995**, *60*, 6448; (b) Tobe, Y.; Sasaki, S.; Mizuno, M.; Hirose, K.; Naemura, K. *J. Org. Chem.* **1998**, *63*, 7481.

(69) Morley, J. S. *J. Chem. Soc. C* **1969**, 809.

(70) (a) Yu, K.-L.; Johnson, R. L. *J. Org. Chem.* **1987**, *52*, 1051; (b) Zabrocki, J.; Smith, G. D.; Dunbar, J. B. Jr., Iijima, H.; Marshall, G. R. *J. Am. Chem. Soc.* **1988**, *110*, 5875.

(71) Demko, Z. P.; Sharpless, K. B. *Org. Lett.* **2002**, *4*, 2525.

(72) Collibe, W. L.; Nakajima, M.; Anselme, J.-P. *J. Org. Chem.* **1995**, *60*, 468.

(73) Stolle, R. *Ber.* **1929**, *62***,** 1118.

(74) Sun, H.; Steeb, J.; Kaifer, A. E. *J. Am. Chem. Soc.* **2006**, *128*, 2820.

(75) Maslak, P.; Varadarajan, S.; Burkey, J. D. *J. Org. Chem.* **1999,** *64,* 8201.

CHAPTER 2

Design, Synthesis and conformational studies of conformationally constrained α-Amino Acid-Aromatic Amino Acid Conjugated Foldamers

-Where nature finishes producing its own species, man begins, using natural things and with the help of this nature, to create an infinity of species.

by Leonardo da Vinci
Born: 15th of April, 1452, Italy.
Death: 2nd May, 1519.

2.1 Introduction: Foldamer Overview

The folding and assembly of biomolecules are two of the most important features in nature. It is beyond doubt that without the ability of nature to form very stable aggregates of small molecules or to form secondary, tertiary and quaternary structures of large molecules, life would have been impossible. The formation of duplex DNA represents one of the most elegant and best known examples of both self assembly and folding of biomacromolecules.[1] To carry out many sophisticated chemical operations, such as catalysis, specific binding, directed flow of electrons, controlled crystallizations of inorganic phases, as well as adopting different functions in different pH, nature relies on large molecules. It attains these various functions on the basis of various noncovalent interactions between molecules. Proteins and RNA are unique relative to other biological and synthetic polymers, because they adopt special and compact conformation that are thermodynamically and kinetically stable. These folding patterns generate "active sites" *via* precise arrangement of functional groups. Naturally occurring twenty amino acid constituents can generate diverse set of structures and can perform different functions in proteins when arranged in a linear sequence. It is a matter of imagination what diverse set of structures and functions are attainable by combining various nonnatural monomers that are available to the chemist. The various levels of structural organizations that are found in proteins are pictorially represented in figure 1.

Within a very short span of time there has been increasing interest in the design and synthesis of oligomeric systems which adopt well ordered and compact folded secondary structures in solution.[2] The field of unnatural folding oligomers (a.k.a.-foldamers) was pioneered by the research groups of Gellman and Seebach, from the studies of secondary structural properties of β-peptides. A foldamer, as defined by Moore, is 'any *oligomer* that folds into a conformationally ordered state in solution, the structures of which are stabilized by a collection of noncovalent interactions between non-adjacent monomer units'.[3] Although more simply, a foldamer can be expressed as an unnatural system that adopts a well defined compact secondary structure.[4] Recently, chemists have tried to

design and synthesize unnatural oligomers with predictable folding propensities. The research in the field of foldamer science has opened a door for applications in the field of

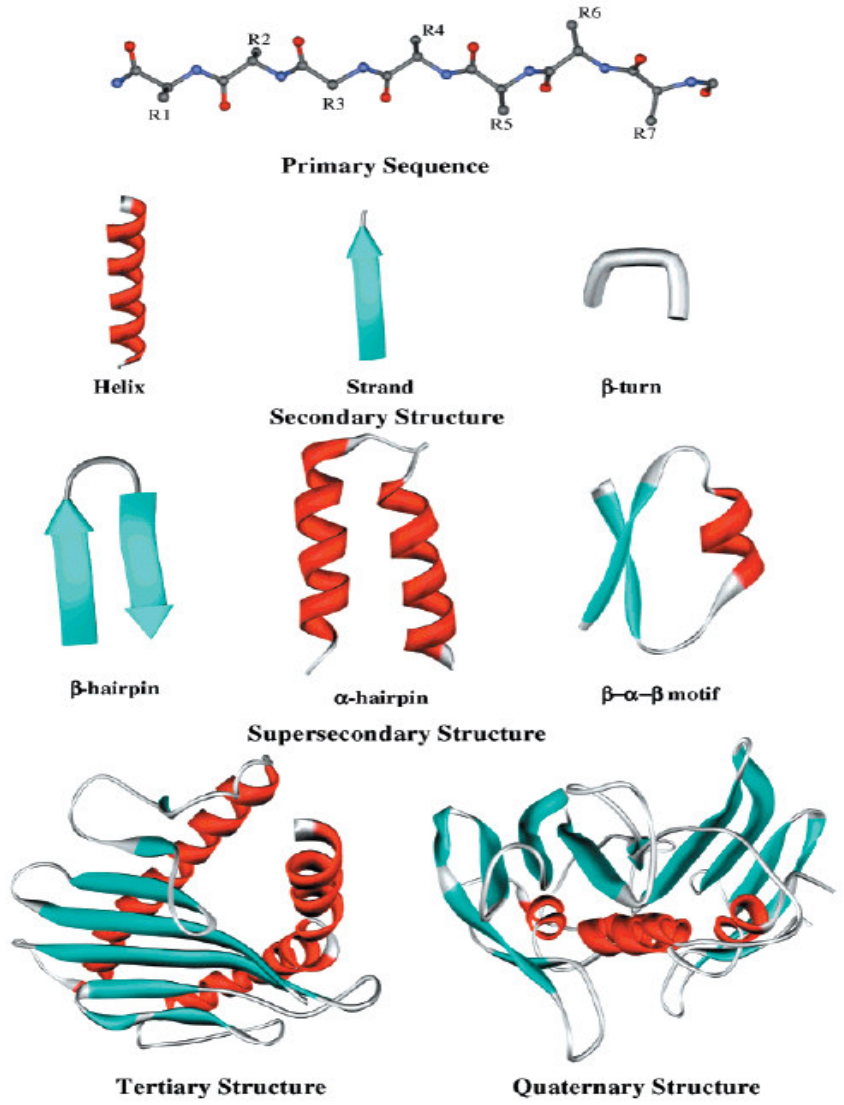

Figure 1: Various levels of structural organization observed in proteins.

biology and material science. It is expected that foldamers research will shed light on (i) answering the question, whether nature has the monopoly on folded structures, (ii) mimicking the functions of biomolecules, and (iii) to see what new functions unseen in nature that can be attained by new designed molecules. Various foldamers with secondary structures such as helices, turns, sheets have been reported. Among reported systems, foldamers adopting various helical conformations represent the overwhelming

majority.[3,4] Among proteins, the term "compact" is associated with tertiary structure, and there is as yet no *synthetic polymer* that displays a specific tertiary structure. Protein tertiary structure arises from the assembly of elements of regular secondary structure (helices, sheets, and turns). Till today, production of high molecular weight polymers that mimic the sophistication of biomacromolecules, either in form or function is far from reality.

2.1.2 Classification of foldamers

In foldamer, a repeating monomeric unit is present within the backbone. Foldamers adopt a particular compact conformation both in solid as well as in solution state. So oligomers where no folding can occur and whose structure is attained by covalent interaction such as in helicines,[5] polyoxapolyspiroalkanones,[6] oligo(naphthalene)s,[7] and "gelander" molecules[8] are not considered as foldamers (figure 2).

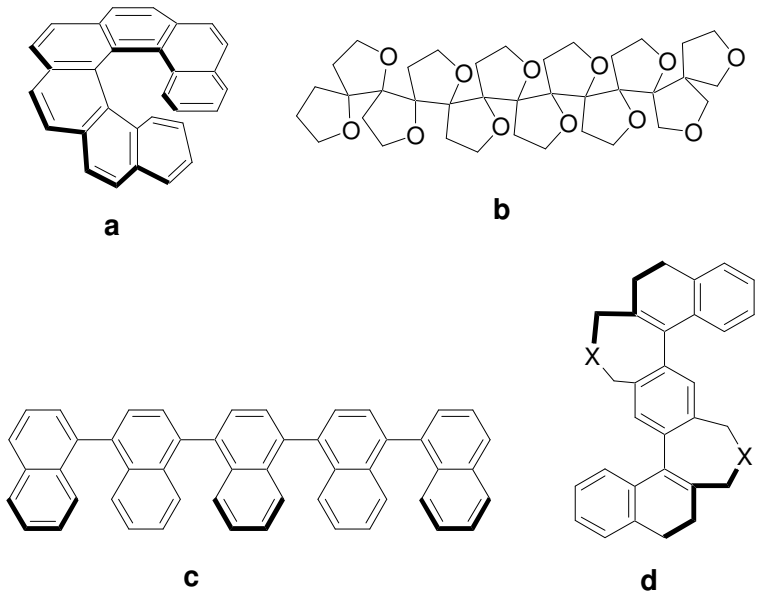

Figure 2: Oligomers not classified as foldamers.

The conformation of a foldamer is effected by change in the environment, such as change in solvent, pH, temperature, addition of specific ligand, etc. Since the conformation of a foldamer is stabilized by weak noncovalent interaction, this can be broken and regenerated easily. This cooperative behaviour is absent in oligomers with stable intrinsic conformations as in helicines.

The foldamers are classified broadly as biotic and abiotic. Research in the field of biotic foldamers include elucidating the sequence specificity of various secondary structures, stabilizing the secondary structure in water and creating tertiary structures such as helical bundles. The research in abiotic foldamer is mainly focused on the monomer geometry design for modulating the structure of resulting oligomers. Conformationally constrained monomers have also been used in biotic foldamers. Examples of some the abiotic (figure 3) and biotic (figure 4) foldamers are as shown below:

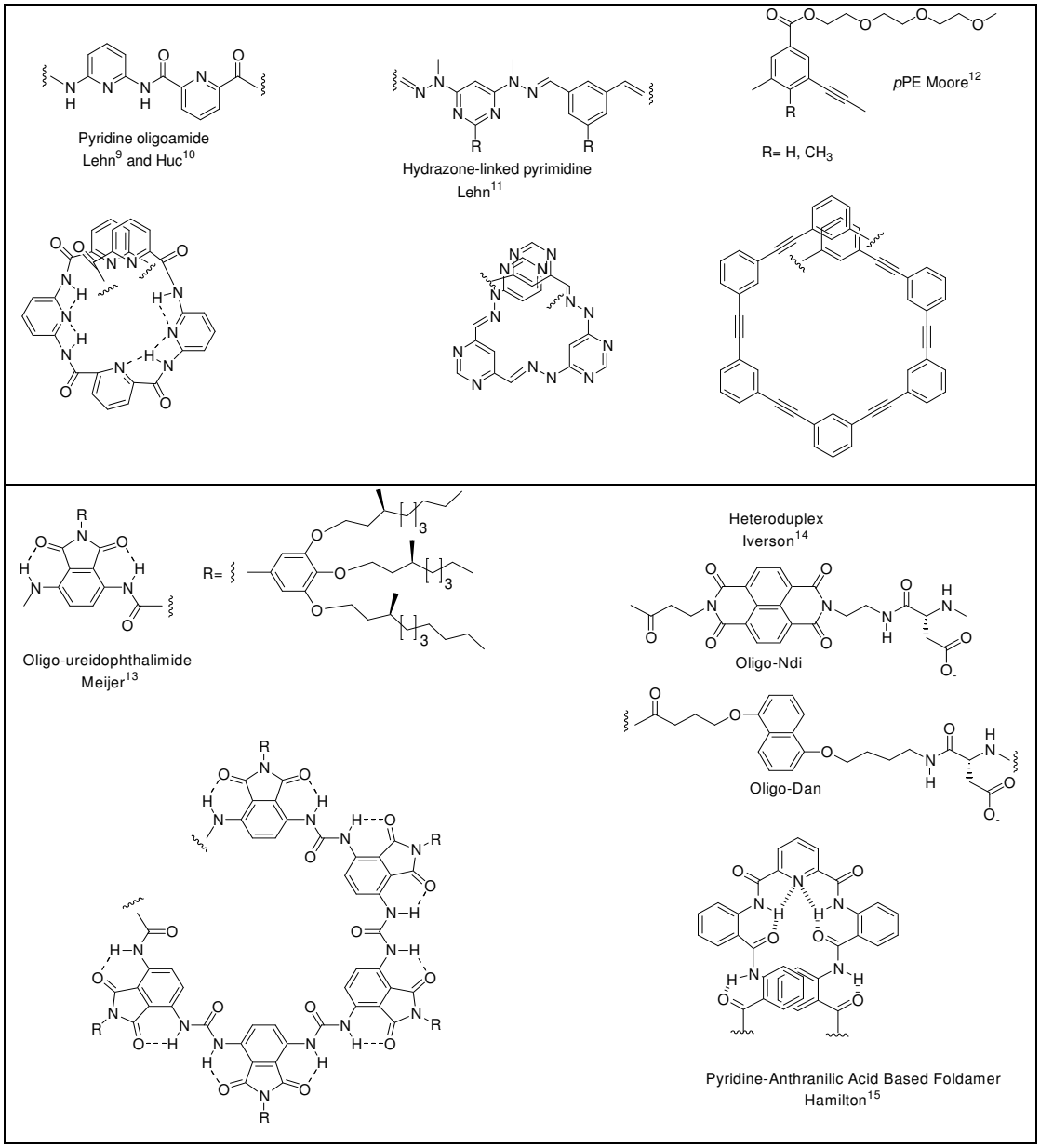

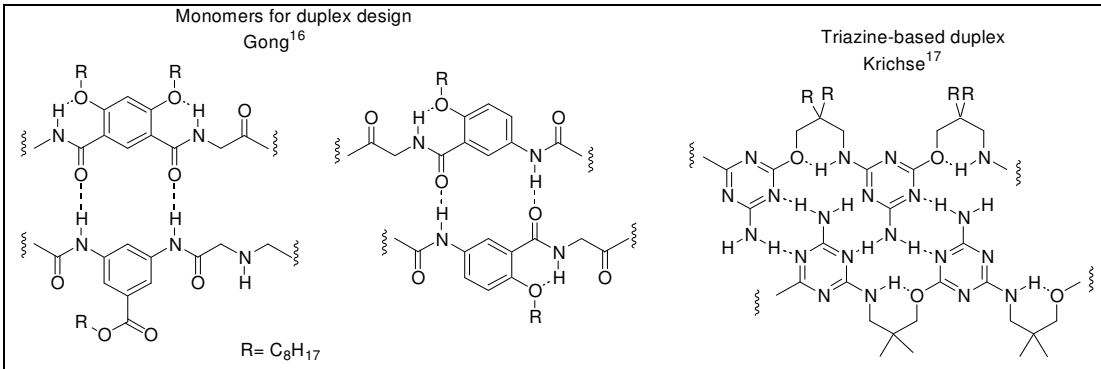

Figure 3: Selected examples of abiotic foldamers.

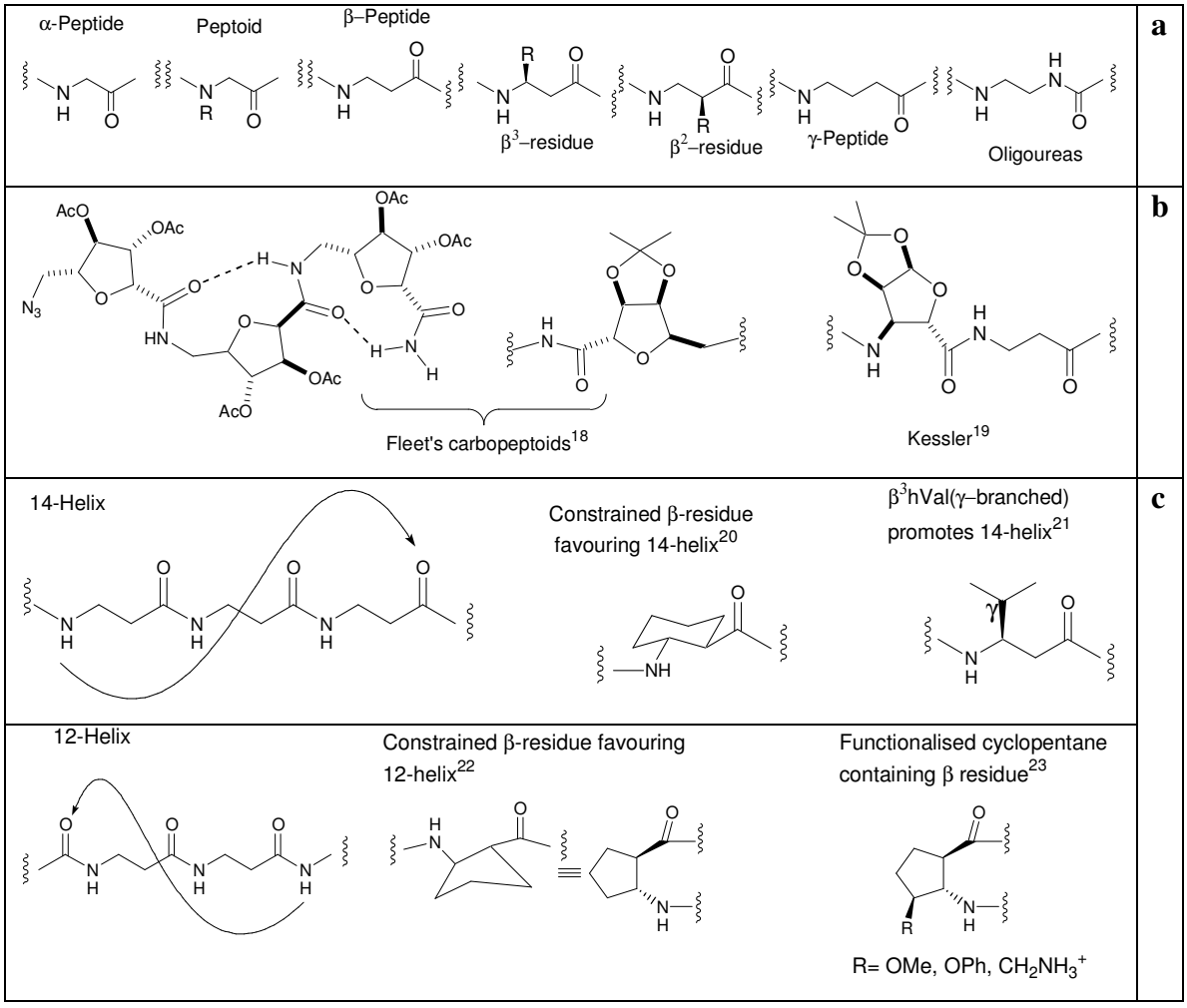

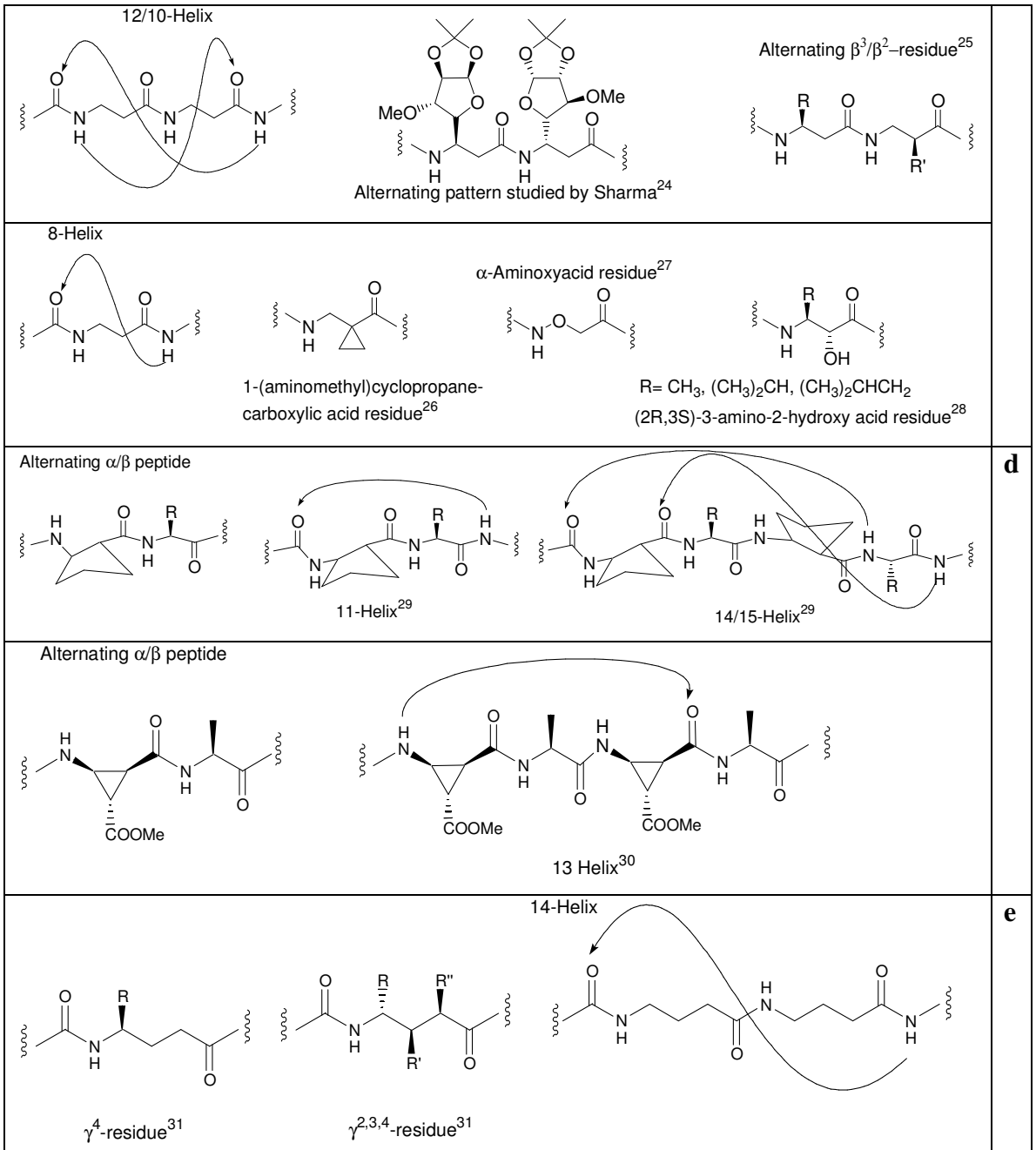

Figure 4: Selected examples of biotic foldamers.

Poly-N-substituted glycines, "peptoids" (figure 4a), were initially developed as highly flexible peptidomimetics.[32] Petoids are regioisomers of conventional peptides with substituents on the amide nitrogens rather than on the α-carbon. They have been shown to adopt a polyproline type I helix in solution and solid state.[33] Analogous to polyproline,

peptoids lack backbone hydrogen-bond donors. The helical 'handedness' of peptoids is dictated by the stereochemistry of the sidechains; α-chiral aromatic and aliphatic sidechains[33] have both been shown to support the polyproline type I helix.

Sugar based amino acids are important class of foldamers adopting secondary structures as has been shown by various groups. Fleet et al. has shown that oligomers of tetrahydrofuran (THFC) amino acids bearing 2,5-*cis* and 2,5-*trans* stereochemistry across the THF ring adopts β-turn like structures (figure 4b).[18] Kessler and co-workers investigated the conformational influence of a range of pyranose carbohydrate amino acids on peptide chains by utilizing them as a replacement for the natural Gly-Gly dipeptide in a linear Leu-enkephalin analogue (figure 4b).[19]

Compared to α-peptides, the chemical similarity and higher stability of β-peptides against proteolytic degradation *in vitro* and *in vivo* have inspired many researchers to design well-defined secondary and tertiary structures of this scaffold. Oligo(β-amino acids), "β-Peptides" (figure 4a, c), can adopt a wide variety of secondary structures, including helices, sheets and turns.[34] The sidechain substitution pattern of the constituting β-amino acids can bias the local backbone conformational preference and thus the overall secondary structure.[34] Among the β-peptide helical conformations, the 14-helix is the most studied.[34a,b] The 14-helix has 14 atoms in the hydrogen-bonded ring N–H(i) ···O=C(i+2) (figure 4c) and an approximately three-residue repeat. Schepartz[21a] and Gellman,[21b] showed independently that γ-branched β^3-amino acids (such as β^3hVal and β^3hIle) can be used to promote the formation of the 14-helix. Gellman et al.[21b] also showed that a single conformationally constrained cyclic residue in the center of the sequence is sufficient to bias a 10-mer to adopt a 14-helix. Furthermore, a 12-mer with four cyclic residues evenly distributed in the sequence was sufficient to stabilize the 14-helix between pH 2 and 12, even though the remainder of the β-peptide comprised charged acylic residues to potentially stabilize the 14-helix through electrostatic interactions.[35] In addition to the known β-peptide antiparallel hairpins, Gellman et al.[36] studied a hairpin structure with parallel sheets composed of β-amino acids. Whereas the α,β-syn-dialkyl configuration of the β-amino acid was critical for parallel hairpin

formation, the stereochemistry of the reverse turn was less important than for α-peptide hairpin formation.

The first report demonstrating that chain molecules based on γ-amino acids form regular secondary structure appeared in 1992.[37] There have been several studies on γ-peptides, revealing helix and turn conformations.[3] The difference between the natural α-peptides and the analogues β- and γ-peptides is that upon homologation of the residues the stability of the helical structures increases.[38] Whereas γ^4-peptides form a 14-helix in solution (figure 4e), $\gamma^{2,4}$-disubstituted residues with the appropriate stereochemistry form a reverse turn. Seebach et al.[31] performed NMR and crystallography studies on oligomers of $\gamma^{2,3,4}$-trisubstituted residues, revealing a 14-helix in methanol. Hanessian et al. has shown that γ^4-peptide analogues of the sequence (-L-Ala- L-Val-) adopted stable right-handed helical conformations in solution.[39] It was also discovered that as the α-carbon was methylated (to the S conformer) the helical structure was strengthened. Conversely, with methylation at the α -carbon leading to the R configuration, helix formation did not occur due to unfavorable nonbonding interactions. Seebach probed the effects of substituent patterns and stereoisomers of γ-amino acids on the folding of helical γ-peptides.[40] These γ-peptides are of great interest as biologically active compounds, as they may show greater durability in the biological environment. Elaborate discussions about abiotic foldamers have been made in the next chapter.

2.1.3 Design and synthesis of foldamers

Predictability of the folding is an essential prerequisite for the functioning of a particular foldamer. With increase in time spent on protein folding, researchers were able to develop reasonably large and complex peptides.[41] The following points have to be considered while designing a foldamer:

1. The molecular design of monomer geometry plays the central role in design and modulating of a foldamer structure. So while designing a foldamer we have to select a monomer with specific groups orienting in such a way that the oligomer has no other option but to fold in a particular way.

2. The stability of the folded structure has to be taken care of. Although conformational lability is a desired phenomenon, sometimes it may lead to complications relating to predictability of the folded structures.
3. Further for a foldamer to be useful in technologically, it should be easy to prepare, as well as it should be possible to synthesize the monomeric units in stereo chemically pure form. There are a lot of synthetic procedures available for small molecules but to synthesize larger molecules very few numbers are known. For the ease of synthesis, amide functions are a choice of chemists.
4. A foldamer has to be tunable for generating diverse set of secondary structure using the same design principle.

In an effort to augment the repertoire of conformational space available for foldamer design, chemists have very recently ushered into the construction of foldamers containing different residues of independent conformational preferences. For instance, Gellman et al. demonstrated that α-β-hybrid peptides composed of alternately changing α- and β-amino acid constituents showed convincing evidence for the formation of compact special helix types.[29] Hybrid oligomers carrying alternately changing chirality have been shown to adopt novel compact conformational features, as demonstrated recently by various groups.[24, 30] Hoffmann et al. have recently provided considerable theoretical insights into the helix formation propensities in α,β- and β,γ- hybrid peptides.[42]

Our knowledge on protein secondary structures is based on the X-ray structure of an increasing number of proteins.[43] The most stable and frequent types of regular, periodic secondary structures are the α-helix and the parallel and antiparallel β-pleated sheets. Another abundant structure is the β-turn (β-bend, reverse turn), which has many types.[43a,44] On the basis of X-ray crystallography, α- and γ- turns also have a significant frequency of occurrence in globular proteins.[45] The various protein secondary structures are assigned by their torsion angles. The tabular form of the dihedral angles of some of these secondary structures are shown below (Table 1).

Table 1: Ordered (regular) polypeptide secondary structures

Torsion angles (deg)		
	ϕ (deg)	ψ (deg)
Periodic		
α-Helix (right-handed 3.6_{13}-helix)	-48	-57
	-45	-55
3_{10}-Helix	-60	-30
β-Pleated sheet (β-strand or β-structure)		
Parallel	-139	135
Antiparallel	-119	113
PolyprolineII (left handed extended helix, PPII)	-78	149
Aperiodic		
β-Turn, TypeI	-60	-30 (i+1)
	-90	0 (i+2)
β-Turn, TypeII	-60	120 (i+1)
	80	0 (i+2)
β-Turn, TypeIII	-60	-30
	-60	-30
β-Turn, TypeVIa	-60	120 (i+1)
	-90	0 (i+2)
β-Turn, TypeVIb	-120	120 (i+1)
	-60	0 (i+2)
γ-Turn, inverse	-70 to -85	60 to 70 (i+1)
γ-Turn, classic	70 to 85	-60 to -70 (i+1)

Although not ubiquitous as its related cousin β-turn, γ-turn (figure 6) has been implicated in several important biological events.[46] Furthermore, γ-turn has been frequently postulated to represent an important feature of peptide secondary structure as determined

by ^{1}H NMR,[47] X-ray crystallography[48] and molecular modeling.[49] Two types of γ-turns have been characterized, the classical and the inverse ones, which are defined by the torsion angles of the central amino acid residue. Whereas inverse γ-turns are more frequently observed in proteins,[50] classical γ-turns are rather rare.[45a] The various β- and γ-turn structures are as shown below in figure 5, 6 respectively.

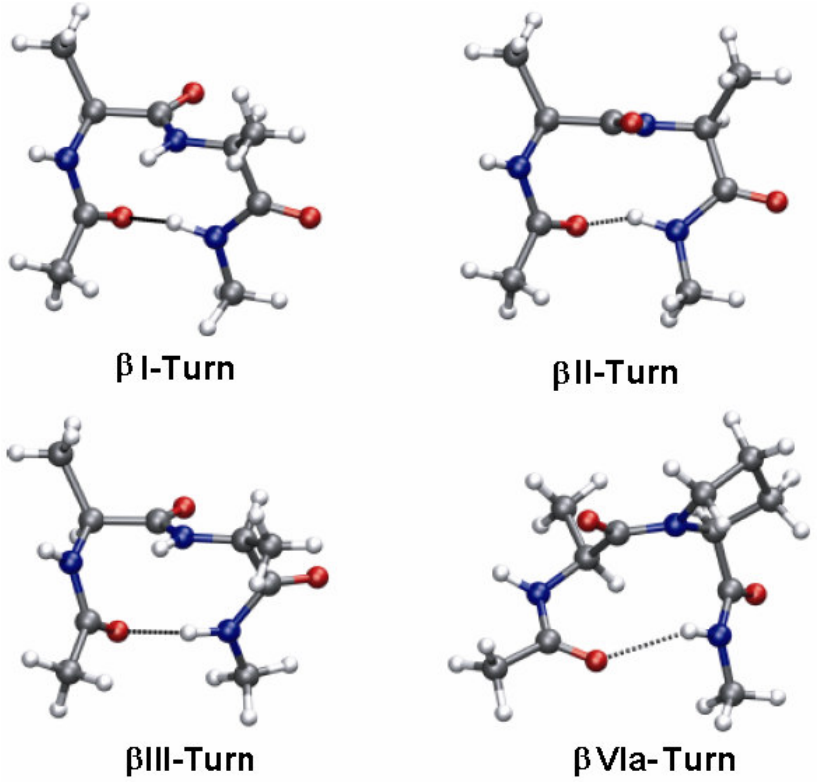

Figure 5: β-Turns featuring a 1←4 (C_{10}) intramolecular H-bond.

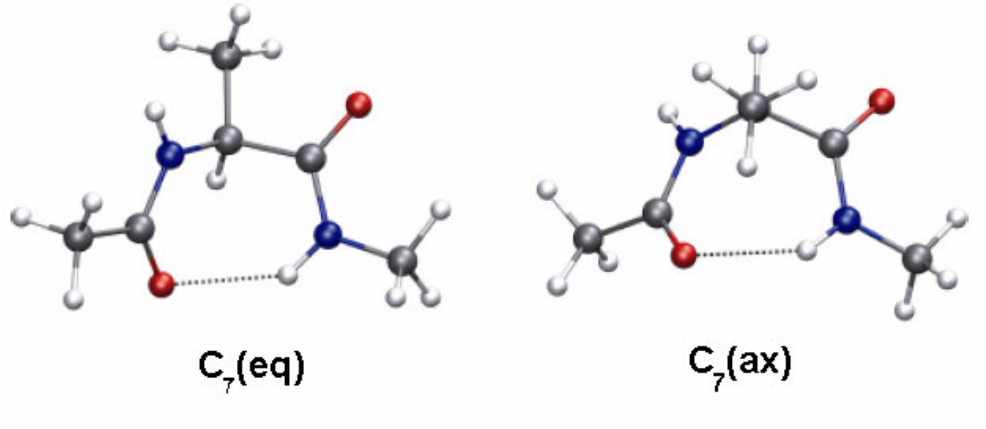

Figure 6: Classical and inverse γ-turns with a 1←3 (C_7^{ax} or C_7^{eq}) intramolecular H-bond.

However, it has been challenging to investigate the roles of γ-turns in protein-peptide recognition because they seldom exist in stable conformation in short, linear peptides, unless constrained by ring formation (backbone cyclization)[51,52] or by the closer positioning of proline to highly constrained cyclopropane amino acid residues with overwhelmingly restricted torsion angles.[53] Interestingly, α-aminoxy acids have recently been shown to be stabilizing γ-turn conformation presumably due to the increased acidity of the aminoxy amide NH that facilitates the "N-O" turn formation.[54]

2.2.1 Objective of the present work

The main objective of the work described in this chapter is to design and synthesize hybrid foldamers derived form natural and constrained synthetic amino acid residues and to study their folding patterns both in solution and solid state.

2.2.2 Design principles

We designed the foldamer based on proline (Pro) and 3-Amino-5-bromo-2-methoxy-benzoic acid (Amb) anticipating that the corresponding oligomers would adopt a well-defined, compact, three dimensional structure, governed by a combined conformational restriction imposed by both Pro and Amb residues (highlighted in bold bonds, figure 7). Whereas the Pro residue, with its torsion angle ϕ constrained at about −60°, is known to promote PPII helical conformation in its homo oligomers;[55] analogs of the backbone-rigidified aromatic amino acid residue Amb is known to induce a crescent conformation in the oligomers[2e,56] *via* localized S(5) and S(6) type[57] hydrogen bonding interactions. Thus we reasoned that hetero-oligomers composed of Pro-Amb repeat motif would also display a three dimensional conformationally rigid structure. It is noteworthy that the understanding of structural factors that influence the secondary structures of peptides has profound implications in several areas ranging from protein–protein interactions[58] and protein–self-assembly.[59]

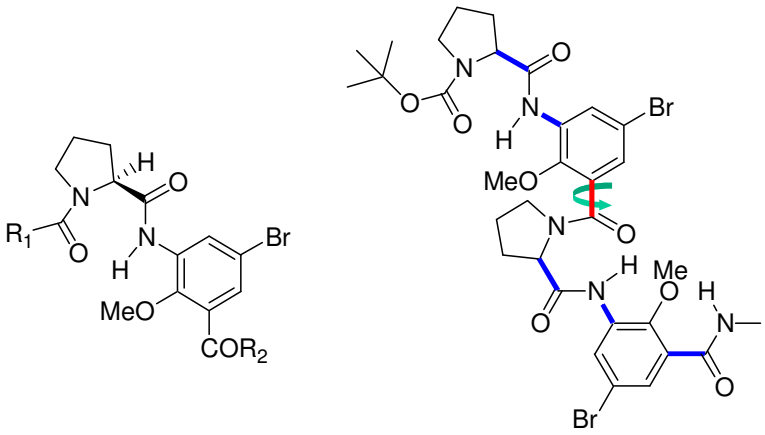

8

Pro-Amb motif

9

Pro-Amb based foldamer

Figure 7: Foldamers designed for the study. *Note*: For aiding quick identification, the conformational restriction imposed by both Pro and Amb residues in **9** is highlighted in blue bold bonds.

2.2.3 Synthesis

3-Amino-5-bromo-2-methoxy-benzoic acid methyl ester **3** was synthesized starting from salicylic acid as shown in scheme 1.

Scheme 1:

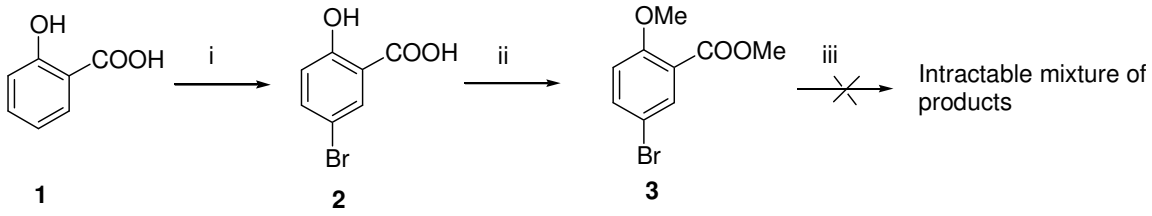

Reagents and conditions: (i) Br_2, CH_3COOH; (ii) CH_3I, K_2CO_3, acetone; (iii) Nitration.

Salicylic acid **1** was converted to the 5-bromosalicylic acid **2** by treatment with Br_2 in acetic acid.[60] **2** was then dimethylated using methyl iodide and potassium carbonate in acetone to obtain **3**. **3** was then subjected to nitration using various nitrating agents, such

as nitric acid and sulphuric acid mixture; acetic anhydride and nitric acid; nitric acid, DCM, aliquat; etc. but the reactions yielded complex mixture of products.

Finally 5-bromosalicylic acid **2** was converted to 5-Bromo-2-methoxybenzoic acid **4** by treatment with dimethyl sulphate and potassium hydroxide. Nitration of **4** was then achieved by dissolving it in minimum amount of sulphuric acid and by slow addition of conc. nitric acid at 0^0C. Esterification of 5-Bromo-2-methoxy-3-nitro-benzoic acid **5** by methyl iodide and potassium carbonate furnished **6**. 5-Bromo-2-methoxy-3-nitro-benzoic acid methyl ester **6** was then reduced with stannous chloride in ethyl acetate to afford the free amine **7**, which was isolated as hydrochloride salt **7a** (scheme 2).

Scheme 2:

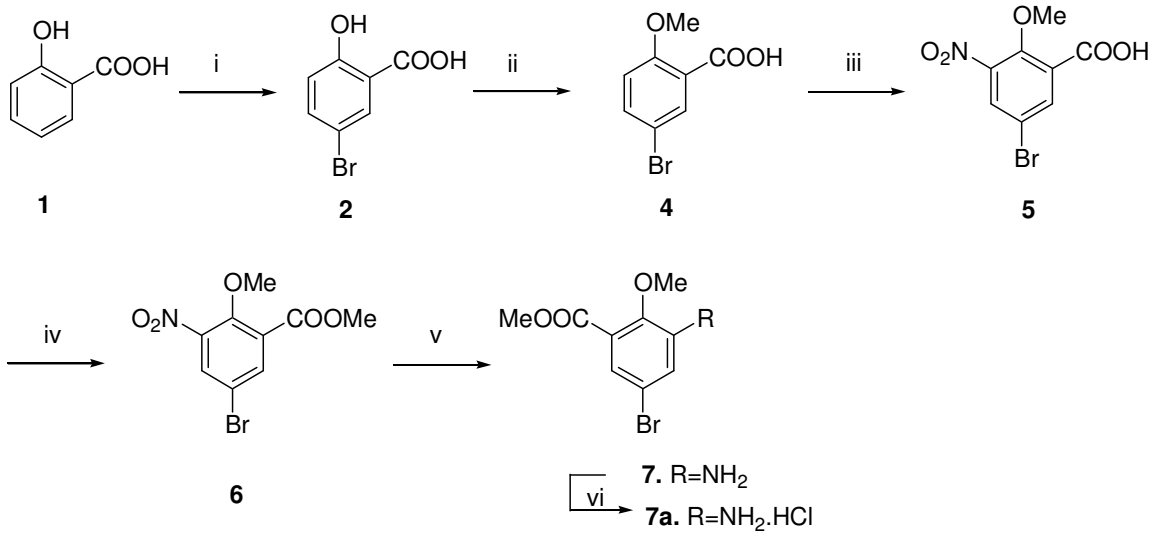

Reagents and conditions: (i) Br_2, CH_3COOH (ii) $(CH_3O)_2SO_2$, KOH (iii) HNO_3, H_2SO_4 (iv) CH_3I, K_2CO_3, acetone (v) $SnCl_2.H_2O$, AcOEt (vi) $SOCl_2$, MeOH.

The Pro-Amb motif-based foldamer **9** was assembled, using "segment doubling strategy", from Boc-Pro-Amb-OMe building block **8a**, which in turn was synthesized by coupling the protected amino acids Pro and Amb using TBTU (O-(Benzotriazol-1-yl)-N,N,N',N'-tetramethyluronium tetrafluoroborate) as a coupling agent DIEA (N,N-diisopropylethylamine) as the base (scheme 3).

Scheme 3:

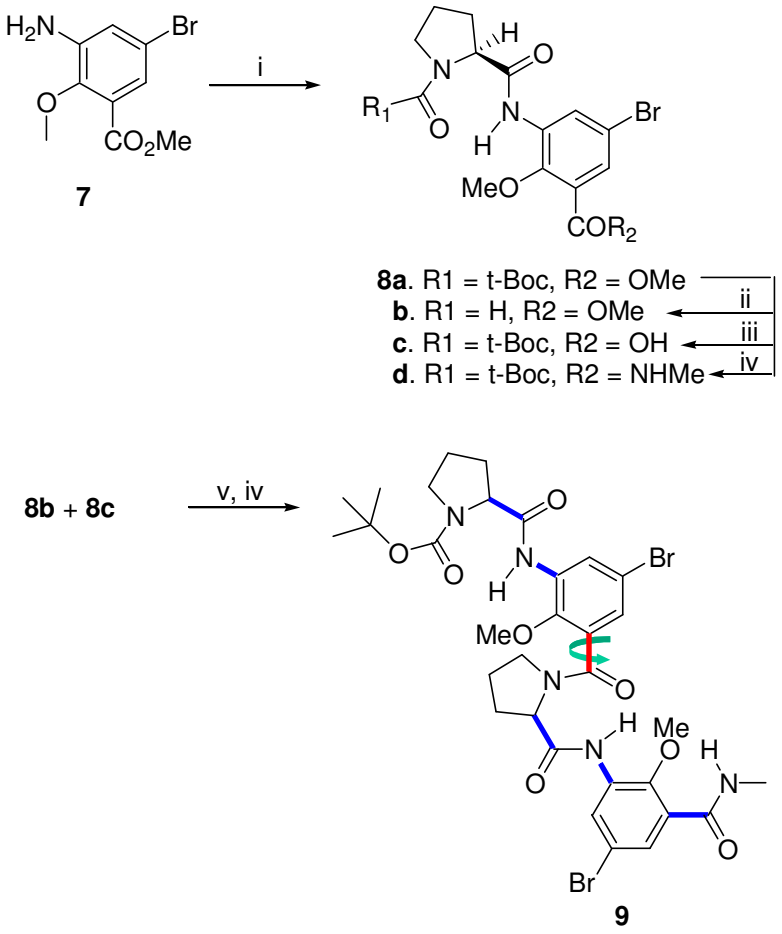

Reagents and conditions: (i) Boc-Pro-OH, DIEA, TBTU, MeCN, rt, 12 h; (ii) dry HCl (gas), dioxane, RT, 15 min; (iii) LiOH, MeOH, RT, 24h; (iv) methanolic $MeNH_2$, 24h, RT; (v) DIEA, TBTU, MeCN, RT, 12h. *Note*: For aiding quick identification, the conformational restriction imposed by both Pro and Amb residues in **9** is highlighted in blue bold bonds.

2.2.4 Results and discussion

Interestingly, the γ-turn stabilization, presumably through bifurcated hydrogen bonding, was realized in the early stage itself. Investigation of the crystal structure of the dipeptide foldamer Boc-Pro-Amb-NHMe **8d** clearly showed the existence of bifurcated hydrogen bond stabilized γ-turn conformation. It should be noted that simple N-acyl prolyl-amide

model peptides are known to exist in multiple conformations, involving γ-turn conformation as one of them, presumably due to the absence of further conformational restriction.[61] A closer inspection of the crystal structure of Boc-Pro-Amb-NHMe **8d** revealed the occurrence of a γ-turn secondary structure with the 1←3 (C_7) H-bonding pattern, between the t-BOC carbonyl [CO(i)], and the aryl amide NH [NH(i+2)] groups (figure 8a). The hydrogen bonding geometry of the γ-turn is well in accordance with the inverse γ-turn pattern ($\phi = -87^0$, and $\psi = 53^0$).

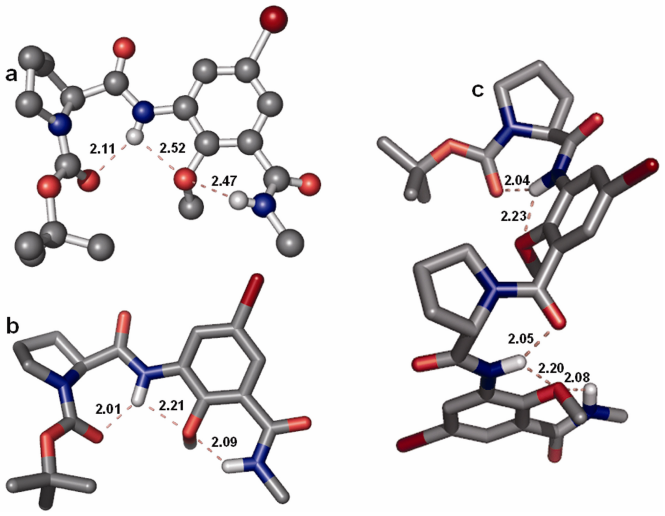

Figure 8: Conformation of the foldamers **8d** and **9** showing bifurcated H-bond stabilized γ-turn motifs: (a) single crystal X-ray structure of **8d**; (b) conformation of **8d** at the HF/6-31G* level of ab initio MO theory; (c) conformation of **9** at the HF/6-31G* level of ab initio MO theory.

Moreover, in addition to its involvement in the S(7)-type 7-membered ring γ-turn formation, the aryl amide NH is also engaged in a S(5) type hydrogen bonding[57] with the aromatic carbonyl oxygen, resulting in the formation of a bifurcated hydrogen bonding that presumably stabilizes the γ-turn conformation. As noted earlier, in the absence of further conformational restriction, simple N-acyl prolyl-amide model peptides are known to exist in multiple conformations, involving γ-conformation as one of them.[61] As expected, the C-terminal S(6) type hydrogen bonding[57] involving aromatic carbonyl and NHMe was extant. The Pro-Amb motif-based tetrapeptide foldamer **9** could not be

crystallized, despite best efforts. However, it was possible to confirm the essential structural aspects by NMR data and by theoretical calculations. The theoretical conformational analysis strongly suggests the occurrence of periodic γ-turn motifs in **9**, as observed in the crystal structure of the shorter analog **8d** (figure 8c).

The conformation of both di- and tetrapeptide foldamers **8d** and **9** in solution was investigated by 2D ROESY NMR studies (500 MHz, $CDCl_3$) that strongly suggested the prevalence of γ-turn conformation, similar to the one observed in the solid state of **8d**, as evidenced from the characteristic ROE interactions.

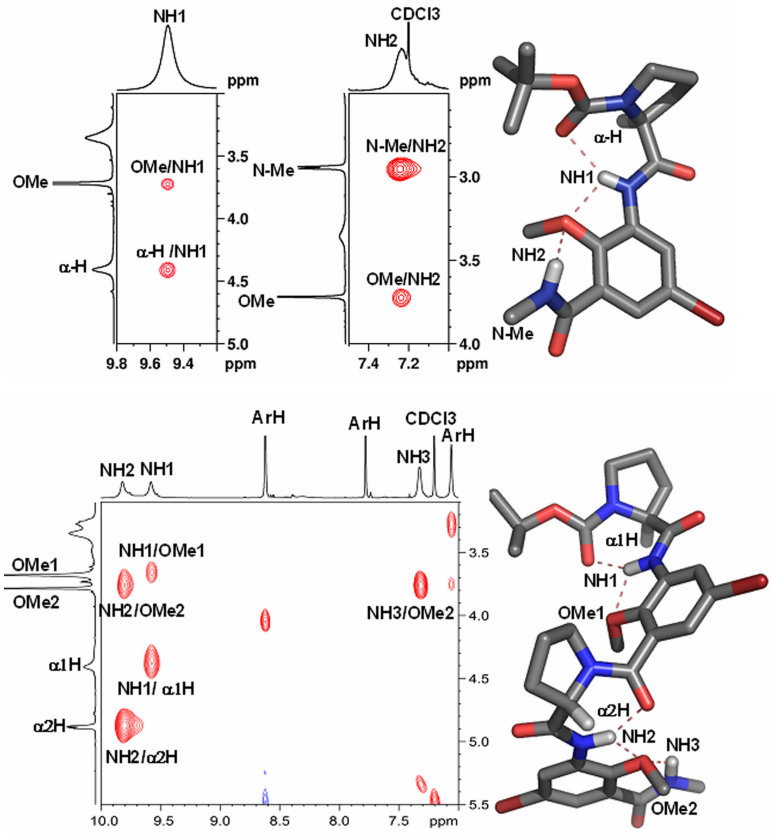

Figure 9: Partial 2D ROESY spectra of **8d** (top) and **9** (bottom) (500 MHz, $CDCl_3$) showing characteristic nOe interactions. Ab initio models of both **8d** and **9** with selected labeled atoms are also shown for aiding easy signal assignments.

One of the most characteristic nOe interactions that can be anticipated for a 1←3 (C_7) H-bonded γ-turn conformation for the foldamers, as observed in the solid state-state

structure of **8d**, would be the requirement of dipolar coupling between proline α-CH vs aryl-NH of adjacent residues. Analysis of the 2D ROESY data indeed revealed the existence of proline α-CH vs aryl-NH dipolar couplings of the adjacent residues in **8d** (α-CH/NH1) and in **9** (NH1/α1-CH, and NH2/α2-CH), as anticipated (figure 9). Furthermore, the characteristic nOes between aryl-NH and the adjacent O-aryloxymethyls in **8d** (OMe/NH1) and in **9** (NH1/OMe1, NH2/OMe2, and NH3/OMe2) also strongly suggested their syn orientation, thereby making room for the S(5) type hydrogen bonded arrangement, a common feature in O-alkoxy arylamines and a prerequisite for the bifurcated hydrogen bonding.[2e,56]

In an effort to confirm that intramolecular hydrogen bonds are clearly prevalent in solution, we also performed [D_6]DMSO titration studies and dilution studies of **8d** and **9**.

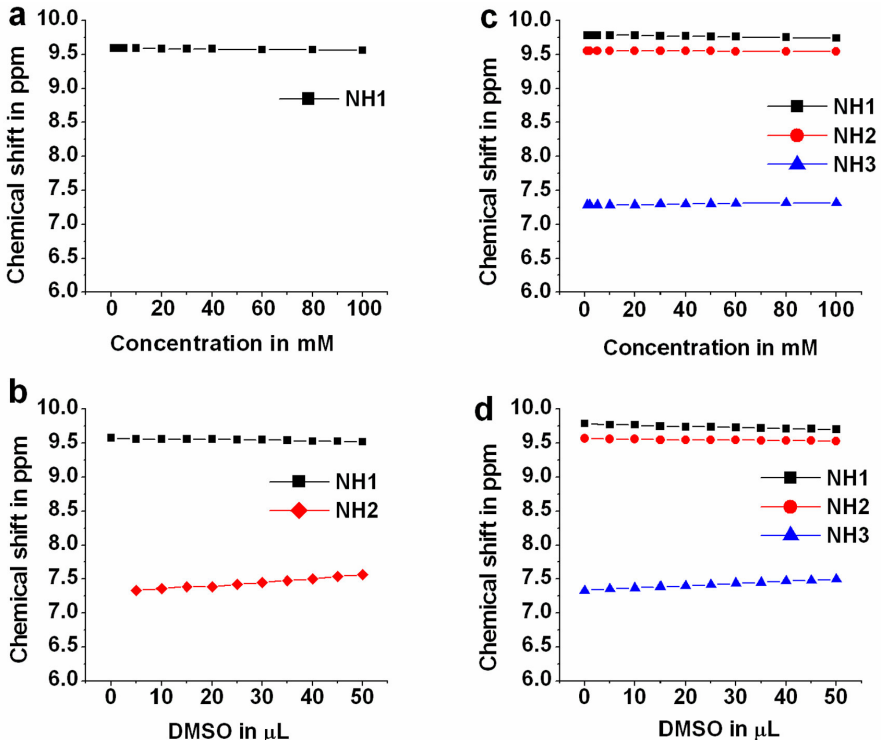

Figure 10: [D_6]DMSO titration and $CDCl_3$ dilution studies of **8d** and **9**. (a), (c) $CDCl_3$ dilution graph of **8d** and **9** respectively; (b), (d) [D_6]DMSO titration graph of **8d** and **9** respectively. *Note*: Due to its overlapping with residual $CHCl_3$, dilution effect on NH_2 in **8d** could not be monitored clearly.

The chemical-shift changes of all the amide protons are presented in figure 10. Notably, all the NH signals of both **8d** and **9** appear at downfield region (figure 10) suggesting their involvement in extensive hydrogen bonding interactions. Remarkably, the protons involved in γ-turn formation show little shift when solutions of **8d** and **9** were titrated gradually with [D_6]DMSO ($\Delta\delta < 0.09$ ppm) or diluted from 100 mM to 1 mM ($\Delta\delta < 0.04$ ppm), suggesting their strong involvement in intramolecular hydrogen bonding. In contrast, the chemical shifts of C-terminal methyl amide protons that partake in S(6) type[57] hydrogen bonding interactions undergo relatively larger chemical shift changes [**8d** (NH_2: $\Delta\delta = 0.24$ ppm), **9** (NH_3: $\Delta\delta = 0.17$ ppm)], on incremental addition of [D_6]DMSO. These results suggest that the amide protons involved γ-turn formations are strongly masked by intramolecular hydrogen bondings.

2.3 Aib-rich Sheet-Forming Abiotic Foldamers

α-Aminoisobutyric (Aib) is a α, α-disubstituted amino acid. It is present in antibiotics of fungal origin, eg. alamethecin and some lantibiotics. It is widely distributed in polypeptide antibiotics produced by diverse species of soil fungi and is one of the nonproteinogenic amino acids and rather rare in nature. Nonproteinogenic amino acids are either not found in proteins, or not coded for in the standard genetic code (like hydroxyproline and selenomethionine). These amino acids often results from posttranslational modification of proteins. Aib and it's homolog isovaline (Iva) are components of amino acid mixtures found in meteorites and have been used as indicator for extraterrestrial origin of rock samples.[62] A high proportion of Aib residue is found in peptaibol class of antibiotics produced by several fungal strains.[63] The structure of the natural peptides such as alamethicin,[64] zervamacin,[65] etc. are largely helical even when the sequence is interspersed with several Pro/Hyp residues due to the presence of Aib in the sequence.

Aib residue has a high propensity to form helical structures. The introduction of Aib residues into polypeptide chains limits the range of accessible conformations and

nucleates β-turns and helical structures and facilitates crystallization presumably by restricting conformational flexibility in crystal lattice.[66] The stereochemical consequences of introducing Aib into peptide chains was extensively investigated by Toniolo and Balaram.[67] Balaram et al. has shown the occurrence of 3_{10}-helical conformation for the Aib oligopeptide Tosyl–$(Aib)_5$–OMe by X-ray crystallography.[68] A 3_{10}-helical structure for p-BrBz-$(Aib)_{10}$-OtBu (p-BrBz = p-bromobenzoyl, O-tBu = tert-butoxy) conformation, stabilised by eight intramolecular $4 \rightarrow 1$ hydrogen bonds was reported by Toniolo et al.[69] In case of mixed peptide sequences such as Boc–Aib–$(Ala–Leu–Aib)_3$–OMe, the peptide adopts a mixed $3_{10}/\alpha$-helical structure with $4 \rightarrow 1$ hydrogen bonds (3_{10}) favored at the N-terminus and $5 \rightarrow 1$ hydrogen bonds (α) occurring at the C-terminus.[70] The decapeptide Boc–Leu–Aib–Val–Ala–Leu–Aib–Val–Ala–Leu–Aib–OMe adopts an almost perfect α-helical conformation stabilized by seven intramolecular $5 \rightarrow 1$ hydrogen bonds.[66] In general, the distinction between 3_{10}, α and mixed helical structures are based on the choice of the intramolecular hydrogen bond type. Relatively small variations in ϕ, ψ dihedral angles can result in switching of $4 \rightarrow 1$ and $5 \rightarrow 1$ hydrogen bonds.

In sequences with relatively less Aib residues, a mixed $3_{10}/\alpha$-helical structure or α-helical structure is prominent.[71] Multiple helical structures have been observed in asymmetric crystallographic unit which adopt different hydrogen bonding pattern.[71,72] It appears that the activation barrier required for the transformation of 3_{10} helical turns into α-helical turns is small, facilitating facile interconversion in solution.

2.3.1 Objective

In the previous section, it was shown that oligomer of Pro-Amb residue adopts double γ-turn conformation. Therefore it was anticipated that introduction of a different amino acid in the sequence should alter the globular conformation of the foldamer. In this context, we have designed and synthesized oligomers containing repeating Aib-Amb motif and studied their folding pattern.

2.3.2 Design

The foldamers, derived from conformationally constrained α-aminoisobutyric acid (Aib) and 3-amino-5-bromo-2-methoxy benzoic acid (Amb)[73] residues (Aib-Amb motif **11a**), were designed anticipating that the corresponding oligomers **12a**, **13a**, and **14** would adopt a well-defined, compact, three dimensional structure, governed by a combined conformational restriction imposed by the constrained Aib and Amb residues (figure 11).

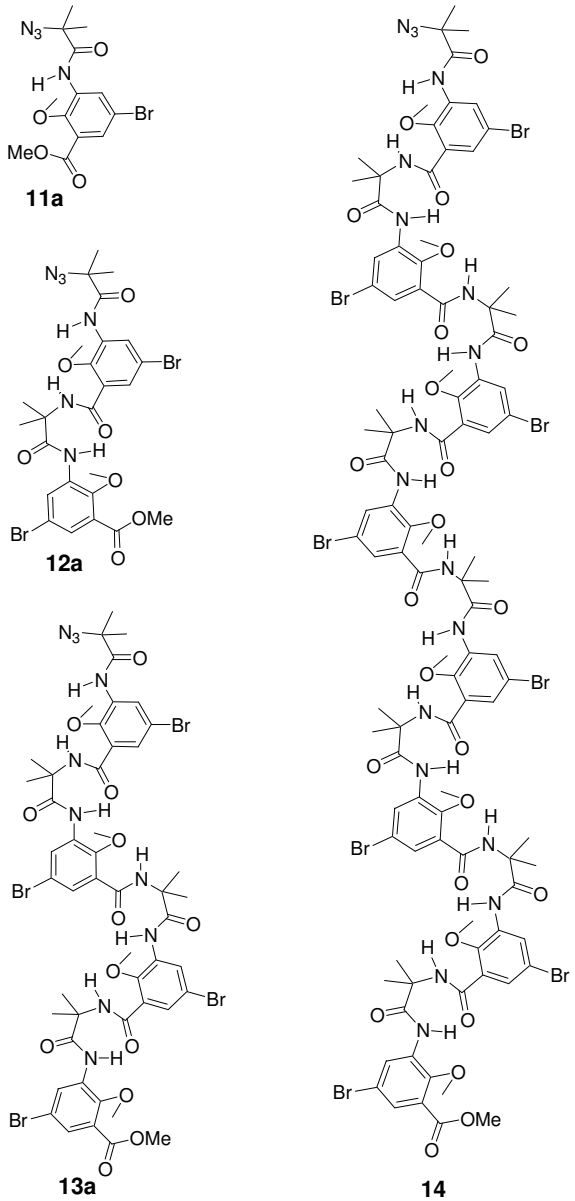

Figure 11: Molecular structure of dipeptide **11a**, tetrapeptide **12a**, octapeptide **13a**, and hexadecapeptide **14** foldamers synthesized in this study.

Whereas the achiral Aib residue is known to play a key role[74] in the conformational restriction of polypeptides due to its overwhelmingly constrained phi ($\phi \pm 60^0$) and psi ($\psi \pm 30^0$) torsion angles, the backbone-rigidified aromatic amino acid residue Amb and its analogs[2e] are known to induce a crescent conformation in its oligomers via localized S(5) and S(6) type[57] hydrogen bonding interactions. Thus, we reasoned that hetero-oligomers made of Aib-Amb repeat motif might also display conformational rigidity. The bromine atoms on the periphery of the aromatic nuclei in the foldamers were meant to aid crystallization easier and to improve the quality of crystal data, due to the presence of heavy bromine atoms.[75] It is noteworthy that one of the biggest challenges in the structural investigation of large synthetic oligomers is their resistance to yield to crystal formation.

2.3.3 Synthesis

In order to assemble the oligomer containing Aib-Amb as repeating units we attempted to couple the hydrochloride salt of 3-Amino-5-bromo-2-methoxy-benzoic acid (Amb), with Boc- and Cbz-Aib using different coupling agents such as TBTU, DCC, and IBCF (scheme 4). Curiously enough, all efforts to couple BOC-Aib-OH with H-Amb-OMe was unsuccessful, under variety of coupling conditions, which prompted us to use different coupling strategy.

Scheme 4:

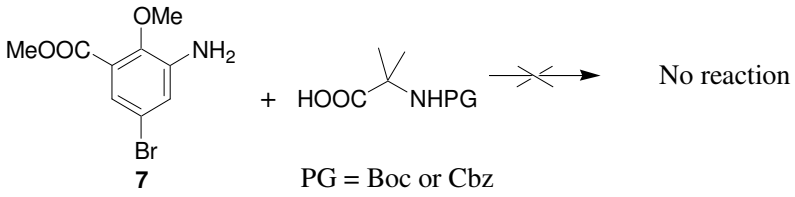

According to this strategy, 2-bromo-2-methylpropanoyl bromide was coupled with 3-amino-5-bromo-2-methoxy-benzoic acid methyl ester to obtain **10** (scheme 5).

Scheme 5:

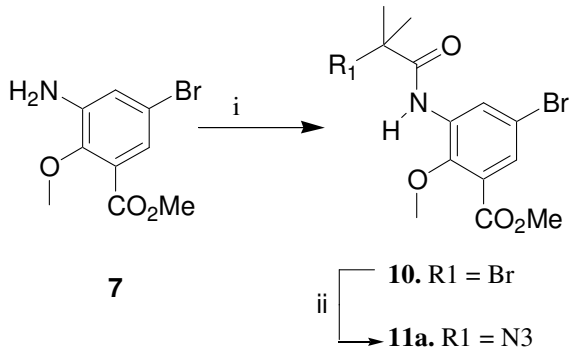

Reagents and conditions: (i) 2-Bromo-2-methylpropanoyl bromide, DIEA, DCM; (ii) LiN_3, DMSO, 40^0C, 48 h.

10 was then subjected to reaction with sodium azide in DMSO for nucleophilic substitution of bromine with azide group. But the reaction was not complete even after 72 hours at 50^0C using excess of sodium azide. Use of lithium azide for the nucleophilic substitution reaction gave us good result and the reaction was complete after heating the reaction mixture at 40-50^0C for 48 hours in DMSO. Having the azide **11a** in hand, we attempted the reduction of the azide **11a** using triphenyl phosphine and water (scheme 6). But the reaction gave us mixture of products and starting material was not fully consumed as was observed from TLC.

Scheme 6:

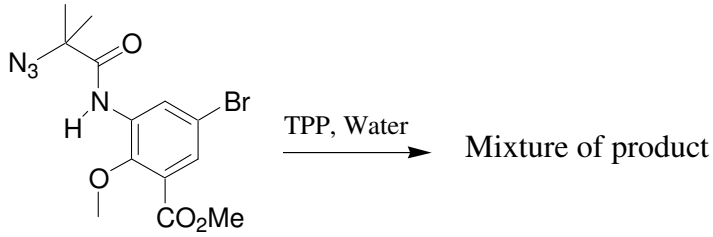

11a

Finally **11a** was reduced with stannous chloride to obtain the free amine **11b**. We further proceeded for the synthesis of the higher oligomers by segment doubling strategy (scheme 7).

Scheme 7:

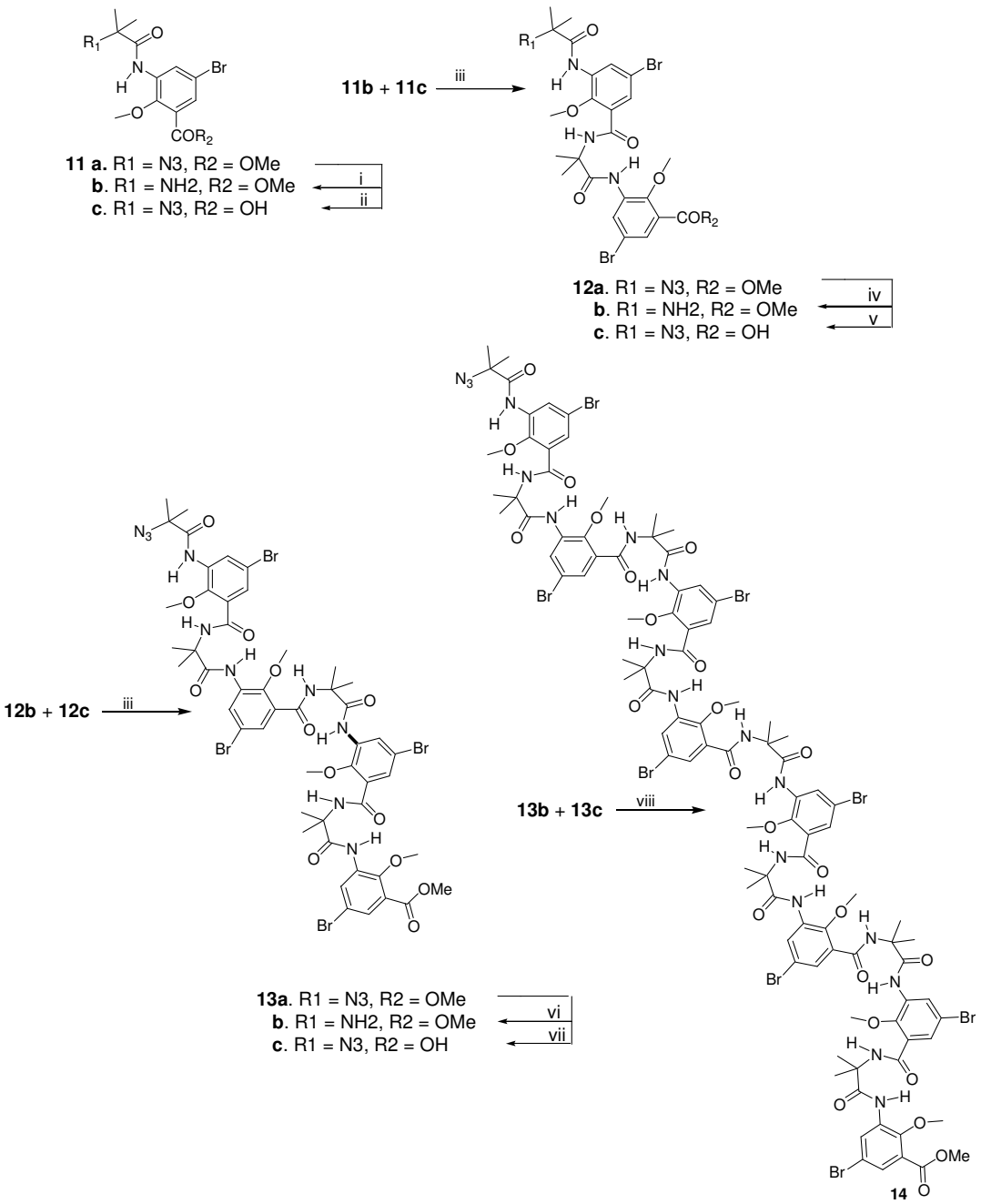

Reagent and condition: (i) 2 equiv. $SnCl_2.2H_2O$, MeOH, 40^0C, 5 h; (ii) 1.5 equiv. $LiOH.H_2O$, aq. MeOH, 18 h; (iii) TBTU, MeCN, DIEA, rt, 12 h; (iv) $SnCl_2.2H_2O$, MeOH, 60^0C, 5 h; (v) 2.5 equiv. $LiOH.H_2O$, aq. MeOH, 18 h; (vi) 6 equiv. $SnCl_2.2H_2O$, MeOH, reflux, 48 h; (vii) 3 equiv. $LiOH.H_2O$, MeOH, dioxane, water, 24 h; (viii) TBTU, MeCN, DCM, DIEA, rt, 12 h.

11a was hydrolyzed using lithium hydroxide as base to afford **11c**. The free acid **11c** and amine **11b** were then coupled using TBTU to obtain the tetrapeptide **12a**. The tetrapeptide **12a** was then reduced to free amine **12b** and and ester group of **12a** was hydrolysed to furnish **12c**. Coupling of **12b** and **12c** gave the octapeptide foldamer **13a**. The hexadecapeptide **14** was obtained by coupling **13b** and **13c** with TBTU as coupling agent. But **14** was only sparingly soluble in DMSO, making it a difficult task to achieve higher oligomers.

2.3.4 Results and discussion

The solubility profile of the oligomers was noted to be progressively deteriorating with increase in size of the oligomer; a fact that is presumably due to extensive aggregation in higher order oligomers. This fact is also vindicated by the results of investigation of the oligomers **12a, 13a** and **14** by Transmission Electron Microscopy (TEM), (*vide infra*). It is noteworthy that increasing tendency of oligomers to self-aggregate is known to be paralleled by a decrease in their solubility profile.[76] The hexadecapeptide foldamer **14** was only sparingly soluble in DMSO. Due to this reason, the synthesis of oligomers larger than the hexadecapeptide foldamer **14** could not be undertaken.

The ^{1}H NMR spectra of the monomer, dimer, tetramer and octamer showed well resolved set of signals showing that they exist in single conformation. Among the oligomers, the tetrapeptide foldamer **12a** crystallized from methanol in monoclinic space group $P2_1/c$, although the higher order oligomers did not yield crystals suitable for single crystal X-ray studies; despite best efforts. Investigation of the crystal structure of **12a** revealed that the intrinsically constrained Aib residues imposed significant twist on the foldamer backbone, as expected, with ϕ and ψ torsion angles of the central Aib residue close to 52^0. This effect was also noted in the previously reported hetero foldamers containing Aib residues reported from our laboratory.[77] Detailed analysis of the crystal structure further revealed self-assembly of the individual strands of the oligomer **12a** (figure 12). The self-complementary individual strands of **12a** undergo self-assembly through intermolecular N–H···O=C hydrogen bonding interactions to afford extended sheet-like

structure; an observation that could provide insights for developing such templates into potential protein-β-sheet mimetics.

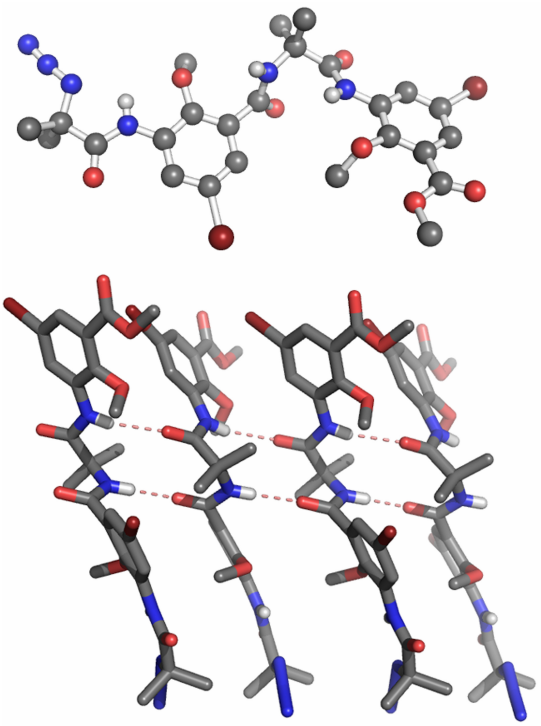

***Figure 12**:* Crystal structure of foldamer **12a** (top, ball and stick representation) and its H-bond-mediated self-assembled structure (bottom, caped stick representation). Hydrogens, other than at the hydrogen bonding sites, have been omitted for clarity.

It may be mentioned here that a similar arrangement is also seen in a recently reported novel acryalmide oligomer-based protein-β-sheet-like structure[78] reported from our laboratory. The striking feature of these Aib-rich synthetic hetero oligomers is their ability to form self-assembled sheet-like structures through extensive intermolecular hydrogen bonding interactions from the backbone amide groups; an observation that is in stark contrast to the general observation that Aib is a proven amino acid as a sheet breaker, at least in oligomers composed of α-amino acids.[67b,e] It is noteworthy that sheet forming structural architectures have tremendous implications in the understanding and development of potential therapies for Alzheimer's disease; a leading cause of dementia

in the elderly, which is pathologically defined by the presence of amyloid plaques, composed of the amyloid β-protein, and neurofibrillary tangles.[79] Indeed, scanning of the morphological architecture of the large hexadecapeptide foldamer **14** shows fibril piles composed of entangled nanofibrils, a morphological signature of extensive self-assembly;[80] which is also substantiated by the results of crystal structure studies (*vide infra*).

A closer inspection of the X-ray structure of the tetrapeptide foldamer **12a** revealed the following facts: NH1 forms five membered S(5) type hydrogen bonding with the the nitrogen of the azide group. Furthermore, in addition to its involvement in the S(5)-type 5-membered hydrogen bond formation, the NH1 is also engaged in a S(5) type hydrogen bonding[57] with the aromatic alkoxy oxygen OMe1, resulting in the formation of a bifurcated hydrogen bonding. The molecule adopts a twisted structure and the NH2 is involved in intermolecular hydrogen bonding with carbonyl oxygen of another molecule. NH3 is involved in S(5) type five membered hydrogen boding with the alkoxy oxygen OMe2 of the second aromatic residue. Interestingly, NH3 is also involved in bifurcated hydrogen bonding with carbonyl oxygen of another molecule.

The extended conformation of the individual strands, as noted in the crystal structure of **12a**, is prevalent in solution-state as well, as evidenced from 2D NOESY NMR studies of the oligomers **12a**, and **13a** (figure 13). One of the most characteristic nOe interactions that can be anticipated for an extended conformation, as seen in the crystal structure of **12a**, would be the requirement of sequential dipolar couplings between the protons of adjacent residues of Aib-Me, Ar-NH, Ar-OMe, and Aib-NHs. Such a sequential interaction is clearly observed for both tetrapeptide **12a** and octapeptide **13a**, suggesting the extended conformation of the individual strands; similar to the one observed for **12a** in its crystal structure (**12a**: Aib1 *vs* NH1 *vs* OMe1 *vs* NH2 *vs* Aib2 *vs* NH3 OMe2). Further, we also note a characteristic dipolar coupling between the NHs of adjacent residues in both **12a** and **13a** (Partial 2D NOESY spectra of **12a** and **13a** showing NH *vs* NH coupling is shown in experimental section, page no. 112). Indeed, closer inspection of the crystal structure of **12a** reveals the close proximity of NHs of adjacent residues in

the extended conformation (d: 2.8 Å). However, the poor solubility of the hexadecapeptide foldamer **14**, presumably due to extensive aggregation (self-assembly), rendered its conformational studies by solution-state NMR difficult.

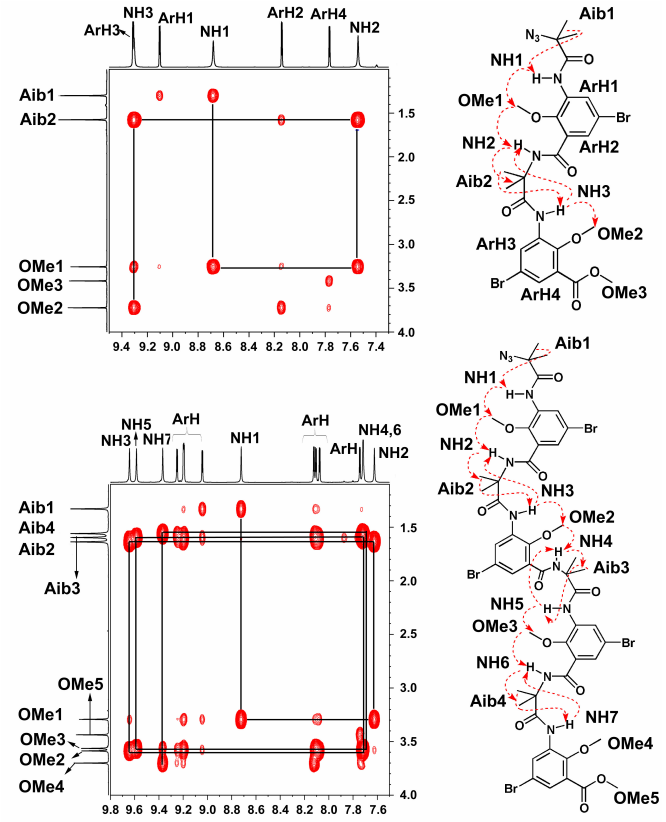

***Figure 13**:* Partial 2D NOESY spectra of **12a** (top) and **13a** (bottom) showing charecteristic nOes. For enabling assignments, the molecular structure with selected numbered atoms are also shown. The dipolar couplings are indicated in red dotted arows.

To investigate the morphological architecture and its effect on the length of the oligomer, we analyzed their self-assembled structures by Transmission Electron Microscopy (TEM). Figures 14A, B, and C show the TEM images of the oligomers **12a**, **13a**, and **14**, respectively, deposited on carbon coated polymer film.

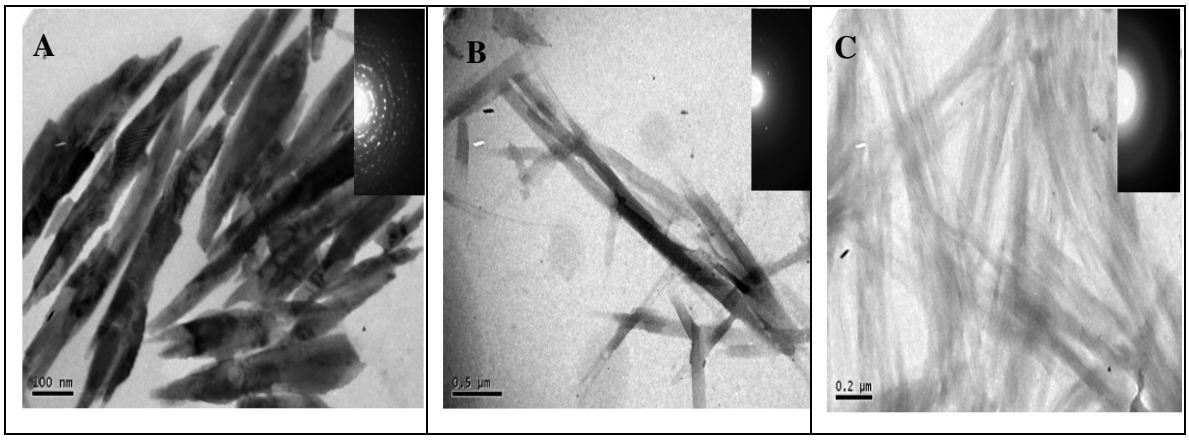

***Figure 14**:* TEM images of the oligomers. (A), (B), and (C): TEM images of the oligomers **12a**, **13a**, and **14**, respectively, deposited on carbon coated polymer film. Corresponding SAED patterns are shown in the inset. *Note:* Full-size figures are available in experimental section (page 114-115).

Comparison of the microscopic images of the oligomers: tetrameric foldamer **12a** *vs* octamer **13a** *vs* hexadecamer **14** reveals an interesting structural aspect. As the oligomer size increases, the morphological architecture transforms from crystalline needle shape (figure 14A) to entangled nanofibrils (figure 14C). In the case of the tetrameric foldamer **12a**, the particles are needle shaped and are flat as evident from the Mòire pattern seen from the overlapping of two needle shaped nanoparticles (indicated by an arrow in figure 14A). Further, the particles of **12a** with size ≈ 400 nm, are crystalline in nature as shown by the SAED pattern in the inset (figure 14A). In the case of octamer **13a**, the size of the particle is ≈ 3 µm and the SAED pattern shown in the inset (figure 14B) is diffused, indicating a loss in the crystalline structure. However, microscopic image of the hexadecamer foldamer **14** (figure 14C) reveals fibril piles composed of entangled nanofibrils, a morphological signature of extensive self-assembly.[80]

2.4 Conclusion

In conclusion, we have developed novel synthetic oligomers that adopt well-defined, compact, three-dimensional architecture, governed by a combined conformational

restriction imposed by the individual amino acids with which they are made of. Conformational investigations by single crystal X-ray studies, solution state NMR, and ab initio MO theory strongly suggest the prevalence of γ-turn motifs in both the di- and tetrapeptide foldamers **8d** and **9**, which are presumably stabilized by strong bifurcated hydrogen bonds in the solid and solution-states. The strategy disclosed herein for the construction of hybrid foldamers with periodic γ-turn motifs has the potential to significantly augment the conformational space available for foldamer design with diverse backbone structures and conformations, and will have a bearing on practical utility. The notable feature of these Aib-rich synthetic oligomers is their ability to form self-assembled sheet-like structures through extensive intermolecular hydrogen bonding interactions from the backbone amide groups; an observation that is in stark contrast to the general observation that Aib is a proven amino acid as a sheet breaker, at least in oligomers composed of α-amino acids. Therefore, these results suggest the utility of hybrid foldamer strategy in modulating conformational preferences of individual amino acids in oligomer sequences. The results of investigation of the morphological architecture of these oligomers further suggest their potential in fabricating novel supramolecular nanoarchitectures. It is noteworthy that sheet promoting structural architectures have tremendous implications in the understanding and development of potential therapies for Alzheimer's disease; a leading cause of dementia in the elderly.[79]

2.5 Experimental Section

General Methods

Unless otherwise stated, starting materials were obtained from commercial suppliers and used without further purification. 5-Bromosalicylic acid 2 and 5-Bromo-2-methoxy-benzoic acid 4 were prepared following the literature procedures.[60] Dry dichloromethane (DCM) was prepared by distillation over P_2O_5. Dry dimethyl sulphoxide (DMSO) and dry acetonitrile (CH_3CN) were freshly prepared by distillation over CaH_2. Dry acetone was freshly distilled over $KMnO_4$ followed by K_2CO_3. Dry reactions were performed under argon atmosphere. Purification by column chromatography was performed in 100-200-mesh silica, unless otherwise stated. NMR spectra were recorded in $CDCl_3$ and d6-DMSO on AC-200 MHz, DRX-400 MHz, DRX-500 MHz Bruker NMR spectrometers. Electrospray ionization mass spectrometry (ESI-MS) was carried out on a Finnigan MAT-1020 mass spectrometer and MALDI-TOF mass spectra on a Voyager-DE STR mass spectrometer. IR spectra, recorded in $CHCl_3$ or nujol were obtained from Perkin–Elmer 68515 PC-FTIR spectrophotometer. Combustion data were recorded on Elmentar-Vario-EL (Heraeus Company Ltd., Germany). Melting points were measured on Buchi 535 melting point apparatus and are uncorrected. Reactions were monitored by thin layer chromatography (TLC) carried out on 0.25 mm E-Merck silica gel plates.

Crystal data for 8d: $C_{19}H_{26}BrN_3O_5$, M= 456.34, crystal size, 0.28 x 0.21 x 0.12 mm^3, T = 297(2) K, crystal system, monoclinic, space group $P2_1$; a = 10.209(2), b = 9.5116(18), c = 11.486(2) Å, β = 95.826(3)°, v = *1109.6(4)* $Å^3$, Z = 2, F(000) = 472, d calc [g cm^{-3}] = 1.366, μ [mm^{-1}] = 1.885, absorption correction, multi-scan, T_{min} = 0.6214; T_{max} = 0.8124; 7929 reflection collected, 3727 unique reflections, 2933 observed reflections, 258 refined parameters, R_1 [$I>2\sigma(I)$] = 0.0418, WR_2 = 0.0961 (all data R = 0.0567, $wR2$ = 0.1032), goodness of fit, 1.016, $\Delta\rho_{max}$, $\Delta\rho_{min}$ (e $Å^{-3}$)= 0.363, -0.264.

Crystal data for 12a: $C_{25}H_{28}Br_2N_6O_7$, M= 684.35, crystal size, 0.84 x 0.14 x 0.13 mm^3, T = 297(2) K, crystal system, monoclinic, space group $P2_1/c$; a = 18.553(4), b = 16.680(4), c = 9.608(2) Å, β = 101.480(4)°, V = 2913.8(11) $Å^3$, Z = 4, F(000) = 1384, d calc [g cm^{-3}] = 1.560, μ [mm^{-1}] = 2.835, absorption correction, multi-scan, T_{min} = 0.1990; T_{max} = 0.7130; 20883 reflection collected, 5136 unique reflections, 4077 observed

reflections, 368 refined parameters, R_1 [I>2σ(I)] = 0.0370, WR_2 = 0.0873 (all data R = 0.0512, wR2 = 0.0942), goodness of fit, 1.008, $\Delta\rho_{max}$, $\Delta\rho_{min}$ (e $Å^{-3}$)= 0.575, -0.528.

5-Bromo-2-methoxy-3-nitro-benzoic acid 5: To a stirred solution of 5-Bromo-2-methoxy-benzoic acid[60] (1 g, 4.33 mmol, 1 equiv.) in conc. H_2SO_4 (6mL) at 0° C, conc. HNO_3 (0.29 ml, 6.49 mmol, 1.5 equiv.) was slowly added and stirred for 30 minutes. The resulting solution was poured into ice-cold water, filtered, washed with water, and dried over P_2O_5 desiccator. The crude product was further purified by recrystallization from aqueous methanol. Yield 0.9 g (75.3 %); mp 176-177 ^{0}C; IR ($CHCl_3$) ν (cm^{-1}): 3020, 2923, 1710, 1681, 1537, 1363; ^{1}H NMR (200 MHz, $CDCl_3$ + Acetone-d_6): δ 8.09 (d, *J* = 2.35 Hz, 1H), 7.90 (d, *J* = 2.74 Hz, 1H), 6.32 (bs, 1H), 3.87 (s, 3H); ^{13}C NMR (50 MHz, DMSO-d_6): δ 164.4, 151.1, 145.9, 137.5, 130.2, 115.2, 64.1; ESI Mass: 299.92 (M + Na^+) ; Anal. Calcd. for $C_8H_6BrNO_5$: C = 34.81, H = 2.19, Br = 28.95, N = 5.07; Found: C = 34.92, H = 1.93, N = 4.91, Br = 29.13.

5-Bromo-2-methoxy-3-nitro-benzoic acid methyl ester 6: To a mixture of 5-Bromo-2-methoxy-3-nitro-benzoic acid **5** (1 g, 3.62 mmol, 1 equiv.) and potassium carbonate (1 g, 7.25 mmol, 2 equiv.) in acetone (10 mL), methyl iodide (0.45 mL, 7.25 mmol, 2 equiv.) was added. The reaction mixture was refluxed for 3 hours, cooled and the solution filtered. The filtrate was stripped off solvent under reduced pressure. The resulting solid was dissolved in ethyl acetate and washed with water and brine. The crude product was purified by column chromatography. Yield 0.8 g (76.1%); mp 63-64 ^{0}C; IR ($CHCl_3$) ν (cm^{-1}): 3024, 2954, 1736, 1541, 1361; ^{1}H NMR (200 MHz, $CDCl_3$): δ 8.1 (d, *J* =2.35 Hz, 1H), 8.0 (d, *J* = 2.34 Hz, 1H), 4.00 (s, 3H), 3.97 (s, 3H); ^{13}C NMR (50 MHz, $CDCl_3$): δ 163.3, 152.3, 145.8, 138.0, 130.9, 128.9, 115.6, 64.2, 52.8; ESI Mass: 313.93 (M + Na^+); Anal. Calcd. for $C_9H_8BrNO_5$: C = 37.27, H = 2.78, Br = 27.55, N = 4.83; Found: C = 37.44, H = 2.69, Br = 27.65, N = 4.96.

3-Amino-5-bromo-2-methoxy-benzoic acid methyl ester hydrochloride salt 7a: To a solution of $SnCl_2.2H_2O$ (2.33 g, 10.3 mmol, 3 equiv.) in ethyl acetate (15 mL), 5-Bromo-2-methoxy-3-nitro-benzoic acid methyl ester **6** (1 g, 3.4 mmol, 1 equiv.) was added and the reaction mixture was heated at 40° C for 6 hours. The reaction mixture was poured into saturated sodium bicarbonate solution. The suspension was filtered through celite and the organic layer was separated. The water layer was further extracted with ethyl

acetate (2x30 ml). The combined organic layer was sequentially washed with water, and brine and dried over sodium sulphate. After removing the solvent under vacuum, the crude free amine was treated with methanol containing 1% thionyl chloride at 0^0 C. The solid hydrochloride salt was filtered and dried in KOH desiccator and was used without further purification in the next step. Yield 0.95 g (88.4%).

Methyl 5-bromo-3-(1-(tert-butoxycarbonyl)pyrrolidine-2-carboxamido)-2-methoxybenzoate 8a: To an ice-cold stirred solution of Boc-proline (0.94 g, 4.4 mmol, 1 equiv.) and 3-amino-5-bromo-2-methoxy-benzoic acid methyl ester hydrochloride salt (1.3 g, 4.4 mmol, 1 equiv.) in dry acetonitrile (10 mL), DIEA (2.25 mL, 13.1 mmol, 3 equiv.) was added followed by the addition of TBTU (1.69 g, 5.3 mmol, 1.2 equiv.). The resulting reaction mixture was stirred overnight at room temperature. The solvent was stripped off under reduced pressure. The residue was dissolved in dichloromethane (80 mL) and washed sequentially with potassium hydrogen sulphate solution, saturated sodium bicarbonate and water. Drying and concentration in vacuum yielded the crude ester **2a**, which was directly used for the next reactions without further purification.

Methyl 5-bromo-2-methoxy-3-(pyrrolidine-2-carboxamido)benzoate, hydrochloride salt 8b: To an ice cold solution of **8a** (0.9 g, 1.97 mmol) in dry dioxane (5 mL) dry HCl gas was passed for fifteen minutes. The solvent was stripped off under reduced pressure and the residue dried under KOH desiccator overnight. The crude product was used for the next step without further purification.

5-Bromo-3-(1-(tert-butoxycarbonyl)pyrrolidine-2-carboxamido)-2-methoxybenzoic acid 8c: To a solution of **8a** (0.9 g, 1.97 mmol, 1 equiv.) in methanol (15 mL) was added $LiOH{\cdot}H_2O$ (0.33 g, 7.89 mmol, 4 equiv.) in water (4 mL) and the reaction mixture was stirred for 24 hours. The solvent was stripped off under reduced pressure and the product dried under P_2O_5 vacuum desiccators overnight. The crude product was used for the next step without further purification.

Tert-butyl 2-[5-Bromo-2-methoxy-3-(methylcarbamoyl) phenyl carbamoyl] pyrrolidine-1-carboxylate 8d: The crude ester **8a** was taken in a RB containing saturated methanolic methylamine solution (15 mL) and stirred at room temperature for 24 hrs. The solvent was removed under reduced pressure, and the crude product was purified by column chromatography to furnish **8d**. Yield 1.46 g (73 %); mp 135-137 ^{0}C;

$[\alpha]_D$ = -66.5 (c = 1.1, MeOH); IR ($CHCl_3$) ν (cm^{-1}): 3408, 3304, 3014, 2980, 1693, 1662, 1527, 1414, 1215 ; ^1H NMR (400 MHz, $CDCl_3$): δ 9.6 (s, 1H), 8.7 (d, *J* = 2.75 Hz, 1H), 7.8 (d, *J* = 2.75 Hz, 1H), 7.3 (bs, 1H), 4.5 (m, 1H), 3.8 (s, 3H), 3.4 (m, 2H), 3.0 (d, *J* = 4.88, 3H), 2.5 (m, 1H), 1.9 (m, 3H), 1.5 (s, 9H); ^{13}C NMR (50 MHz, $CDCl_3$): δ 170.3, 164.4, 156.3, 145.8, 133.1, 127.9, 127.7, 125.7, 117.8, 80.7, 62.3, 60.8, 47.2, 28.2, 27.2, 26.6, 24.4; MALDI-TOF: 456.5 (M+); Anal. Calcd. for $C_{19}H_{26}BrN_3O_5$: C = 50.01%, H = 5.74, Br = 17.51, N = 9.21; Found: C = 49.84, H = 5.93, Br = 17.89, N = 8.92.

Tert-butyl 2-(5-bromo-3-(2-(5-bromo-2-methoxy-3- [(methylcarbamoyl) phenylcarbamoyl) pyrrolidine-1-carbonyl)-2-methoxyphenylcarbamoyl)] pyrrolidine-1-carboxylate 9: To an ice-cold stirred solution of the acid **8c** (0.7 g, 1.6 mmol, 1 equiv.) and amine **8b** (0.56 g, 1.6 mmol, 1 equiv.) in dry acetonitrile (8 mL), DIEA (0.68 mL, 3.9 mmol, 2.5 equiv.) was added followed by the addition of TBTU (0.71 g, 2.2 mmol, 1.4 equiv.). The resulting reaction mixture was stirred overnight at room temperature. The solvent was stripped off under reduced pressure; the residue was dissolved in dichloromethane (50 mL) and washed sequentially with potassium hydrogen sulphate solution, saturated sodium bicarbonate, and water. Drying and concentration in vacuum yielded the crude ester, which was directly used for the next amidation reaction, without further purification. The crude ester was taken in a RB containing saturated methanolic methylamine solution (15 mL) and stirred at room temperature for 24h. The solvent was removed under reduced pressure, and the crude product was purified by column chromatography to furnish **9**. Yield 0.78 g (63 %); mp 98-100 ^0C; $[\alpha]_D$ = - 76.0 (c = 1.0, MeOH); IR ($CHCl_3$) ν (cm^{-1}): 3414, 3292, 3256, 3018, 2981, 1693, 1666, 1659, 1595, 1537, 1529, 1516, 1454, 1414, 1369; ^1H NMR (500 MHz, $CDCl_3$): δ 9.9 (s, 1H), 9.6 (s, 1H), 8.7 (d, *J* = 2.51, 2H), 7.8 (d, *J* = 2.51, 1H), 7.4 (d, *J* = 4.27, 1H), 7.1 (s, 1H), 5.0 (s, 1H), 4.5 (m, 1H), 3.8 (s, 3H), 3.7 (s, 3H), 3.4-3.3 (m, 4H), 3.0 (d, *J* = 4.86, 3H), 2.7 (m, 1H), 2.5 (m, 1H), 2.1-1.9 (m, 6H), 1.5 (s, 9H); ^{13}C NMR (125 MHz, $CDCl_3$): δ 170.4, 168.7, 168.2, 164.3, 156.5, 146.1, 144.0, 133.6, 133.2, 130.4, 128.4, 128.0, 126.0, 124.4, 118.2, 117.5, 81.0, 62.6, 62.4, 60.8, 48.9, 47.3, 28.3, 27.3, 26.7, 24.8, 24.6; MALDI-TOF: 805.0 (M+ Na); Anal. Calcd. for $C_{32}H_{39}Br_2N_5O_8$: C = 49.18, H = 5.03, Br = 20.45, N = 8.96; Found: C = 49.32, H = 4.99, Br = 20.19, N = 8.81.

Methyl 5-bromo-3-(2-bromo-2-methylpropanamido)-2-methoxybenzoate 10: To a ice cold solution of hydrochloride salt of methyl 3-amino-5-bromo-2-methoxybenzoate **7** (3.30 g, 11.2 mmol, 1 equiv) and N,N'-diisopropylethylamine, DIEA (5.72 mL, 33.3 mmol, 3 equiv) in dry DCM (10 mL) was added slowly bromo isobutyryl bromide (1.65 mL, 13.4 mmol, 1.2 equiv). The reaction mixture was allowed to come at room temperature and stirred for additional 12 hrs. The reaction mixture was diluted with DCM (100 mL) and washed sequentially with saturated sodium bicarbonate, dil. HCl and brine solution. The organic layer was dried over Na_2SO_4, filtered and solvent was stripped off under reduced pressure. The crude product was purified by column chromatography. Yield 4.28 g (93.8%); mp 41 ^{0}C; IR ($CHCl_3$) ν (cm^{-1}): 3367, 3107, 3022, 2986, 2951, 1732, 1693, 1514, 1421, 1317, 1275, 1227, 1149, 991; ^{1}H NMR (200 MHz, $CDCl_3$): δ 9.27 (s, 1H), 8.73 (d, *J* = 2.52 Hz, 1H), 7.73 (d, *J* = 2.53 Hz, 1H), 3.94 (s, 3H), 3.93 (s, 3H), 2.05 (s, 6H); ^{13}C NMR (50 MHz, $CDCl_3$): δ 169.9, 164.2, 148.2, 133.4, 128.6, 126.0, 124.6, 116.8, 62.5, 62.2, 52.4; ESI Mass: 411.2 (M^+); Anal. Calcd. For $C_{13}H_{15}Br_2NO_4$: C = 38.17, H = 3.70, N = 3.42; Found: C = 38.27, H = 3.51, N = 3.57.

Methyl 3-(2-azido-2-methylpropanamido)-5-bromo-2-methoxybenzoate 11a: To a solution of **10** (4.09 g, 10 mmol, 1 equiv) in dry DMSO (15 mL) was added lithium azide (2.45 g, 50 mmol, 5 equiv) and the reaction mixture was heated at 40 ^{0}C for 48 hrs. The reaction mixture was cooled and added to water. The water layer was extracted with ethyl acetate. The combined organic layer was given water and brine wash. The organic layer was dried over Na_2SO_4, filtered and solvent was stripped off under reduced pressure. The crude product was purified by column chromatography. Yield 3.2 g (86.2%); mp 60-61 ^{0}C; IR ($CHCl_3$) ν (cm^{-1}): 3377, 3022, 2980, 2953, 2116, 1732, 1693, 1514, 1421, 1315, 1269, 1149, 991; ^{1}H NMR (200 MHz, $CDCl_3$): δ 9.07 (s, 1H), 8.76 (d, *J* = 2.53 Hz, 1H), 7.71 (d, *J* = 2.52 Hz, 1H), 3.93 (s, 3H), 3.90 (s, 3H), 1.63 (s, 6H); ^{13}C NMR (50 MHz, $CDCl_3$): δ 170.3, 164.1, 148.2, 133.0, 128.4, 126.1, 124.6, 116.6, 64.6, 62.1, 52.2, 24.2; ESI Mass: 371.3 (M + 1), 393.4 (M + Na); Anal. Calcd. For $C_{13}H_{15}BrN_4O_4$: C = 42.07, H = 4.07, N = 15.09; Found: C = 42.26, H = 4.23, N = 15.28.

Methyl 3-(2-amino-2-methylpropanamido)-5-bromo-2-methoxybenzoate 11b: To a stirred suspension of $SnCl_2.2H_2O$ (3.29 g, 14.6 mmol, 2 equiv.) in methanol (15 mL) was added **11a** (2.71 g, 7.3 mmol, 1 equiv.) and the reaction mixture was heated at 40 ^{0}C for 5

hrs.[81] Methanol was removed under reduced pressure. The residue was dissolved in ethyl acetate (50 mL) and slowly added to a saturated sodium bicarbonate solution. Filtered through celite and organic layer separated. The water layer was further extracted with ethyl acetate (2 x 30 mL). The combined organic layer was given water and brine wash (2 x 50 mL each). The organic layer was dried over Na_2SO_4 and used for next step without further purification. Yield 2.46 (97.6%).

3-(2-Azido-2-methylpropanamido)-5-bromo-2-methoxybenzoic acid 11c: To a solution of **11a** (2.71 g, 7.3 mmol, 1 equiv.) in methanol (25 mL) was added $LiOH.H_2O$ (0.63 g, 15 mmol, 1.5 equiv.) in water (5 mL) and stirred for 18 hrs. The solvent was stripped off under reduced pressure. To the residue was added water (50 mL) and acidified with dilute HCl. The water layer was extracted with ethyl acetate (3 x 50 mL). The combined organic layer was given water and brine wash, dried over Na_2SO_4 and used for next reaction without further purification. Yield 2.52 (96.6%).

Methyl 3-(2-(3-(2-azido-2-methylpropanamido)-5-bromo-2-methoxybenzamido)-2-methylpropanamido)-5-bromo-2-methoxybenzoate 12a: To an ice-cold stirred solution of the acid **11c** (2.5 g, 7 mmol, 1 equiv.) and amine **11b** (2.42 g, 7 mmol, 1 equiv.) in dry acetonitrile (15 mL), DIEA (1.80 mL, 10.5 mmol, 1.5 equiv.) was added followed by the addition of TBTU (2.70 g, 8.4 mmol, 1.2 equiv.). The resulting reaction mixture was stirred overnight at room temperature. The solvent was stripped off under reduced pressure; the residue was dissolved in dichloromethane (100 mL) and washed sequentially with dilute HCl, saturated sodium bicarbonate, and water. Drying and concentration in vacuum yielded the crude ester, which was purified by column chromatography to furnish **12a**. Yield 3.42 g (71.3%); mp 163-164^{0}C; IR ($CHCl_3$) ν (cm^{-1}): 3375, 3020, 2978, 2943, 2118, 1730, 1697, 1518, 1412, 1315, 1217, 1149, 987; ^{1}H NMR (400 MHz, $CDCl_3$): δ 9.10 (s, 1H), 8.92 (s, 1H), 8.78 (d, *J* = 2.26 Hz, 1H), 8.72 (d, *J* = 2.51 Hz), 8.05 (s, 1H), 7.89 (d, *J* = 2.51 Hz, 1H), 7.71 (d, *J* = 2.51 Hz, 1H), 3.93 (s, 3H), 3.92 (s, 3H), 3.86 (s, 3H), 1.79 (s, 6H), 1.67 (s, 6H); ^{13}C NMR (100 MHz, $CDCl_3$): δ 172.1, 170.4, 164.4, 163.3, 148.3, 146.3, 133.7, 132.3, 128.5, 128.4, 127.2, 126.8, 126.3, 124.6, 118.5, 116.8, 64.8, 62.5, 62.4, 58.4, 52.4, 25.2, 24.4; ESI Mass: 685.1 (M + 1), 707.0 (M + Na), 723.0 (M + K); Anal. Calcd. For $C_{25}H_{28}Br_2N_6O_7$: C = 43.88, H = 4.12, N = 12.28; Found: C = 43.73, H = 4.21, N = 12.19.

Methyl 3-(2-(3-(2-amino-2-methylpropanamido)-5-bromo-2-methoxybenzamido)-2-methylpropanamido)-5-bromo-2-methoxybenzoate 12b: To a stirred suspension of $SnCl_2.2H_2O$ (2.87 g, 12.7 mmol, 2 equiv.) in methanol (20 mL) was added **12a** (2.9 g, 4.2 mmol, 1equiv.) and the reaction mixture was heated at 60 ^{0}C for 5 hrs. Methanol was removed under reduced pressure. The residue was dissolved in ethyl acetate (70 mL) and slowly added to a saturated sodium bicarbonate solution. Filtered through celite and organic layer separated. The water layer was further extracted with ethyl acetate (2 x 30 mL). The combined organic layer was given water and brine wash (2 x 50 mL each). The organic layer was dried over Na_2SO_4 and used for next step without further purification. Yield 2.65 g (95%).

3-(2-(3-(2-Azido-2-methylpropanamido)-5-bromo-2-methoxybenzamido)-2-methylpropanamido)-5-bromo-2-methoxybenzoic acid 12c: To a solution of **12a** (2.95 g, 4.3 mmol, 1 equiv.) in methanol (40 mL) was added $LiOH.H_2O$ (0.45 g, 10.8 mmol, 2.5 equiv.) in water (5 mL) and stirred for 18 hrs. The solvent was stripped off under reduced pressure. To the residue was added water (50 mL) and acidified with dilute HCl. The water layer was extracted with ethyl acetate (3 x 50 mL). The combined organic layer was given water and brine wash, dried over Na_2SO_4 and used for next reaction without further purification. Yield 2.75 g (95.2%).

Methyl 3-(2-(3-(2-(3-(2-(3-(2-azido-2-methylpropanamido)-5-bromo-2-methoxybenzamido)-2-methylpropanamido)-5-bromo-2-methoxybenzamido)-2-methylpropanamido)-5-bromo-2-methoxybenzamido)-2-methylpropanamido)-5-bromo-2-methoxybenzoate 13a: To an ice-cold stirred solution of the acid **12c** (2.63 g, 3.9 mmol, 1equiv.) and amine **12b** (2.58 g, 3.9 mmol, 1 equiv.) in dry acetonitrile (15 mL), DIEA (1 mL, 5.9 mmol, 1.5 equiv.) was added followed by the addition of TBTU (1.51 g, 4.7 mmol, 1.2 equiv.). The resulting reaction mixture was stirred overnight at room temperature. The solvent was stripped off under reduced pressure; the residue was dissolved in dichloromethane (100 mL) and washed sequentially with dilute HCl, saturated sodium bicarbonate, and water. Drying and concentration in vacuum yielded the crude ester, which was purified by column chromatography to furnish **13a**. Yield 3.52 g (68.4%); mp 213-215^{0}C; IR ($CHCl_3$) ν (cm^{-1}): 3371, 3018, 2978, 2941, 2118, 1693, 1668, 1514, 1456, 1410, 1313, 1215, 982; ^{1}H NMR (400 MHz, $CDCl_3$): δ 9.75 (s, 1H), 9.69 (s,

1H), 9.45 (s, 1H), 9.36 (d, *J* = 2.51, 1H), 9.31 (m, 2H), 9.14 (d, *J* = 2.51, 1H), 8.73 (s, 1H), 8.22 (d, *J* = 2.51, 1H), 8.19 (d, *J* = 2.51, 1H), 8.15 (d, *J* = 2.51, 1H), 7.80 (d, *J* = 2.51, 1H), 7.67 (s, 1H), 7.65 (s, 1H), 7.55 (s, 1H), 3.74 (s, 3H), 3.57 (s, 3H), 3.56 (s, 3H), 3.45 (s, 3H), 3.25 (s, 3H), 1.64 (s, 6H), 1.60 (s, 6H), 1.57 (s, 6H), 1.34 (s, 6H); ^{13}C NMR (100 MHz, $CDCl_3$): δ 172.1, 170.5, 164.4, 164.0, 163.9, 163.5, 148.3, 146.5, 146.4, 146.3, 133.8, 133.3, 133.2, 132.4, 128.4, 128.3, 128.2, 127.4, 127.2, 127.1, 127.0, 126.8, 126.6, 124.6, 118.6, 118.43, 118.36, 116.8, 64.8, 62.64, 62.62, 62.5, 62.4, 58.63, 58.62, 58.4, 52.4, 25.33, 25.30, 25.25, 24.44; MALDI-TOF: 1334.0 (M + Na), 1350.0 (M + K); Anal. Calcd. For $C_{49}H_{54}Br_4N_{10}O_{13}$: C = 44.90, H = 4.15, N = 10.69; Found: C = 45.13, H = 4.24, N = 10. 43.

Methyl 3-(2-(3-(2-(3-(2-(3-(2-amino-2-methylpropanamido)-5-bromo-2-methoxybenzamido)-2-methylpropanamido)-5-bromo-2-methoxybenzamido)-2-methylpropanamido)-5-bromo-2-methoxybenzamido)-2-methylpropanamido)-5-bromo-2-methoxybenzoate 13b: To a stirred suspension of $SnCl_2.2H_2O$ (0.41 g, 1.8 mmol, 6 equiv.) in methanol (20 mL) was added **13a** (0.40 g, 0.3 mmol, 1equiv.) and the reaction mixture was refluxed for 48 hrs. Methanol was removed under reduced pressure. The residue was dissolved in ethyl acetate (50 mL) and slowly added to a saturated sodium bicarbonate solution. Filtered through celite and organic layer separated. The water layer was further extracted with ethyl acetate (2 x 30 mL). The combined organic layer was given water and brine wash (2 x 50 mL each). The organic layer was dried over Na_2SO_4 and used for next step without further purification. Yield 2.65 g (90%).

3-(2-(3-(2-(3-(2-(3-(2-azido-2-methylpropanamido)-5-bromo-2-methoxybenzamido)-2-methylpropanamido)-5-bromo-2-methoxybenzamido)-2-methylpropanamido)-5-bromo-2-methoxybenzamido)-2-methylpropanamido)-5-bromo-2-methoxybenzoic acid 13c: To a solution of **13a** (0.40 g, 0.3 mmol, 1equiv.) in a mixture of methanol (15 mL) and dioxane (15 mL) was added $LiOH.H_2O$ (0.38 g, 0.9 mmol, 3 equiv.) in water (3 mL) and stirred for 24 hrs. The solvent was stripped off under reduced pressure. To the residue was added water (50 mL) and acidified with dilute HCl. The water layer was extracted with ethyl acetate (3 x 50 mL). The combined organic layer was given water and brine wash, dried over Na_2SO_4 and used for next reaction without further purification. Yield 2.75 g (95.2%).

Methyl 3-(2-(3-(2-(3-(2-(3-(2-(3-(2-(3-(2-(3-(2-azido-2-methylpropanamido)-5-bromo-2-methoxybenzamido)-2-methylpropanamido)-5-bromo-2-methoxybenzamido)-2-methylpropanamido)-5-bromo-2-methoxybenzamido)-2-methylpropanamido)-5-bromo-2-methoxybenzamido)-2-methylpropanamido)-5-bromo-2-methoxybenzamido)-2-methylpropanamido)-5-bromo-2-methoxybenzamido)-2-methylpropanamido)-5-bromo-2-methoxybenzoate 14 To an ice-cold stirred solution of the acid **13b** (0.38 g, 0.3 mmol, 1equiv.) and amine **13c** (0.38 g, 0.3 mmol, 1 equiv.) in a mixture of dry acetonitrile (10 mL) and dry DCM (10 mL), DIEA (0.1 mL, 0.6 mmol, 2 equiv.) was added followed by the addition of TBTU (0.14 g, 0.4 mmol, 1.5 equiv.). The resulting reaction mixture was stirred overnight at room temperature. The solid precipitate obtained was filtered, washed with DCM, dilute HCl, saturated sodium bicarbonate, and water. Dried over P_2O_5 vacuum desiccator to furnish **14**. Yield 0.28 (36.9%); mp > 300^0C; IR (Nujol) ν (cm^{-1}): 3400, 3275, 2116, 1707, 1647, 1522, 1508, 1462, 1377, 1321, 1148, 997; ^{1}H NMR (400 MHz, $CDCl_3$): δ 9.42 (s, 1H), 9.31 (s,1H), 9.25 (m, 6H), 8.94 (m, 7H), 8.28 (m, 1H), 8.20 (m, 6H), 8.07 (m, 1H), 7.64 (m, 1H), 7.61 (m, 1H), 7.58 (m, 1H), 7.57 (m, 5H), 3.85 (s, 3H), 3.79 (s, 3H), 3.70 (m, 21H), 1.56 (m, 48H); ^{13}C NMR (100 MHz, $CDCl_3$): δ 173.2, 173.1, 171.1, 164.8, 164.7, 164.5, 149.8, 149.0, 147.8, 134.4, 133.4, 132.6, 131.3, 131.1, 131.0, 128.7, 1218.1, 128.0, 127.9, 126.8, 126.6, 126.2, 115.2, 115.0, 64.6, 62.2, 62.0, 59.9, 57.5, 52.8, 24.7, 24.3; MALDI-TOF: 2562.8 (M+), 2586.1 (M + Na); Anal. Calcd. For $C_{97}H_{106}Br_8N_{18}O_{25}$: C = 45.45, H = 4.17, N = 9.84; Found: C = 45.62, H = 4.21, N = 9.56.

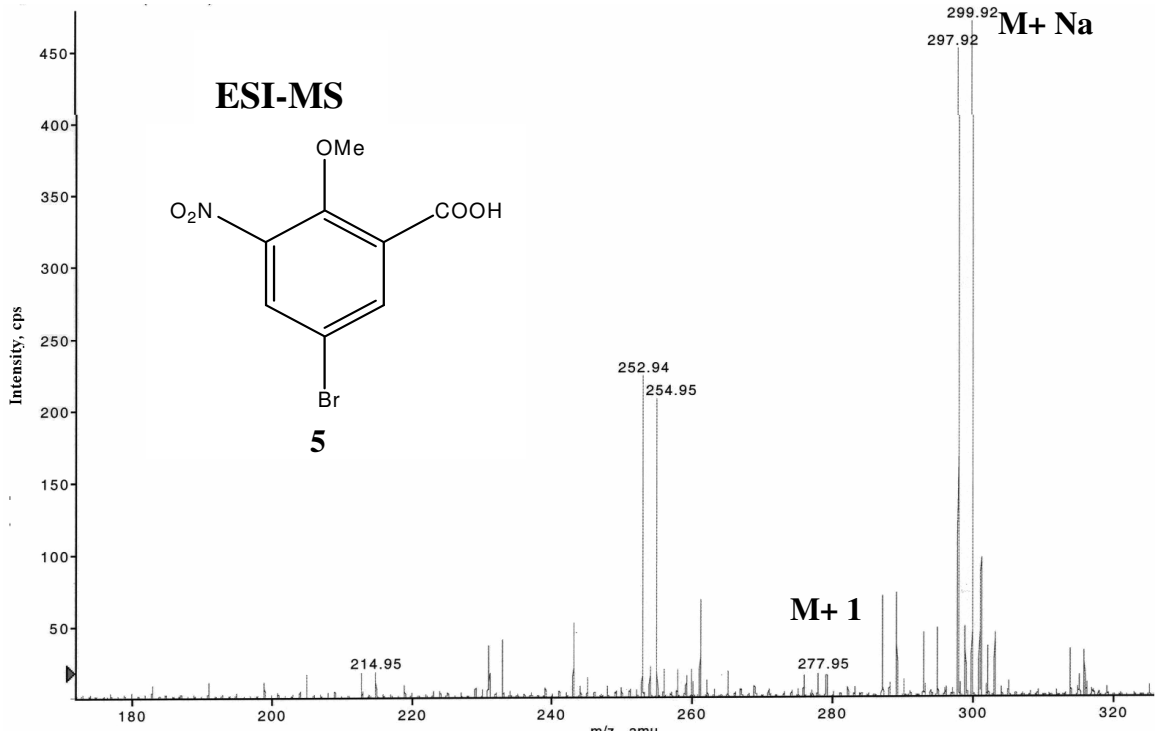
ESI-MS
OMe
O2N
COOH
Br
5
299.92
297.92
M+ Na
252.94
254.95
M+ 1
214.95
277.95
Intensity, cps
m/z, amu

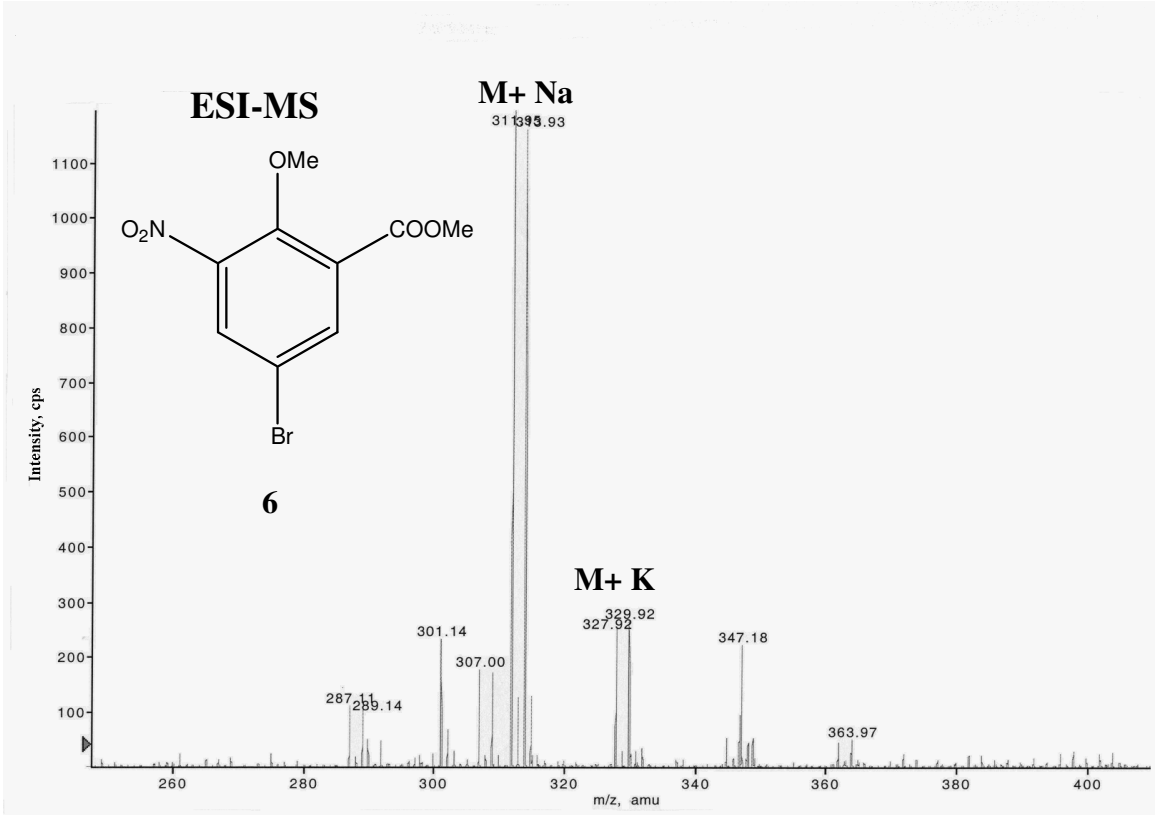
ESI-MS
M+ Na
OMe
O2N
COOMe
Br
6
M+ K
329.92
327.92
301.14
307.00
347.18
287.11
289.14
363.97
Intensity, cps
m/z, amu

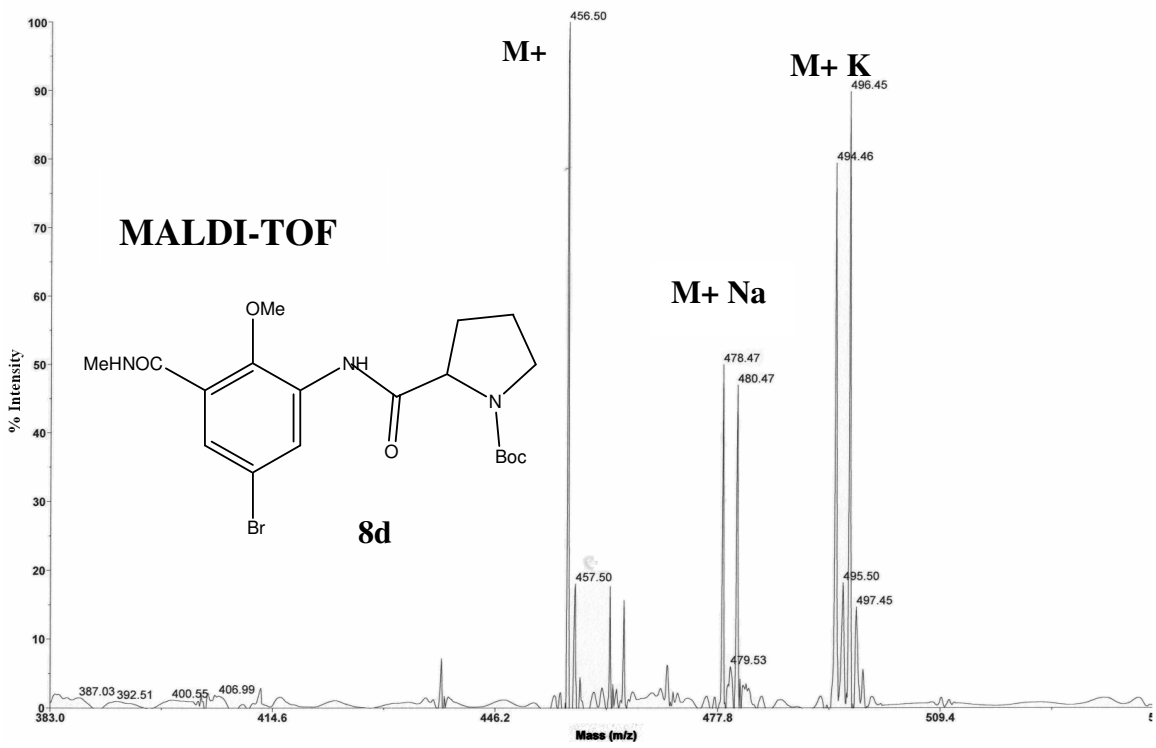
MALDI-TOF
M+
M+ K
M+ Na
456.50
496.45
494.46
478.47
480.47
457.50
495.50
497.45
479.53
387.03
392.51
400.55
406.99
% Intensity
Mass (m/z)
OMe
MeHNOC
NH
N
O
Boc
Br
8d

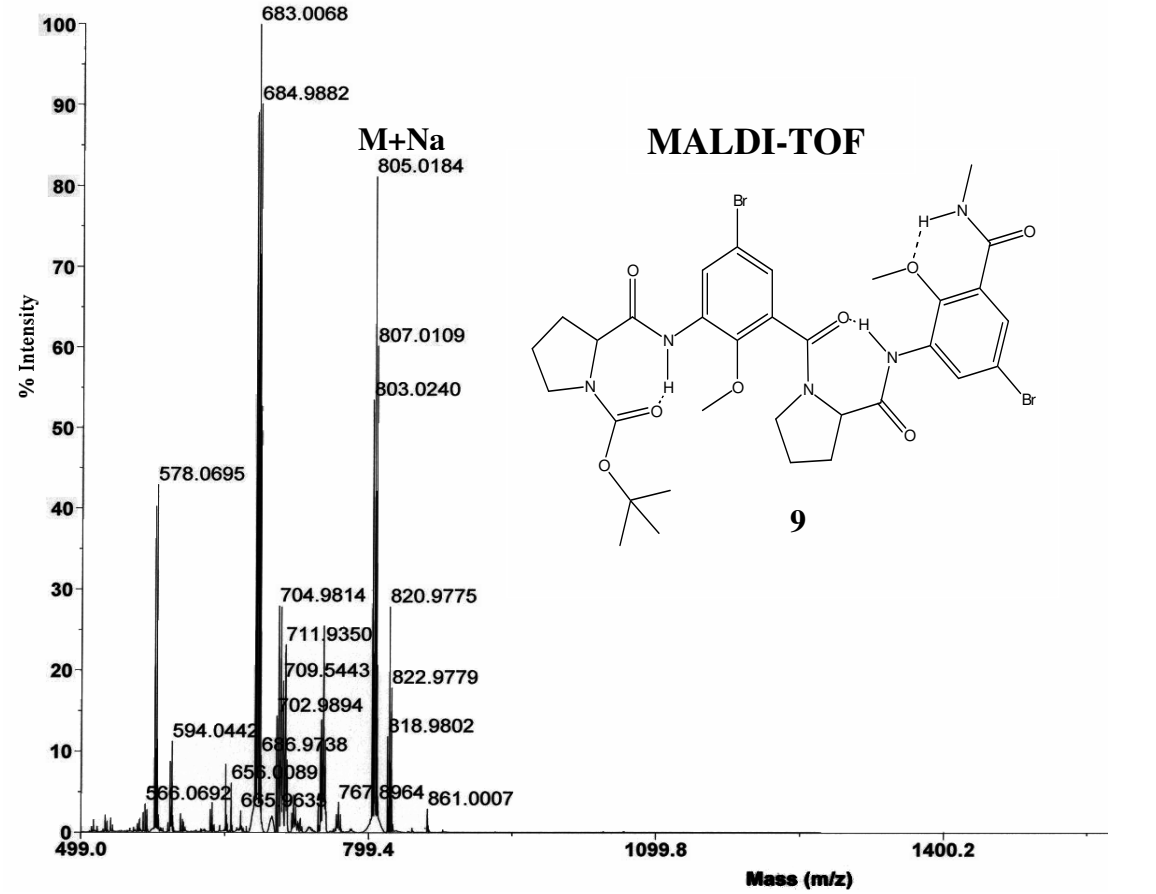
MALDI-TOF
M+Na
683.0068
684.9882
805.0184
807.0109
803.0240
578.0695
704.9814
820.9775
711.9350
709.5443
822.9779
702.9894
818.9802
594.0442
686.9738
656.0089
566.0692
685.9634
767.8964
861.0007
% Intensity
Mass (m/z)
Br
N
H
O
9

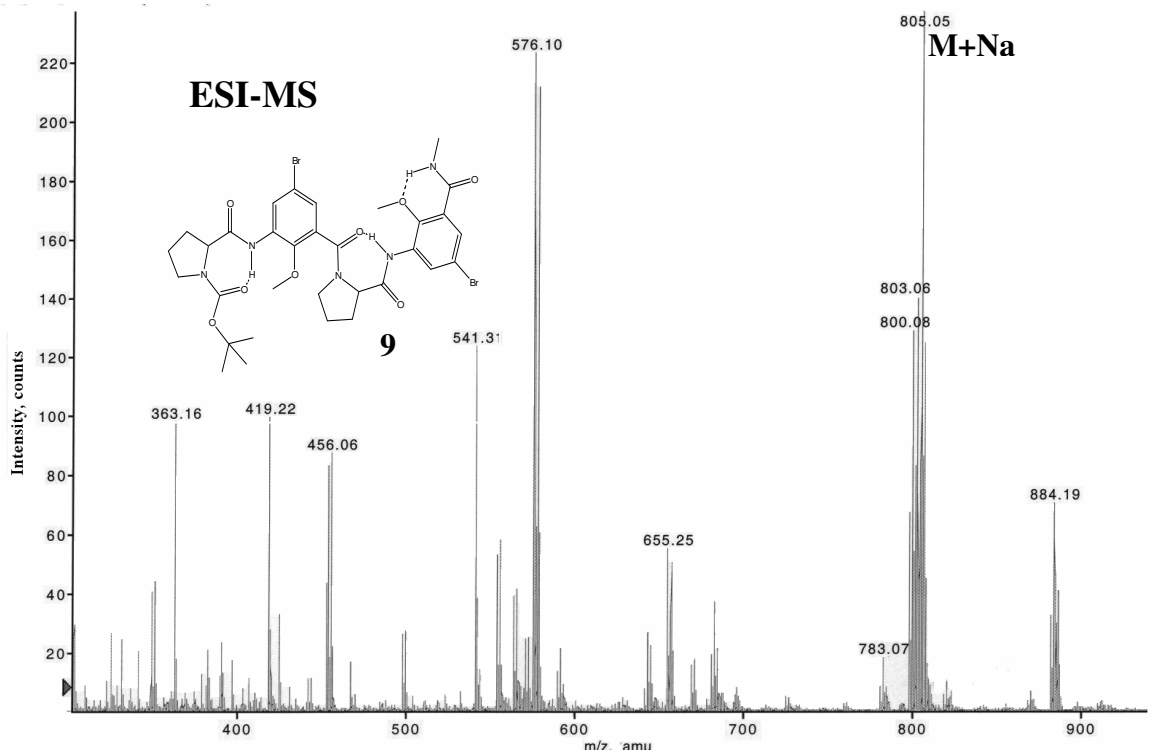
ESI-MS
M+Na
805.05
576.10
803.06
800.08
541.31
363.16
419.22
456.06
655.25
884.19
783.07
Intensity, counts
m/z, amu

9

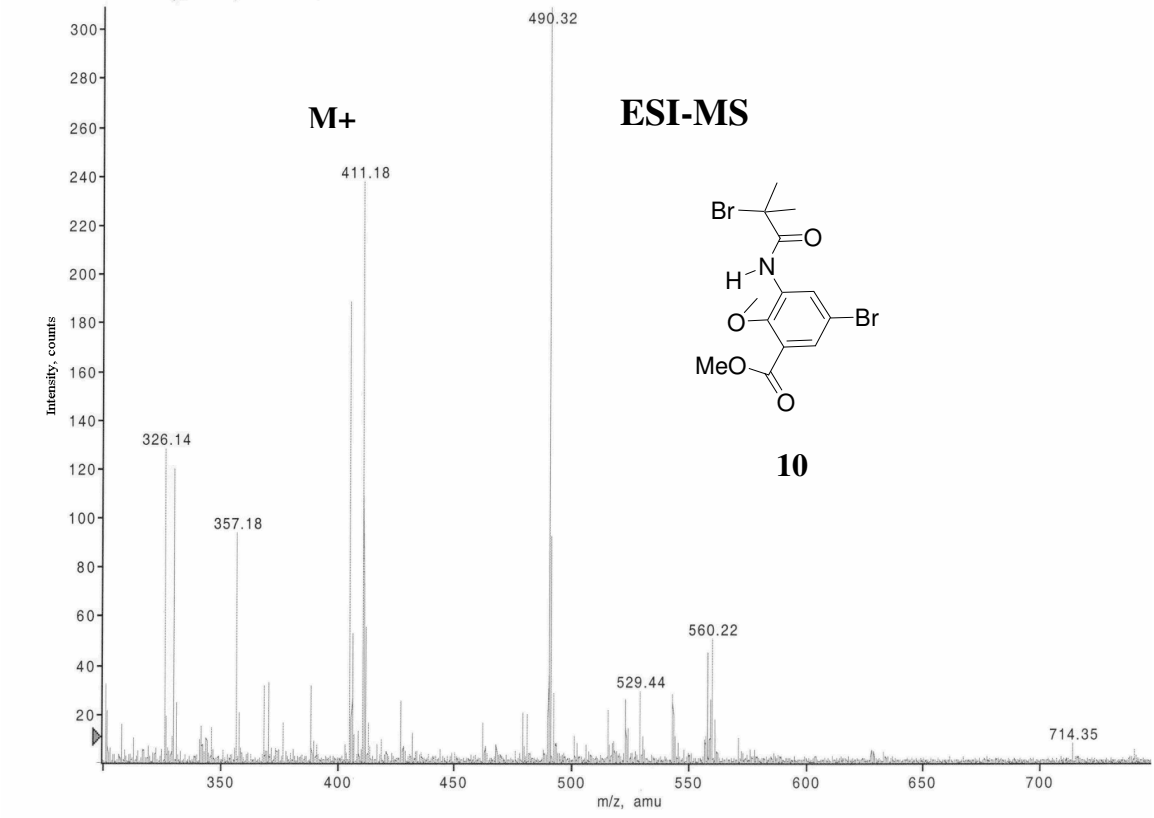
M+
ESI-MS
490.32
411.18
326.14
357.18
560.22
529.44
714.35
Intensity, counts
m/z, amu

10

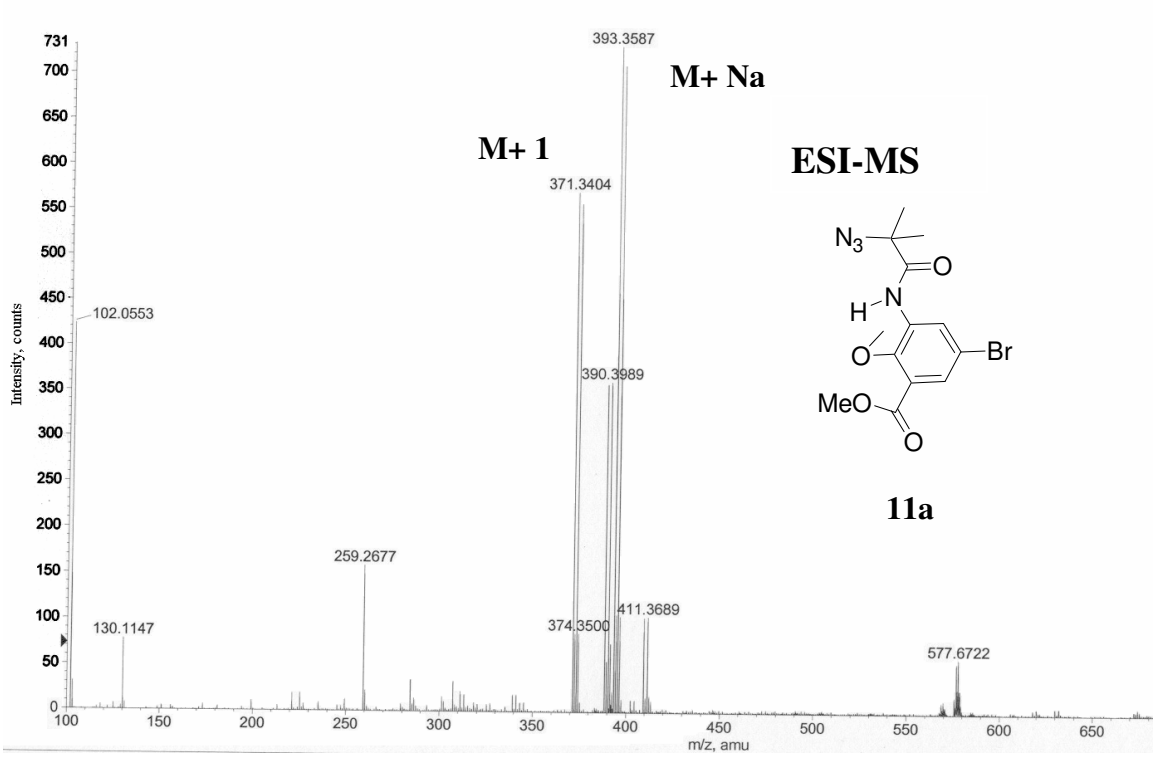
393.3587
M+ Na
M+ 1
ESI-MS
371.3404
102.0553
390.3989
259.2677
130.1147
374.3500
411.3689
577.6722
Intensity, counts
m/z, amu
11a

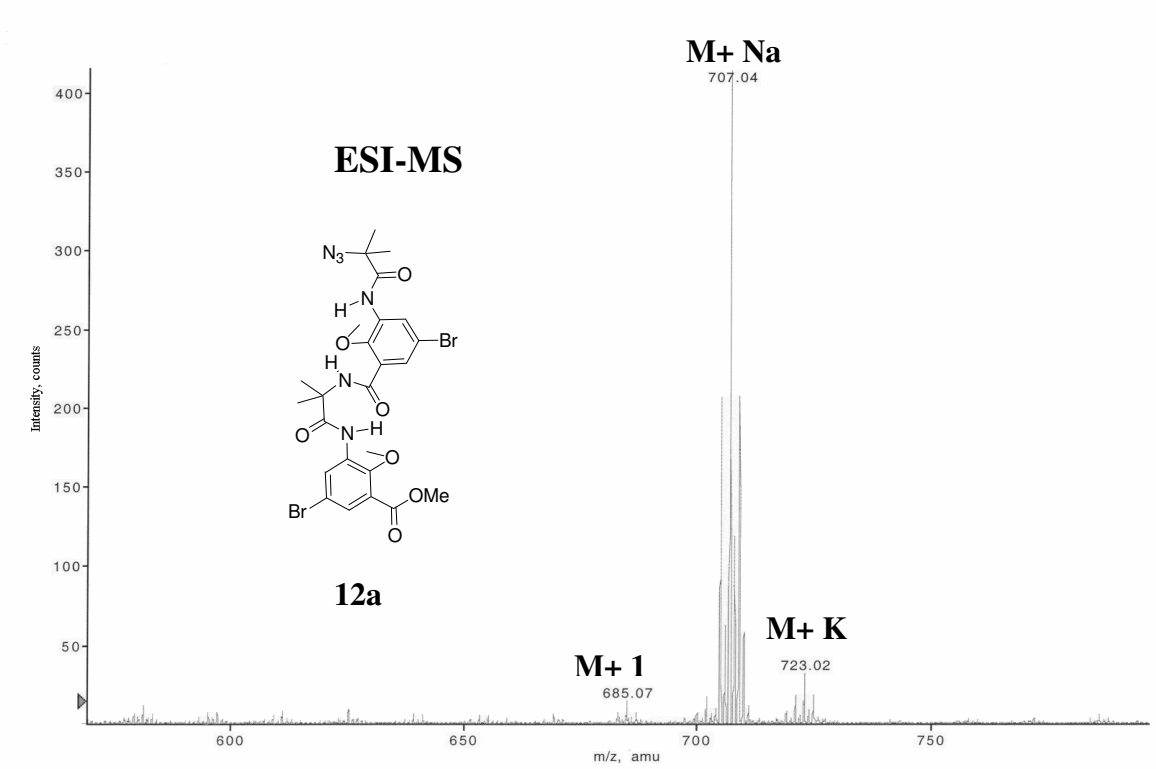
M+ Na
707.04
ESI-MS
M+ K
723.02
M+ 1
685.07
Intensity, counts
m/z, amu
12a

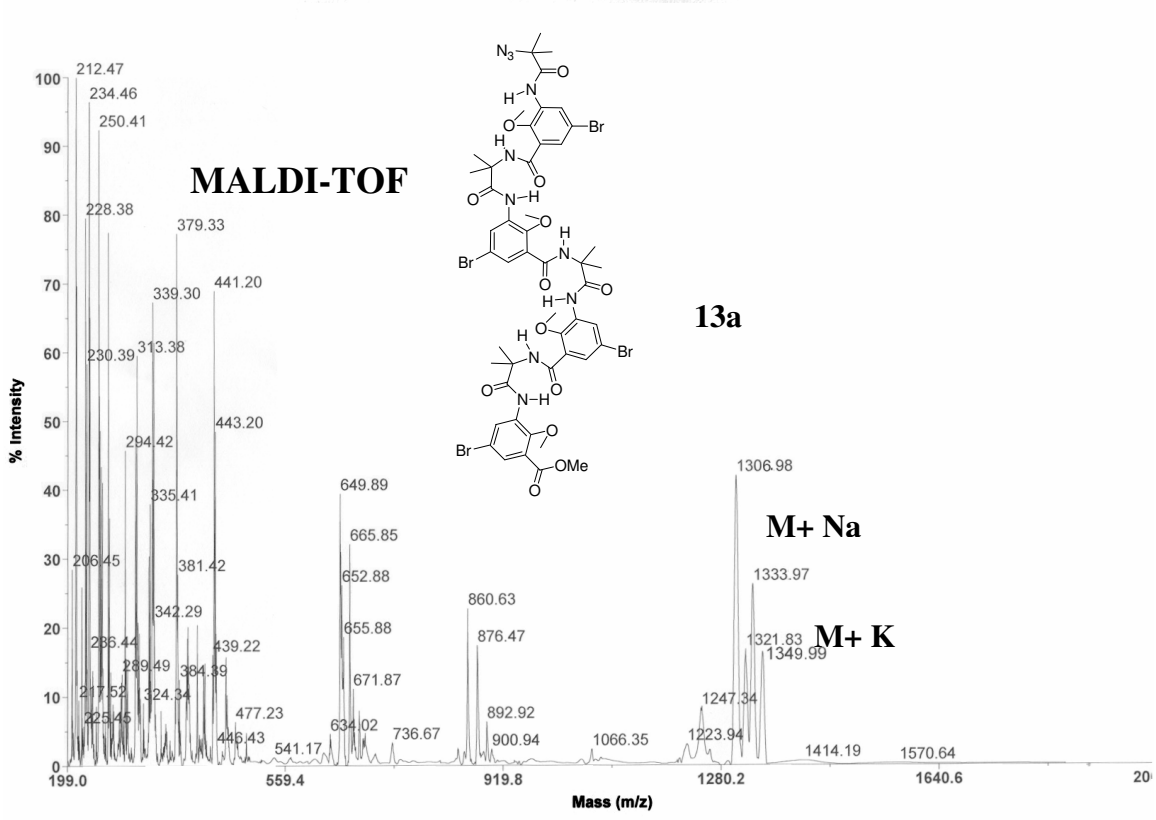
MALDI-TOF
13a
M+ Na
M+ K
% Intensity
Mass (m/z)
212.47
234.46
250.41
228.38
379.33
339.30
441.20
230.39
313.38
443.20
294.42
335.41
649.89
665.85
206.45
381.42
652.88
342.29
860.63
655.88
286.44
439.22
876.47
671.87
289.49
384.39
217.52
324.34
225.45
477.23
634.02
892.92
446.43
736.67
541.17
900.94
1066.35
1306.98
1333.97
1321.83
1349.99
1247.34
1223.94
1414.19
1570.64
199.0
559.4
919.8
1280.2
1640.6

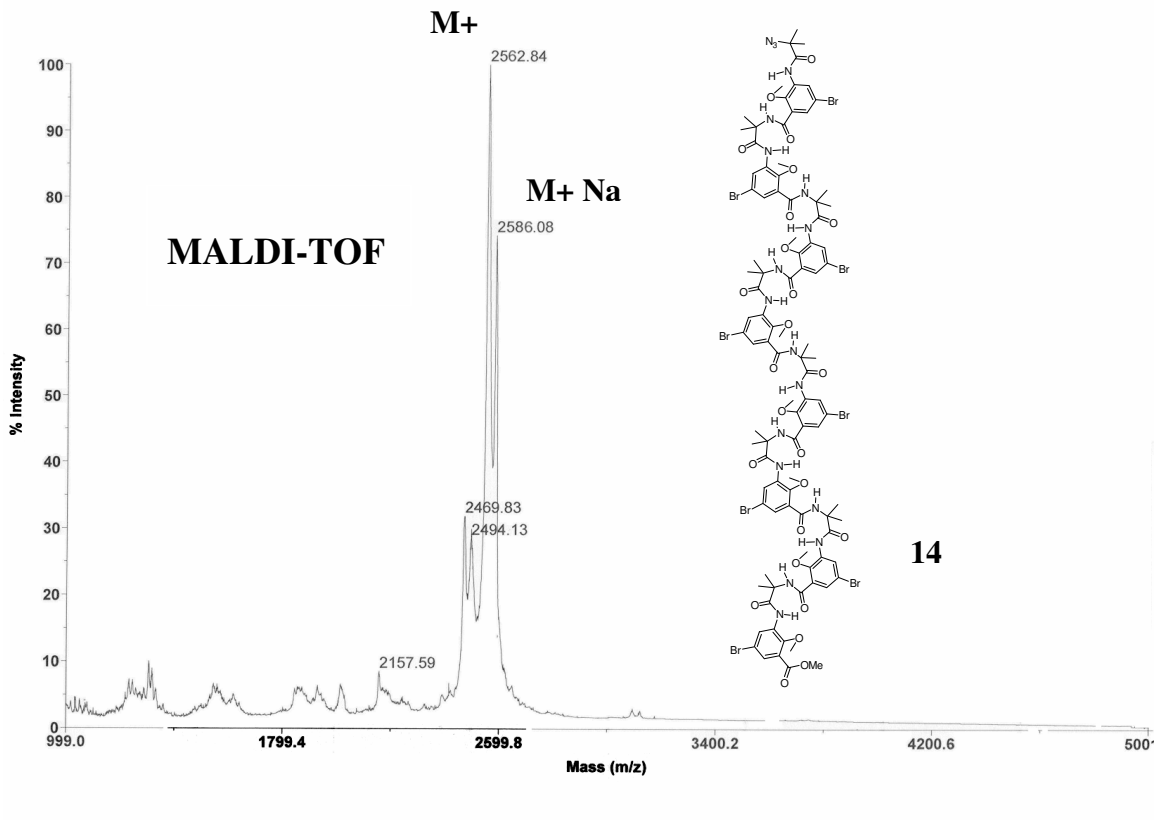
M+
MALDI-TOF
M+ Na
14
% Intensity
Mass (m/z)
2562.84
2586.08
2469.83
2494.13
2157.59
999.0
1799.4
2599.8
3400.2
4200.6

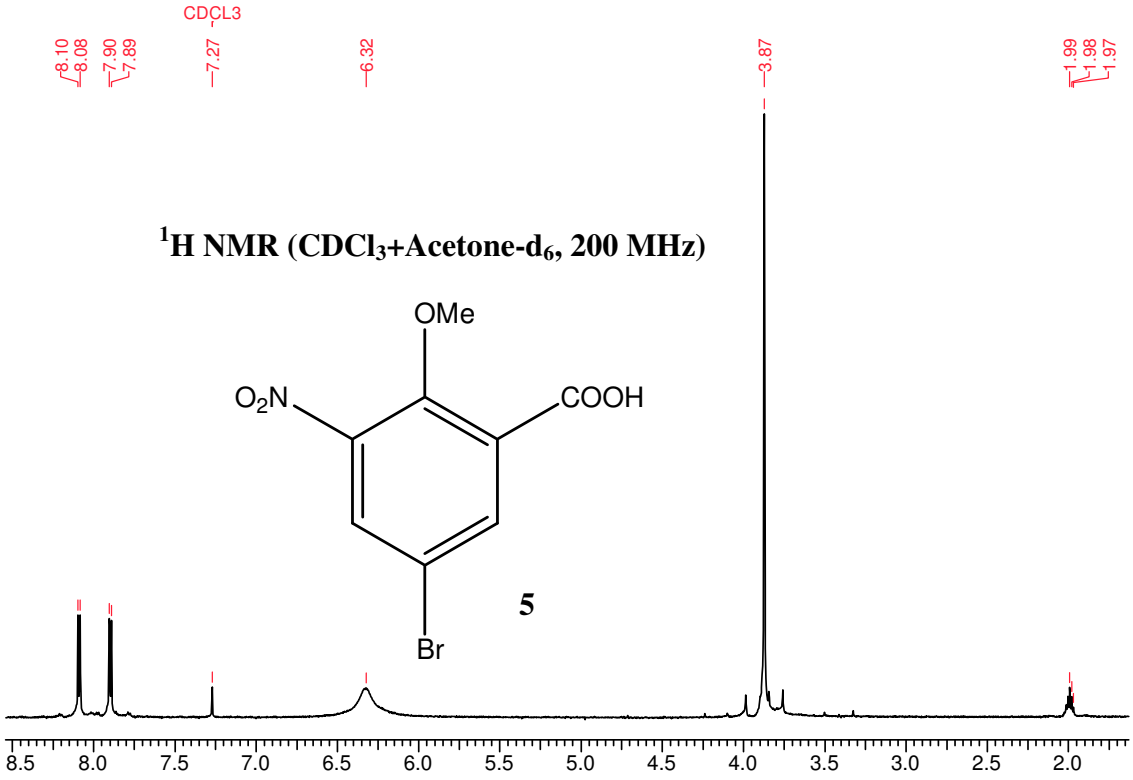

^{1}H NMR ($CDCl_3$+Acetone-d_6, 200 MHz)

5

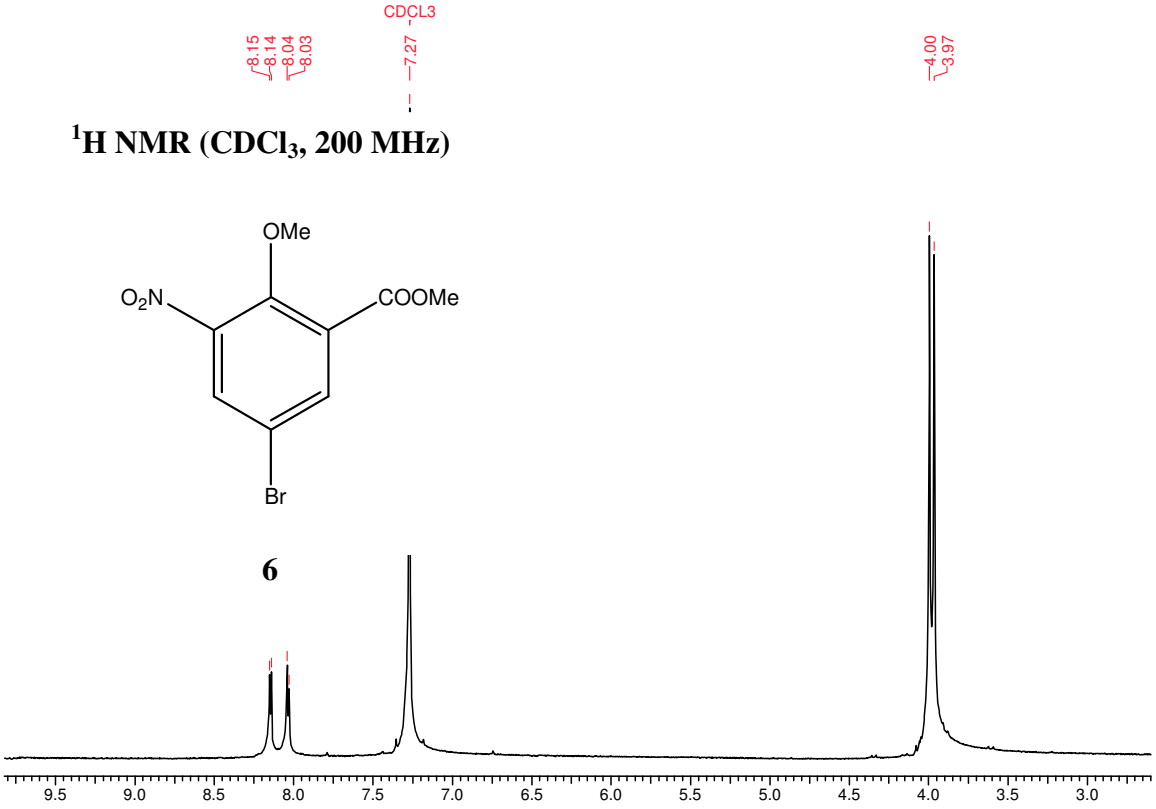

^{1}H NMR ($CDCl_3$, 200 MHz)

6

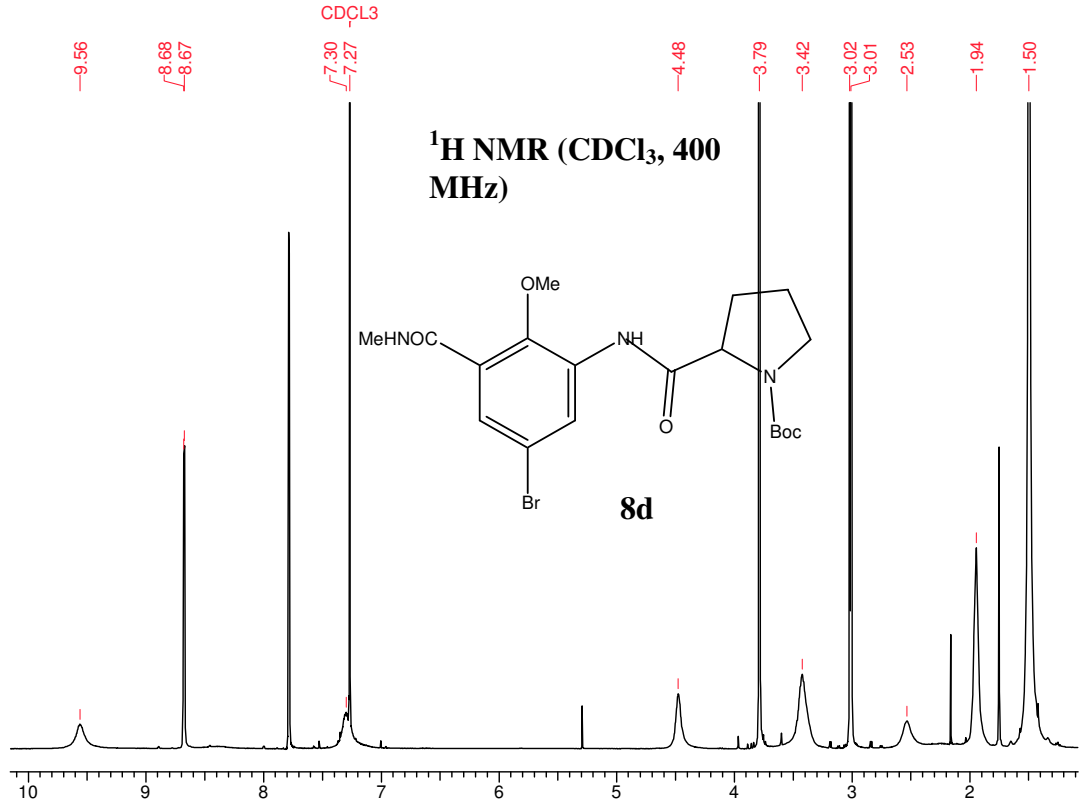
CDCL3
9.56
8.68
8.67
7.30
7.27
4.48
3.79
3.42
3.02
3.01
2.53
1.94
1.50
^{1}H NMR (CDCl$_3$, 400 MHz)
OMe
MeHNOC
NH
N
Boc
O
Br
8d
10
9
8
7
6
5
4
3
2

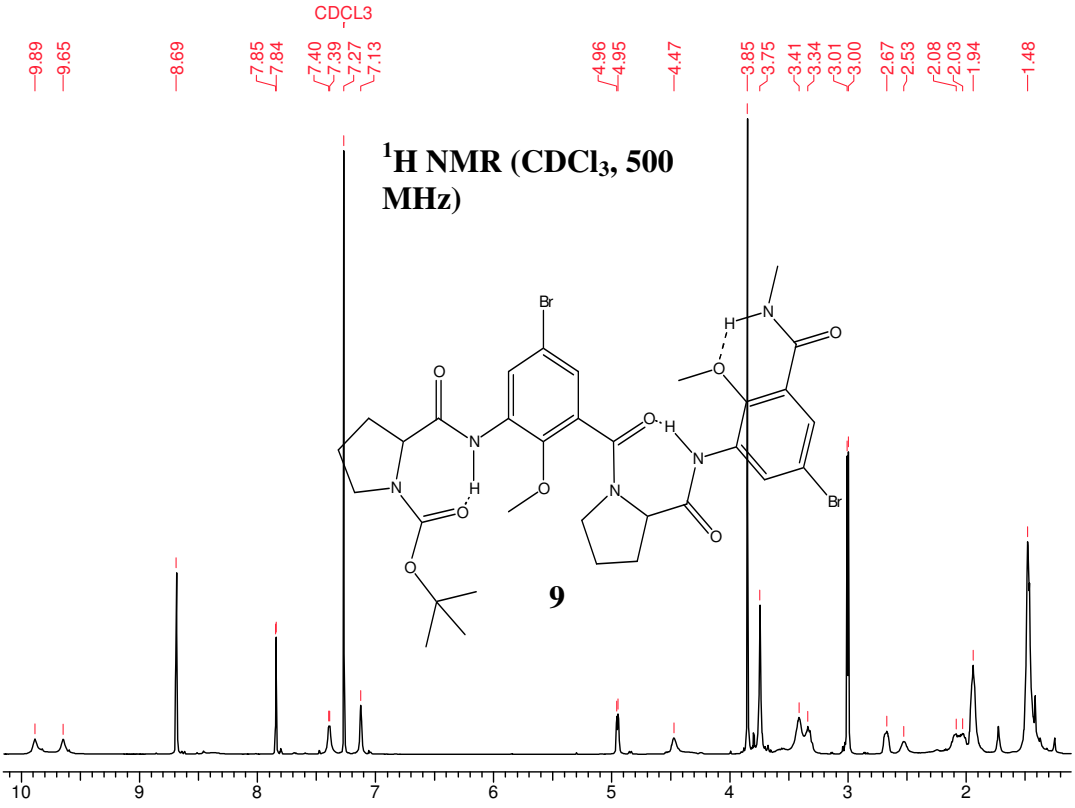
CDCL3
9.89
9.65
8.69
7.85
7.84
7.40
7.39
7.27
7.13
4.96
4.95
4.47
3.85
3.75
3.41
3.34
3.01
3.00
2.67
2.53
2.08
2.03
1.94
1.48
^{1}H NMR (CDCl$_3$, 500 MHz)
Br
H
N
O
9
10
9
8
7
6
5
4
3
2

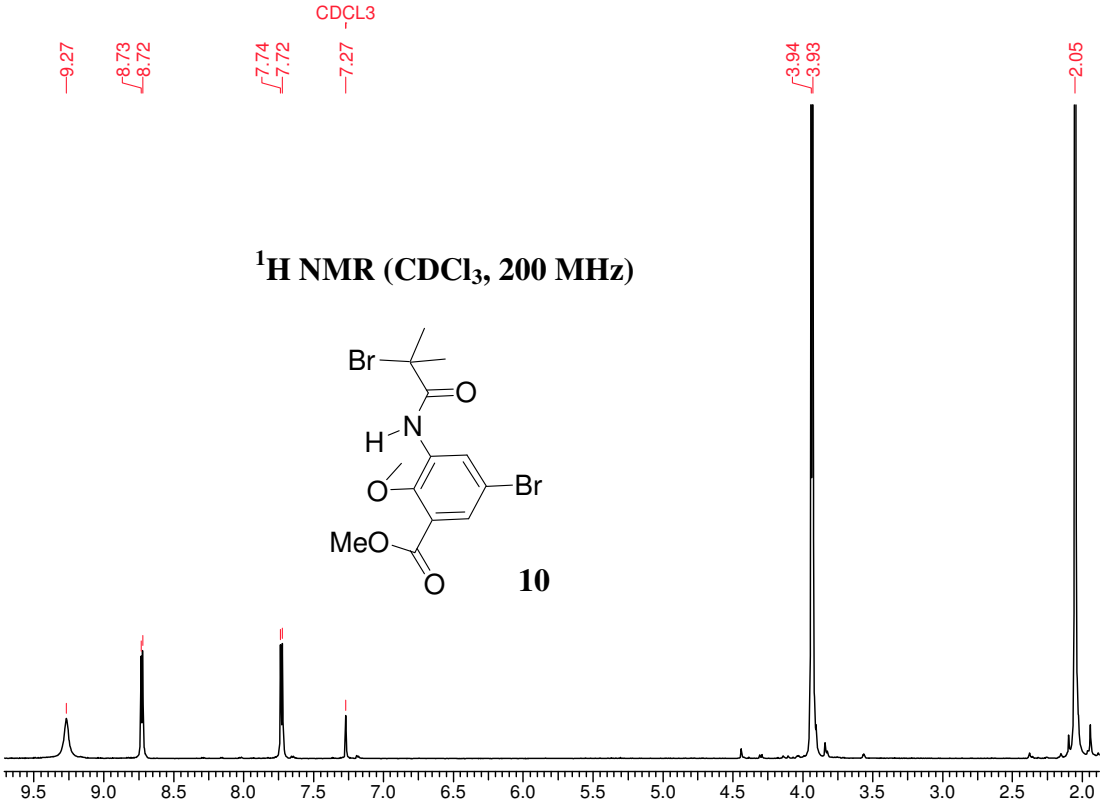

^{1}H NMR ($CDCl_3$, 200 MHz)

10

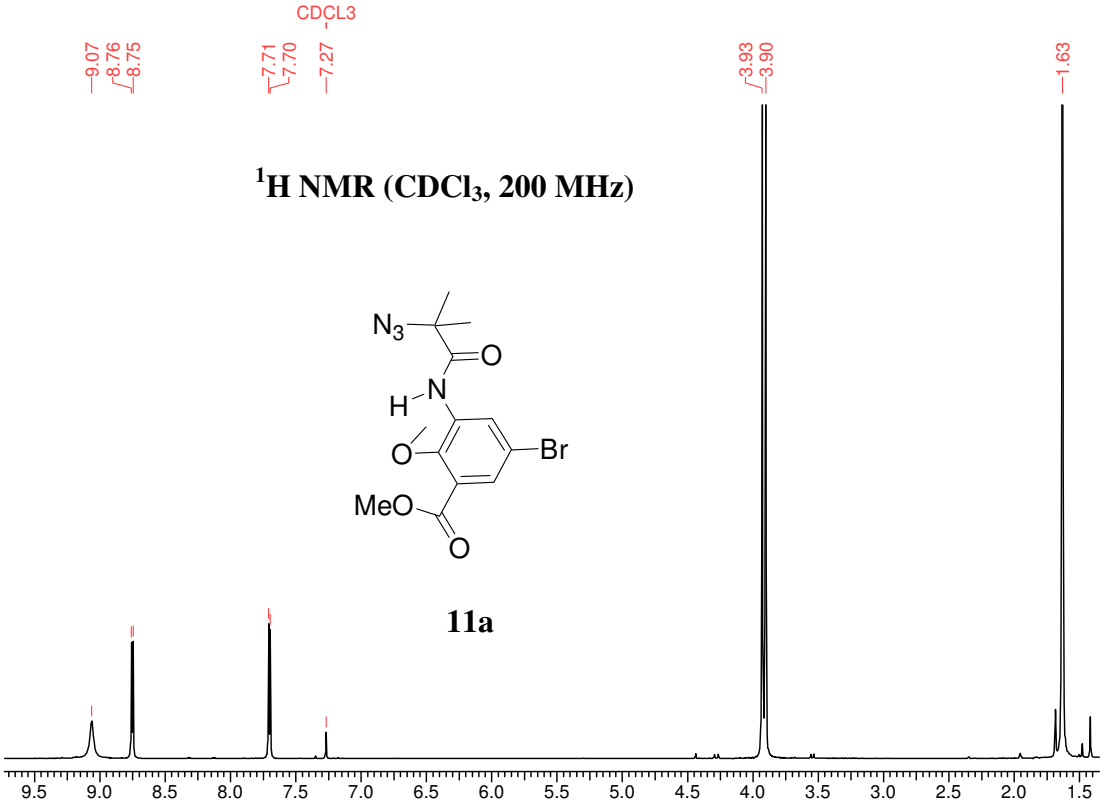

^{1}H NMR ($CDCl_3$, 200 MHz)

11a

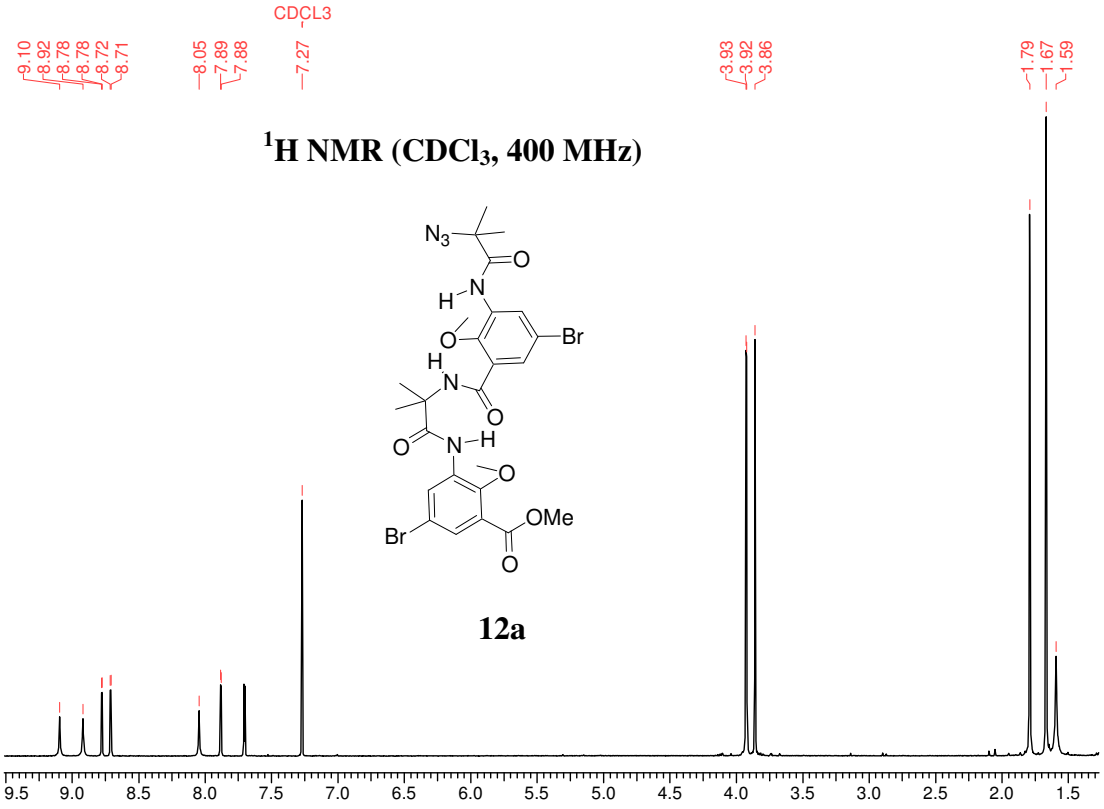

^{1}H NMR ($CDCl_3$, 400 MHz)

12a

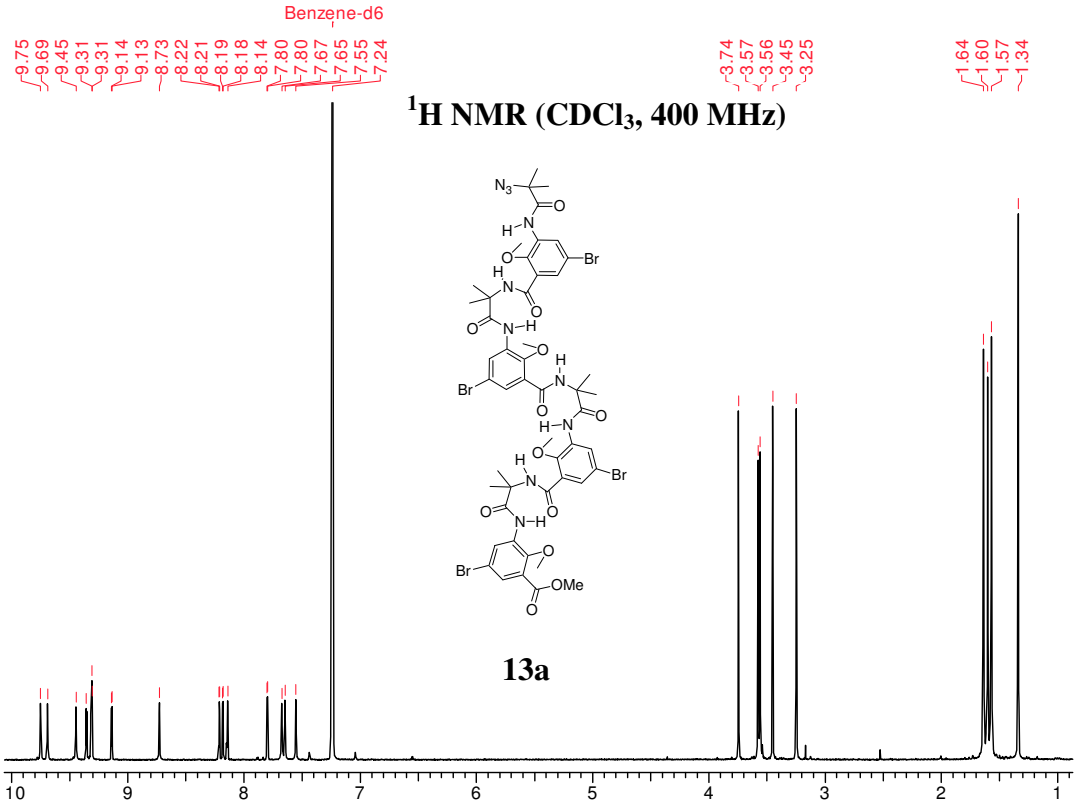

^{1}H NMR ($CDCl_3$, 400 MHz)

13a

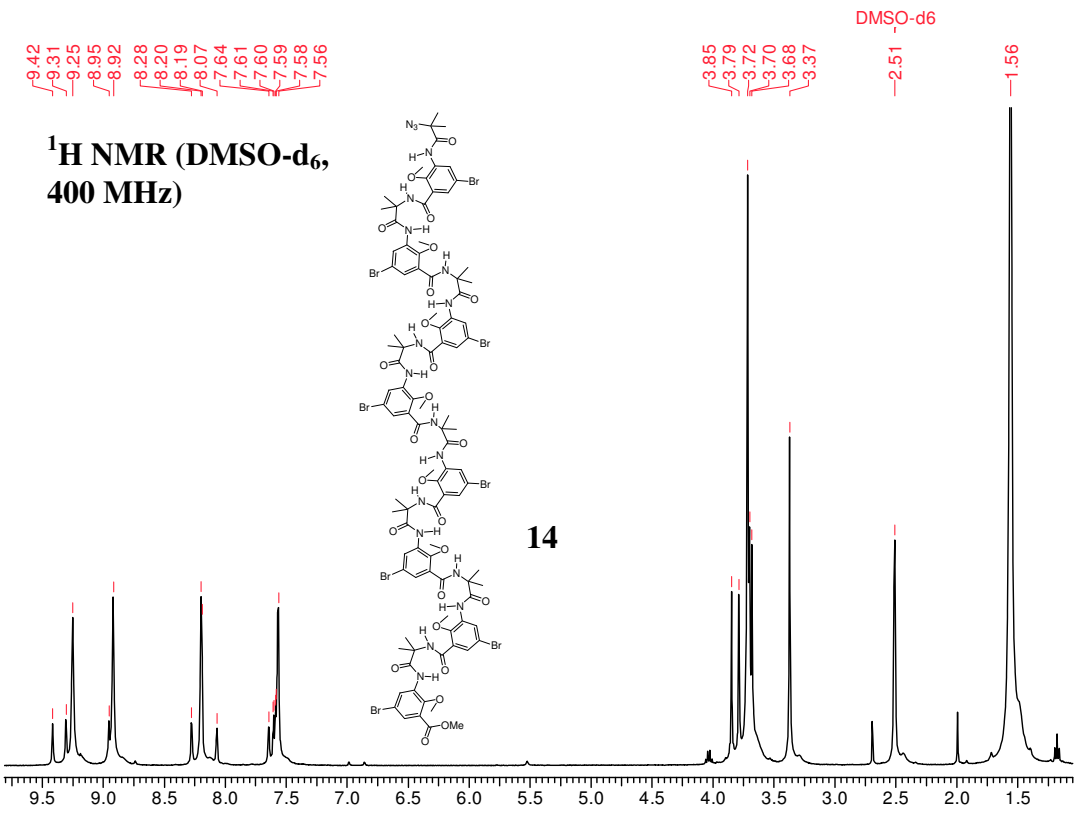

^{1}H NMR (DMSO-d$_6$, 400 MHz)

14

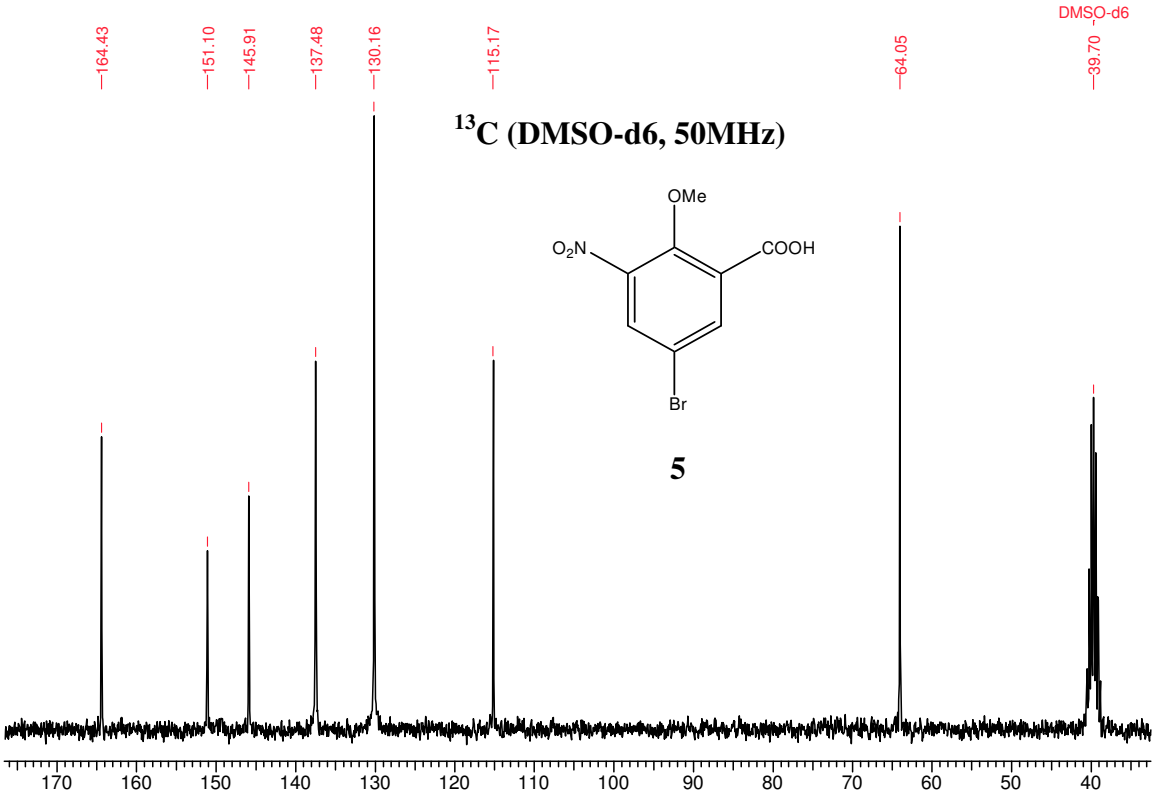

^{13}C (DMSO-d6, 50MHz)

5

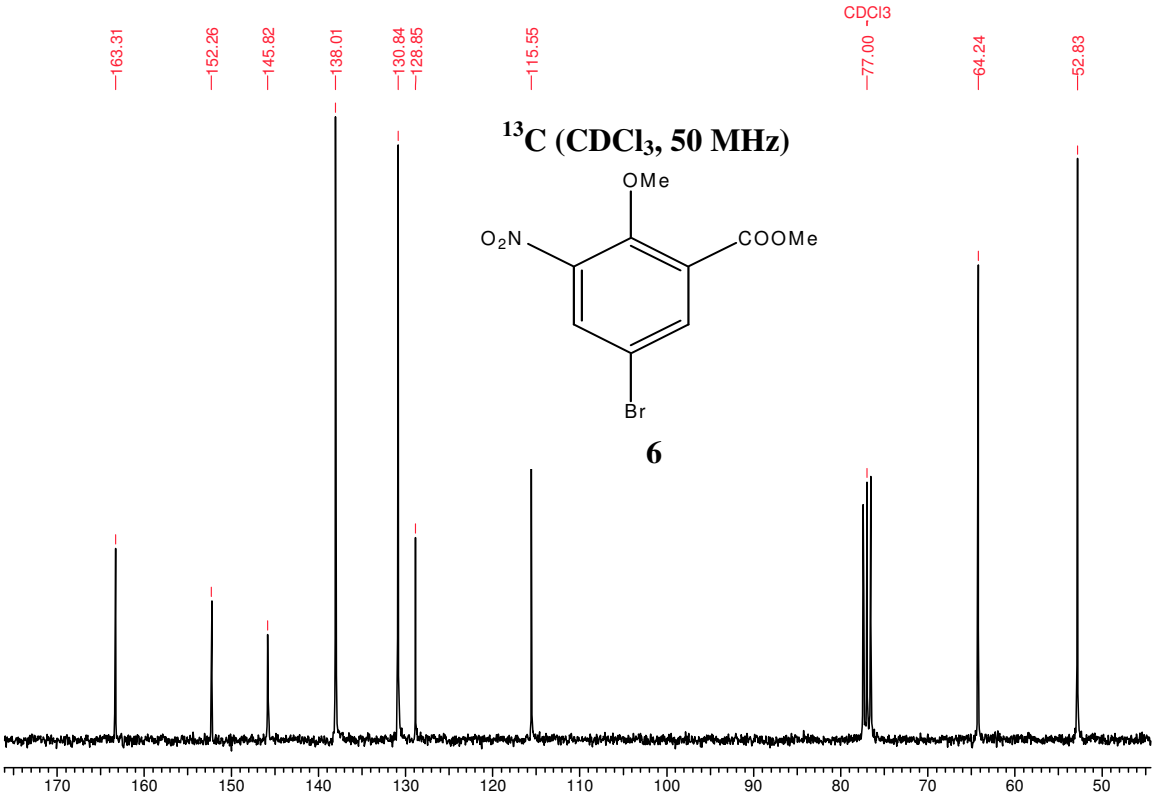
CDCl3
163.31
152.26
145.82
138.01
130.84
128.85
115.55
77.00
64.24
52.83
13C (CDCl3, 50 MHz)
OMe
O2N
COOMe
Br
6
170
160
150
140
130
120
110
100
90
80
70
60
50

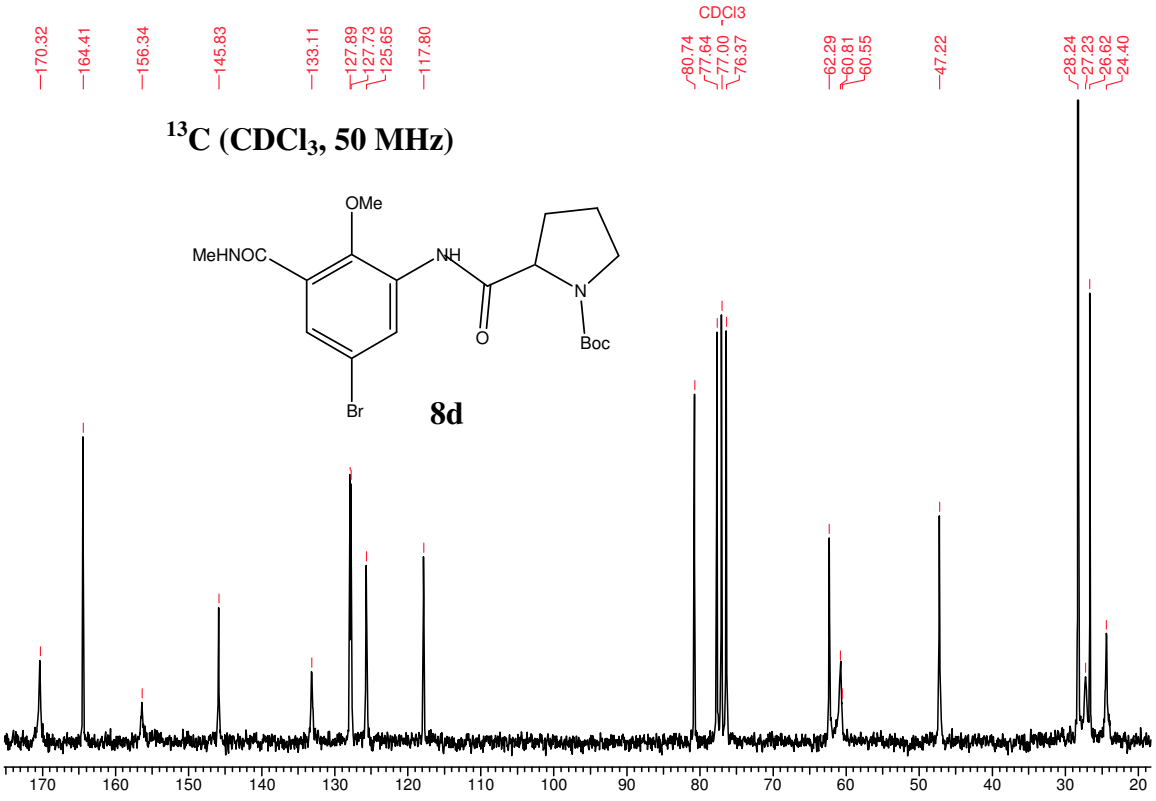
CDCl3
170.32
164.41
156.34
145.83
133.11
127.89
127.73
125.65
117.80
80.74
77.64
77.00
76.37
62.29
60.81
60.55
47.22
28.24
27.23
26.62
24.40
13C (CDCl3, 50 MHz)
OMe
MeHNOC
NH
N
O
Boc
Br
8d
170
160
150
140
130
120
110
100
90
80
70
60
50
40
30
20

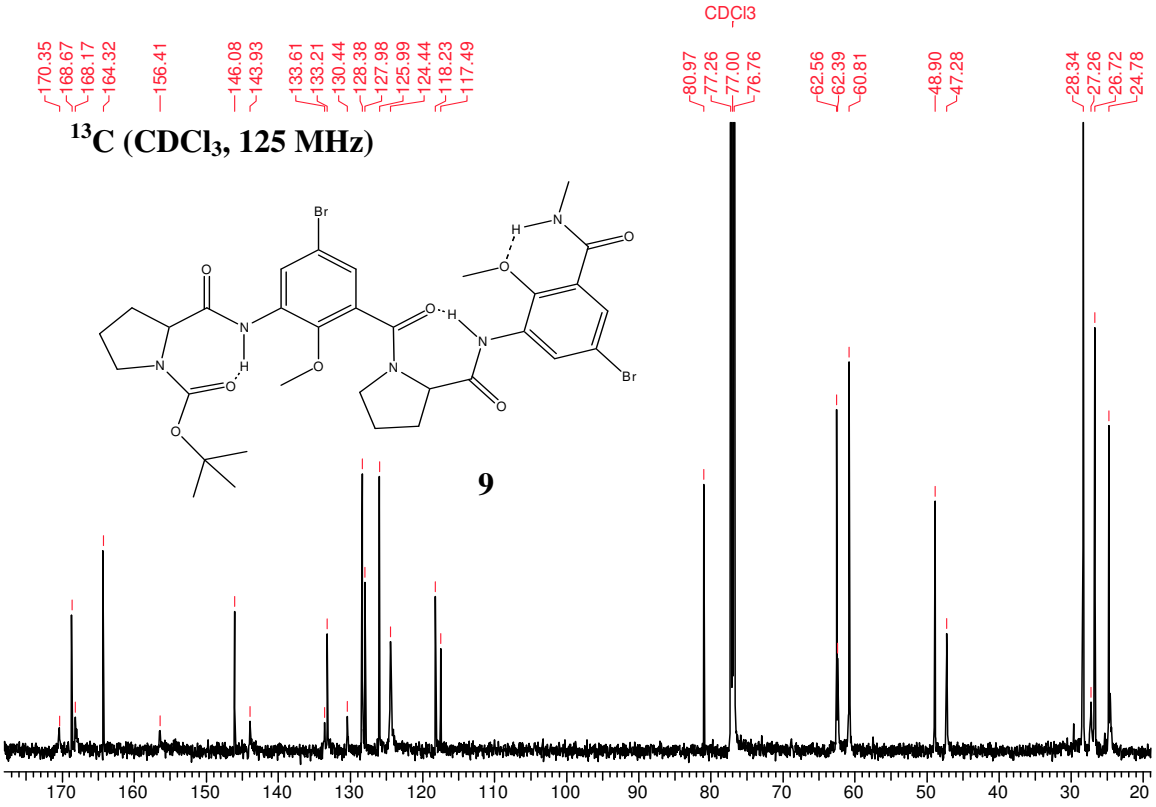

^{13}C ($CDCl_3$, 125 MHz)

9

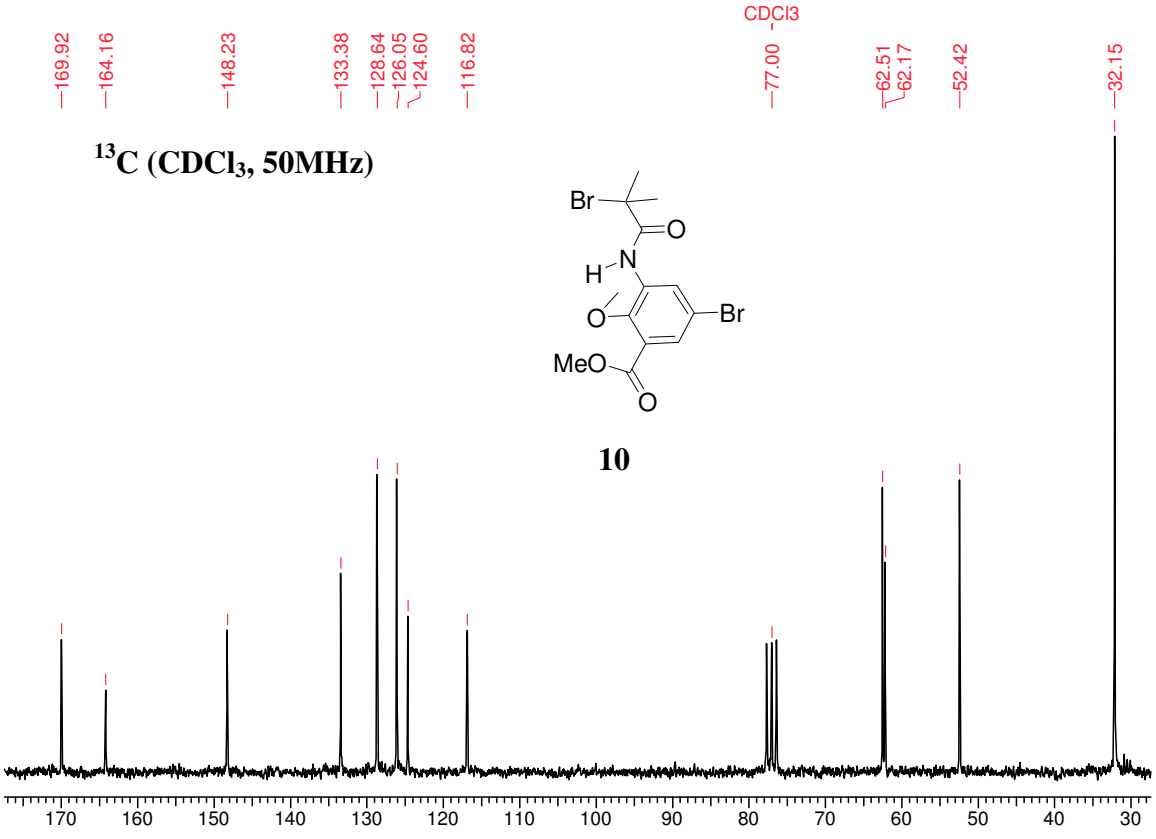

^{13}C ($CDCl_3$, 50MHz)

10

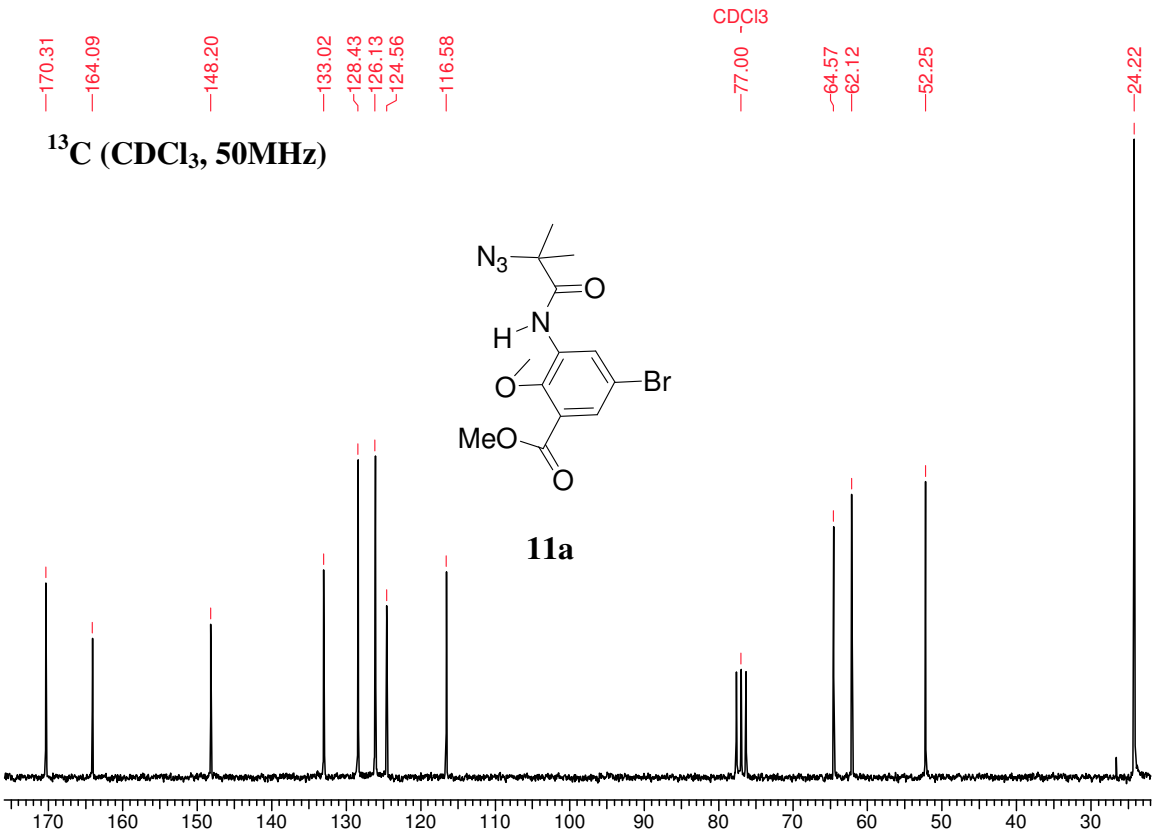
CDCl3
170.31
164.09
148.20
133.02
128.43
126.13
124.56
116.58
77.00
64.57
62.12
52.25
24.22
13C (CDCl3, 50MHz)
N3
O
N
H
O
Br
MeO
O
11a
170
160
150
140
130
120
110
100
90
80
70
60
50
40
30

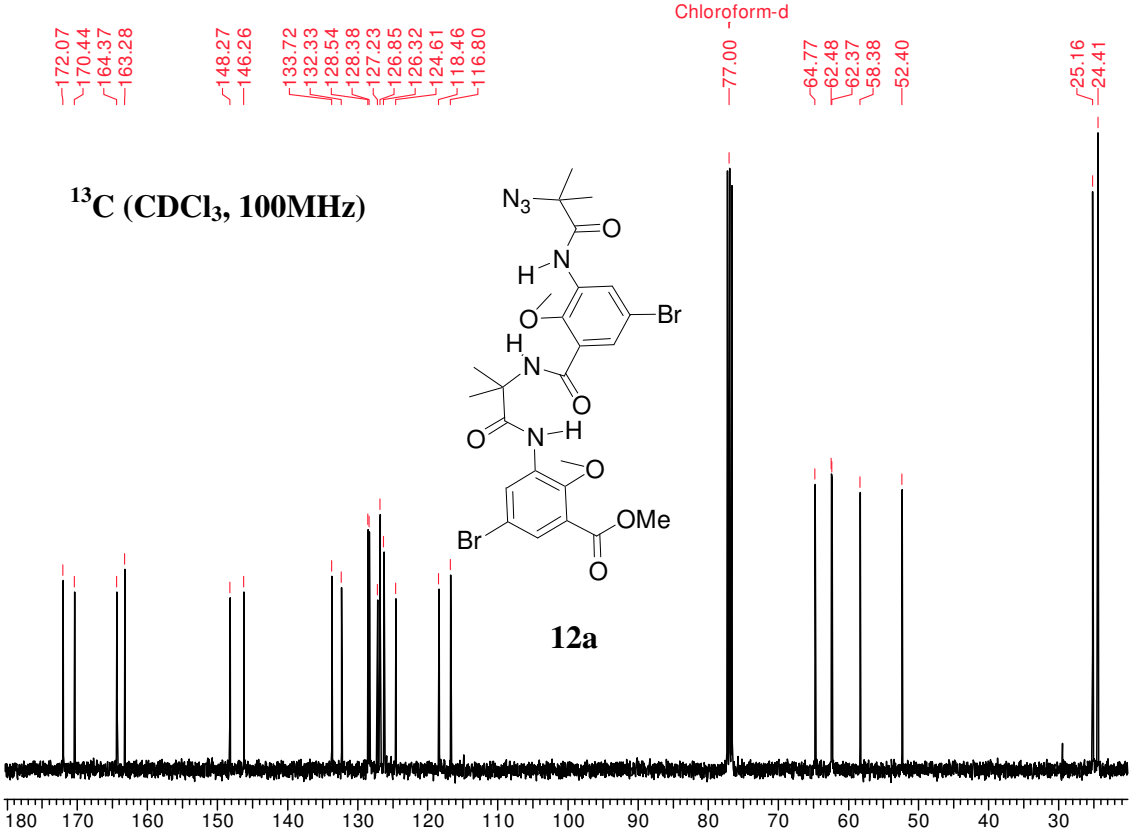
Chloroform-d
172.07
170.44
164.37
163.28
148.27
146.26
133.72
132.33
128.54
128.38
127.23
126.85
126.32
124.61
118.46
116.80
77.00
64.77
62.48
62.37
58.38
52.40
25.16
24.41
13C (CDCl3, 100MHz)
N3
O
N
H
O
Br
H
N
O
O
N
H
O
Br
OMe
O
12a
180
170
160
150
140
130
120
110
100
90
80
70
60
50
40
30

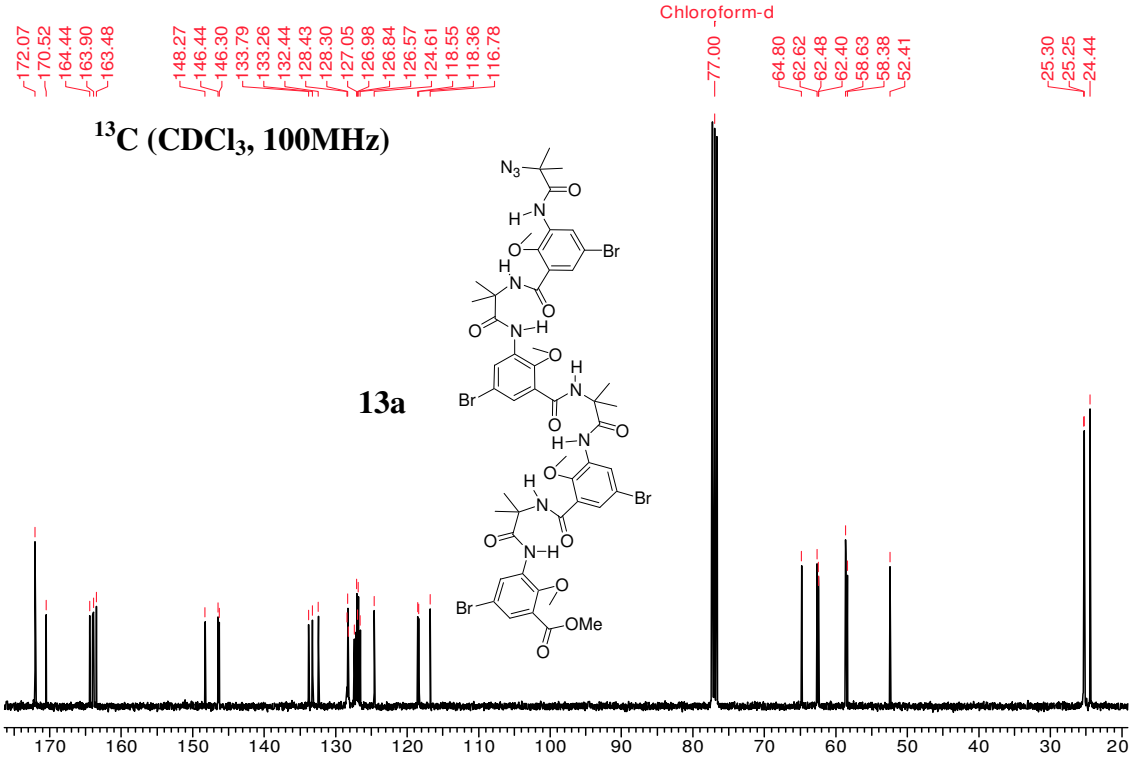

^{13}C ($CDCl_3$, 100MHz)

13a

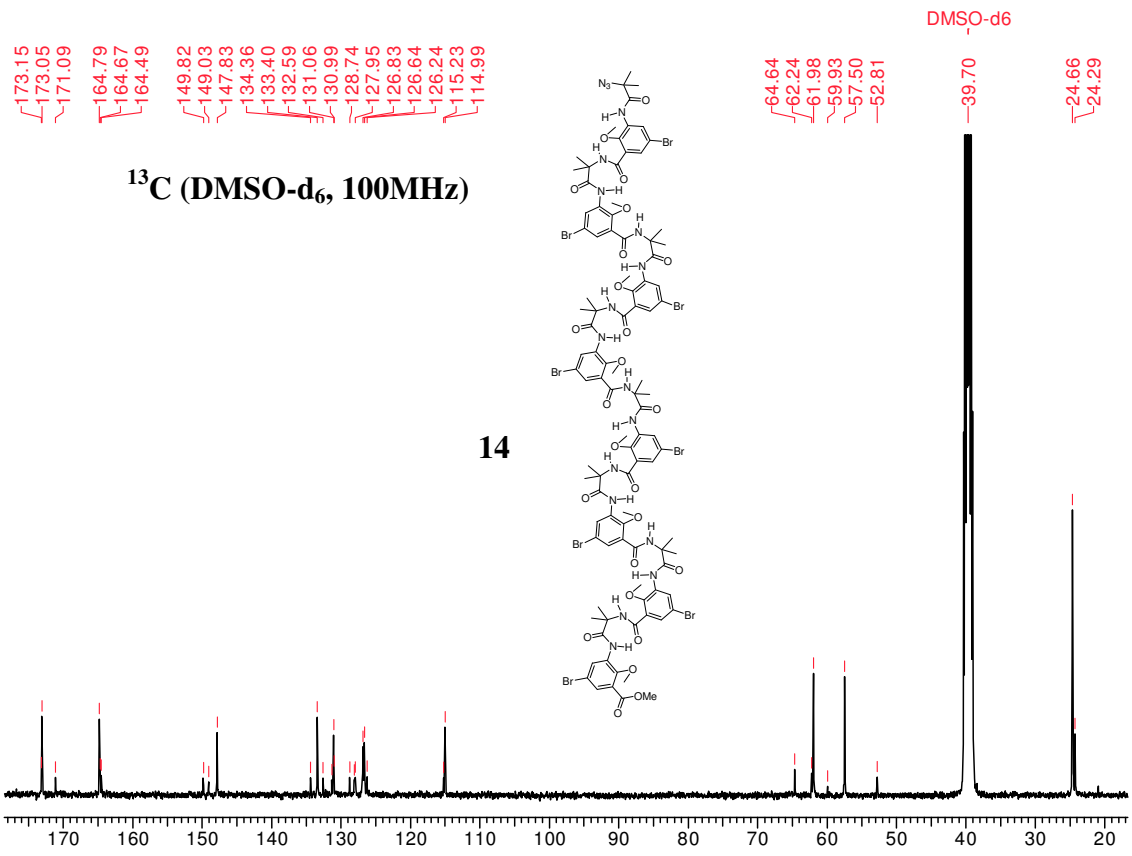

^{13}C ($DMSO\text{-}d_6$, 100MHz)

14

Partial 2D NOESY spectra of **12a**, (NH *vs* NH and OMe *vs* Aib), (top) and **13a** (NH *vs* NH) (bottom) showing charecteristic nOes. For enabling assignments, the molecular structure with selected numbered atoms are also shown. The dipolar couplings are indicated in red dotted arows.

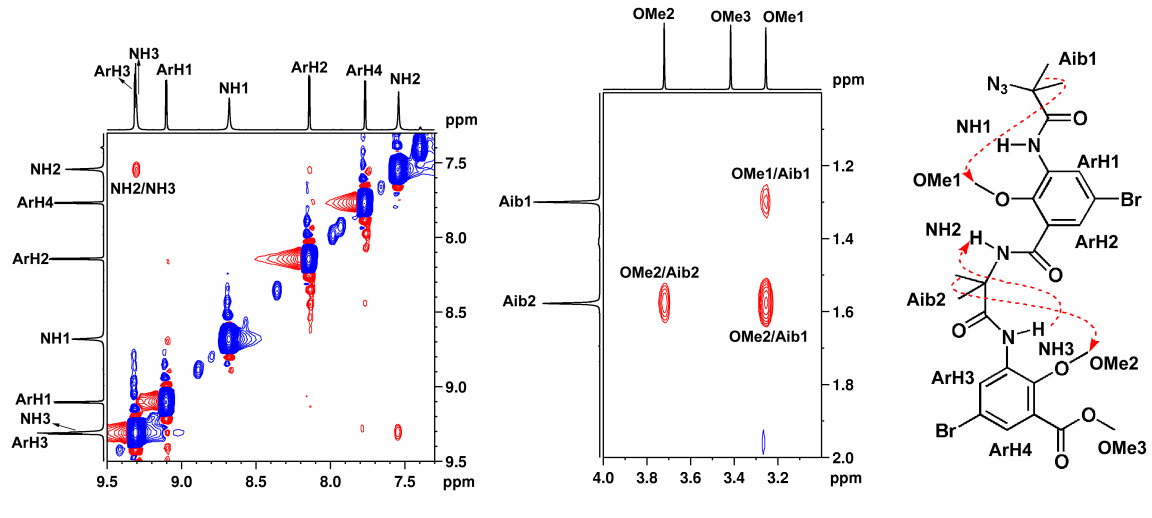

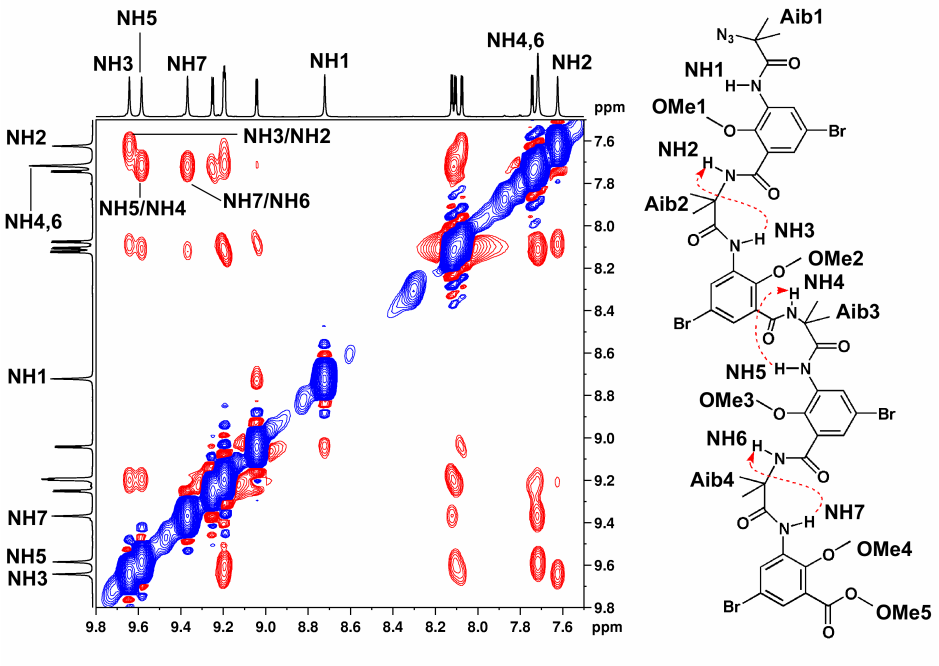

$CDCl_3$ Dilution data for 8d:

Concn. (mM)	Chemical shift ppm
100	9.56
80	9.57
60	9.57
40	9.58
30	9.58
20	9.58
10	9.59
5	9.59
2	9.59
1	9.59

Note: Due to its overlap with residual $C\underline{H}Cl_3$, dilution effect on *NH2* could not clearly be monitored.

DMSO titration for 8d:

Amount of DMSO	Chemical shift in ppm	Chemical shift in ppm
0	9.58	--
5	9.56	7.33
10	9.56	7.36
15	9.56	7.39
20	9.56	7.39
25	9.55	7.42
30	9.55	7.45
35	9.54	7.48
40	9.53	7.50
45	9.53	7.54
50	9.52	7.57

$CDCl_3$ Dilution data for 9:

Concn. (mM)	Chemical shift in ppm (NH2)	Chemical shift in ppm (NH1)	Chemical shift in ppm (NH3)
100	9.74	9.54	7.315
80	9.75	9.54	7.315
60	9.76	9.54	7.305
50	9.76	9.55	7.300
40	9.77	9.55	7.295
30	9.77	9.55	7.295
20	9.78	9.55	7.285
10	9.78	9.55	7.285
5	9.78	9.55	7.285
2	9.78	9.55	7.285
1	9.78	9.55	7.285

DMSO titration for 9:

Amount of DMSO in μL	Chemical shift in ppm (NH2)	Chemical shift in ppm (NH1)	Chemical shift in ppm (NH3)
0	9.79	9.57	7.330
5	9.77	9.56	7.355
10	9.77	9.56	7.370
15	9.75	9.55	7.385
20	9.74	9.55	7.400
25	9.74	9.55	7.420
30	9.73	9.55	7.440
35	9.72	9.54	7.450
40	9.71	9.54	7.470
45	9.71	9.54	7.480
50	9.70	9.53	7.500

TEM image of tetrapeptide foldamer 12a (SAED pattern is shown in the inset)

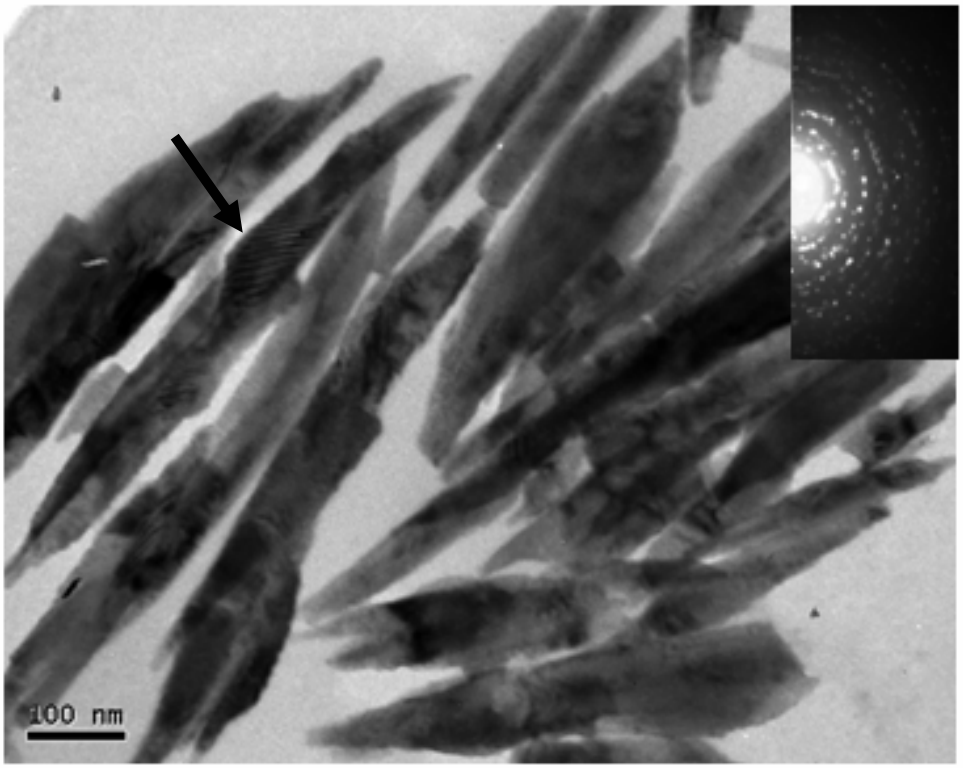

TEM image of octapeptide foldamer 13a (SAED pattern is shown in the inset)

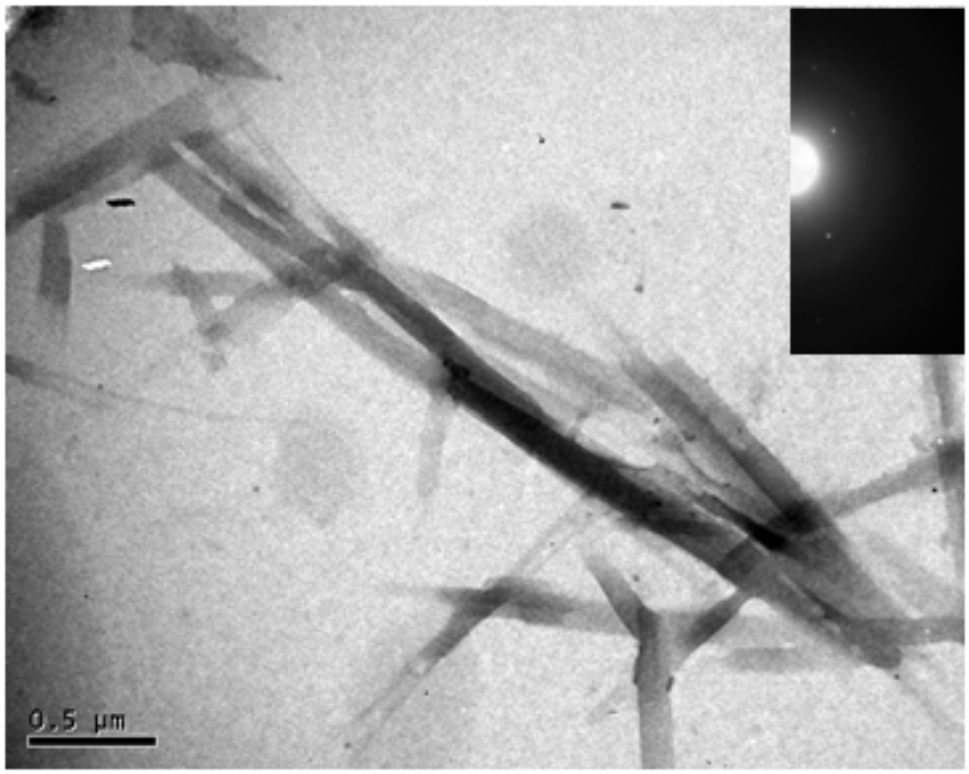

TEM image of hexadecapeptide foldamer 14 (SAED pattern is shown in the inset)

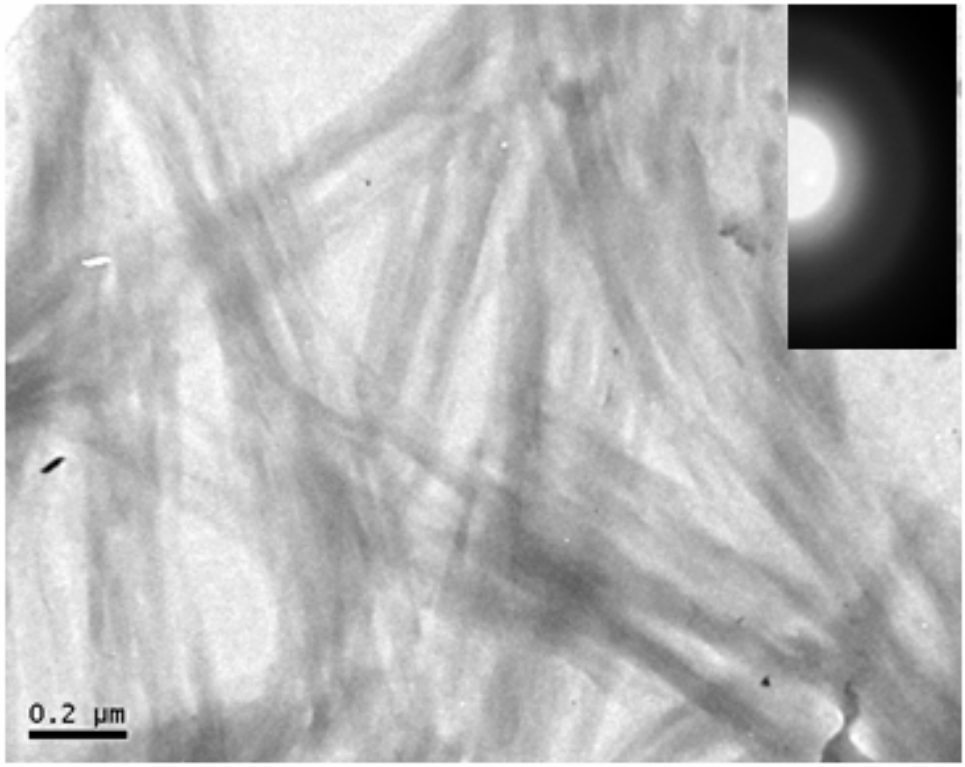

Quantum chemical calculations

The conformation of the compounds **8d** and **9** was investigated at the HF/6-31G* and the DFT/B3LYP/6-31G* levels of ab initio MO theory. After confirmation of the bifurcated hydrogen bonding system in the basic unit **8d**, the remaining conformational degrees of freedom in oligomers of **8d** like **9** are the rotations around the single bonds connecting the aromatic rings and the carboxyamide groups. Several starting conformations for **9** with different values for this angle were selected and their geometries were completely optimized. The most stable structure is illustrated in figure 7. The HF total energies are E_T = -3842.255084 a.u. for **8d** and E_T = -7245.524523 a.u. for **9**. The calculations were performed with the Gaussian03 program package (Gaussian, Inc.).

2.6 References and notes

(1) Saenger, W. *Principles of Nucleic Acid Structure*, Springer, New York, **1984**.

(2) For representative recent reviews, see: (a) Smith, M. D.; Fleet, G. W. J. *J. Peptide Sci.* **1999**, *5*, 425; (b) Stigers, K. D.; Soth, M. J.; Nowick, J. S. *Curr. Opin. Chem. Biol.* **1999**, *3*, 714; (c) Brunsveld, L.; Folmer, B. J. B.; Meijer, E. W.; Sijbesma, R. P. *Chem. Rev.* **2001,** *101,* 4071; (d) Schmuck, C. *Angew. Chem. Int. Ed.* **2003**, *42*, 2448; (e) Sanford, A. R.; Yamato, K.; Yang, X.; Yuan, L.; Han, Y.; Gong, B. *Eur. J. Biochem.* **2004**, *271*, 1416; (f) Huc, I. *Eur. J. Org. Chem.* **2004**, 17; (g) Cheng, R. P. *Curr. Opin. Struct. Biol.* **2004**, *14*, 512; (h) Licini, G.; Prins, L.J.; Scrimin, P. *Eur. J. Org. Chem.* **2005**, 969; (i) Yin, H.; Hamilton, A. D. *Angew. Chem. Int. Ed.* **2005**, *44*, 4130; (j) Zhang, W.; Moore, J. S. *Angew. Chem. Int. Ed.* **2006**, *45*, 4416; (k) Davis, J. M.; Tsou, L. K.; Hamilton, A. D. *Chem. Soc. Rev.* **2007**, *36*, 326.

(3) Hill, D. J.; Mio, M. J.; Prince, R. B.; Hughes,T. S.; Moore, J. S. *Chem. Rev.* **2001,** *101,* 3893.

(4) Gellman, S. H. *Acc. Chem. Res.* **1998,** *31,* 173.

(5) (a) Deshayes, K.; Broene, R. D.; Chao, I.; Knobler, C. B.; Diederich, F. *J. Org. Chem.* **1991**, *56*, 6787; (b) Paruch, K.; Katz, T. J.; Incarvito, C.; Lam, K.-C.; Rhatigan, B.; Rheingold, A. L. *J. Org. Chem.* **2000**, *65*, 7602 and references therein.

(6) Gange, D.; Magnus, P.; Bass, L.; Arnold, E. V.; Clardy, J. *J. Am. Chem. Soc.* **1980**, *102*, 2134.

(7) Fuji, K.; Furuta, T.; Tanaka, K. *Org. Lett.* **2001**, *3*, 169.

(8) Kiupel, B.; Niederalt, C.; Nieger, M.; Grimme, S.; Vögtle, F. *Angew. Chem. Int. Ed.* **1998**, *37*, 3031.

(9) (a) Berl, V.; Huc, I.; Khoury, R; Lehn, J.-M. *Chem. Eur. J.* **2001**, *7*, 2798; (b) Kolomiets, E.; Berl, V.; Odriozola, I.; Stadler, A.-M.; Kyritsakas, N.; Lehn, J.-M. *Chem. Commun.* **2003**, 2868.

(10) Dolain, C.; Maurizot, V.; Huc, I. *Angew. Chem. Int. Ed.* **2003**, *2*, 2738.

(11) Schmitt, J.-L.; Stadler, A.-M.; Kyritsakas, N.; Lehn, J.-M. *Helv. Chim. Acta* **2003**, *86*, 1598.

(12) (a) Brunsveld, L.; Meijer, E. W.; Prince, R. B.; Moore, J. S. *J. Am. Chem. Soc.* **2001,** *123,* 7978; (b) Hill, D. J.; Moore, J. S. *PNAs* **2002**, *99*, 5053.

(13) (a) van Gorp, J. J.; Vekemans, J. A. J. M.; Meijer, E. W. *Chem. Commun.* **2004**, 60; (b) Sinkeldam, R. W.; Hoeben, F. J. M.; Pouderoijen, M. J.; De Cat, I.; Zhang, J.; Furukawa, S.; De Feyter, S.; Vekemans, J. A. J. M.; Meijer, E. W. *J. Am. Chem. Soc.* **2006**, *128*, 16113.

(14) Gabriel, G. J.; Iverson, B. L. *J. Am. Chem. Soc.* **2002**, *124*, 15174.

(15) (a) Hamuro, Y.; Geib, S. J.; Hamilton, A. D. *J. Am. Chem. Soc.* **1996**, *118*, 7529; (b) Hamuro, Y.; Geib, S. J.; Hamilton, A. D. *J. Am. Chem. Soc.* **1997**, *119*, 10587.

(16) Yang, X.; Martinovic, S.; Smith, R. D.; Gong, B. *J. Am. Chem. Soc.* **2003**, *125*, 9932.

(17) Archer, E. A.; Krische, M. J. *J. Am. Chem. Soc.* **2002**, *124*, 5074.

(18) (a) Smith, M. D.; Long, D. D.; Claridge, T. D. W.; Marquess, D. G.; Fleet, G. W. J. *Chem. Commun*. **1998**, 2039; (b) Long, D. D.; Smith, M. D.; Marquess, D. G.; Claridge, T. D. W.; Fleet, G. W. J. *Tetrahedron Lett.* **1998**, *39*, 9293; (c) Claridge, T. D. W.; Long, D. D.; Hungerfor, N. L.; Aplin, R. T.; Smith, M. D.; Marquess, D. G.; Fleet, G. W. J. *Tetrahedron Lett.* **1999**, *40*, 2199; (d) Watterson, M. P.; Pickering, L.; Smith, M. D.; Hudson, S. J.; Marsh, P. R.; Mordaunt, J. E.; Watkin, D. J.; Newman, C. J.; Fleet, G. W. J. *Tetrahedron Asymm.* **1999**, *10*, 1855; (e) Edwards, A. A.; Sanjayan, G. J.; Hachisu, S.; Trantera, G. E.; Fleet, G. W. J. *Tetrahedron* **2006**, *62*, 7718.

(19) (a) von Roedern, E. G.; Lohof, E.; Hessler, G.; Hoffmann, M.; Kessler, H. *J. Am Chem. Soc*. **1996**, *118*, 10156; (b) von Roedern, E. G.; Kessler, H. *Angew. Chem. Int. Ed.* **1994**, *34*, 687; (c) Gruner, S. A. W.; Truffault, V.; Voll, G.; Locardi, E.; Stöckle, M.; Kessler, H. *Chem. Eur. J.* **2002**, *8*, 4365.

(20) Apella, D. H.; Christianson, L. A.; Karle, I. L.; Powel, D. R.; Gellman, S. H. *J. Am. Chem. Soc.* **1996**, *118*, 13071.

(21) (a) Hart, S. A.; Bahadoor, A. B. F.; Matthews, E. E.; Qiu, X. J.; Schepartz, A. *J. Am. Chem. Soc.* **2003**, *125*, 4022; (b) Raguse, T. L.; Lai, J. R.; Gellman, S. H. *Helv. Chim. Acta* **2002**, *85*, 4154.

(22) Cheng, R. P.; Gellman, S. H.; DeGrado, W. F. *Chem. Rev.* **2001**, *101*, 3219.

(23) Woll, M. G.; Fisk, J. D.; LePlae, P. R.; Gellman, S. H. *J. Am. Chem. Soc.* **2002**, *124*, 12447.

(24) (a) Sharma, G. V. M.; Reddy, K. R.; Krishna, P. R.; Sankar, A. R.; Narsimulu, K.; Kumar, S. K.; Jayaprakash, P.; Jagannadh, B.; Kunwar, A. C. *J. Am. Chem. Soc.* **2003**, *125*,13670; (b) Sharma, G. V. M.; Nagendar, P.; Jayaprakash, P.; Krishna, P. R.; Ramakrishna, K. V. S.; Kunwar, A. C. *Angew. Chem. Int. Ed.* **2005**, *44*, 5878.

(25) Rueping, M.; Schreiber.; J. V.; Lelais, G.; Jaun, B.; Seebach, D. *Helv. Chim. Acta* **2002**, *85*, 2577.

(26) Abele, S.; Seebach, D. *Helv. Chim. Acta* **1999**, *82*, 1559.

(27) Yang, D.; Qu, J.; Li, B.; Ng, F.-F.; Wang, X.-C.; Cheung, K.-K.; Wang, D.-P.; Wu, Y.-D. *J. Am. Chem. Soc.* **1999**, *121*, 589.

(28) Gademann, K.; Häne, A.; Rueping, M.; Jaun, B.; Seebach, D. *Angew. Chem. Int. Ed.* **2003**, *42*, 1534.

(29) Hayen, A.; Schmitt, M. A.; Ngassa, F. N.; Thomasson, K. A.; Gellman, S. H. *Angew. Chem. Int. Ed.* **2004**, *43*, 505.

(30) De Pol, S.; Zorn, C.; Klein, C. D.; Zerbe, O; Reiser, O. *Angew. Chem. Int. Ed.* **2004**, *43*, 511.

(31) Seebach, D.; Brenner. M.; Rueping, M.; Jaun, B. *Chem. Eur. J.* **2002**, *8*, 573.

(32) Simon, R. J.; Kania, R. S.; Zuckermann, R. N.; Huebner, V. D.; Spellmeyer, D. C.; Tan, R.; Frankel, A. D.; Santi, D. V.; Cohen, F. E.; Bartlett, P. A. *PNAs* **1992**, *89*, 9367.

(33) Wu, C. W.; Kirshenbaum, K.; Sanborn, T. J.; Patch, J. A.; Huang, K.; Dill, K.; A.; Zuckermann, R. N.; Barron, A. E. *J. Am. Chem. Soc.* **2003**, *125*, 13525.

(34) (a) Seebach, D.; Matthews, J. L. *Chem. Commun.* **1997**, 2015; (b) Cheng, R. P.; Gellman, S. H.; DeGrado, W. F. *Chem. Rev.* **2001**, *101*, 3219; (c) Martinek, T. A.; Fülöp, F. *Eur. J. Biochem.* **2003**, *270*, 3657.

(35) Raguse, T. L.; Lai, J. R.; Gellman, S. H. *J. Am. Chem. Soc.* **2003**, *125*, 5592.

(36) Langenhan, J. M.; Guzei, I. A.; Gellman, S. H. *Angew. Chem. Int. Ed.* **2003**, *42*, 2402.

(37) Hagihara, M.; Anthony, N. J.; Stout, T. J.; Clardy, J.; Schreiber, S. L. *J. Am. Chem. Soc.* **1992**, *114*, 6568.

(38) Hintermann, T.; Gademann, K.; Jaun, B.; Seebach, D. *Helv. Chim. Acta* **1998**, *81*, 983.

(39) Hanessian, S.; Luo, X.; Schaum, R.; Michnick, S. *J. Am. Chem. Soc.* **1998**, *120*, 8569.

(40) (a) Hintermann, T.; Gademann, K.; Juan, B.; Seebach, D. *Helv. Chim. Acta* **1998**, *81*, 983; (b) Seebach, D.; Schreiber, J. V.; Abele, S.; Daura, X. van Gunsteren, W. F. *Helv. Chim. Acta* **2000,** *83,* 34.

(41) Imperiali, B.; Ottesen, J. J. *J. Pept. Res.* **1999**, *54*, 177.

(42) (a) Baldauf, C.; Gunther, R.; Hofmann, H.-J. *Helv. Chim. Acta* **2003**, *86*, 2573; (b) Baldauf, C.; Gunther, R.; Hofmann, H.-J. *J. Org. Chem.* **2004**, *69*, 6214; (c) Baldauf, C.; Gunther, R.; Hofmann, H.-J. *Biopolymers* **2006**, *84*, 408; (d) Baldauf, C.; Gunther, R.; Hofmann, H.-J. *J. Org. Chem.* **2006**, *71*, 1200.

(43) (a) Richardson, J. S. *Adv. Protein Chem.* **1981**, *34*, 167; (b) Burley, S. K.; Almo, S. C.; Bonanno, J. B.; Capel, M.; Chance, M. R.; Gaasterland, T.; Lin, D.; Sali, A.; Studier, F. W.; Swaminathan, S. *Nat. Genet.* **1999**, *23*, 151.

(44) Chou, P.; Fasman, G. G. *J. Mol. Biol*. **1977**, *115*, 135.

(45) (a) Milner-White, E. J.; Ross, B. M.; Ismail, R.; Belhadj-Mostefa, K.; Poet, R. *J. Mol. Biol.* **1988**, *204*, 777; (b) Milner-White, E. J. *J. Mol. Biol.* **1990**, *216*, 385; (c) Pavone, V.; Gaeta, A. L.; Nastri, F.; Maglio, O.; Isernia, C.; Saviano, M. *Biopolymers* **1996**, *38*, 705; (d) Chou, K.-C. *Biopolymers* **1997**, *42*, 837.

(46) (a) Yuan, Z. Q.; Blomberg, D.; Sethson, I.; Brickmann, K.; Ekholm, K.; Johansson, B.; Nilsson, A.; Kihlberg, J. *J. Med. Chem*. **2002**, *45*, 2512; (b) Hedenstroem, M.; Yuan, Z. Q.; Brickmann, K.; Carlsson, J.; Ekholm, K.; Johansson, B.; Kreutz, E.; Nilsson, A.; Sethson, I.; Kihlberg, J. *J. Med. Chem*. **2002**, *45*, 2501; (c) Rosenstroem, U.; Skoeld, C.; Plouffe, B.; Beaudry, H.; Lindeberg, G.; Botros, M.; Nyberg, F.; Wolf, G.; Karlen, A.; Gallo-Payet, N.; Hallberg, A. *J. Med. Chem*. **2005**, *48*, 4009.

(47) Narutis, V. P.; Kopple, K. D. *Biochemistry* **1983**, *22*, 6233.

(48) Loosi, H. R.; Kessler, H.; Oschkinat, H.; Weber, H. P.; Petcher, T. J.; Widmer, A. *Helv. Chim. Acta* **1985**, *68*, 682.

(49) Hagler, A. T.; Osguthorpe, D. J.; Dauber-Osguthorpe, P.; Hempel, J. C. *Science* **1985**, *227*, 1309.

(50) Frishman, D.; Argos, P. *Proteins* **1995,** *23*, 566.

(51) For heterocyclic γ-turns, see: (a) Callahan, J. F.; Bean, J. W.; Burgess, J. L.; Eggleston, D. S.; Hwang, S. M.; Kopple, K. D.; Koster, P. F.; Nichols, A.; Peishoff, C. E.; Samanen, J. M.; Vasko, J. A.; Wong, A.; Huffman, W. F. *J. Med. Chem.* **1992**, *35*, 3970; (b) Callahan, J. F.; Newlander, K. A.; Burgess, J. L.; Eggleston, D. S.; Nichols, A.; Wong, A.; Huffman, W. F. *Tetrahedron* **1993**, *49*, 3479; (c) Newlander, K. A.; Callahan, J. F.; Moore, M. L.; Tomaszek, Jr, T. A.; Huffman, W. F. *J. Med. Chem.* **1993**, *36*, 2321; (d) Alkorta, I.; Suarez, M. L.; Herranz, R.; Gonzalez-Muniz, R.; Garcia-Lopez, M. T. *J. Mol. Model.* **1996**, *2*, 16; (e) Etzkorn, F. A.; Travins, J. M.; Hart, S. A. *Ad*v. *Amino Acid Mimetics Peptidomimetics* **1999**, *2*, 125.

(52) For γ-turns induced by 2,3-methanoamino acids, see: (a) Burgess, K.; Ho, K.-K.; Pettitt, B. *J. Am. Chem. Soc.* **1994**, *116*, 799; (b) Burgess, K.; Ke, C.-Y. *J. Org. Chem.* **1996**, *61*, 8627; (c) Moye-Sherman, D.; Jin, S.; Li, S.; Welch, M. B.; Reibenspies, J.; Burgess, K. *Chem. Eur. J.* **1999**, *5*, 2730.

(53) Jimenez, A. I.; Ballano, G.; Cativiela, C. *Angew. Chem. Int. Ed.* **2005**, *44*, 396.

(54) Chen, F.; Zhu, N. Y.; Yang, D. *J. Am. Chem. Soc***. 2004**, *126*, 15980.

(55) Creamer, T. P.; Campbell, M. N. *Adv. Protein. Chem*. **2002**, *62*, 263.

(56) (a) Zhu, J.; Parra, R. D.; Zeng, H.; Jankun, E. S.; Zeng, X. C.; Gong, B. *J. Am. Chem. Soc.* **2000**, *122,* 4219; (b) Gong, B. *Chem. Eur. J.* **2001**, *7*, 4336.

(57) Etter, M. C. *Acc. Chem. Res.* **1990**, *23*, 120.

(58) Kritzer, J. A.; Hodsdon, M. E.; Schepartz, A. *J. Am. Chem. Soc*. **2005**, *127*, 4118.

(59) Liu, D.; Choi, S.; Chen, B.; Doerksen, R. J.; Clements, D. J.; Winkler, J. D.; Klein, M. L.; DeGrado, W. F. *Angew. Chem. Int. Ed.* **2004**, *43*, 1158.

(60) Hussey, A. S.; Wilk, I. J. *J. Am. Chem. Soc*. **1950**, *72*, 830.

(61) (a) Ishimoto, B.; Tonan, K.; Ikawa, S. *Spectrochim. Acta Part A* **2000**, *56*, 201; (b) Jin, Y.; Tonan, K.; Ikawa, S. *Spectrochim. Acta Part A* **2002**, *58*, 2795.

(62) (a) Zhao, M.; Bada, J. L. *Nature* **1989**, *339*, 463; (b) Ehrenfreund, P.; Charnley, S. B.; *Annu. Rev. Astron. Astrophys.* **2000**, *38*, 427.

(63) (a) Brückner, H.; Nicholson, G. J.; Jung, G.; Kruse, K.; König, W. A. *Chromatographia* **1980**, *13*, 209; (b) Sansom, M. S. P. *Prog. Biophys. Mol. Biol.* **1991**, *55*, 139; (c) Sansom, M. S. P. *Q. Rev. Biophys*. **1993**, *26*, 365; (d) Karle, I. L.; Perozzo,

M. A.; Mishra, V. K.; Balaram, P. *PNAs* **1998**, *95*, 5501; (e) Snook, C. F.; Woolley, G. A.; Oliva, G.; Patthabi, V.; Wood, S. F.; Blundell, T. L.; Wallace, B. A. *Structure* **1998**, *6*, 783; (f) Tieleman, D. P.; Biggin, P. C.; Smith, G. R.; Sansom, M. S. P. *Q. Rev. Biophys.* **2001**, *34*, 473; (g) Chugh, J. K.; Wallace, B. A. *Biochem. Soc. Trans.* **2001**, *29*, 565.

(64) (a) Pandey, R. C.; Cook, J. C. Jr.; Rinehart, K. L. Jr. *J. Am. Chem. Soc.* **1977**, *99*, 8469; (b) Fox, R. O. Jr.; Richards, F. M. *Nature* **1982**, *300*, 325.

(65) (a) Rinehart, K. L.; Gaudioso, L. A.; Moore, M. L.; Pandey, R. C.; Cook, J. C. Jr; *J. Am. Chem. Soc.* **1981**, *103*, 6517; (b) Karle, I. L.; Flippen-Anderson, J. L.; Agarwalla, S.; Balaram, P. *PNAs* **1991**, *88*, 5307.

(66) Arvinda, S.; Shmala, N.; Roy, R. S.; Balaram, P. *Proc. Indian Acad. Sci.* (*Chem. Sci.*) **2003**, *115*, 373.

(67) For excellent reviews, see: (a) Prasad, B. V.; Balaram, P. *CRC critical reviews in biochemistry* **1984**, *16*, 307; (b) Venkatraman, J.; Shankaramma, S. C.; Balaram, P.; *Chem. Rev.* **2001**, *101*, 3131; (c) Toniolo, C.; Crisma, M.; Formaggio, F.; Peggion, C. *Biopolymers (Peptide Science)* **2001**, *60*, 396; (d) Crisma, M.; Moretto, A.; Rainaldi, M.; Formaggio, F.; Broxterman, Q. B.; Kaptein, B.; Toniolo, C. *J. Peptide Sci.* **2003**, *9*, 620; (e) Toniolo, C.; Formaggio, F.; Kaptein, B.; Broxterman, Q. B. *Synlett.* **2006**, 1295; (f) Mahalakshmi, R.; Balaram, P. *Methods in molecular biology (Clifton, N. J.)* **2006**, *340*, 71.

(68) Shamala, N.; Nagaraj, R.; Balaram, P. *Chem. Commun.* **1978**, 996.

(69) Toniolo, C.; Crisma, M.; Bonora, G. M.; Benedetti, E.; Di Blasio, B.; Pavone, V.; Pedine, C.; Santini, A. *Biopolymers* **1991**, *31*, 129.

(70) Karle, I. L.; Flippen-Anderson, J. L.; Sukumar, M.; Uma, K.; Balaram, P. *PNAs* **1988**, *85*, 299.

(71) Karle, I. L.; Balaram, P. *Biochemistry* **1990**, *29*, 6747.

(72) (a) Karle, I. L.; *Acta Crystallogr.* **1992**, *B48*, 341; b) Benedetti, E. *Biopolymers* (*Peptide Science*) **1996**, *40*, 3.

(73) (a) Zeng, H.; Miller, R. S.; Flowers, R. A; Gong, B. *J. Am. Chem. Soc.* **2000**, *122*, 2635; (b) Zeng, H. Q.; Yang, X. W.; Brown, A. L.; Martinovic, S.; Smith, R. D.; Gong, B. *Chem. Commun.* **2003**, 1556.

(74) (a) Toniolo, C.; Crisma, M.; Formaggio, F.; Peggion, C. *Biopolymers* **2001**, *60*, 396; (b) Kaul, R.; Balaram, P. *Bioorg. Med. Chem.* **1999**, *7*, 105.

(75) Desiraju, G. R.; Parthasarathy, R. *J. Am. Chem. Soc.* **1989**, *111*, 8725.

(76) α-aminoisobutyric acid (Aib) residue has been shown to be significantly more effective than L-Proline in inducing β-sheet disruption in short model peptides. Formaggio, F.; Bettio, A.; Moretto, V.; Crismo, M.; Toniolo, C.; Broxterman, Q. B. *J. Peptide Sci.* **2003**, *9*, 461.

(77) Srinivas, D.; Gonnade, R.; Ravindranathan, S.; Sanjayan, G. J. *Tetrahedron* **2006**, *62*, 10141.

(78) Kendhale, A.; Gonnade, R.; Rajamohanan, P. R.; Sanjayan. G. J. *Chem. Commun.* **2006**, 2756.

(79) Cuello, A.C.; Bell, K.F.S. *Curr. Med. Chem. – Central Nervous System Agents,* **2005***, 5,* 15.

(80) Smeenk, J. M.; Otten, M. B. J.; Thies, J.; Tirrell, D. A.; Stunnenberg, H. G.; van Hest, J. C. M. *Angew. Chem. Int. Ed*. **2005**, *44*, 1968.

(81) Maiti, S. N.; Singh, M. P.; Micetich, R. G. *Tetrahedron Lett.* **1986**, *27*, 1423.

CHAPTER 3

BINOL-Based Foldamers - Access to Oligomers with Diverse Structural Architectures

-Man needs his difficulties because they are necessary to enjoy success.

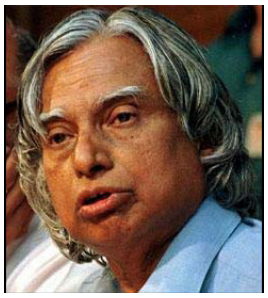

by A. P. J. Abdul Kalam
Born: 15th October 1931, India

3.1 Aromatic foldamers: An overview

The previous chapter has an elaborate discussion about foldamers in general, their various types and importance. This chapter primarily describes about the synthesis and conformation of a new family of aromatic oligoamide foldamers based on binaphthol (BINOL) monomeric building blocks.

The discovery of foldamers with biological activity[1] and special material properties[2,3] was of particular importance and increased the activities to find novel foldamers with diverse backbone structures not easily achievable by their small molecule counterparts.[3] Several classes of aromatic foldamers have been designed and synthesized using the bottom-up approach. This involves the identification of novel abiotic backbones that can fold into secondary structures such as helices, sheets, etc. Among them the aromatic structures which bear close analogy with peptide secondary structures are aromatic oligoamides. The conformation of these oligoamides can be stabilized by hydrogen bonding interactions between amide groups and donors and acceptors belonging to the adjacent aromatic rings. Several oligomers based on different building blocks such as pyridines,[4] anthranilic acids,[5] pyrazines,[6] 1,3-dimethoxybenzenes,[7] etc. are reported. Some aromatic oligomers based on ureas[8] and hydrazides[9] have also been reported. Oligo(m-phyleneethylene)s has been shown to adopt secondary structures controlled by non covalent interactions.[10] Oligomers with mixed building blocks such as pyridine-pyrimidine,[11] pyridine-pyridazines,[12] pyridine-pyrimidine with hydrazide linkers[13] have also been reported. The salient features of aromatic oligomers are (i) they often exhibit high resistance towards hydrolytic cleavage, (ii) their structures can often be accurately predicted.

Rotation about the bond connecting the aryl group to the amide is not feasible and they are coplanar or nearly coplanar due to the conjugation between amide and aryl group (figure 1).[14]

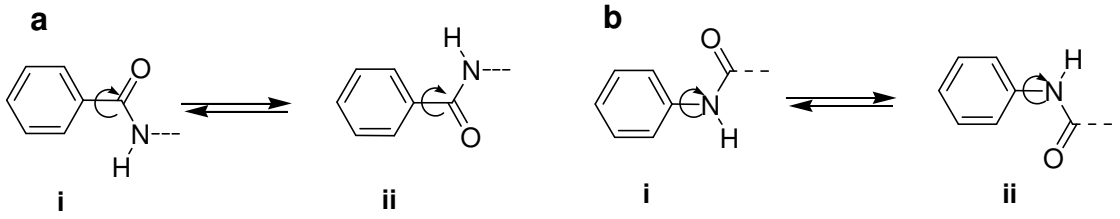

***Figure 1*:** Rotation around (a) aryl-CONH bond and (b) aryl-NHCO bond.

The stability of particular conformer e.g. *syn* or *anti* can be further increased by using specific attractive and repulsive interaction between the amide and other functional groups in the aryl moiety. Intramolecular hydrogen bonding provides the most-simple, efficient, and reliable approach for this purpose.[7a,15] Figure 2 shows the typical intramolecular hydrogen-bonding patterns that have been used to restrict the rotation of the Ar-CONHAr bond in folding oligomers. The six- and five-membered rings formed by O···H-N and N···H-N hydrogen bonding (figure 2a–e) are well-established.[5a,16] Replacement of the OR (figure 2a) with an OH group lowers the stability of the conformation shown, because the OH proton can also form a six-membered hydrogen bond with the neighboring carbonyl oxygen atom.[15] On the other hand, a phenoxide salt

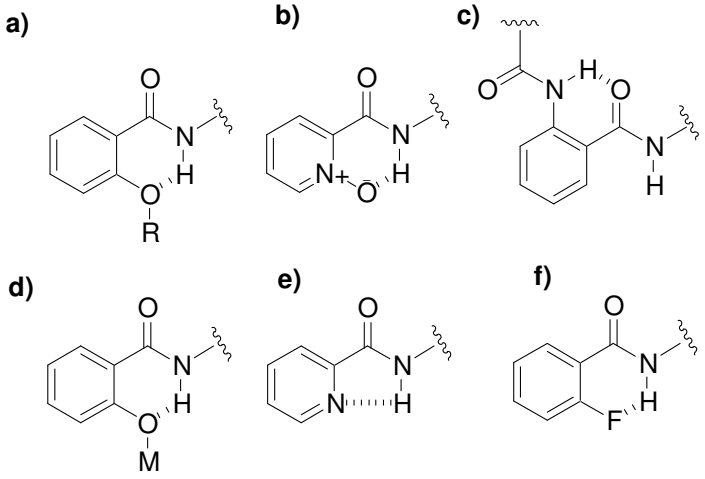

Figure 2: Typical example of intramolecular bond in aromatic units for restriction of Ar-CONHAr bond.

(figure 2d, M=K) was reported to form the expected intramolecular hydrogen bonding that is used to induce the formation of ionic foldamers.[17] It is well-established that fluoride ion is a very strong proton acceptor. Covalently bound fluorine is considered a very weak hydrogen bond acceptor.[18] But Li et al.[19] has demonstrated that intramolecular F···H-N hydrogen bonding, as shown in figure 2f, can be readily formed.

Some representative examples of intramolecular hydrogen-bonding patterns in aromatic foldamers that restrict the rotation of the Ar-NHCOAr bond in foldamers are shown in figure 3.

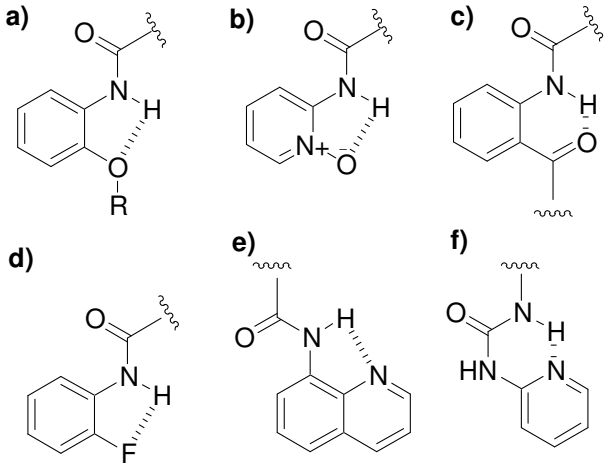

***Figure 3*:** Typical example of intramolecular hydrogen bond in aromatic units for restriction of Ar-NHCOAr bond.

These rotational restrictions are strong enough to design an aromatic oligomer with predictable conformation. This has been well demonstrated in the case of oligomers derived from pyridine diamines and pyridine carboxylic acid[4] or those derived from 4,6-dimethoxy-3-amino-benzoic acid.[7] When a oligomer is made from a repeated structural motif the computational and/or experimental studies of a short oligomer provides accurate data on relative positioning of consecutive units that may be extrapolated to higher oligomers. But in case of α- or β-peptides the conformational study of short oligomer does not give much information about the folding pattern of a higher oligomer.

This is due to the fact that interactions which stabilize a particular conformation are not consecutive in nature.

Depending upon the monomeric building block, aromatic oligomers are shown to adopt stable linear, bent and helical structures.[15] The angle between the amine and acid substituents defines the structure of the aromatic foldamers. When the angle is 180^0 it prefers linear structure and if it is less than 180^0 it prefers bend structures. For example, oligomers of 6-alkoxy-5-aminopicolinic acid[20] adopts a linear structure (figure 4a) but in the case of oligomers derived from 2,6-diaminopyridine and/or 2,6-pyridinedicarboxylic acid,[4b,21] and 4,6-dialkoxy-3-aminobenzoic acid[7a,22] adopts helical structure (figure 4c).

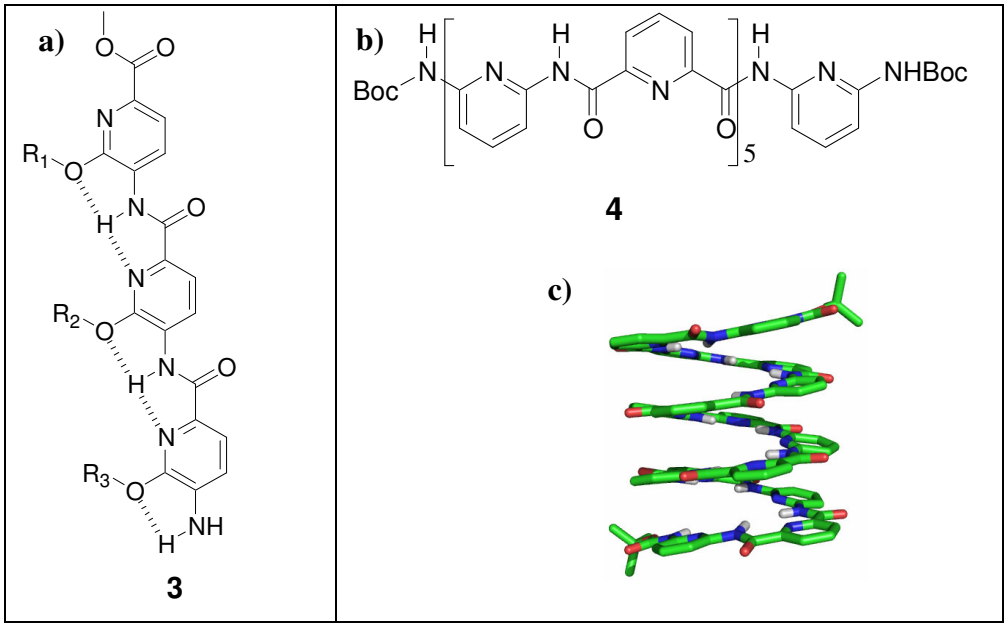

***Figure 4*:** (a) Oligomers of 6-alkoxy-5-aminopicolinic acid adopting linear structure.[20] (b) Molecular structure of oligomer derived from 2,6-diaminopyridine and 2,6-pyridinedicarboxylic acid. (c) X-ray structure of **4** adopting helical structure.[23]

A large variety of structures can be obtained by just changing the substituent position in the aromatic ring. Gong et al. has shown that by changing the *meta* and *para*-substituted monomeric units, one can get helices with large diameters. The diameters of these helices

can be very easily tuned by simply varying the ratio of *meta* and *para* substituted monomeric units (figure 5).[7,22] These helical foldamers find extensive application in the field of molecular recognition, catalysis or transport.[24] Helices with very few units per turn permit easy access to objects with a high aspect ratio which can be synthesized easily.[16,25]

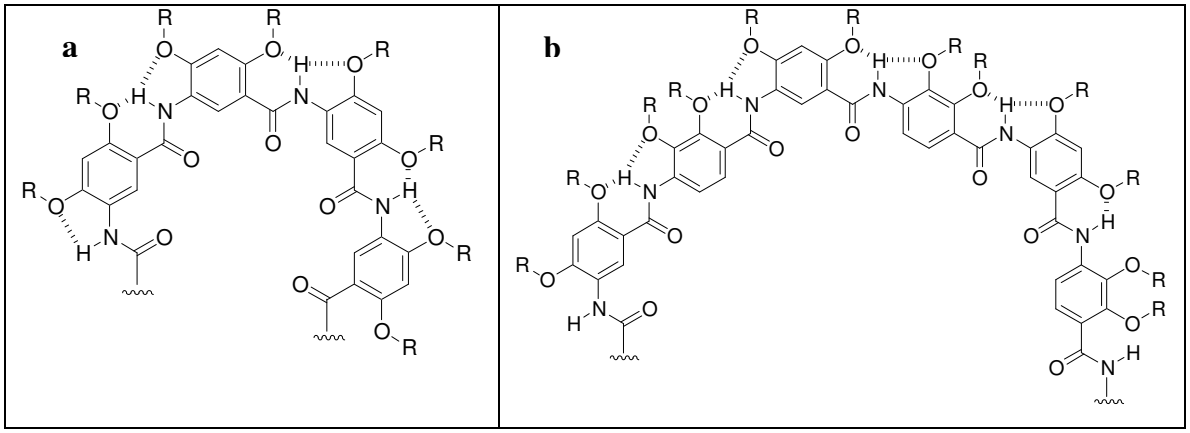

***Figure 5*:** The diameter of the helical backbone can be easily tuned by changing the substituents[7,22] in the monomeric building blocks; (a) backbone with *meta*, *meta*, *meta* sequence and (b) backbone with *meta*, *para*, *meta* sequence.

3.2 BINOL-Based Foldamers: Oligomers with diverse structural archietectures

3.2.1 Atropisomerism in BINOLs

Atropisomerism is the phenomenon that is exhibited by variety of biaryl compounds.[26] The type of isomerism which arises due to the restricted rotation around a single bond is termed as *atropisomerism* and the isomers are called *atropisomers* (figure 6). In the case of biphenyls, the two phenyl groups are joined by a single bond (sp^2-sp^2), called a pivotal bond. The distance between ortho H's in adjacent rings in the planar conformation is appreciably greater (0.29 nm) than twice the van der Waals radius of hydrogen (2 x 0.12 nm) so that the rotation around the pivotal bond is not *impeded* by the steric factor. So, by introduction of bulky substituents at the *ortho* position, energy barrier between the

enantiomers can be increased. The enantiomers are separable at room temperature when the energy barrier is 80-100 KJ mol^{-1}. The preferred conformations of the enantiomers are those in which the two phenyl planes are approximately, but not exactly, perpendicular to each other.

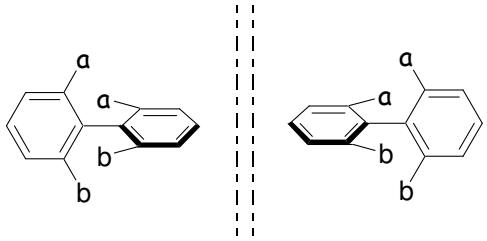

***Figure 6*:** Principle of optically active biphenyls.

Absolute configurations of chiral binaphthyl compounds were originally proposed by Mislow on the basis of a study of optical properties, stereochemical mechanisms, and thermal analysis.[27] This was later confirmed by Yamada and co-workers from the X-ray analysis of (*R*)-(+)-2,2'-Dihydroxy-[1,1']binaphthalenyl-3,3'-dicarboxylic acid dimethyl ester and its chemical correlation with other binaphthyl molecules.[28] The dihedral angle between the naphthalene rings in this molecule is about 77°. 2,2'-substituted 1,1'-binaphthyls have been extensively used to control many asymmetric processes because of their highly stable chiral configuration, and have demonstrated outstanding chiral discrimination properties.[29]

Research on the application of binaphthyls to molecular recognition was pioneered by Cram et al. who used chiral binaphthyl-based crown ethers as hosts for molecular recognition.[30] Katz et al. have prepared oligomers with more than one helical turn based on bis-salicylaldimine.[31] The helical conformation of these molecules has a marked effect on their optical properties; *i.e.* very intense absorption bands and CD effects were observed compared to those of the low-molecular-weight parent compounds. Pu et al.[32] made use of binaphthyl linkers to connect a large variety of conjugated molecules such as aryleneethynylenes, phenylenevinylenes, polythiophenes, oligophenylenes, and oligoethynylenes (e.g., **6**, figure 7). In the cases where the linkers contain phenyl groups,

meta as well as *para* substitution has been used. In the former case, this leads to the introduction of an extra turn in the polymer backbone, whereas, in the latter case, the turns are exclusively due to the binaphthyl groups. The resulting materials have a rigid helical comformation and can be applied to anchor catalytic complexes based on Al(III) and Zn(II) via the hydroxyl groups on their naphthyl units. Tanaka et al. has reported stepwise construction of chiral tetranaphthalenes (**5,** figure 7)[33] and their higher oligomers[34] and they exist in rod like structure.

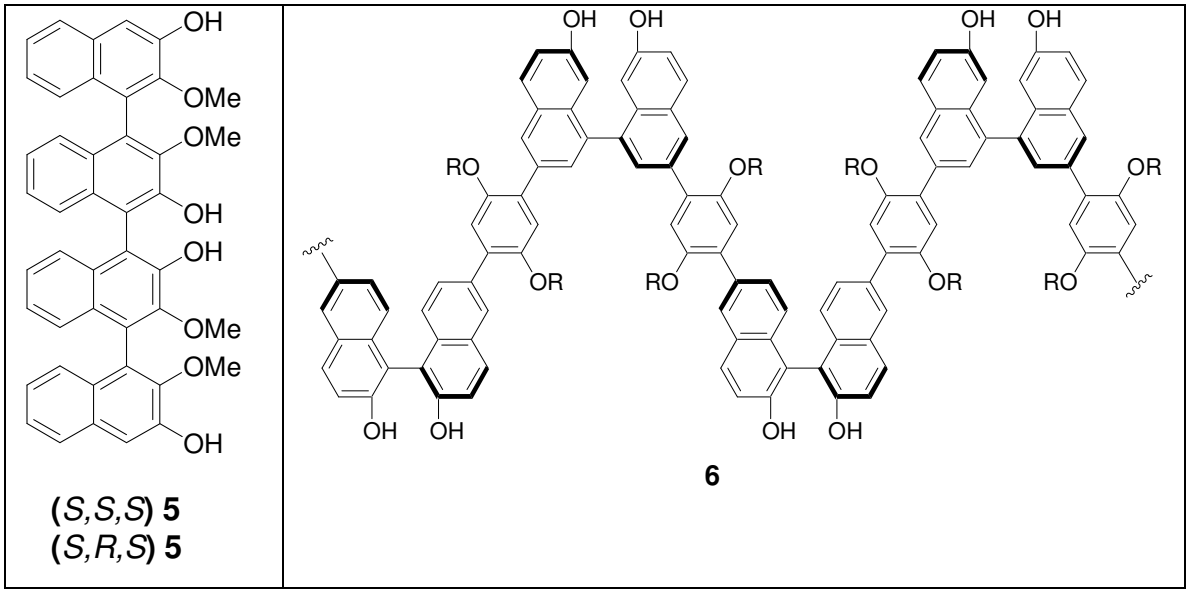

***Figure 7*:** Optically active binaphthyl oligomers.[33, 34]

3.2.2 BINOL-Based Foldamer: Design principles

The designing of a new foldamer requires the identification of new backbones with well-defined structural preferences, and foldamers are thus further defined as oligomers of modest length that in solution display such a specific conformational preference. Rotation around the aryl-amide bond is not feasible as discussed earlier in this chapter and the hydrogen bonds between the amide groups and donors and acceptor atoms belonging to the adjacent aromatic units stabilize a particular conformation.[25] Again, due to the ease in synthesis acid-amine coupling strategy is the preferred one for the foldamer synthesis to assemble the monomeric building blocks. Although 1,1'-Binaphthols have been used in

several applications, their use in foldamer synthesis as monomeric building block is largely unexplored. We chose 1,1'-Binaphthols, also known as BINOLs as monomeric building block due to ease of synthesis and coupled with the fact that they can be obtained in enantiomerically pure form in multigram scale. We designed the following foldamer **1** for our study as shown in figure 8. It was expected that each oligomer would have a single possibility of conformer formation due to extensive intramolecular bifurcated hydrogen bonding, which precludes the possibility of conformer alternatives.

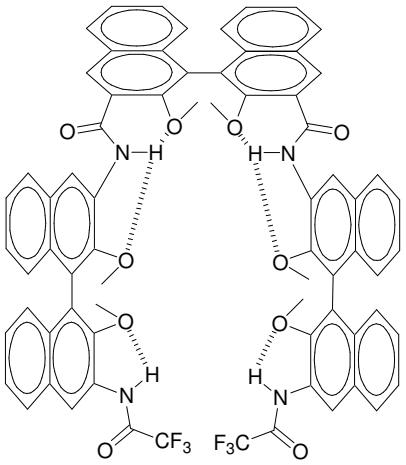

1

Figure 8: The foldamers having all BINOL units **1** with expected hydrogen bonding pattern is shown.

In general, the number of foldamers that can be obtained from *n* building blocks of the same class, considering chirality, is 2^n. For *n*=3, this provides, for instance, eight foldamers: [*R*][*R*][*R*], [*R*][*R*][*S*], [*R*][*S*][*R*], [*S*][*R*][*R*], [*R*][*S*][*S*], [*S*][*R*][*S*], [*S*][*S*][*R*], and [*S*][*S*][*S*]. A closer inspection reveals that the pairs [*R*][*R*][*S*] / [*S*][*R*][*R*] and [*R*][*S*][*S*] / [*S*][*S*][*R*], respectively, are degenerated in shape (figure 9). Therefore, the number of foldamers of different shape accessible (excluding the degenerated ones) can be calculated for an *odd* number of *n* building blocks, according to $2^{n-1} + 2^{(n-1)/2}$ and to $2^{n-1} + 2^{(n-2)/2}$, for an *even* number of same foldamer building blocks. Thus, for n=3 there would be six oligomers of different shapes, but for n=10 a library of 528 foldamers of different shape will be available.

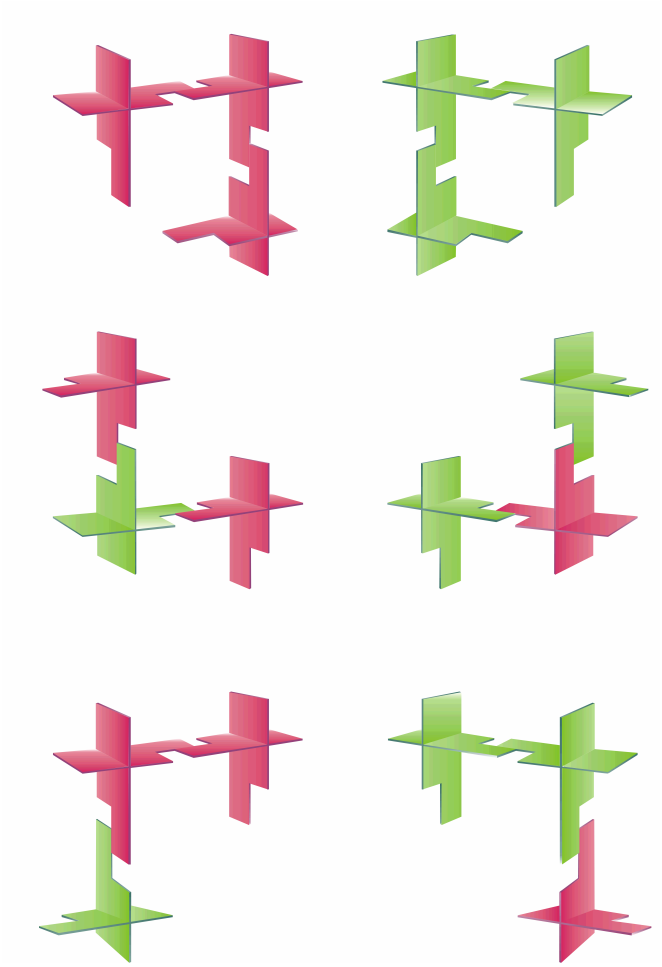

***Figure 9*:** Cartoon representation showing the number of oligomers of different shape accessible from three building blocks of [*R*] or [*S*] BINOL units. The purple and green coloured blocks indicates BINOLs with [*R*] or [*S*] configuration, respectively.

3.2.3 Synthesis

The monomeric building block **8** can in principle be accessed by two routes as shown in scheme 1. The protection of hydroxyl group of commercially available optically pure BINOL **7** by methoxymethyl chloride, ortholithiation with n-butyllithium followed by carboxylation and acidification affords **8**.[35] Alternatively **10**, dimethyl ester of 3,3-dicarboxylic acid **8**, can be obtained in a single step by oxidative coupling[36] of methyl ester of 3-hydroxy-2-naphthoic acid **9** using Cu(OH)Cl.TMEDA as a catalyst in

multigram scale. We chose the second route as it does not involve use of pyrophoric reagents like sodium hydride, n-butyllithium, etc. and can be scaled up very easily.

Scheme 1:

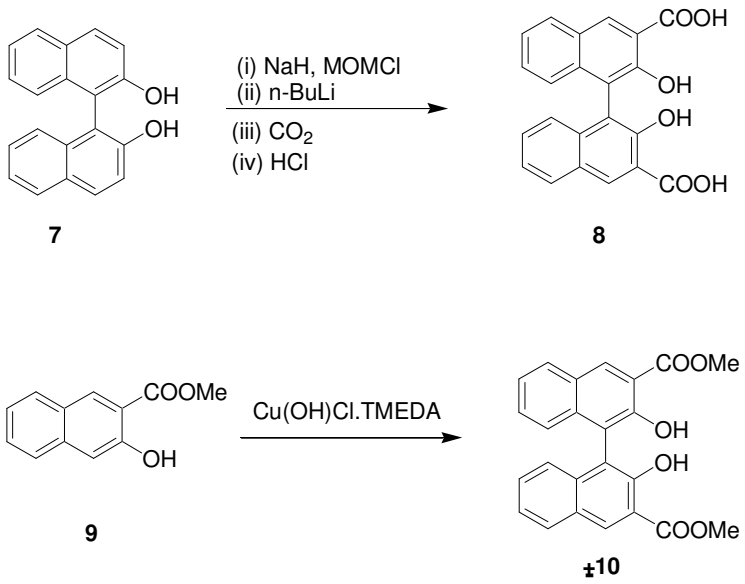

The racemic BINOL ester **10**, obtained by the oxidative coupling of methyl ester of 3-hydroxy-2-naphthoic acid **9**, was saponified to furnish the BINOL bis-acid **11**, which was subjected to kinetic resolution[37] using Leucine methyl ester as the base to afford both [*R*] and [*S*] antipodes of **11** (scheme 2).

Scheme 2:

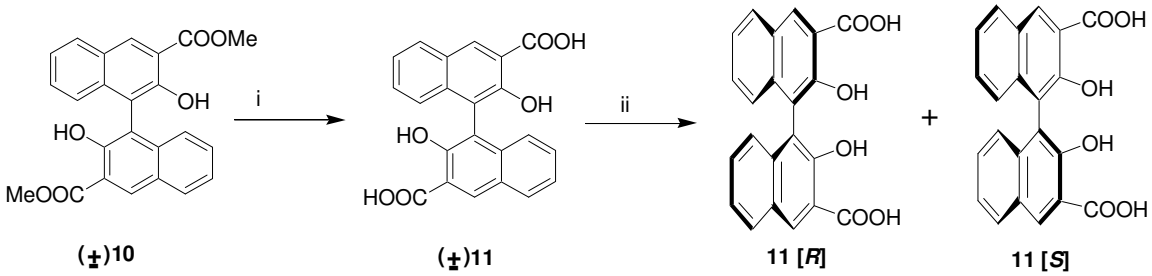

Reagents and conditions: (i) KOH, MeOH, reflux, 2h; (ii) leucine methyl ester (resolution).[37]

Both the [*R*] and [*S*] antipodes of the BINOL acid **11** were subjected to a series of transformations, involving Curtious rearrangement as a key step, [38] to furnish the BINOL bis-amines **15** [*R*] and **15** [*S*] (scheme 3).

Scheme 3:

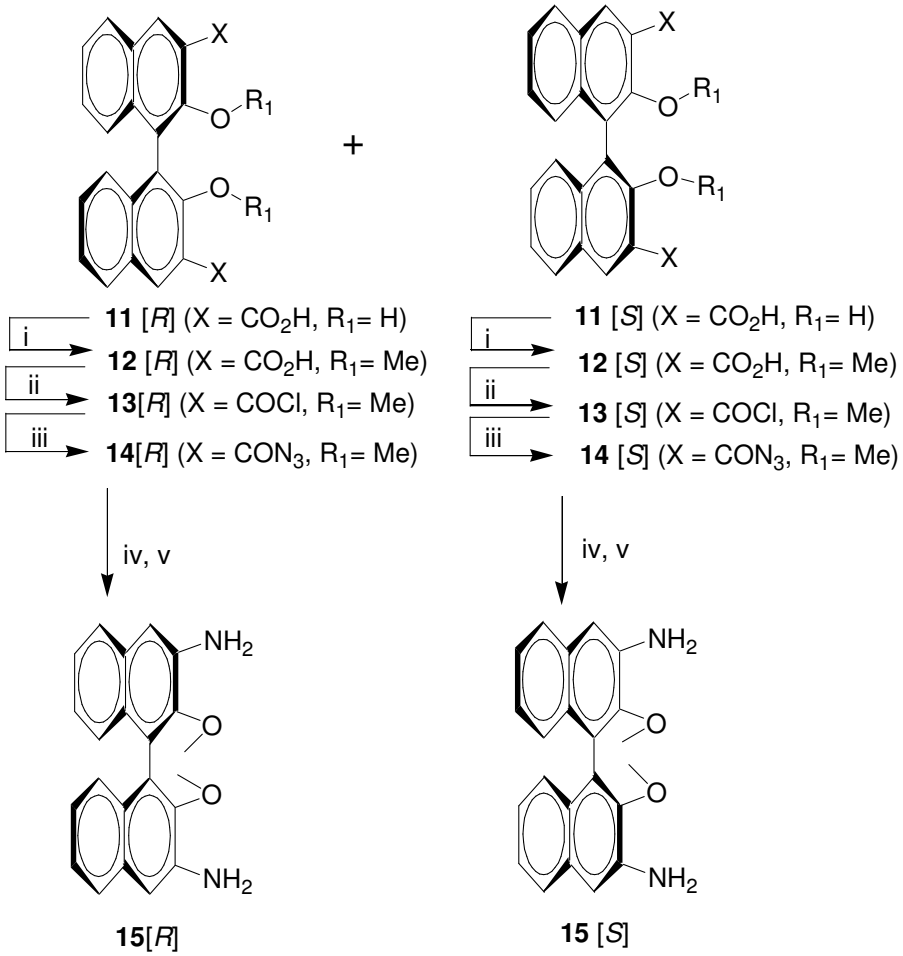

Reagent and conditions: (i) (a) Dimethyl sulphate, K_2CO_3, acetone, reflux, 6h; (b) KOH, MeOH, reflux, 2h; (ii) oxalyl chloride, DCM, DMF (cat.), RT, 2h; (iii) NaN_3, acetone, water, 15min; (iv) benzene, reflux, 1h; (v) NaOH, benzene, water, reflux, 1h;

Finally the oligomers **1** were made accessible by coupling excess BINOL amines **15** [*R*]/**15** [*S*] with the acid chlorides **13** [*S*]/ **13** [*R*] followed by capping the terminal amines as trifluoroacetamides (scheme 4).

Scheme 4:

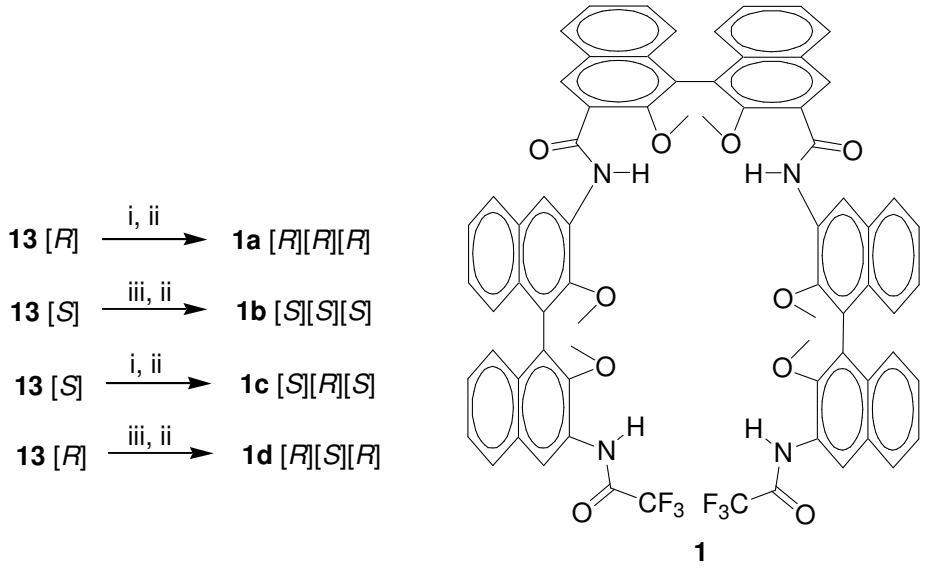

Reagents and conditions: (i) **15** [*R*] (4 eq.), triethylamine, DCM; (ii) TFA, DCC, DCM; (iii) **15** [*S*] (4 eq.), triethylamine, DCM.

All efforts to investigate the solid-state conformation of the trimers **1a-d** by single crystal X-ray studies did not succeed, since diffraction-quality crystals could not be grown in any of the cases, despite best efforts.

3.2.4 ab initio modeled structures of BINOL oligomers

To get an insight into the conformational features of the oligomers we performed the theoretical calculations based on the ab initio MO theory at the HF/6-31G* level. The phenomenon of atropisomerism restricts the conformational space considerably. Therefore, it is relatively easy to perform a systematic conformational search by quantum chemical methods. It has frequently been shown that Hartree-Fock theory at the HF/6-31G* level and Density Functional Theory at the B3LYP/6-31G* level are reliable enough to describe the conformational characteristics of peptides and peptide foldamers. [39,40] The conformational search according to both formalisms led in perfect agreement to the conformers visualized in figure 10.

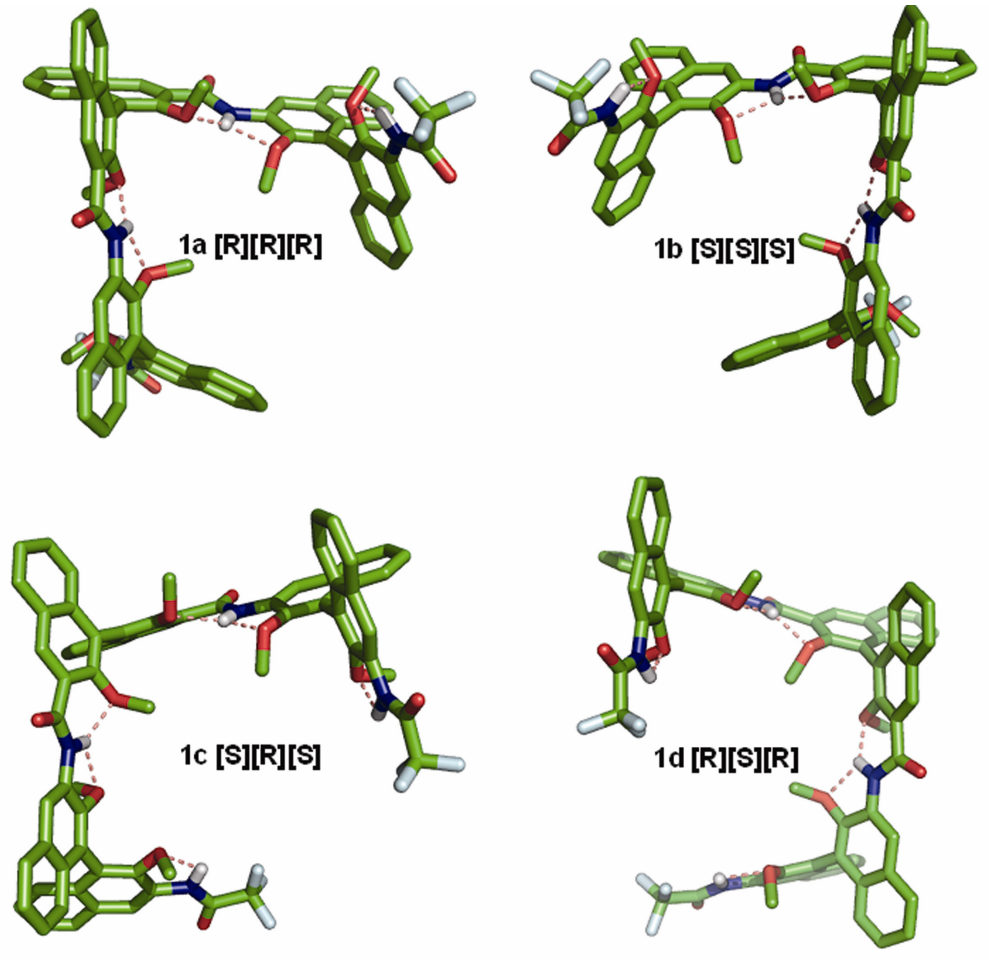

***Figure 10*:** Structural architecture of the oligomers **1a-d** obtained at the HF/6-31G* level of ab initio MO theory. The positioning of the BINOL enantiomers [*R*] and [*S*] is given in the inset along with the compound number.

Each oligomer has a single possibility of conformer formation due to extensive intramolecular bifurcated hydrogen bonding that precludes the possibility of conformer alternatives. The comparison of the structures revealed that all the conformers are endowed with two sets of intramolecular bifurcated hydrogen bonding, as anticipated. These bifurcated hydrogen bonded networks with S(5) and S(6)-type arrangements[41] maintain the rigidity of the foldamer backbone. The N-termini are relatively close to each other in the *SRS*/*RSR* stereo pairs. The closest distance between the fluorine atoms of the terminal CF_3 groups is 7 Å. A comparable arrangement is not observed in the other oligomers. A closer inspection further reveals that the four oligomer sets are composed of

two oligomer sub-sets with their non-super imposable mirror images ([*R*][*R*][*R*] *vs* [*S*][*S*][*S*] and [*R*][*S*][*R*] *vs* [*S*][*R*][*S*]).

3.2.5 NMR studies of BINOL oligomers

All two-dimensional foldamer oligomers are highly soluble in non-polar organic solvents (>>100 mM in $CDCl_3$) at ambient temperature. This observation suggested that the polar hydrogen-bonding groups of **1a-d** are strongly involved in intramolecular hydrogen bonding, thus preventing the formation of polymeric aggregates.[42] The ^{1}H NMR spectra (400 MHz) of all oligomers showed well resolved single set of signals in $CDCl_3$ at ambient temperature, which suggests that these oligomers exist in single conformation.

The comparison of ^{1}H NMR spectra of BINOL oligomers revealed that [*R*][*R*][*R*] *vs*. [*S*][*S*][*S*] and [*R*][*S*][*R*] *vs.* [*S*][*R*][*S*] shows similar chemical shifts. But in case of [*R*][*R*][*R*] *vs*. [*R*][*S*][*R*] and [*S*][*S*][*S*] *vs.* [*S*][*R*][*S*], the value of chemical shifts differs (figure 11). This observation strongly suggests that pairs of enantiomers of the oligomers [*R*][*R*][*R*]/[*S*][*S*][*S*] and [*R*][*S*][*R*]/[*S*][*R*][*S*] exists in their mirror-image architecture at the oligomer level as well.

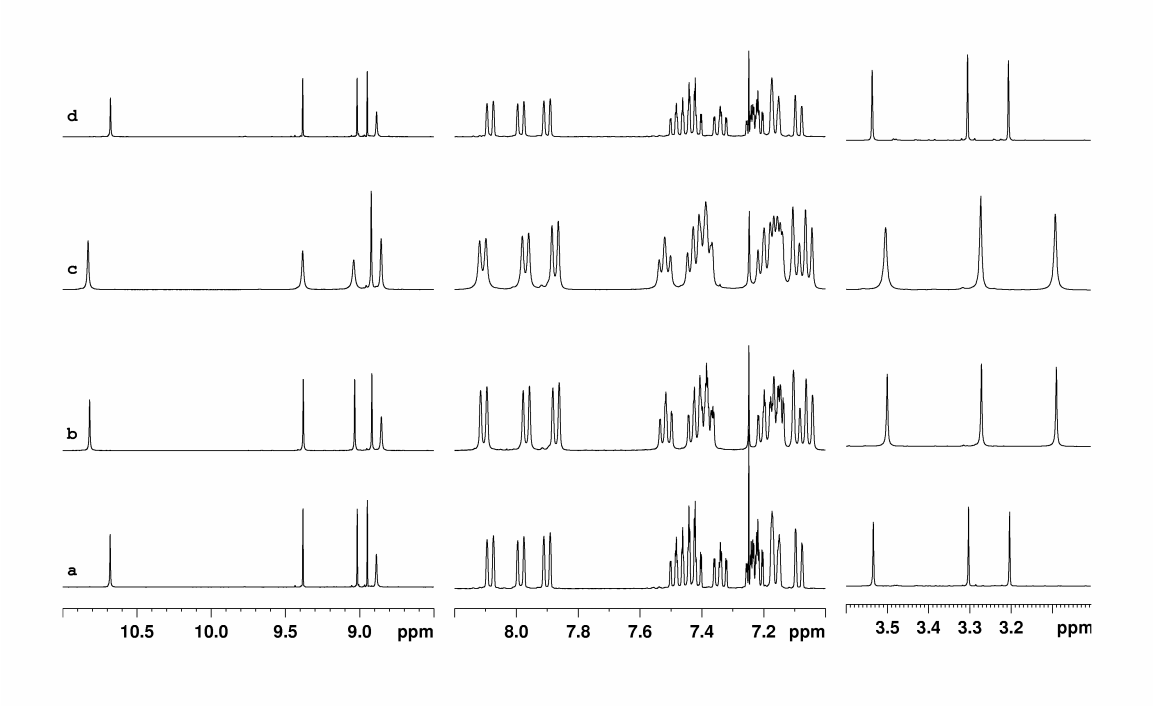

***Figure 11*:** Comparison of ^{1}H NMR spectra of BINOL oligomers (a) **1c**, [*S*][*R*][*S*]; (b) **1b**, [*S*][*S*][*S*]; (c) **1a**, [*R*][*R*][*R*] and (d) **1d**, [*R*][*S*][*R*].

The signal assignments were made using a combination two-dimensional COSY, HMBC, HSQC (^{1}H-^{13}C), HSQC (^{1}H-^{15}N), and NOESY NMR experiments. Details of COSY, HMBC, HSQC (^{1}H-^{13}C), HSQC (^{1}H-^{15}N) spectra are given in the experimental section. Conformational investigations in solution by 2D NOESY studies (400 MHz, $CDCl_3$) clearly supported the bifurcated hydrogen bond arrangements observed in the calculated structures of the oligomers. One of the most characteristic nOe interactions that can be anticipated for a bifurcated hydrogen bonded network with S(5) and S(6) type arrangements,[41] as seen in the structures of **1a-d**, would be the requirement of dipolar coupling between the aryl NH and the adjacent aryloxy methyls. The analysis of the 2D NOESY data (figure 12) indeed revealed the existence of such dipolar couplings.

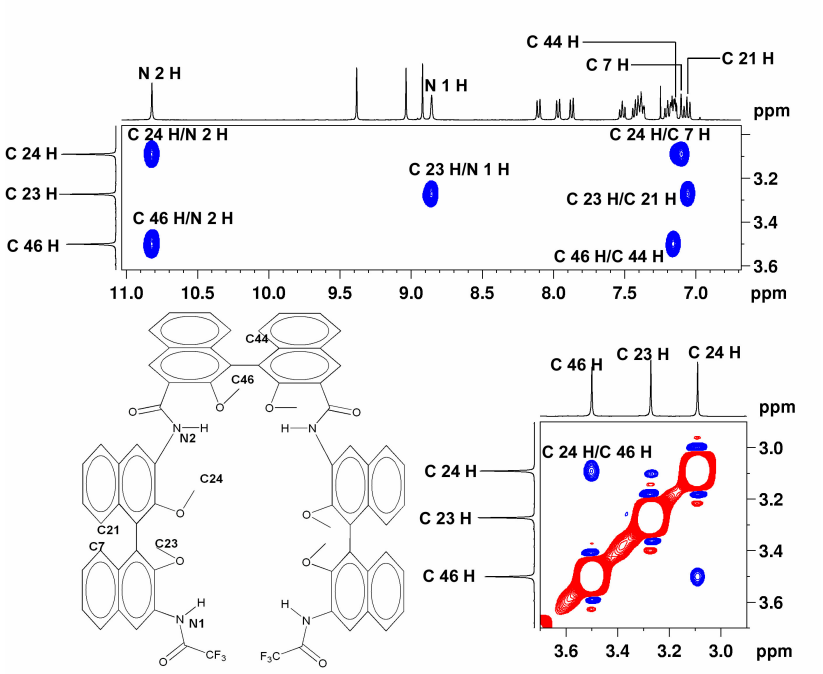

***Figure 12*:** Partial 2D NOESY spectra of **1b** [*S*][*S*][*S*] (400 MHz, $CDCl_3$) showing characteristic nOe interactions. The chemical structure with selected labeled atoms is also shown to facilitate signal assignments.

Furthermore, the characteristic nOe interactions between aryl-NH and the adjacent *O*-aryloxymethyls strongly suggest their *syn* orientation thereby making space for the S(5)-

type hydrogen bonded arrangement, which is a common feature in *O*-alkoxy arylamines and a prerequisite for the bifurcated hydrogen bonding[43] in S(5) and S(6) type arrangements. A strong support to the perpendicular disposition of the napthyl rings in BINOLs, as seen in their crystal structure,[36] are the characteristic nOes observed between the methoxy and the peripheral aryl protons of the adjacent napthyl rings.

Additional support for the prevalence of intramolecular hydrogen bonds came from [D_6]DMSO titration studies of **1a** and **1d** as representative examples (figure 13). Notably, all the NH signals appear at downfield region suggesting their involvement in extensive hydrogen bonding interactions. They showed little shift when solutions of **1a** and **1d** were titrated gradually with [D_6]DMSO ($\Delta\delta < 0.09$ ppm), which confirmed the involvement of strong intramolecular hydrogen bonding.

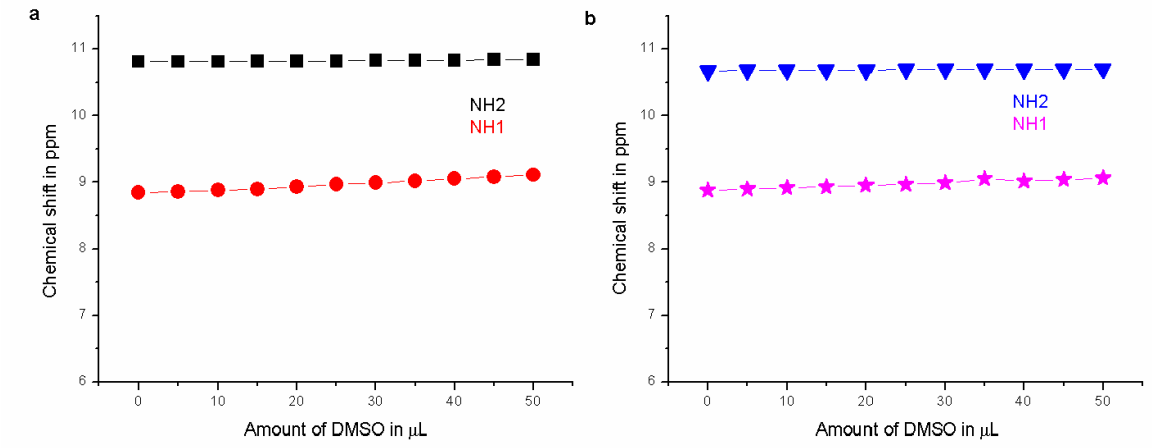

***Figure 13*:** DMSO titration graph of (a) **1a**, [*R*][*R*][*R*]; (b) **1d**, [*R*][*S*][*R*] BINOL foldamers.

3.2.6 CD spectra of BINOL-based two-dimensional foldamers 1a-d

In order to gain insight into the CD signature of these novel oligomers, we recorded their CD spectra (figure 14). Circular Dichroism (CD) spectroscopy is a useful tool to investigate the secondary structure of peptides and synthetic oligomers.[44,45] The CD spectra of the BINOL foldamers **1a-d** were recorded in acetonitrile at 8.019×10^{-4} M

concentration. As expected, mirror image CD profiles were clearly evident for the oligomers with opposite chirality. It should be remembered that the pairs of the enantiomers [*R*][*R*][*R*]/[*S*][*S*][*S*] and [*R*][*S*][*R*]/[*S*][*R*][*S*], respectively, show identical ^{1}H NMR spectra, which confirmed their mirror-image architecture at the oligomer level.

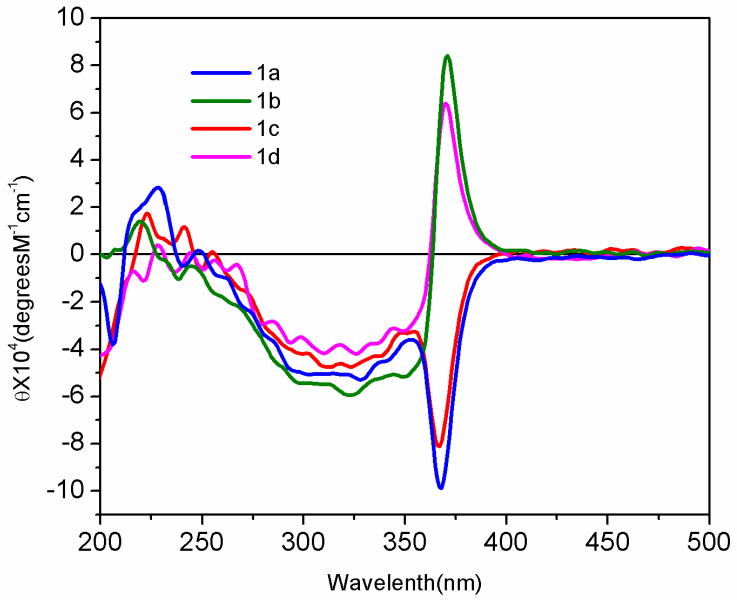

Figure 14: CD spectra of BINOL foldamers **1a-d** in acetonitrile.

3.3 BINOL-pyridyl hybrid foldamer

For further demonstration of the overwhelming ability of BINOL foldamer building blocks to breed dazzling structural architectures, we designed and synthesized the BINOL-pyridine-based hybrid foldamer structures **2a** and **2b** (figure 15), which differ only in their chirality, yet diverge distinctly in their structural architecture. It has been observed that the foldamers derived from 2,6-diaminopyridine and 2,6-pyridinedicarboxylic acid exist in helical conformation as has been shown by Lehn's group.[23] These foldamers adopt helical structure due to conformational preferences at the pyridine-NH and CO-NH linkages that restrict rotations about these bonds: the amide bond prefers a trans conformation; the carbonyls establish favorable contacts with aromatic protons in position 3 or 5 of the diaminopyridine rings; and the $N^{\delta-}H^{\delta+}$ dipoles are antiparallel to the neighboring pyridine nitrogen lone pairs. This sets the

pyridinaminocarbonyl moiety in an overall planar geometry. Based on the above mentioned conformational preferences of 2,6-pyridinecarboxamides, we designed a hybrid foldamer composed of BINOL and 2,6-diaminopyridine as its subunits. The foldamer was expected to adopt a three dimensional compact structure stabilized by intramolecular bifurcated hydrogen bonding interactions.

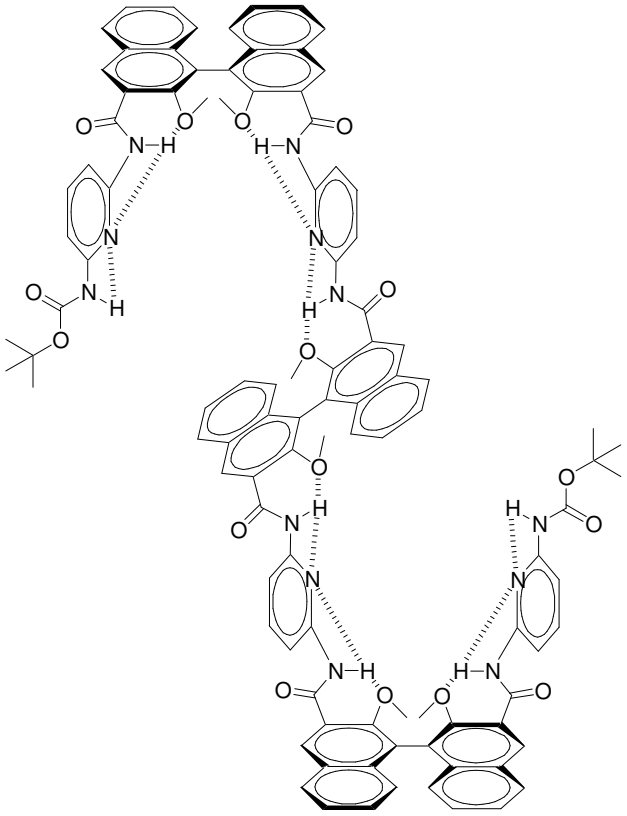

2

Figure 15: Hybrid foldamers having BINOL-pyridyl units, **2** with expected hydrogen bonding pattern is shown.

3.3.1 Synthesis:

Reaction of excess mono-boc 2,6-diamnopyridine **16**[23] with the BINOL [*S*] acid chloride **13** [*S*], gave the bis-boc protected diamine **17**, which after mono-boc deprotection with trimethyl silyl iodide followed by coupling with the BINOL acid chloride **13** [*S*] gave the hybrid foldamer **2a**, wherein all the three BINOLs are in [*S*] configuration (scheme 5). The hybrid foldamer **2b** was made accessible by reacting the mono-boc protected amine

18 with BINOL acid chloride **13** [*R*]. Herein, the three BINOL building blocks have [*S*][*R*][*S*] configuration (scheme 5).

Scheme 5:

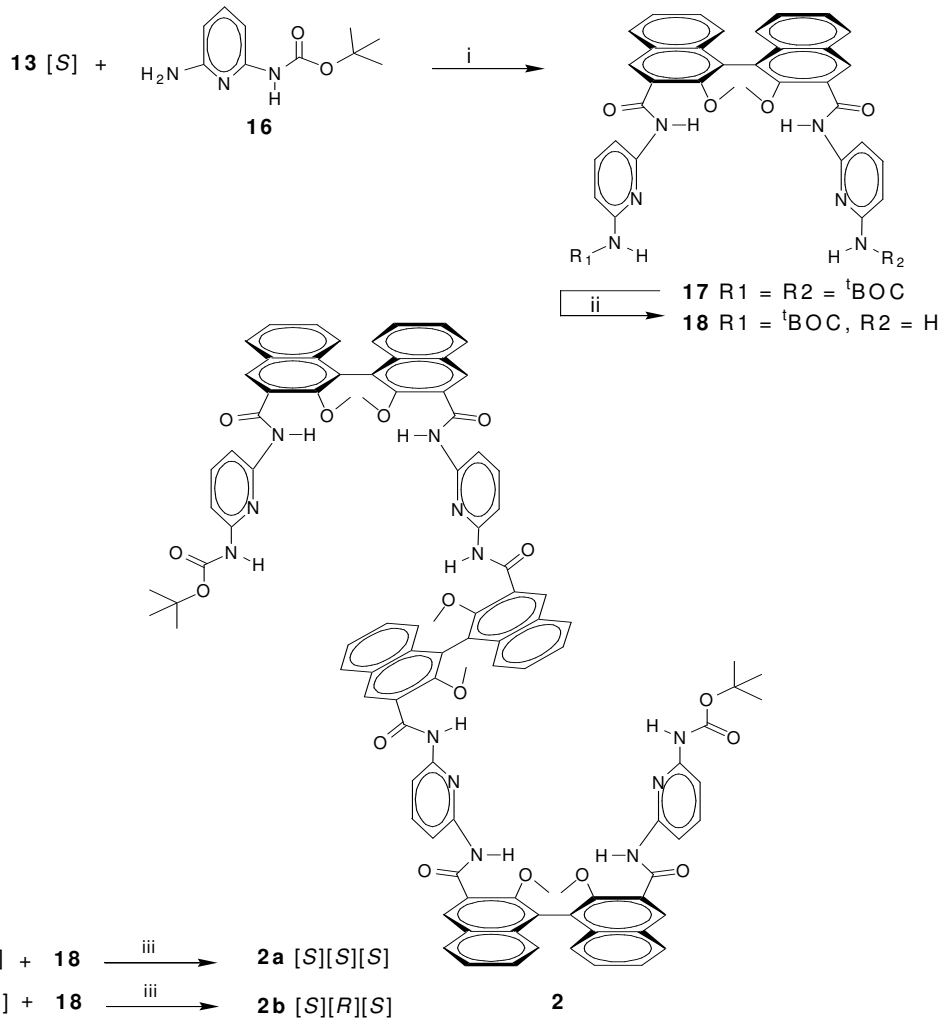

Reagents and conditions: (i) Triethylamine, THF, room tempature; (ii) NaI, TMSCl, acetonitrile, 2 h and then MeOH reflux, 1h; (iii) Triethylamine, THF, 50^0C, 4h.

Since the two foldamers **2a** and **2b** did not yield single crystals suitable for X-ray studies, the investigation of their conformational preferences was again based on NMR and quantum chemical studies. The structures obtained at the HF/6-31G* and B3LYP/6-31G* levels show a strongly different shape for both foldamers, although they only differ in the chirality of the same building block (figure 16).

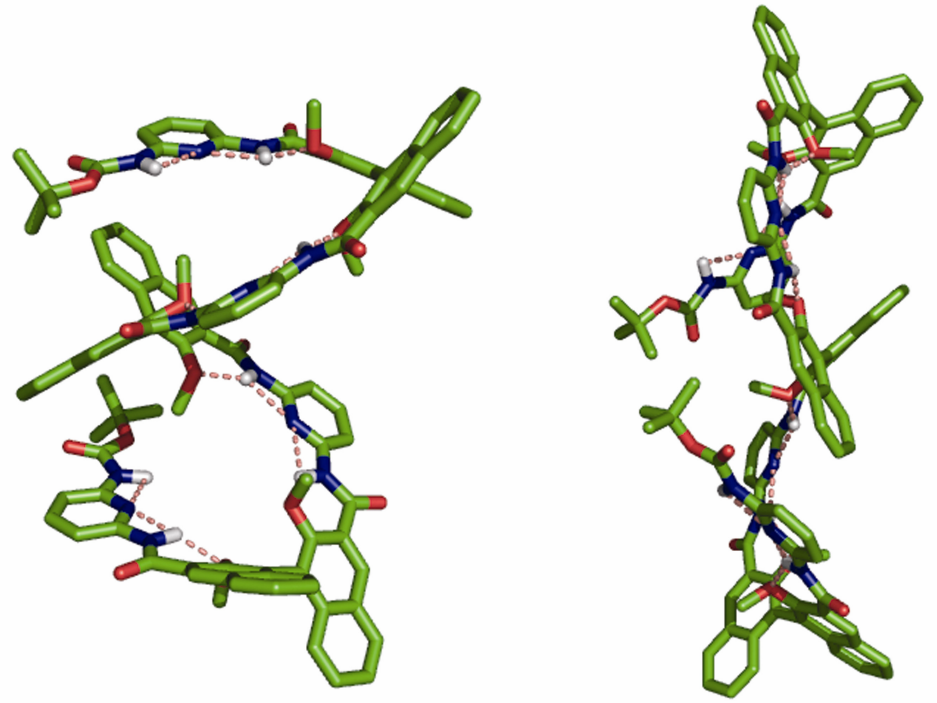

***Figure 16*:** Structural architecture of the hybrid oligomers **2a** (left), and **2b** (right) obtained at the HF/6-31G* level of ab initio MO theory. The two oligomers consisting of three BINOL building blocks differ only in the positioning of the BINOL enantiomers [*R*] and [*S*]: **2a:** [*S*][*S*][*S*], **2b:** [*S*][*R*][*S*].

In both hybrid foldamer structures **2a** and **2b**, extensive hydrogen bonding interactions of three-center S(4)-type are visible which is a common feature found in bis-acylated 2,6-diaminopyridines.[23] In addition to the S(4)-type interactions, bifurcated hydrogen bonding interactions involving the amino pyridine NHs can also be seen in the ab initio modeled structures.

3.3.2 NMR studies of BINOL-pyridyl oligomers

All the arguments for the existence of an extensive intramolecular hydrogen bonding network coming from the experimental studies on the oligomers **1a**-**d** can be repeated for the hybrid foldamers **2a** and **2b**. To study the solution state conformation of the hybrid foldamers we performed the 2D NMR experiments. Both **2a** and **2b** are highly soluble in nonpolar organic solvents (>>100 mM in $CDCl_3$) at ambient temperature suggesting the

involvement of the pre-organized hydrogen-bonding groups in intramolecular hydrogen-bonded interactions. Thus, the formation of polymeric aggregates can be excluded.[42] The ^{1}H NMR spectra (400 MHz) of oligomers **2a** and **2b** showed well resolved single set of signals in $CDCl_3$ at ambient temperature, which suggested that these oligomers exist in single conformation. The signal assignments were made using a combination two-dimensional COSY, HMBC, HSQC (^{1}H-^{13}C), HSQC (^{1}H-^{15}N), and NOESY NMR experiments. Details of COSY, HMBC, HSQC (^{1}H-^{13}C), HSQC (^{1}H-^{15}N) spectra are given in the experimental section. The characteristic nOes that support the bifurcated hydrogen bonding arrangement and the perpendicular disposition of the napthyl rings in BINOLs are clearly visible (figure 17).

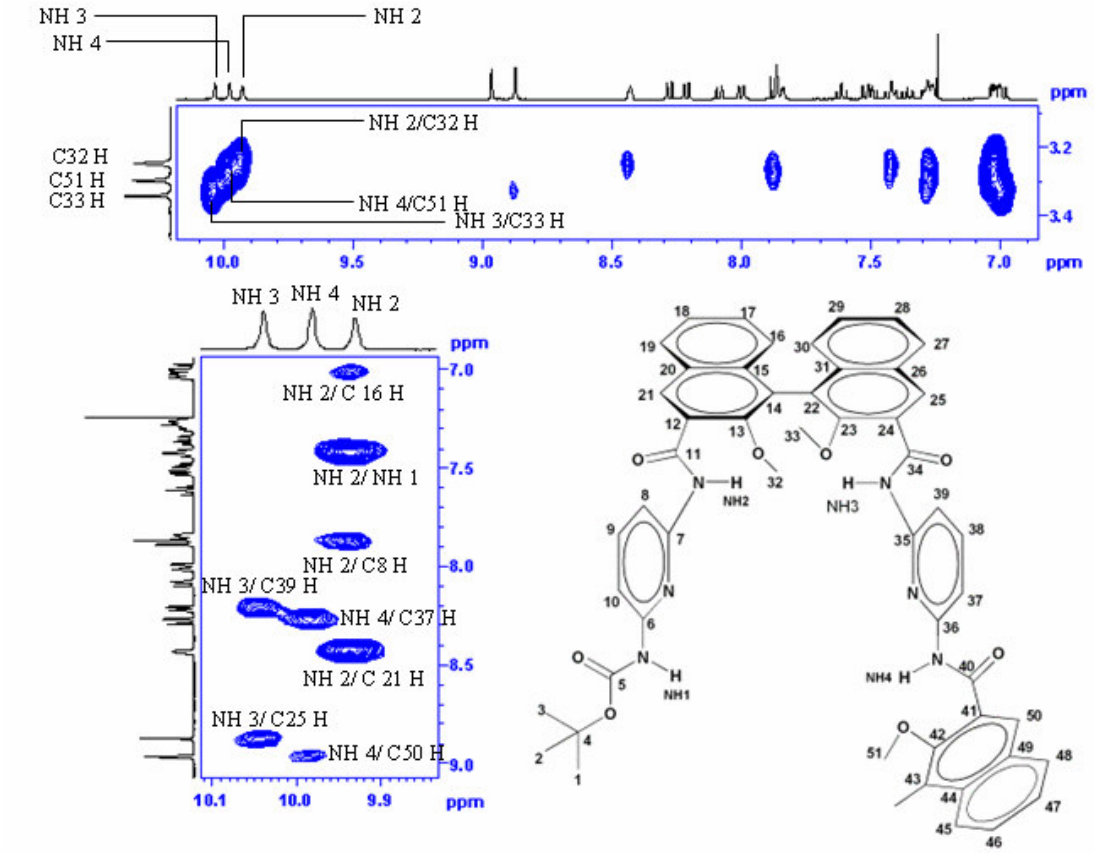

***Figure 17*:** Partial 2D NOESY spectra of **2b** [*S*][*R*][*S*] (400 MHz, $CDCl_3$) showing characteristic nOe interactions. The partial chemical structure with selected labeled atoms is also shown to facilitate signal assignments.

The strong involvement of all amide NHs in intramoleculear hydrogen bonding was supported by [D_6]DMSO titration studies (figure 18). Notably, all the NH signals appeared at downfield region suggesting their involvement in extensive hydrogen bonding interactions. They showed little shift when solutions of **2a** and **2b** were titrated gradually with [D_6]DMSO ($\Delta\delta < 0.09$ ppm), which confirmed the involvement of strong intramolecular hydrogen bonding.

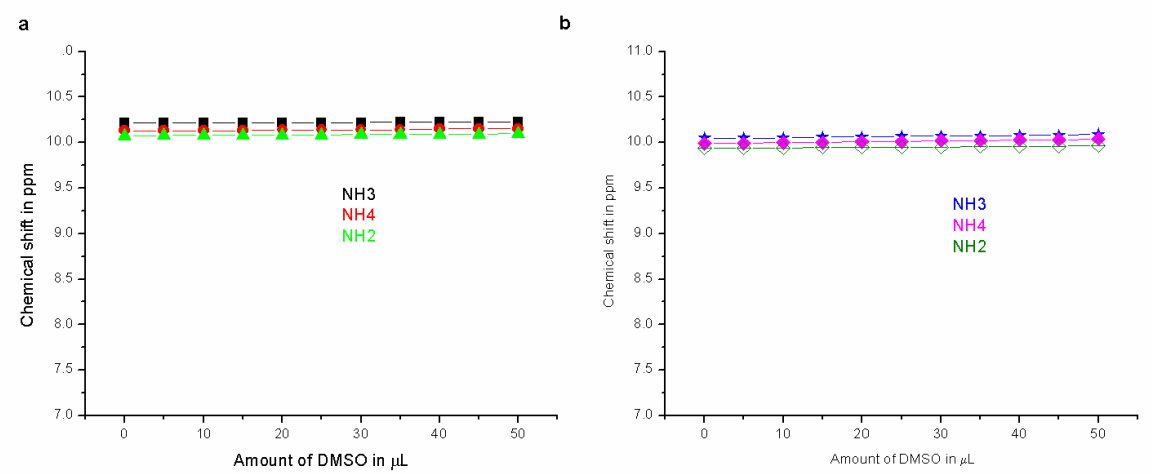

***Figure 18*:** DMSO titration graph of (a) **2a**, [*S*][*S*][*S*]; (b) **2b**, [*S*][*R*][*S*] BINOL-pyridyl hybrid foldamers.

3.4 Conclusion

The aromatic oligoamide foldamers based on the BINOL building blocks described here demonstrate convincingly the ability of such building blocks to generate conformationally ordered structures even in short oligomers. The controlled modulation of the direction of the oligomeric strands composed of the same building blocks differing only in their intrinsic chirality provide access to a great number of diverse structural architectures distinct from those classically observed. In principle, such immense conformational diversity could be achieved by all rigid aromatic building blocks, whose backbones are inherently chiral. Apart from the vast family of conformationally restricted biaryls,[46] building blocks of spirobiindanols[47] and conformationally restricted aryl amides[48] might also be suited for the design of such novel foldamer structures.

3.5 Experimental Section

General Methods

Unless otherwise stated, starting materials and dry solvents were obtained from commercial suppliers and used without further purification. Cu(OH)Cl.TMEDA complex was prepared according to the literature procedure.[49] Dry reactions were performed under argon atmosphere. Purification by column chromatography was performed in 100-200 mesh silica, unless otherwise stated. NMR spectra were recorded in $CDCl_3$ or [D_6]-DMSO on DRX-400 MHz Bruker NMR spectrometers. Electrospray ionization mass spectrometry (ESI-MS) was carried out on a Finnigan MAT-1020 mass spectrometer and MALDI-TOF mass spectra on a Voyager-DE STR mass spectrometer. CD spectra were recorded in JASCO J-715 spectrometer. Reactions were monitored by thin layer chromatography (TLC) carried out on 0.25 mm E-Merck silica gel plates. The quantum chemical calculations were performed employing the Gaussian 03 program package (Gaussian, Inc., Wallingford, CT 06492, USA).

N^3,$N^{3'}$-bis-(*R*,*R*)-(2,2'-dimethoxy-3'-(2,2,2-trifluoroacetamido)-1,1'-binaphthyl-3-yl)-(*R*)- 2,2'-dimethoxy-1,1'-binaphthyl-3,3'-dicarboxamide 1a: To a solution of 2,2′-dimethoxy-1,1′-binaphthyl-3,3′-dicarboxylic acid **12** [*R*][37,38] (0.52 g, 1.3 mmol, 1 equiv.) in dry DCM (5 mL), oxalyl chloride (0.45 mL, 5.2 mmol, 4 equiv.) and a catalytic amount of DMF were added. The reaction mixture was stirred for 2 hours at room temperature. The solvent was stripped off under reduced pressure and dried under high vacuum. The resulting diacid chloride **13** [*R*] was dissolved in dry DCM (3 mL) and slowly added to a solution of 2,2′-dimethoxy-1,1′-binaphthyl-3,3′-diamine **15** [*R*][38] (1.78 g, 5.2 mmol, 4 equiv.) in dry DCM (10 mL) containing triethylamine (0.9 mL, 6.5 mmol, 5 equiv.). The reaction mixture was stirred at room temperature for 12 hours. The solvent was stripped off under reduced pressure, and a solution of dry DCM (10 mL) containing trifluoroacetic acid (1.15 mL, 15.5 mmol, 12 equiv.), and dicyclohexylcarbodiimide, DCC (3.20 g, 15.5 mmol, 12 equiv.) was added to the residue at 0°C. After stirring the reaction mixture for 12 h, at room temperature, DCU was filtered off, and the solvent was evaporated under vacuum to afford a crude product, which was further purified by

column chromatography. The column purified product was further purified by dissolving it in minimum amount of ether and then filtering to get rid of DCU. The product was further purified by dissolving in minimum amount of DCM and precipitating it with petether. Yield 2.13 g (68.7%); mp 229-231 ^{0}C; $[\alpha]_D$ = - 124.6 (c = 1.01, THF); IR ($CHCl_3$) ν (cm^{-1}): 3396, 3306, 3018, 2935, 2856, 1726, 1699, 1664, 1529, 1350, 1310, 1215, 1003; ^{1}H NMR (400 MHz, $CDCl_3$): δ 10.85 (s, 2H), 9.41 (s, 2H), 9.06 (s, 2H), 8.95 (s, 2H), 8.88 (s, 2H), 8.13 (m, 2H), 7.99 (m, 2H), 7.90 (m, 2H), 7.54 (m, 2H), 7.42 (m, 6H), 7.20 (m, 6H), 7.10 (m, 4H), 3.53 (s, 6H), 3.30 (s, 6H), 3.11 (s, 6H); ^{13}C NMR (100 MHz, $CDCl_3$): δ 163.6, 155.2, 154.8, 154.5, 154.1, 153.2, 147.2, 146.4, 135.7, 134.6, 131.3, 131.0, 130.3, 130.2, 129.7, 128.9, 128.4, 127.7, 126.6, 126.1, 126.0, 125.9, 125.7, 125.5, 125.4, 125.1, 123.1, 122.6, 119.9, 118.9, 118.8, 117.0, 114.2, 111.3, 62.1, 61.0, 60.7; MALDI-TOF MS: 1270.3 (M+ Na), 1286.4 (M+K); Anal. Calcd. for $C_{72}H_{52}F_6N_4O_{10}$: C = 69.34, H = 4.20, N = 4.49; Found: C = 69.09, H = 4.01, N = 4.62.

N^3,$N^{3'}$-bis-(*S,S*)-(2,2'-dimethoxy-3'-(2,2,2-trifluoroacetamido)-1,1'-binaphthyl-3-yl)-(*S*)- 2,2'-dimethoxy-1,1'-binaphthyl-3,3'-dicarboxamide 1b: It was synthesized according to the procedure described for **1a** (scheme 4). Yield 2.3 g (74.1%); mp 223-226 ^{0}C; $[\alpha]_D$ = + 124.0 (c = 0.91, THF); IR ($CHCl_3$) ν (cm^{-1}): 3396, 3315, 3065, 3014, 2941, 2874, 1726, 1666, 1581, 1537, 1493, 1458, 1412, 1350, 1244, 1211, 1151, 1003; ^{1}H NMR (400 MHz, $CDCl_3$): δ 10.84 (s, 2H), 9.40 (s, 2H), 9.05 (s, 2H), 8.94 (s, 2H), 8.87 (s, 2H), 8.12 (m, 2H), 7.99 (m, 2H), 7.89 (m, 2H), 7.54 (m, 2H), 7.42 (m, 6H), 7.2 (m, 6H), 7.09 (m, 4H), 3.52 (s, 6H), 3.29 (s, 6H), 3.10 (s, 6H); ^{13}C NMR (100 MHz, $CDCl_3$): δ 163.6, 155.2, 154.8, 154.4, 154.1, 153.2, 147.2, 146.4, 135.7, 134.6, 131.3, 131.1, 131.0, 130.3, 130.3, 130.2, 129.7, 128.9, 128.3, 127.7, 126.6, 126.1, 126.0, 125.9, 125.7, 125.5, 125.4, 125.3, 125.1, 123.1, 122.6, 119.9, 118.9, 118.8, 117.0, 114.1, 111.3, 62.1, 61.0, 60.7; MALDI-TOF MS: 1270.3 (M+ Na), 1286.2 (M+K); Anal. Calcd. for $C_{72}H_{52}F_6N_4O_{10}$: C = 69.34, H = 4.20, N = 4.49; Found: C = 69.13, H = 4.31, N = 4.59.

N^3,$N^{3'}$-bis-(*S,S*)-(2,2'-dimethoxy-3'-(2,2,2-trifluoroacetamido)-1,1'-binaphthyl-3-yl)-(*R*)- 2,2'-dimethoxy-1,1'-binaphthyl-3,3'-dicarboxamide 1c: It was synthesized according to the procedure described for **1a** (scheme 4). Yield 2.1 g (67.7%); mp 239-241 ^{0}C; $[\alpha]_D$ = - 43.5 (c = 1.1, THF); IR ($CHCl_3$) ν (cm^{-1}): 3396, 3317, 3063, 3018, 2943, 2872, 2837, 1728, 1666, 1581, 1537, 1493, 1454, 1412, 1350, 1310, 1217, 1151, 1001;

^{1}H NMR (400 MHz, $CDCl_3$): δ 10.69 (s, 2H), 9.40 (s, 2H), 9.03 (s, 2H), 8.97 (s, 2H), 8.90 (s, 2H), 8.10 (m, 2H), 8.00 (m, 2H), 7.92 (m, 2H), 7.47 (m, 6H), 7.36 (m, 2H), 7.24 (m, 4H), 7.18 (m, 4H), 7.10 (m, 2H), 3.55 (s, 6H), 3.32 (s, 6H), 3.22 (s, 6H); ^{13}C NMR (100 MHz, $CDCl_3$): δ 163.7, 155.1, 154.8, 154.4, 154.0, 153.1, 147.4, 146.4, 135.5, 134.5, 131.3, 131.0, 130.9, 130.3, 130.3, 129.6, 128.7, 128.3, 127.7, 126.6, 126.2, 126.0, 125.9, 125.8, 125.7, 125.4, 125.2, 125.1, 123.1, 122.4, 119.9, 119.1, 118.9, 117.0, 114.1, 111.3, 62.1, 61.0, 60.9; MALDI-TOF MS: 1270.5 (M+ Na), 1286.6 (M+K); Anal. Calcd. for $C_{72}H_{52}F_6N_4O_{10}$: C = 69.34, H = 4.20, N = 4.49; Found: C = 69.57, H = 4.29, N = 4.71.

N^3,$N^{3'}$-bis-(*R,R*)-(2,2'-dimethoxy-3'-(2,2,2-trifluoroacetamido)-1,1'-binaphthyl-3-yl)-(*S*)-2,2'-dimethoxy-1,1'-binaphthyl-3,3'-dicarboxamide 1d: It was synthesized according to the procedure described for **1a** (scheme 4). Yield 1.9 g (61.3%); mp 242-244 ^{0}C; $[\alpha]_D$ = + 40.9 (c = 1.05, THF); IR ($CHCl_3$) ν (cm^{-1}): 3398, 3308, 3063, 3020, 2943, 1726, 1664, 1581, 1541, 1493, 1458, 1412, 1350, 1310, 1215, 1001; ^{1}H NMR (400 MHz, $CDCl_3$): δ 10.69 (s, 2H), 9.39 (s, 2H), 9.02 (s, 2H), 8.95 (s, 2H), 8.89 (s, 2H), 8.08 (m, 2H), 7.98 (m, 2H), 7.90 (m, 2H), 7.44 (m, 6H), 7.34 (m, 2H), 7.20 (m, 8H), 7.09 (m, 2H), 3.54 (s, 6H), 3.31 (s, 6H), 3.21 (s, 6H); ^{13}C NMR (100 MHz, $CDCl_3$): δ 163.8, 155.2, 154.9, 154.5, 154.1, 153.1, 147.4, 146.4, 135.6, 134.6, 131.4, 131.1, 130.9, 130.4, 130.3, 129.7, 128.7, 128.4, 127.7, 126.6, 126.2, 126.1, 126.0, 125.9, 125.7, 125.5, 125.2, 125.1, 123.2, 122.5, 119.9, 119.2, 118.9, 117.0, 114.2, 111.3, 62.1, 61.0, 60.9; MALDI-TOF MS: 1270.2 (M+Na); Anal. Calcd. for $C_{72}H_{52}F_6N_4O_{10}$: C = 69.34, H = 4.20, N = 4.49; Found: C = 69.29, H = 4.35, N = 4.67.

***tert*-Butyl 6-(3'-(6-(*tert*-butyloxycarbonylamino)pyridin-2-ylcarbamoyl)-(*S*)-2,2'-dimethoxy-1,1'-binaphthyl-3-carboxamido)pyridin-2-ylcabamate 17:** To a solution of 2,2′-dimethoxy-1,1′-binaphthyl-3,3′-dicarboxylic acid **12** [*S*][37,38] (2.5 g, 6.2 mmol, 1 equiv.) in dry DCM (15 mL), oxalyl chloride (2.17 mL, 24.9 mmol, 4 equiv.) and a catalytic amount of DMF were added. The reaction mixture was stirred for 2 hours at room temperature. The solvent was stripped off under reduced pressure and the residue was dried under high vacuum. The resulting diacid chloride **13** [*S*] was dissolved in dry THF (10 mL) and added slowly to a solution of mono Boc 2,6- diaminopyridine **16**[23] (2.6 g, 12.4 mmol, 2 equiv.) in dry THF (15 mL) containing triethylamine (2.6 mL, 18.6 mmol, 3 equiv.). After stirring the reaction mixture for 4 hours at room temperature, it

was filtered and directly purified by column chromatography. Yield 3.49 g (71.6%); mp 285 ^{0}C; $[\alpha]_D$ = + 186.2 (c = 0.992, THF); IR ($CHCl_3$) ν (cm^{-1}): 3423, 3331, 3018, 2980, 2937, 1730, 1672, 1585, 1504, 1454, 1304, 1215, 1155; ^{1}H NMR (400 MHz, $CDCl_3$): δ 10.31 (s, 2H), 8.96 (s, 2H), 8.11 (m, 4H), 7.75 (m, 2H), 7.69 (m, 2H), 7.52 (m, 2H), 7.39 (m, 2H), 7.14 (m, 2H), 3.41 (s, 5H), 1.49 (s, 18H); ^{13}C NMR (100 MHz, $CDCl_3$): δ 163.2, 153.2, 152.2, 150.4, 149.7, 140.5, 135.5, 134.5, 130.2, 129.7, 128.9, 126.0, 125.6, 125.3, 125.2, 108.8, 108.0, 80.9, 61.9, 28.1; ESI Mass: 785.2 (M+1), 807.2 (M+ Na); Anal. Calcd. for $C_{44}H_{44}N_6O_8$: C = 67.33, H = 5.65, N = 10.71; Found: C = 67.14, H = 5.82, N = 10.69.

***tert*-Butyl 6-(3'-(6-aminopyridin-2-ylcarbamoyl)-(*S*)-2,2'-dimethoxy-1,1'-binaphthyl-3-carboxamido)pyridine-2-ylcarbamate 18:** To a solution of **17** (1.5 g, 1.9 mmol, 1 equiv.) and sodium iodide (0.86 g, 5.7 mmol, 3 equiv.) in dry acetonitrile (20 mL), dry TMSCl (0.37 mL, 2.9 mmol, 1.5 equiv.) was slowly added and the mixture was stirred for 2 hours. The reaction mixture was stripped off the solvent, the residue dissolved in methanol (40 mL) and heated to reflux for 1 hour to decompose the unstable silylated amine. The solvent was then evaporated under reduced pressure, and the crude product **18** obtained was dried and used for the next step without further purification ESI Mass: 685.1 (M+1).

***tert*-Butyl 6-(3'-(6-(3'-(6-(3'-(6-(*tert*-butyloxycarbonylamino)pyridin-2-ylcarbamoyl)-(*S*)-2,2'-dimethoxy-1,1'-binaphthyl-3-carboxamido)pyridin-2-ylcarbamoyl)-(*S*)-2,2'-dimethoxy-1,1'-binaphthyl-3-carboxamido)pyridin-2-ylcarbamoyl)-(*S*)-2,2'-dimethoxy-1,1'-binaphthyl-3-carboxamido)pyridine-2-ylcarbamate 2a:** To a solution of 2,2′-dimethoxy-1,1′-binaphthyl-3,3′-dicarboxylic acid **12** [*S*] (0.2 g, 0.5 mmol, 1 equiv.) in dry DCM (5 mL), oxalyl chloride (0.17 mL, 2 mmol, 4 equiv.) and a catalytic amount of DMF were added. The reaction mixture was stirred for 2 hours at room temperature. The solvent was stripped off under reduced pressure and the residue was dried under high vacuum. The resulting diacid chloride **13** [S] was dissolved in dry THF (5 mL) and added slowly to a solution of **18** (0.71 g, 1 mmol, 2.1 equiv.) in dry THF (10 mL) containing triethylamine (0.2 mL, 1.5 mmol, 3 equiv.), at room temperature. The reaction mixture was warmed at 50 °C for 4 hours, filtered, and directly adsorbed on silica gel and purified by column chromatography. Yield 0.59 g

(68.4%); mp > 300 ^{0}C; $[\alpha]_D$ = - 186.1 (c = 1.3, THF); IR ($CHCl_3$) ν ((cm^{-1}): 3421, 3335, 3018, 2980, 2939, 1730, 1682, 1583, 1504, 1454, 1306, 1217, 1153; ^{1}H NMR (400 MHz, $CDCl_3$): δ 10.22 (s, 2H), 10.14 (s, 2H), 10.10 (s, 2H), 8.97 (s, 2H), 8.90 (s, 2H), 8.85 (s, 2H), 8.26 (m, 4H), 8.04 (m, 8H), 7.89 (m, 2H), 7.73 (m, 2H), 7.64 (m, 2H), 7.50 (m, 2H), 7.37 (m, 8H), 7.24 (m, 2H), 7.05 (m, 8H), 3.39 (s, 3H), 3.36 (s, 6H), 1.44 (s, 18 H); ^{13}C NMR (100 MHz, $CDCl_3$): δ 162.97, 153.06, 152.87, 151.86, 150.11, 149.95, 149.38, 140.6, 135.4, 135.2, 134.5, 134.3, 130.1, 130.0, 129.7, 129.6, 128.9, 128.7, 126.1, 125.3, 125.1, 125.1, 110.8, 110.5, 108.8, 107.9, 80.9, 61.9, 28.0; MALDI-TOF MS: 1758.4 (M+Na), 1774.5 (M+K); Anal. Calcd. for $C_{102}H_{86}N_{12}O_{16}$: C = 70.58, H = 4.99, N = 9.68; Found: C = 70.40, H = 5.13, N = 9.46.

***tert*-Butyl 6-(3'-(6-(3'-(6-(3'-(6-(*tert*-butyloxycarbonylamino)pyridin-2-ylcarbamoyl)-(*S*)-2,2'-dimethoxy-1,1'-binaphthyl-3-carboxamido)pyridin-2-ylcarbamoyl)-(*R*)-2,2'-dimethoxy-1,1'-binaphthyl-3-carboxamido)pyridin-2-ylcarbamoyl)-(*S*)-2,2'-dimethoxy-1,1'-binaphthyl-3-carboxamido)pyridine-2-ylcarbamate 2b**: It was synthesized according to the procedure described for **2a** (scheme 5). Yield 0.57 g (66%); mp > 300 ^{0}C; $[\alpha]_D$ = + 62.3 (c = 1.02, THF); IR ($CHCl_3$) ν (cm^{-1}): 3335, 3020, 2984, 2941, 1730, 1678, 1583, 1504, 1454, 1304, 1215, 1155; ^{1}H NMR (400 MHz, $CDCl_3$): δ 10.06 (s, 2H), 10.00 (s, 2H), 9.95 (s, 2H), 8.99 (s, 2H), 8.90 (s, 2H), 8.45 (s, 2H), 8.30 (m, 2H), 8.24 (m, 2H), 8.11 (m, 2H), 8.03 (m, 2H), 7.89 (m, 6H), 7.64 (m, 2H), 7.53 (m, 4H), 7.45 (m, 4H), 7.39 (m, 2H), 7.31 (m, 6H), 7.03 (m, 6H), 3.36 (s, 6H), 3.32 (s, 6H), 3.27 (s, 6H), 1.36 (s, 18 H); ^{13}C NMR (100 MHz, $CDCl_3$): δ 163.7, 163.4, 153.0, 152.8, 152.7, 152.0, 150.2, 149.9, 140.7, 140.6, 135.6, 135.3, 134.6, 133.5, 130.2, 130.1, 130.0, 129.6, 129.5, 128.9, 128.8, 126.6, 126.2, 126.0, 125.5, 125.5, 125.4, 125.3, 125.2, 110.8, 110.5, 108.9, 108.1, 81.0, 62.1, 62.0, 61.9, 28.0; MALDI-TOF MS: 1758.5 (M+Na), 1774.6 (M+K); Anal. Calcd. for $C_{102}H_{86}N_{12}O_{16}$: C = 70.58, H = 4.99, N = 9.68; Found: C = 70.64, H = 5.06, N = 9.51.

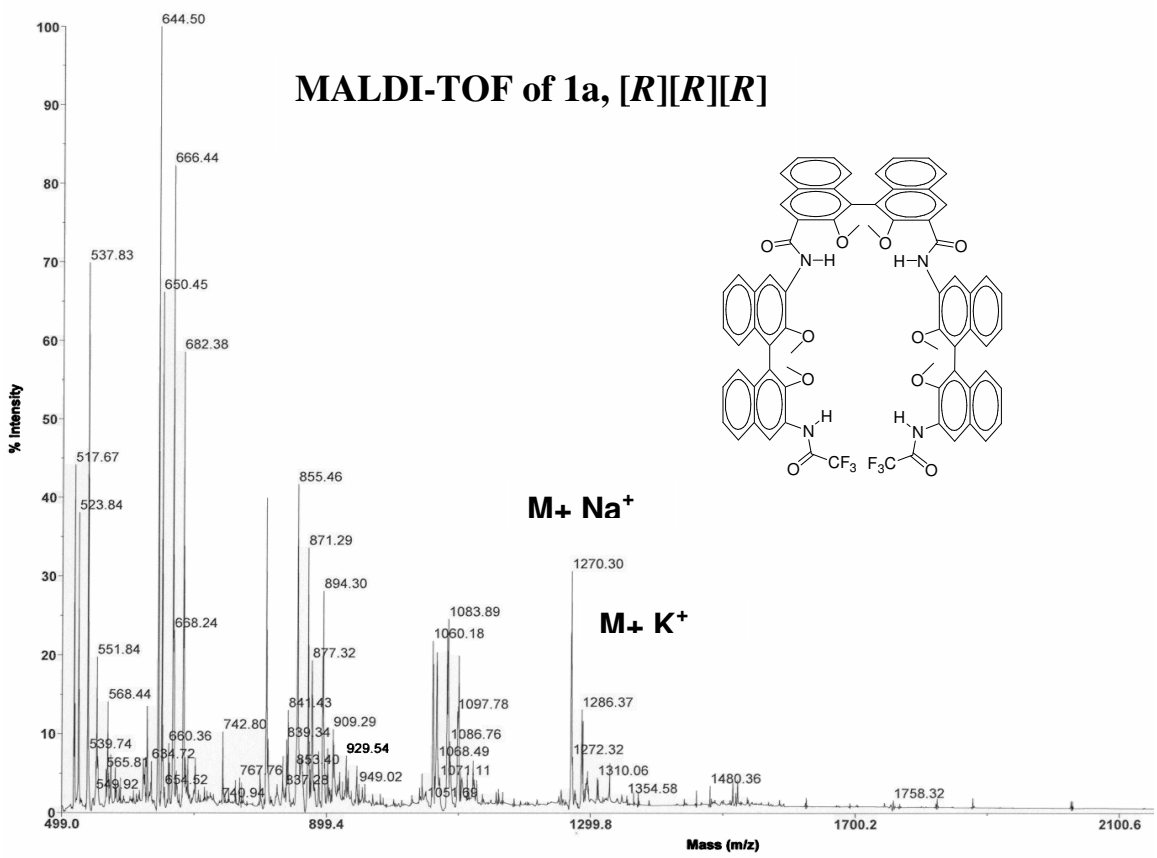
MALDI-TOF of 1a, [R][R][R]
M+ Na+
M+ K+
% Intensity
Mass (m/z)
644.50
666.44
537.83
650.45
682.38
517.67
523.84
855.46
871.29
894.30
1270.30
1083.89
1060.18
658.24
551.84
877.32
568.44
841.43
1097.78
1286.37
742.80
839.34
909.29
660.36
929.54
1086.76
539.74
684.72
1068.49
1272.32
565.81
853.40
1071.11
1310.06
654.52
767.76
837.28
949.02
1354.58
1480.36
549.92
740.94
1051.69
1758.32
499.0
899.4
1299.8
1700.2
2100.6

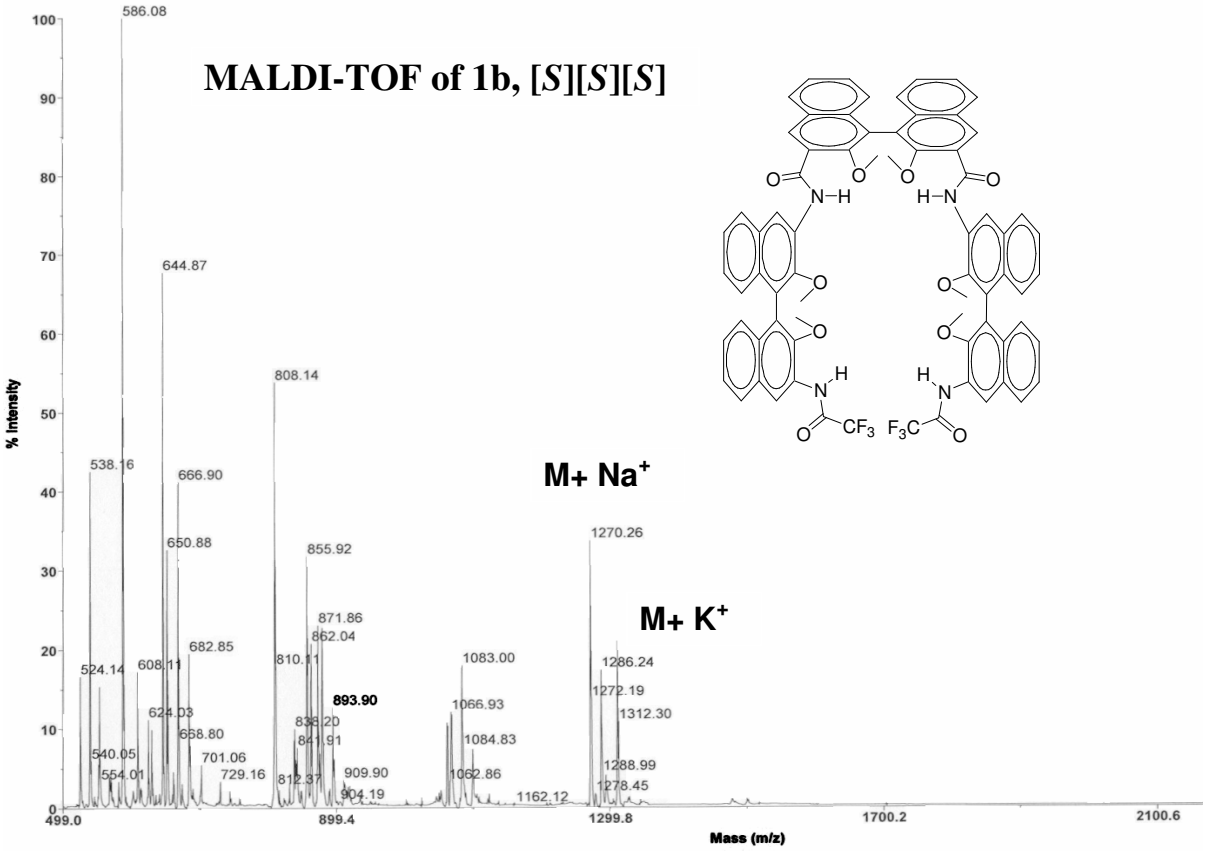
MALDI-TOF of 1b, [S][S][S]
M+ Na+
M+ K+
% Intensity
Mass (m/z)
586.08
644.87
808.14
538.16
666.90
650.88
855.92
1270.26
871.86
862.04
682.85
524.14
608.11
810.11
1083.00
1286.24
893.90
1272.19
624.03
1066.93
1312.30
838.20
658.80
841.91
1084.83
540.05
701.06
554.01
729.16
909.90
812.37
1062.86
1288.99
904.19
1162.12
1278.45
499.0
899.4
1299.8
1700.2
2100.6

MALDI-TOF of 1c, [*S*][*R*][*S*]

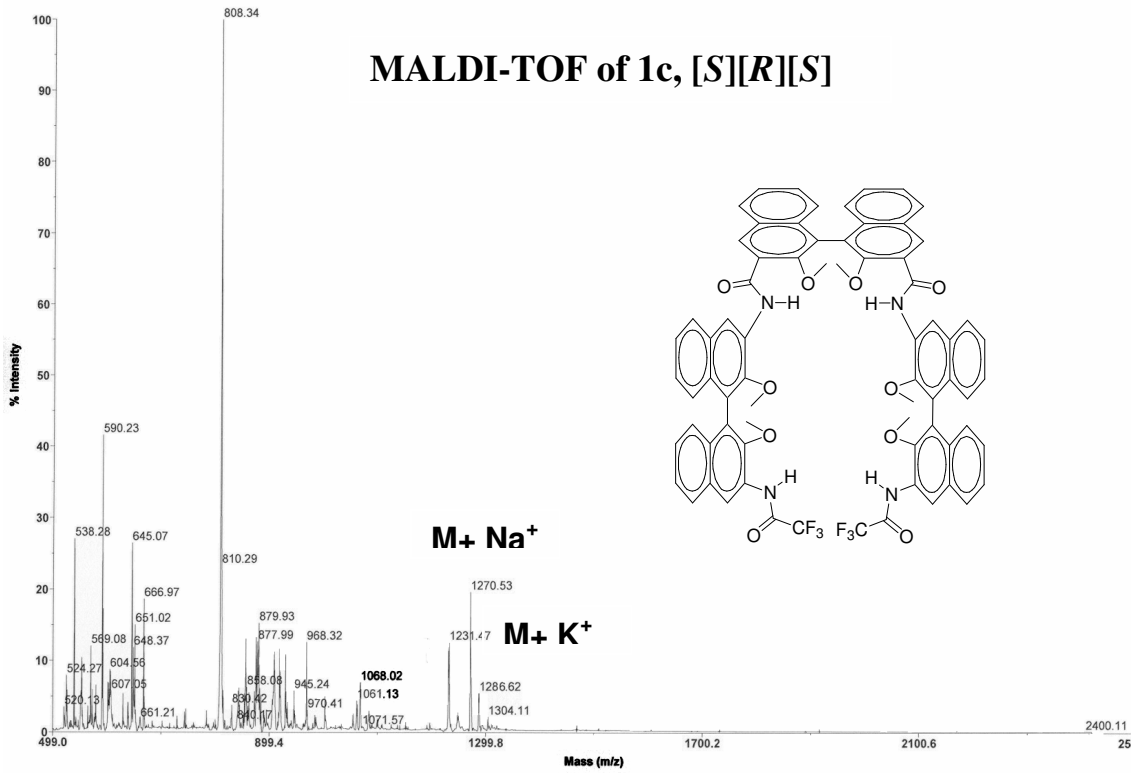

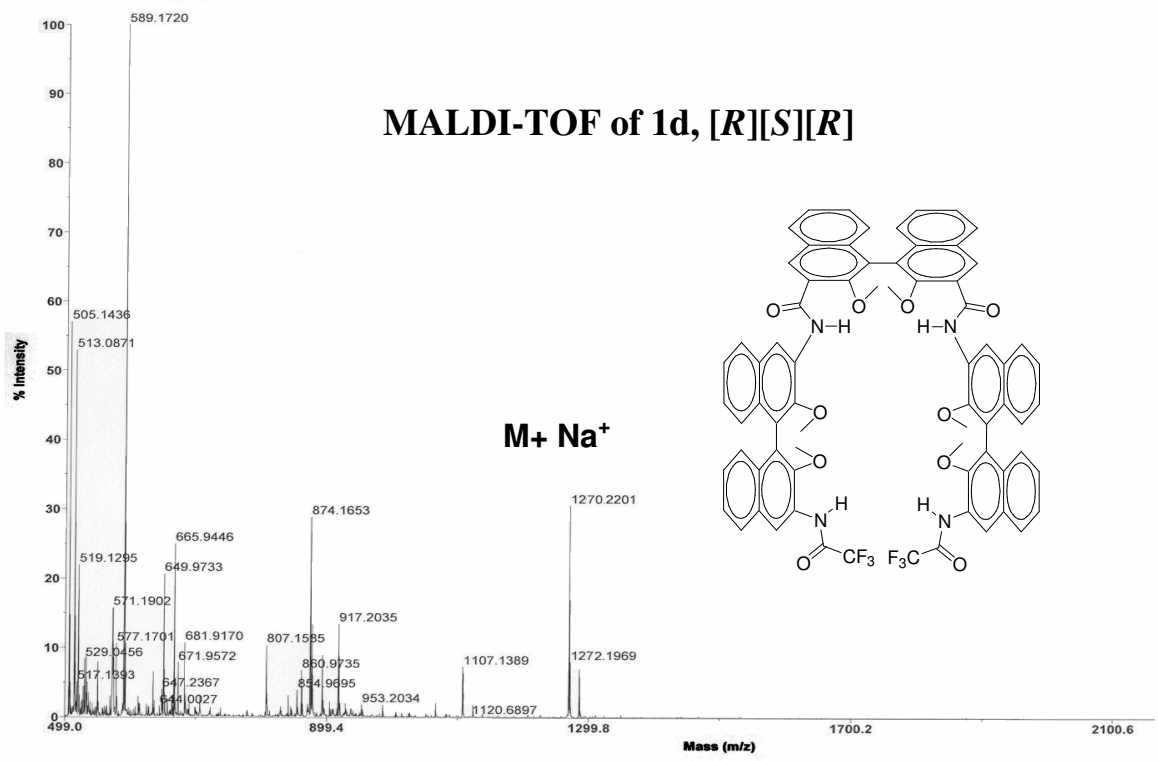

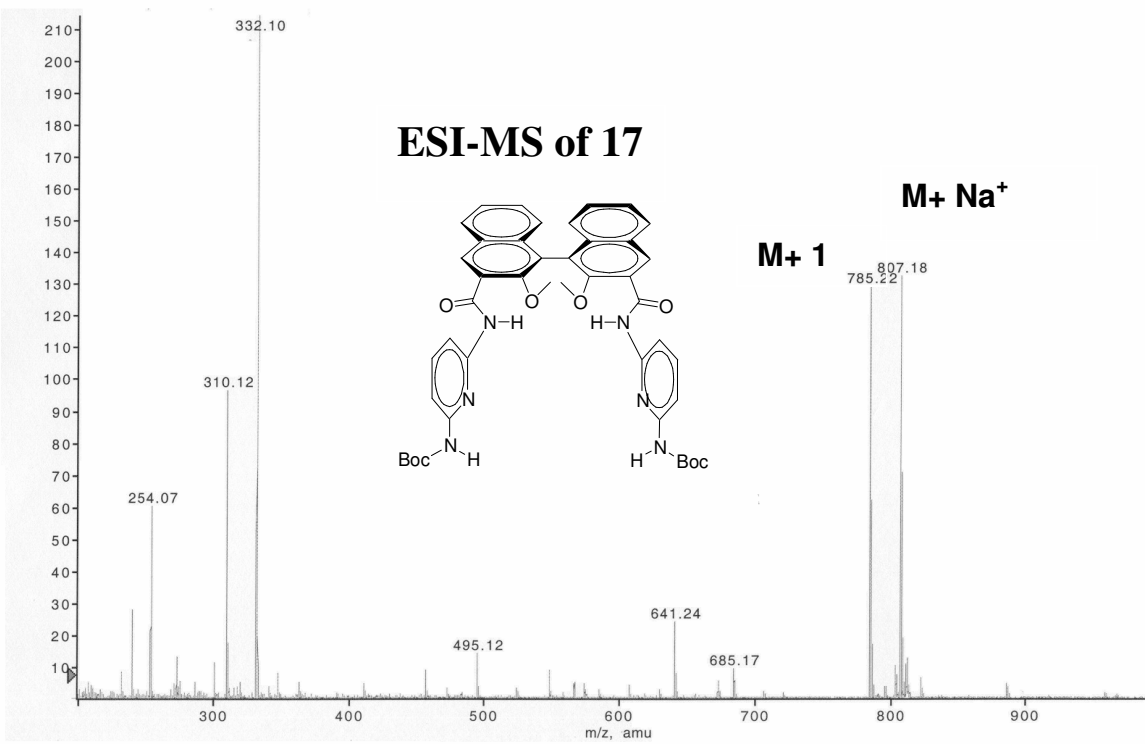
ESI-MS of 17
M+ Na+
M+ 1
332.10
310.12
254.07
495.12
641.24
685.17
785.22
807.18
m/z, amu

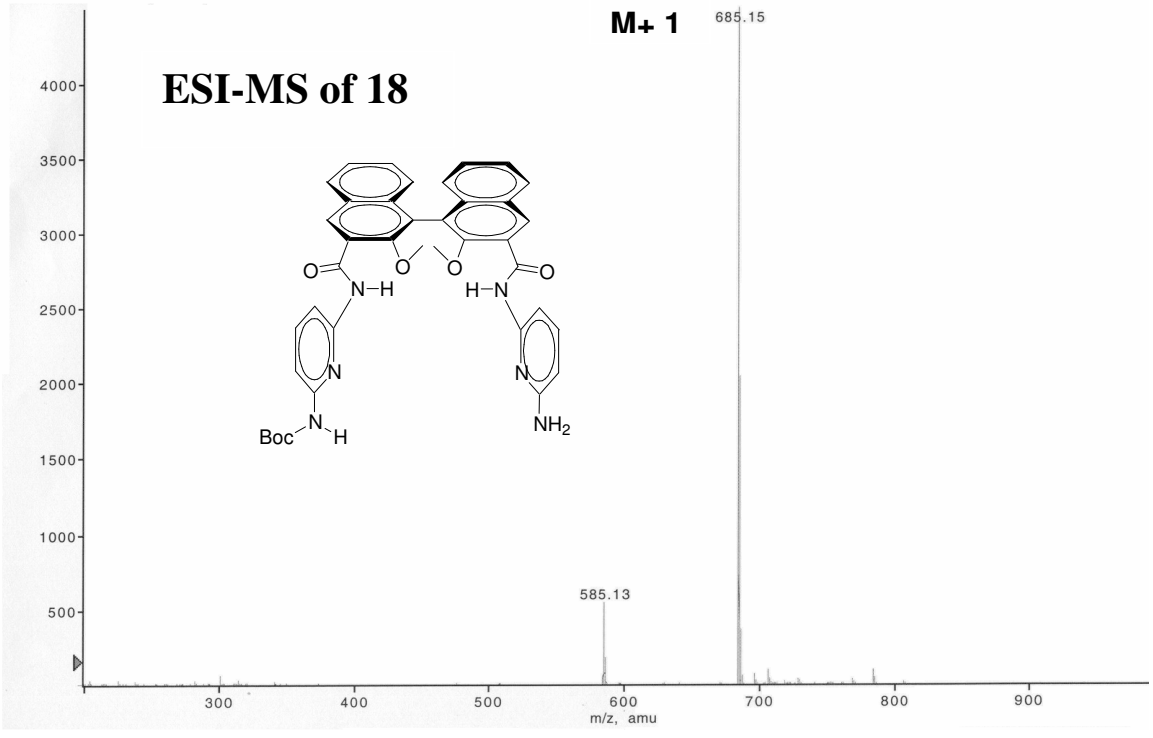
ESI-MS of 18
M+ 1
685.15
585.13
m/z, amu

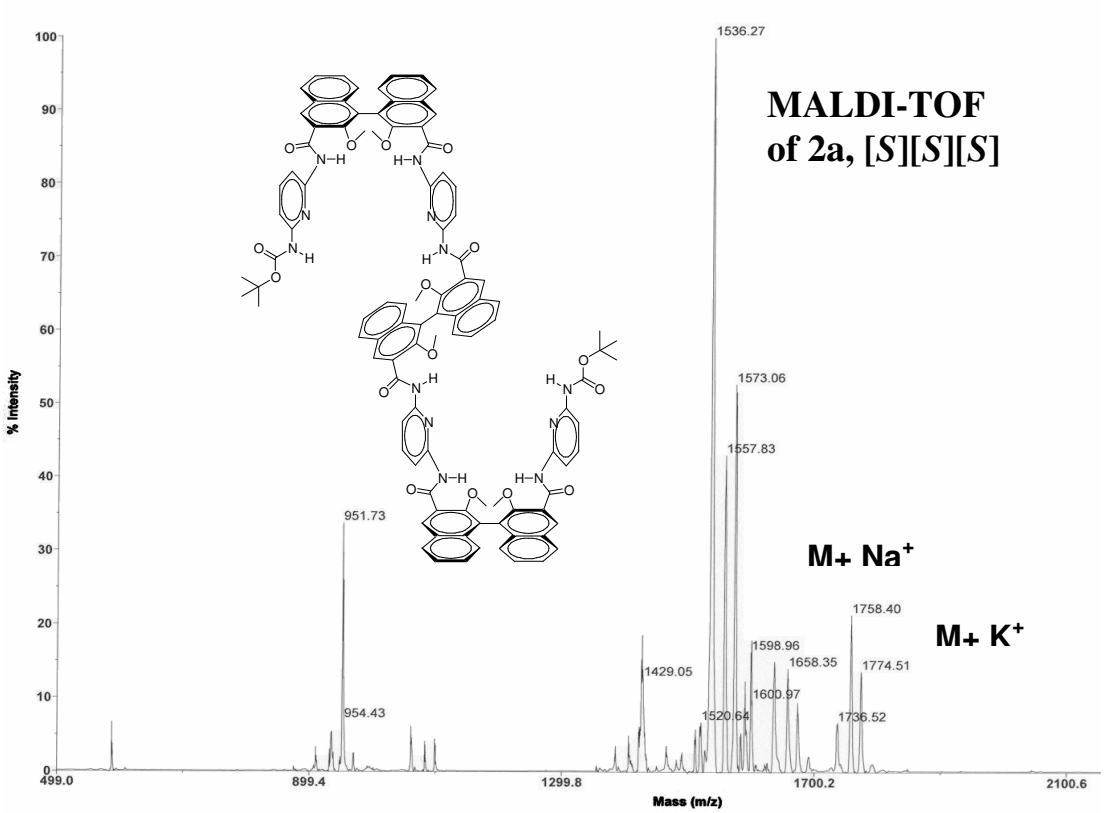
MALDI-TOF
of 2a, [S][S][S]
M+ Na+
M+ K+
% Intensity
Mass (m/z)
1536.27
1573.06
1557.83
951.73
1758.40
1598.96
1658.35
1774.51
1429.05
1600.97
954.43
1520.64
1736.52
499.0
899.4
1299.8
1700.2
2100.6

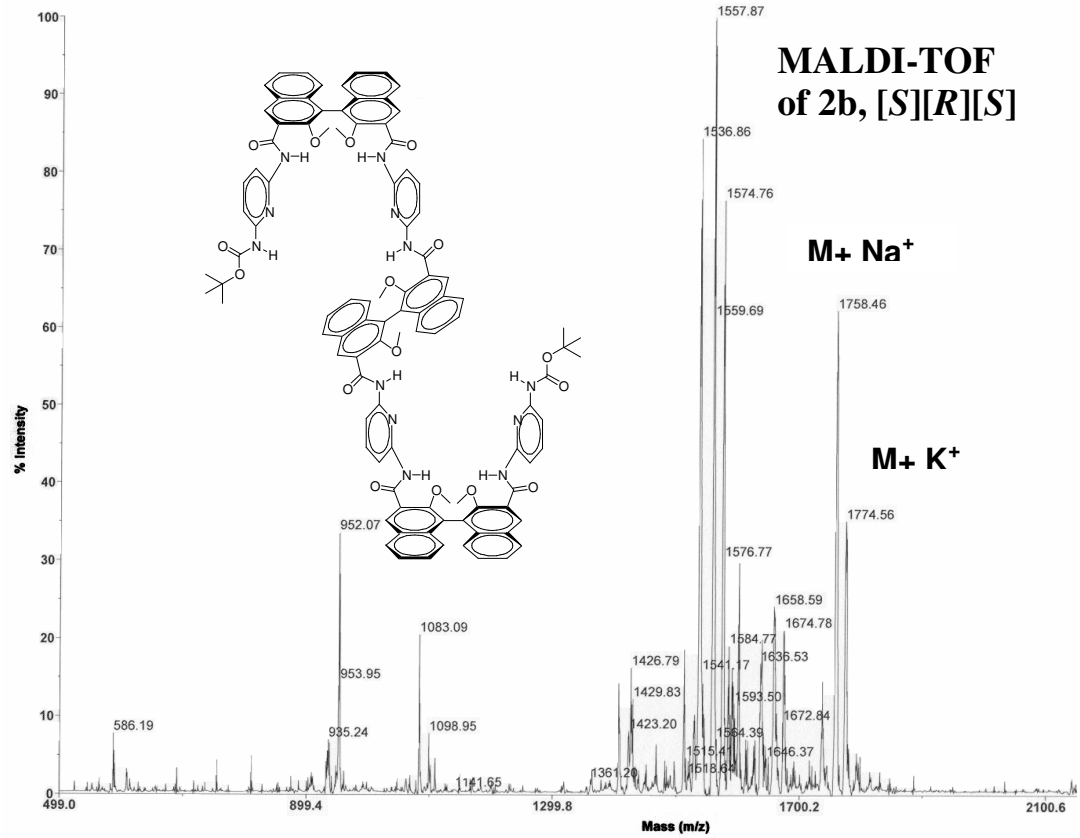
MALDI-TOF
of 2b, [S][R][S]
M+ Na+
M+ K+
% Intensity
Mass (m/z)
1557.87
1536.86
1574.76
1559.69
1758.46
952.07
1774.56
1576.77
1658.59
1674.78
1083.09
1584.77
1636.53
1426.79
953.95
1541.17
1429.83
1593.50
586.19
935.24
1098.95
1423.20
1672.84
1564.39
1515.41
1646.37
1518.84
1361.20
1141.65
499.0
899.4
1299.8
1700.2
2100.6

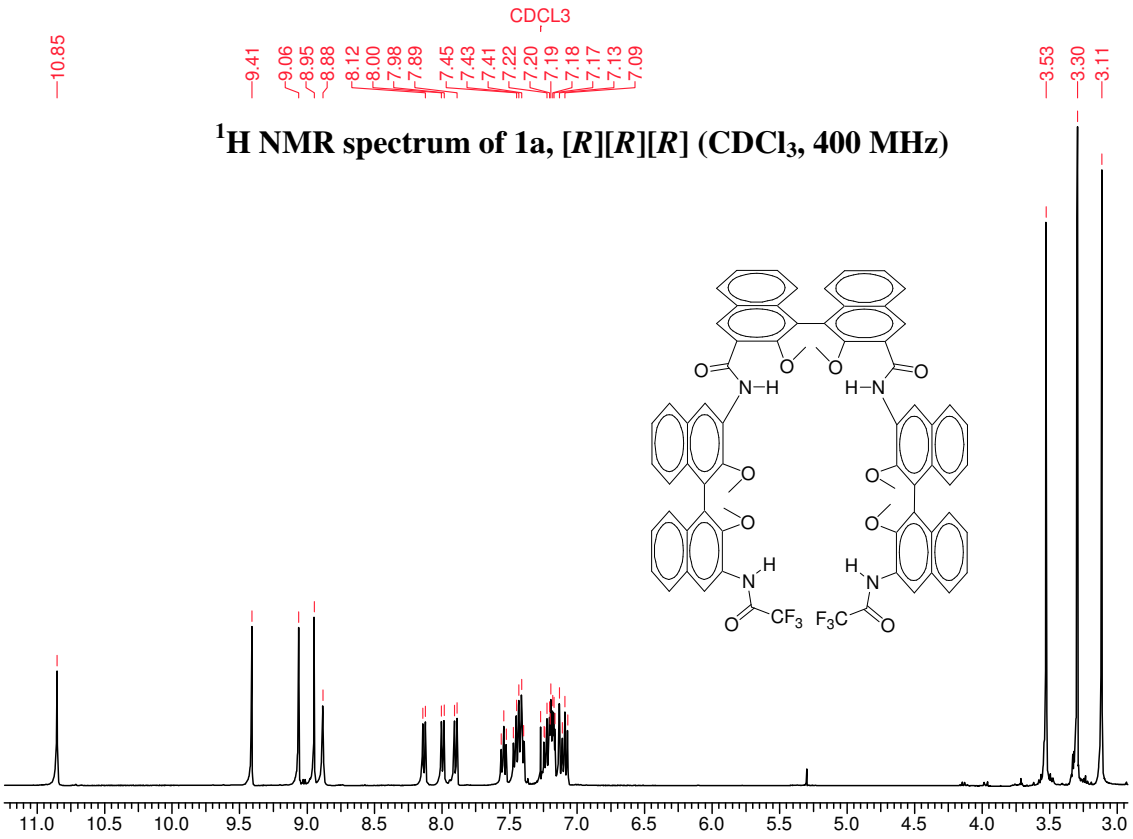

^{1}H NMR spectrum of 1a, [*R*][*R*][*R*] ($CDCl_3$, 400 MHz)

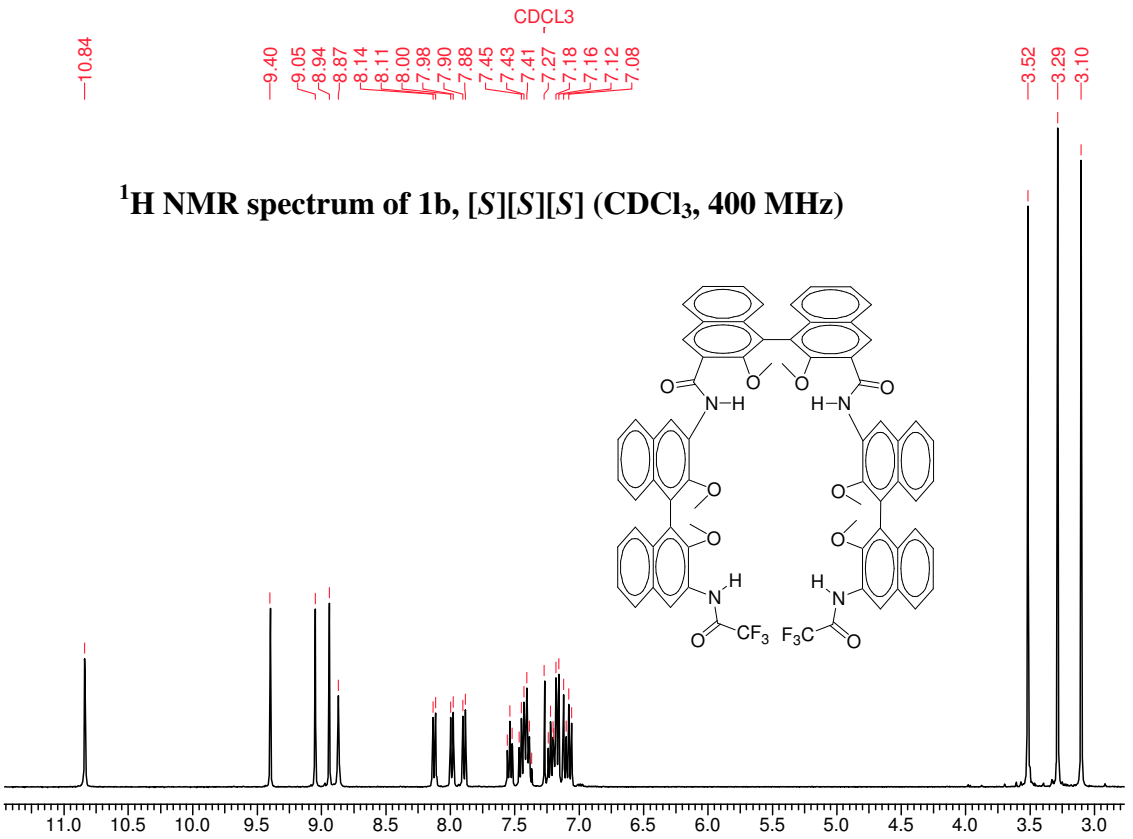

^{1}H NMR spectrum of 1b, [*S*][*S*][*S*] ($CDCl_3$, 400 MHz)

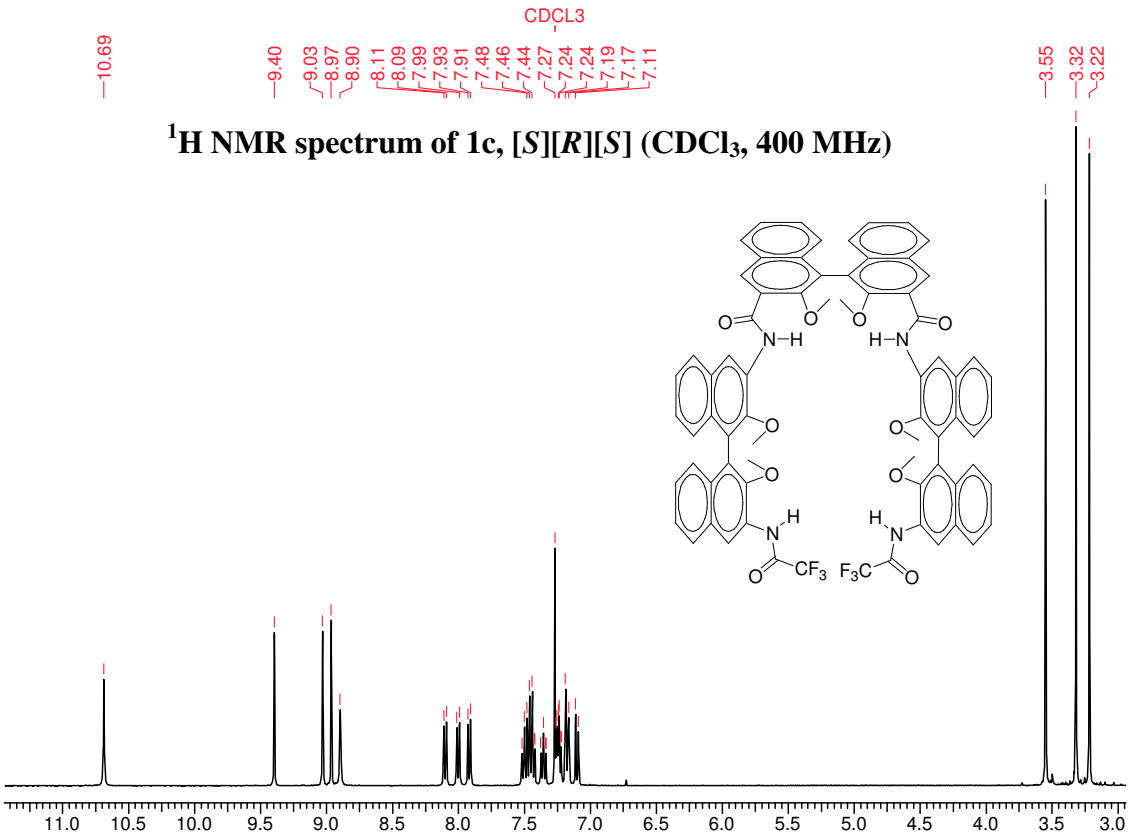

^{1}H NMR spectrum of 1c, [*S*][*R*][*S*] ($CDCl_3$, 400 MHz)

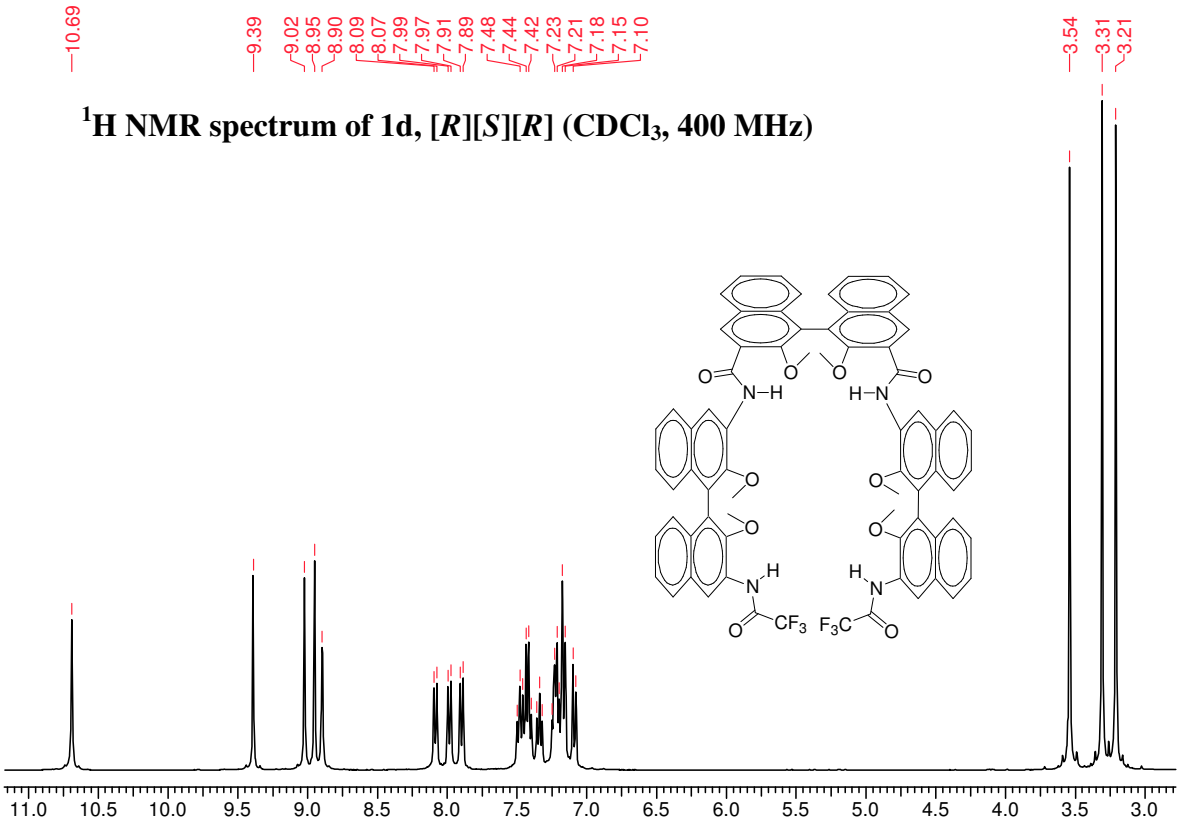

^{1}H NMR spectrum of 1d, [*R*][*S*][*R*] ($CDCl_3$, 400 MHz)

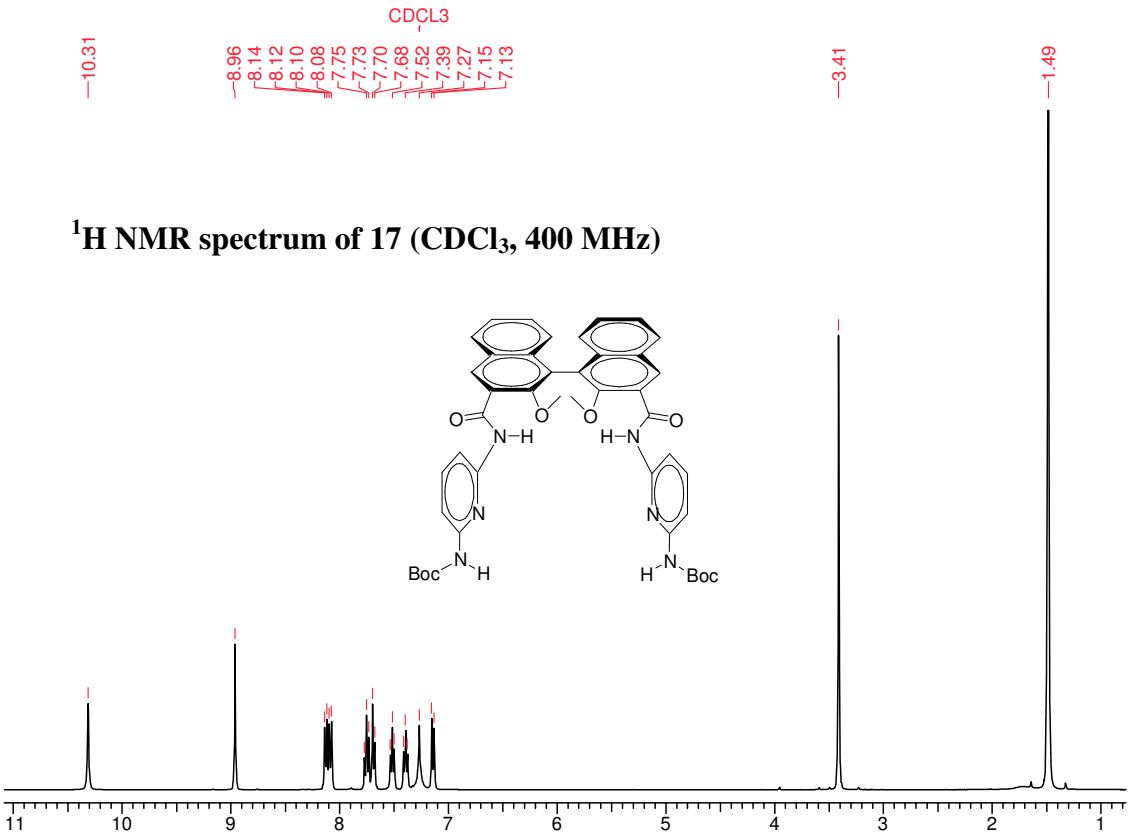

^{1}H NMR spectrum of 17 ($CDCl_3$, 400 MHz)

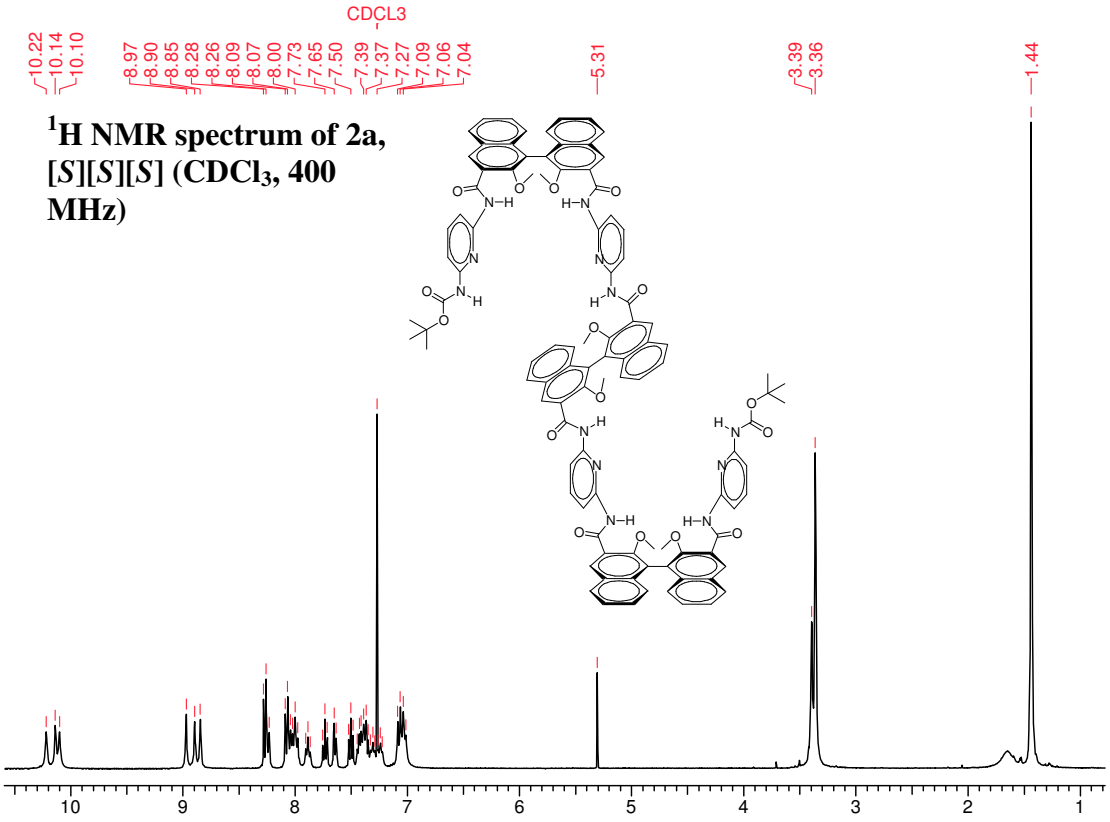

^{1}H NMR spectrum of 2a, [*S*][*S*][*S*] ($CDCl_3$, 400 MHz)

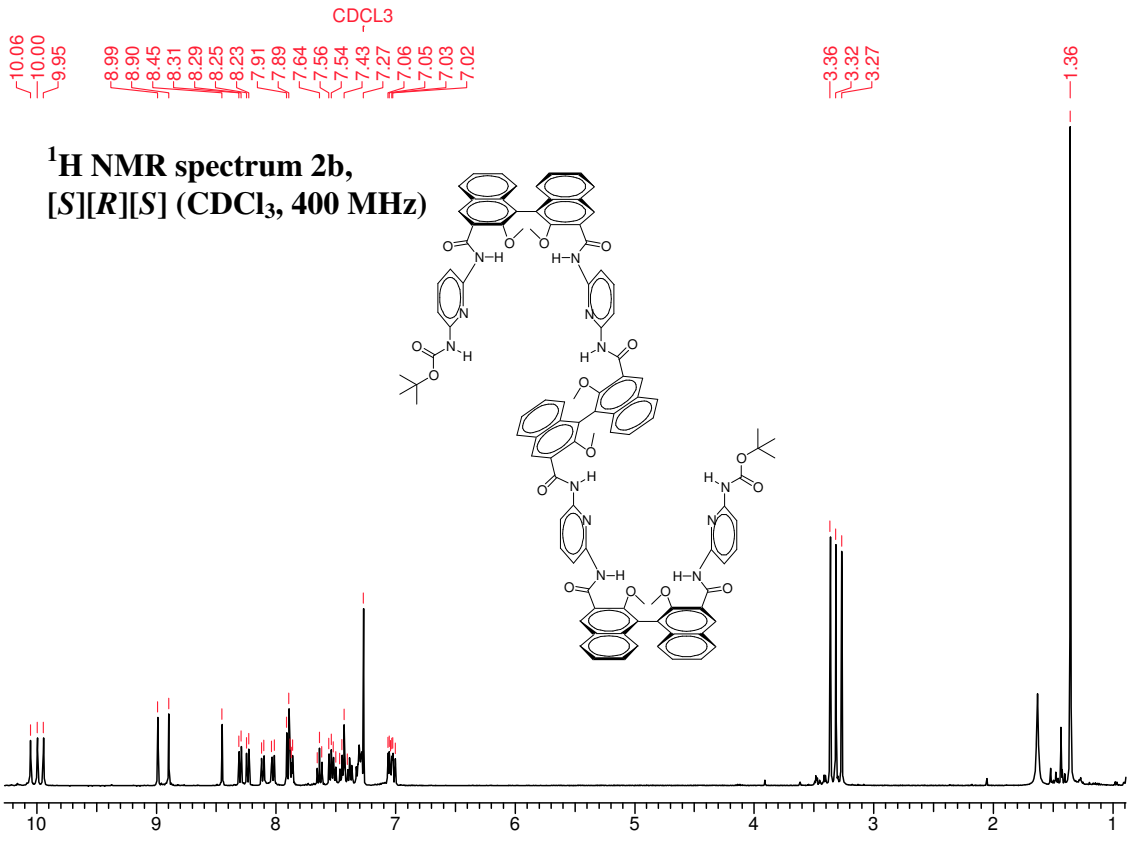

^{1}H NMR spectrum 2b, [*S*][*R*][*S*] ($CDCl_3$, 400 MHz)

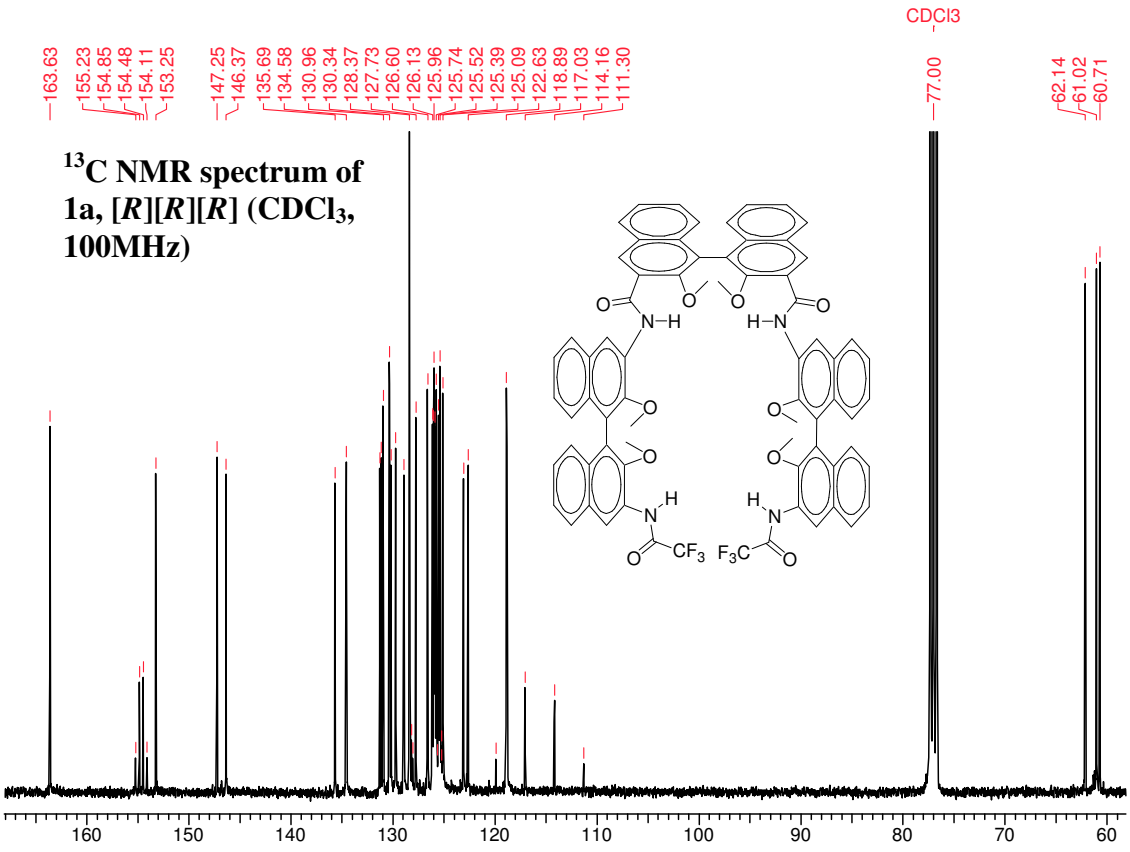

^{13}C NMR spectrum of 1a, [*R*][*R*][*R*] ($CDCl_3$, 100MHz)

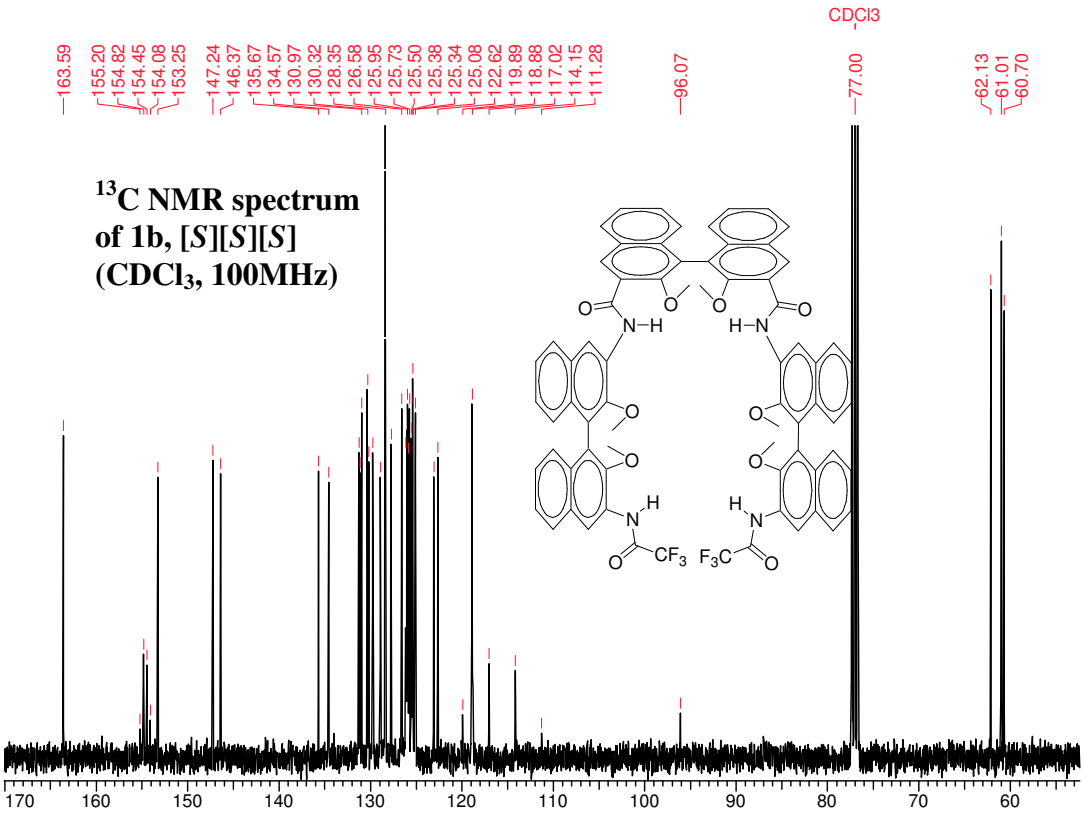

^{13}C NMR spectrum of 1b, [*S*][*S*][*S*] ($CDCl_3$, 100MHz)

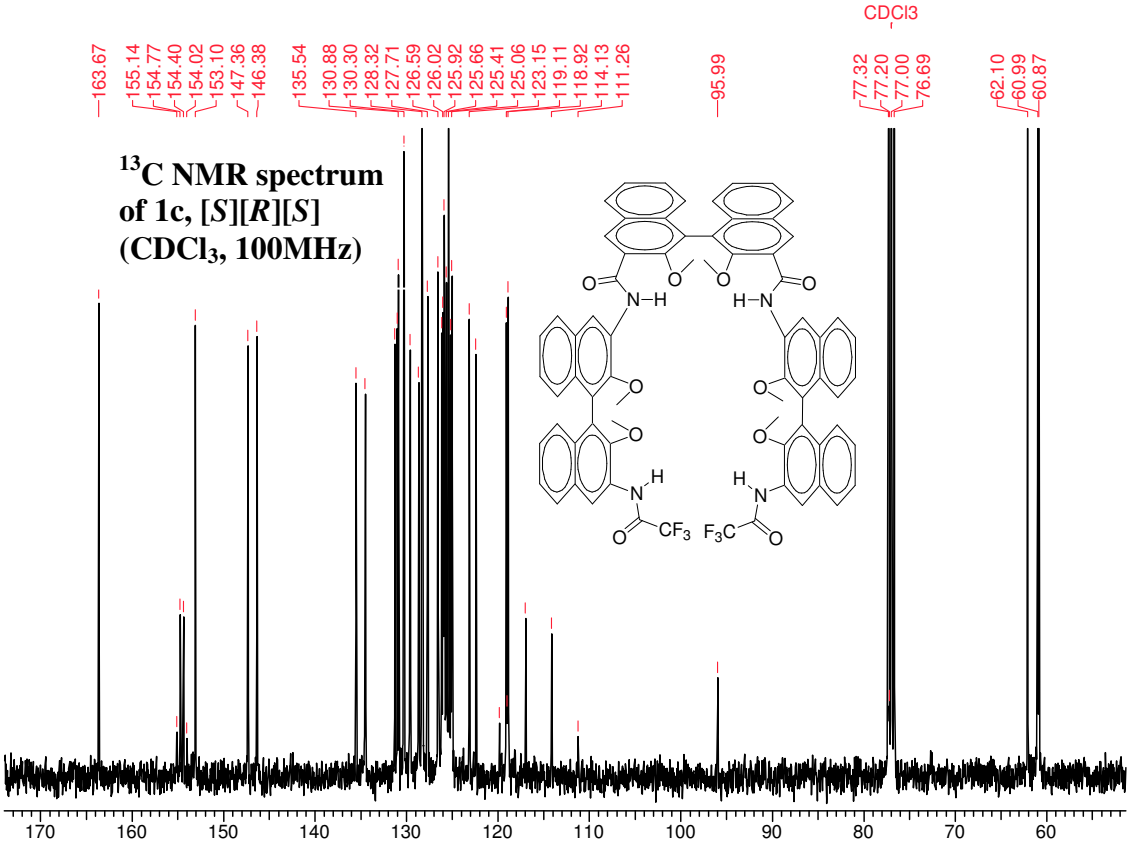

^{13}C NMR spectrum of 1c, [*S*][*R*][*S*] ($CDCl_3$, 100MHz)

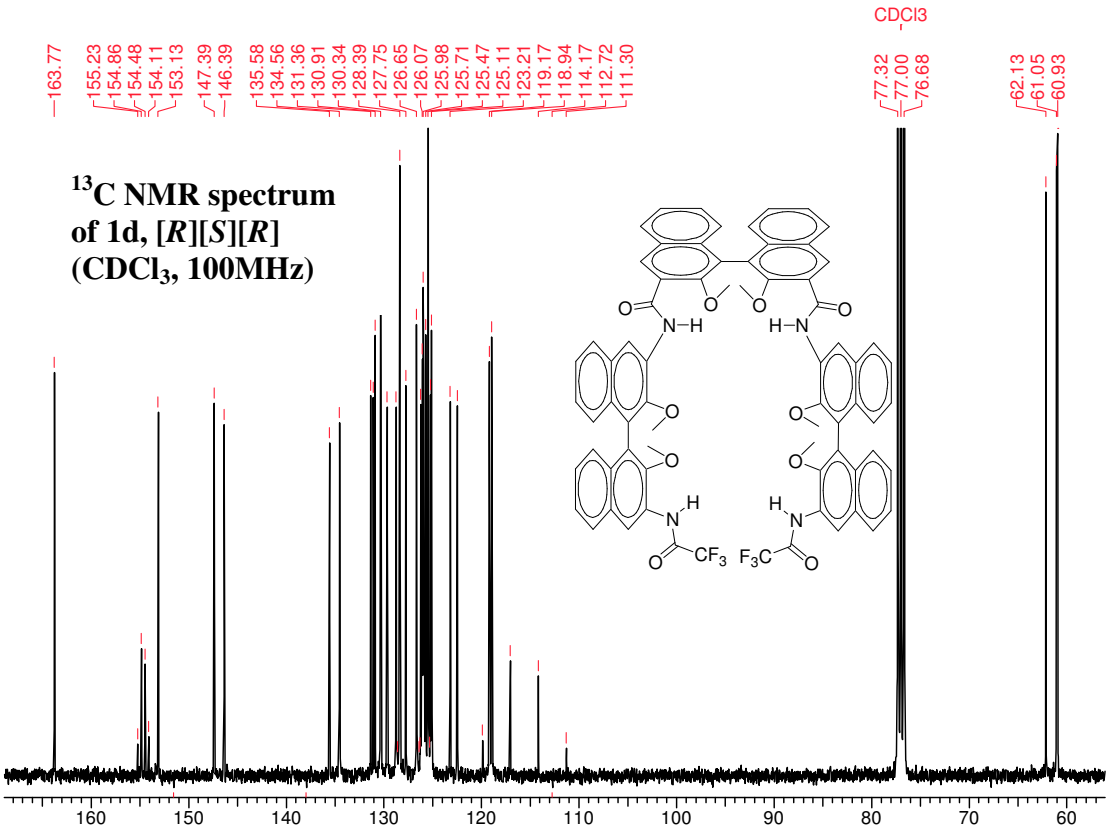

^{13}C NMR spectrum of 1d, [*R*][*S*][*R*] ($CDCl_3$, 100MHz)

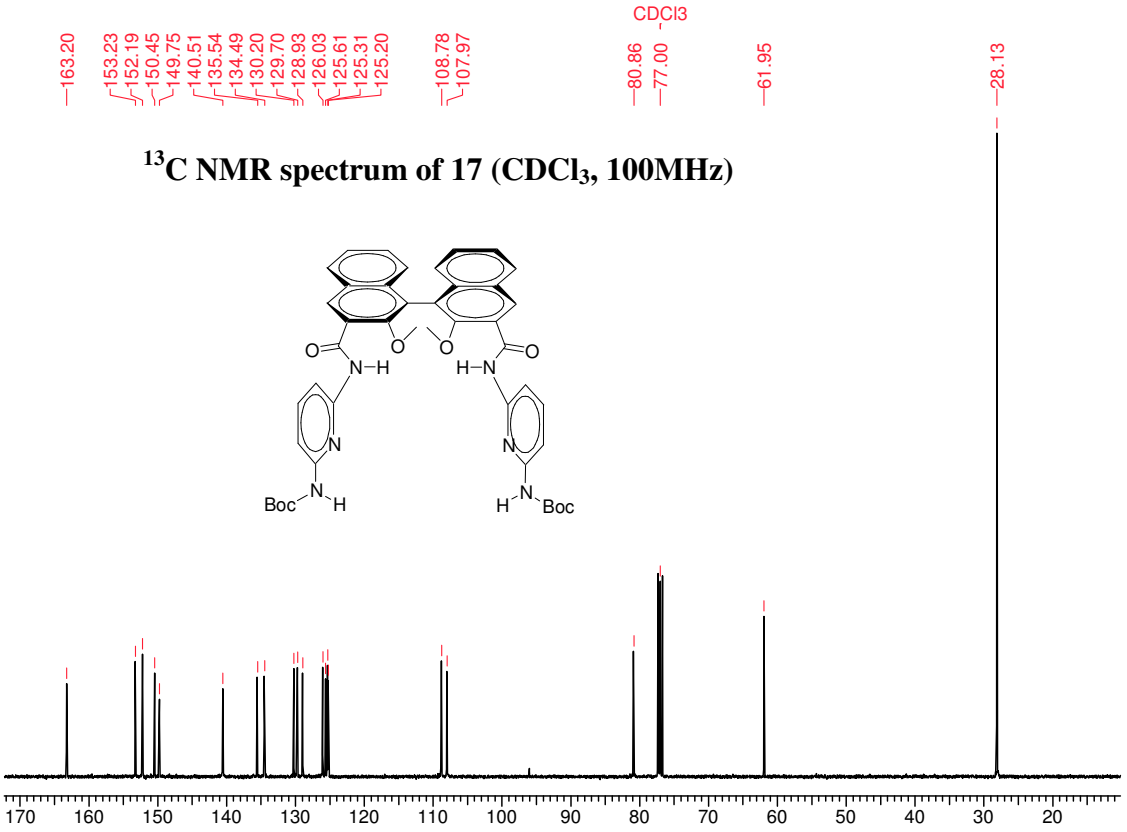

^{13}C NMR spectrum of 17 ($CDCl_3$, 100MHz)

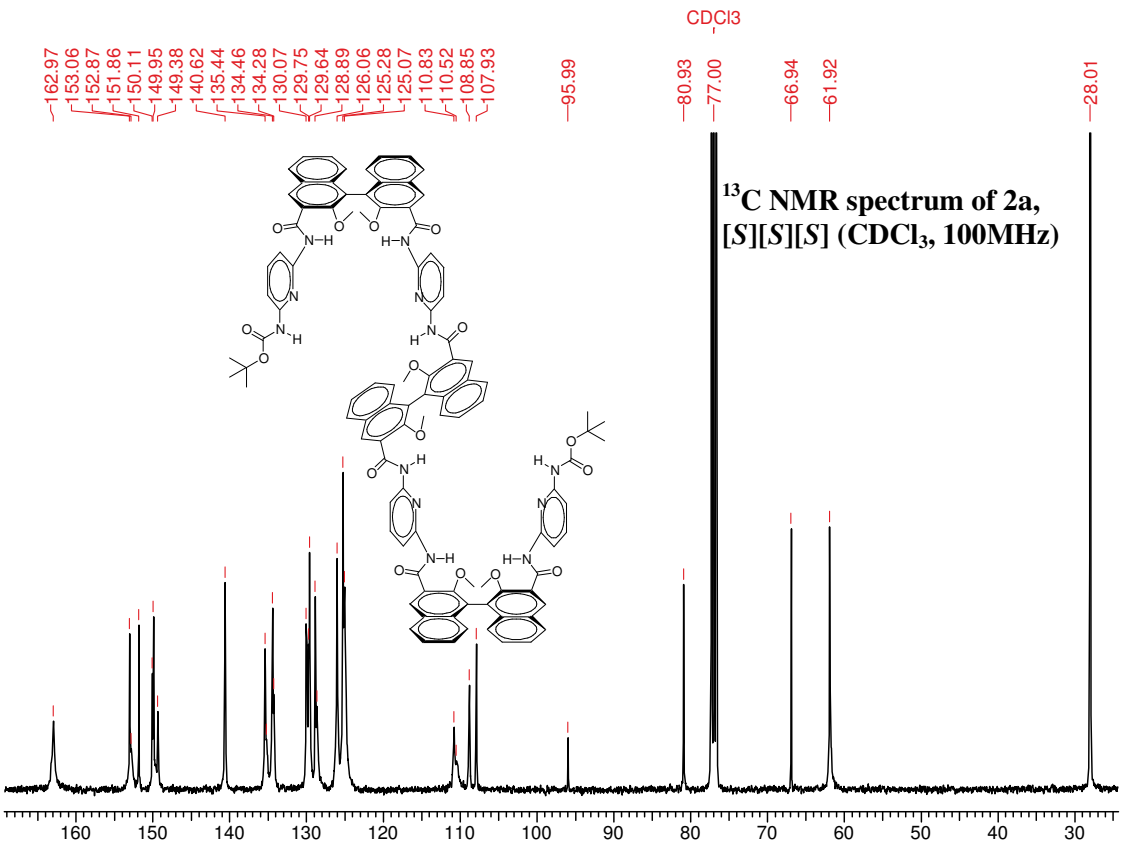

^{13}C NMR spectrum of 2a, [*S*][*S*][*S*] ($CDCl_3$, 100MHz)

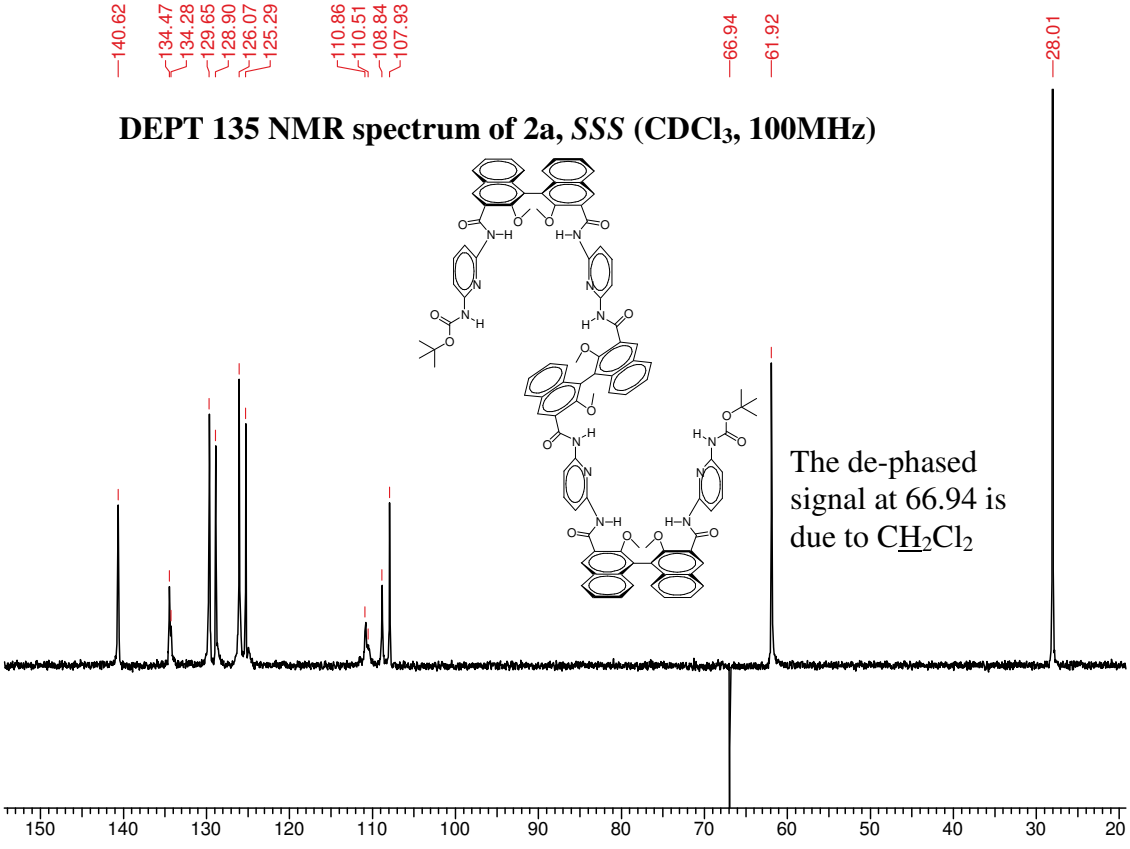

DEPT 135 NMR spectrum of 2a, *SSS* ($CDCl_3$, 100MHz)

The de-phased signal at 66.94 is due to $C\underline{H}_2Cl_2$

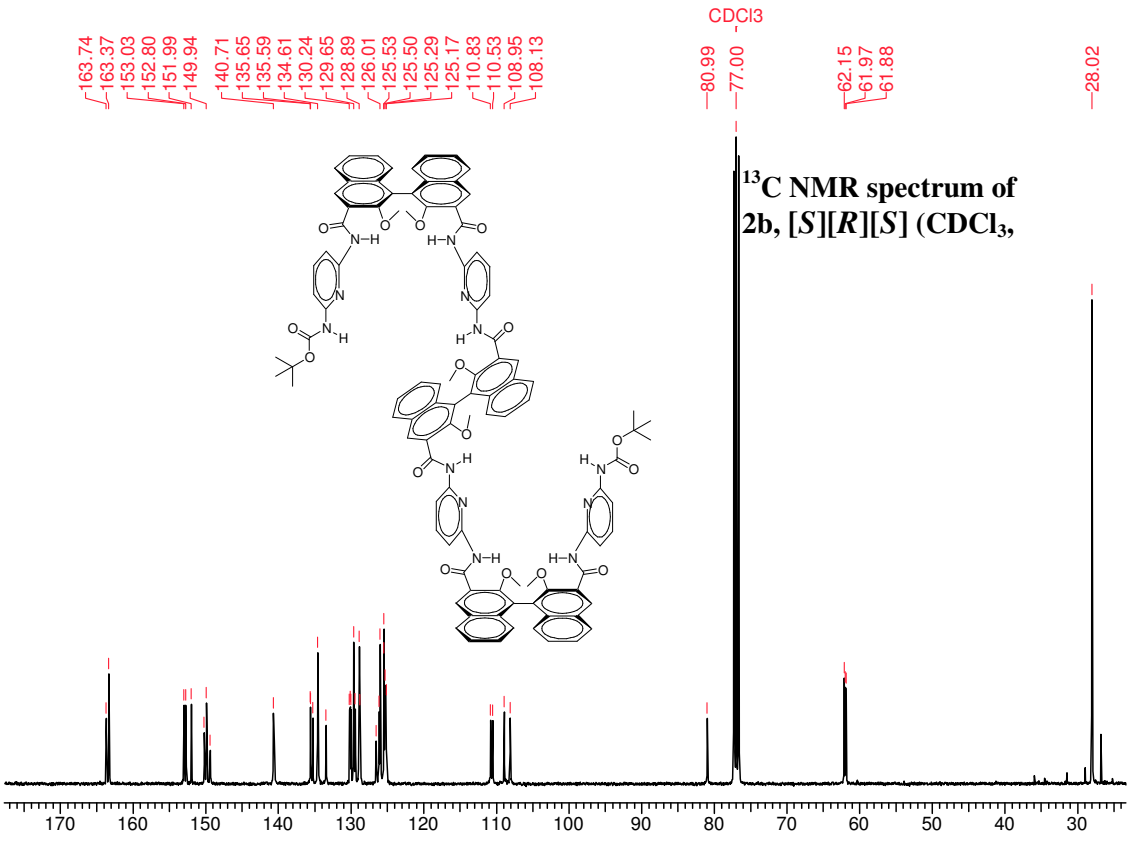

^{13}C NMR spectrum of 2b, [*S*][*R*][*S*] ($CDCl_3$,

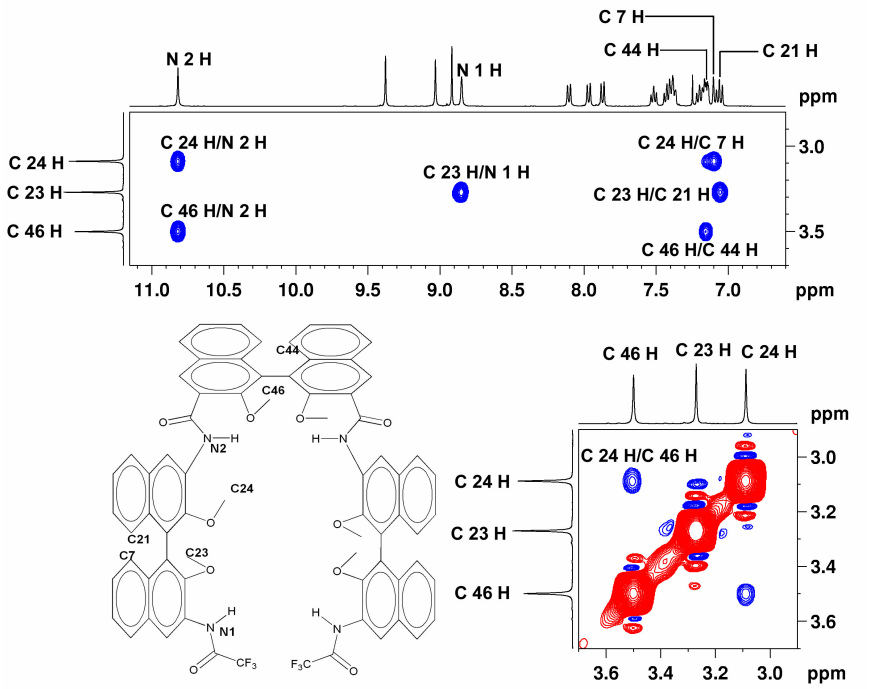	**2D NOESY spectrum of 1a, [*R*][*R*][*R*] (400 MHz, $CDCl_3$):** ***Note:*** *The chemical structure with selected labeled atoms is also shown to facilitate signal assignments.*
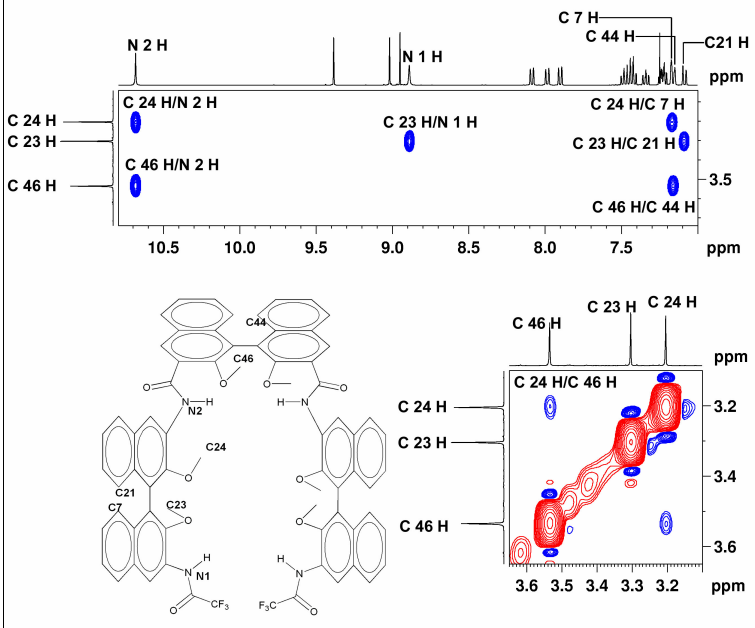	**2D NOESY Spectrum of 1c, [*S*][*R*][*S*] (400 MHz, $CDCl_3$):** ***Note:*** *The chemical structure with selected labeled atoms is also shown to facilitate signal assignments.*

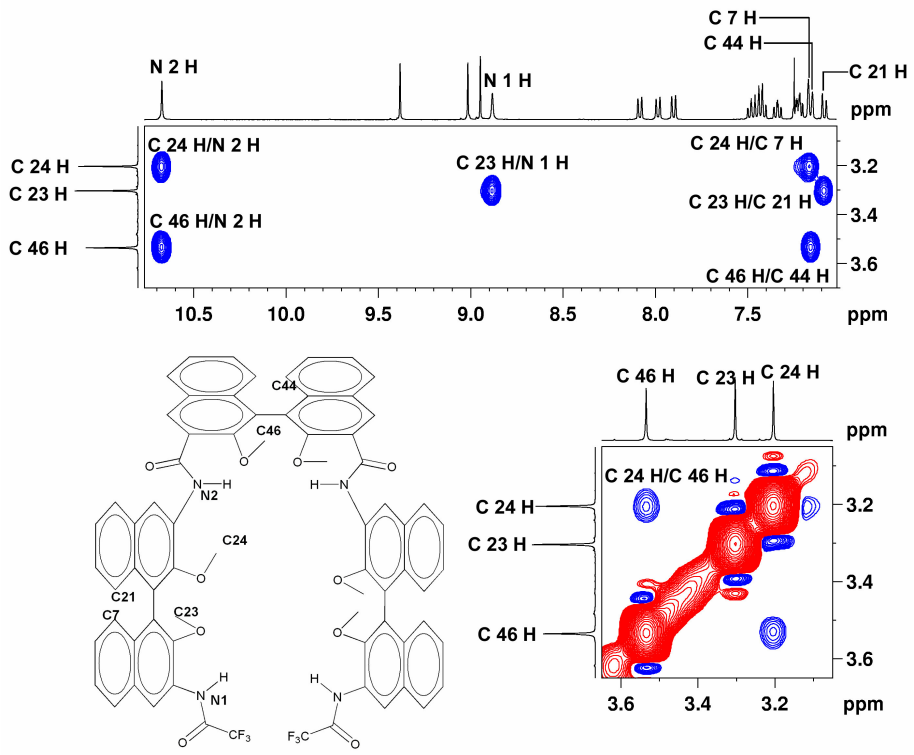	**2D NOESY Spectrum of 1d, [*R*][*S*][*R*] (400 MHz, $CDCl_3$):** ***Note:*** *The chemical structure with selected labeled atoms is also shown to facilitate signal assignments.*
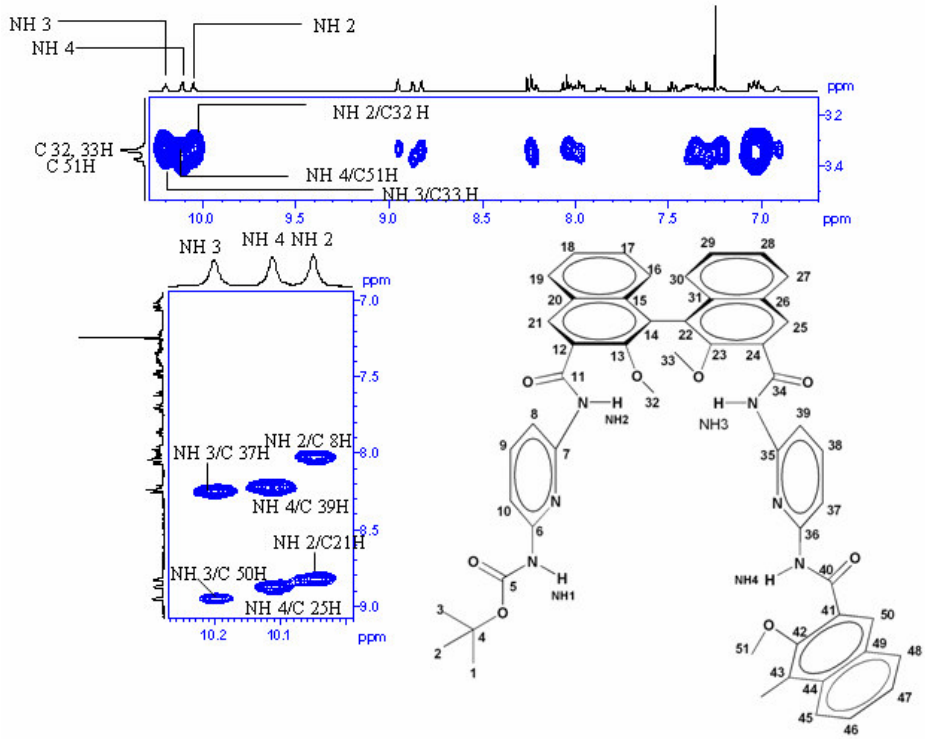	**2D NOESY Spectrum of 2a, [*S*][*S*][*S*] (400 MHz, $CDCl_3$):** ***Note:*** *The partial chemical structure with selected labeled atoms is also shown to facilitate signal assignments.*

2D HSQC (^{1}H-^{13}C) spectrum of 1b, [*S*][*S*][*S*] (400 MHz, $CDCl_3$):

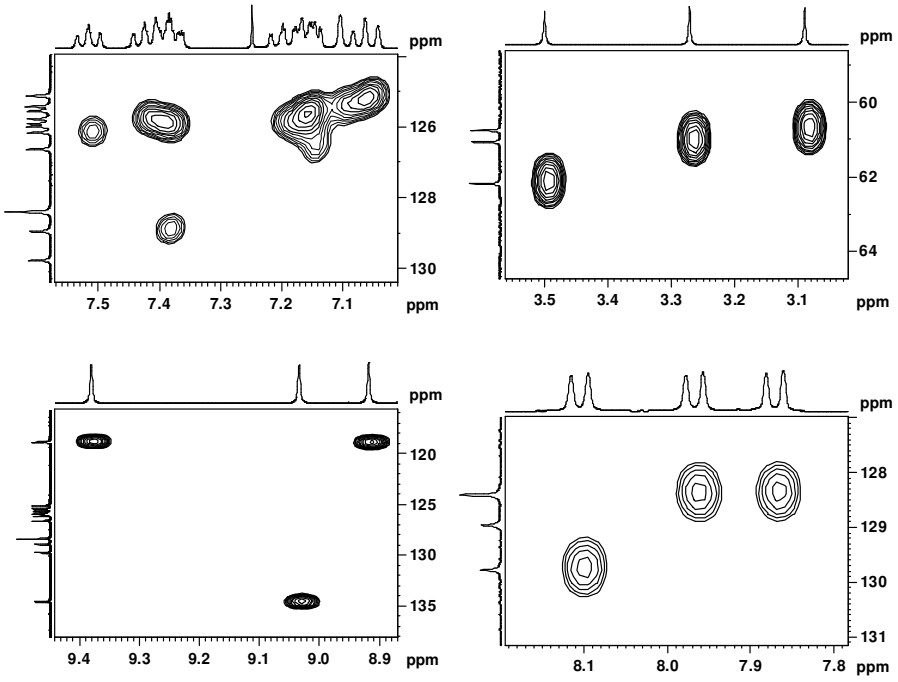

2D HSQC (^{1}H-^{13}C) spectrum of 1c, [*S*][*R*][*S*] (400 MHz, $CDCl_3$):

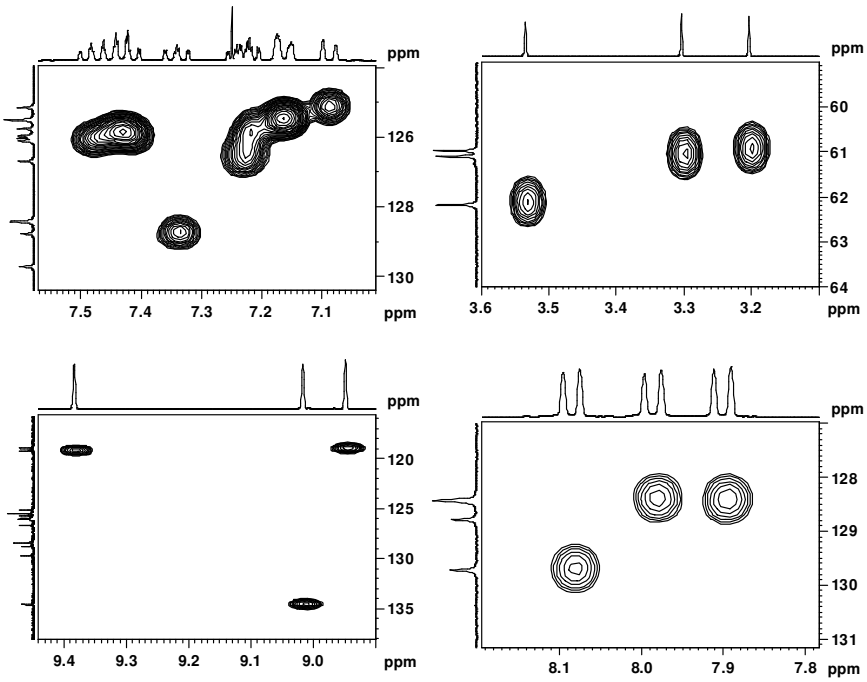

2D HSQC (^{1}H-^{13}C) spectra of 2a, [*S*][*S*][*S*] (400 MHz, $CDCl_3$):

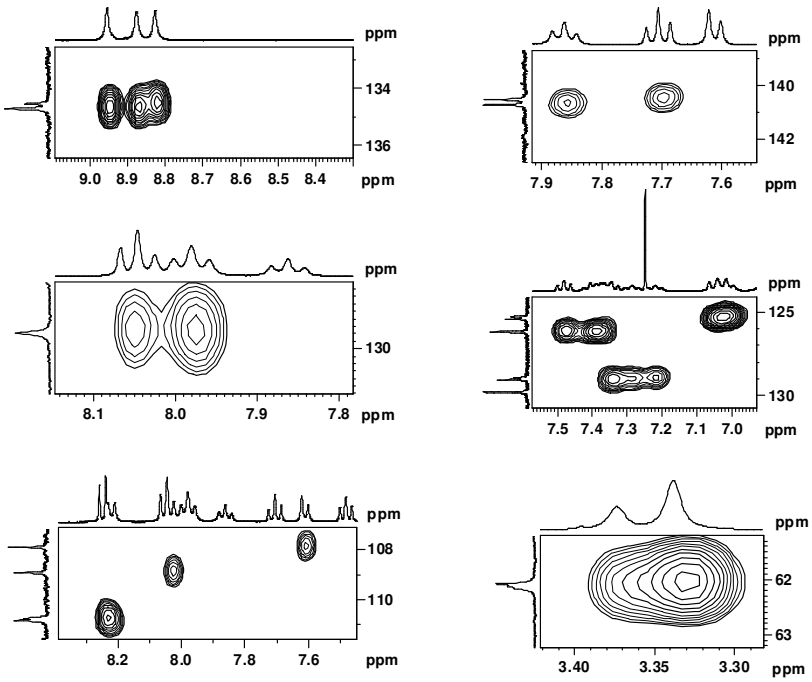

2D HSQC (^{1}H-^{13}C) spectra of 2b, [*S*][*R*][*S*] (400 MHz, $CDCl_3$):

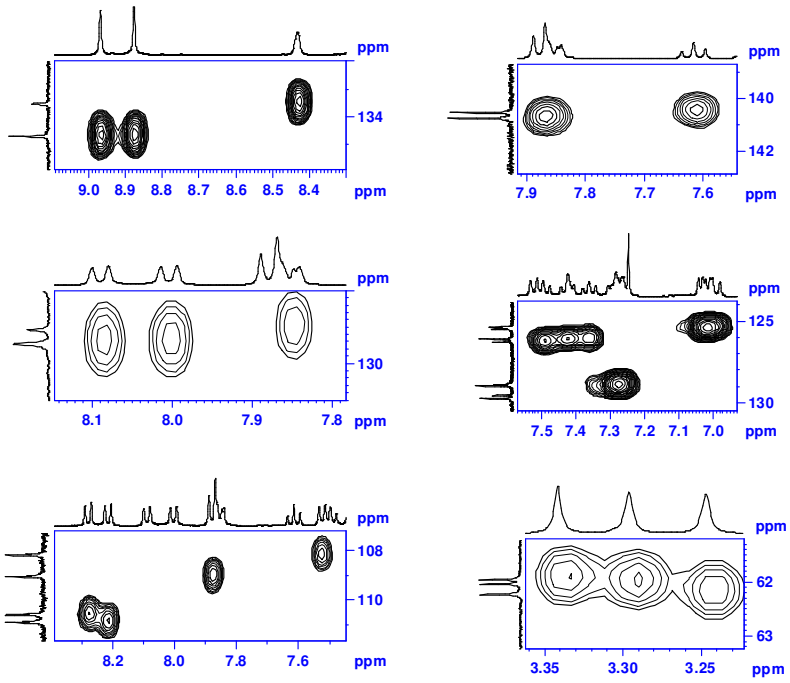

2D HMBC (^{1}H-^{13}C) spectrum of 1b, [*S*][*S*][*S*] (400 MHz, $CDCl_3$):

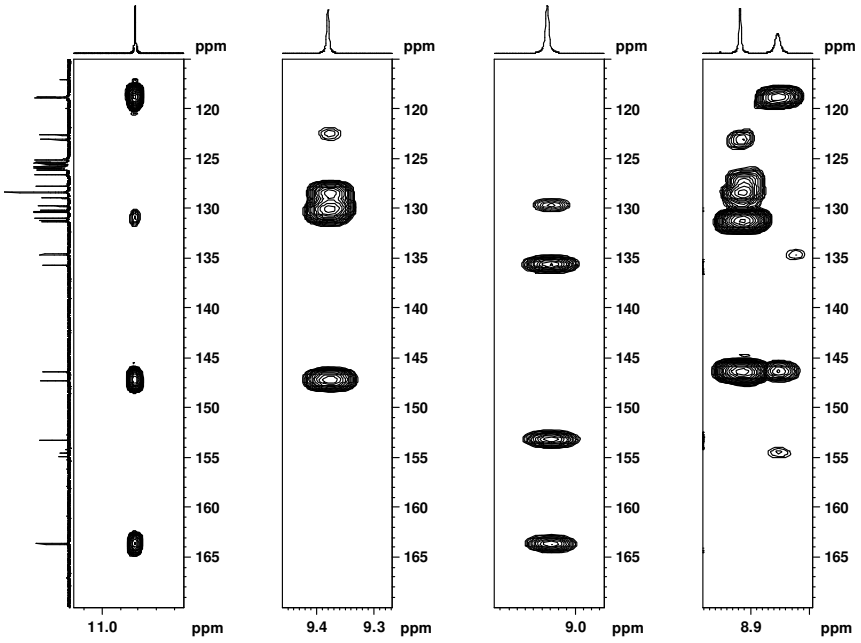

2D HMBC (^{1}H-^{13}C) spectrum of 1b, [*S*][*S*][*S*] (400 MHz, $CDCl_3$):

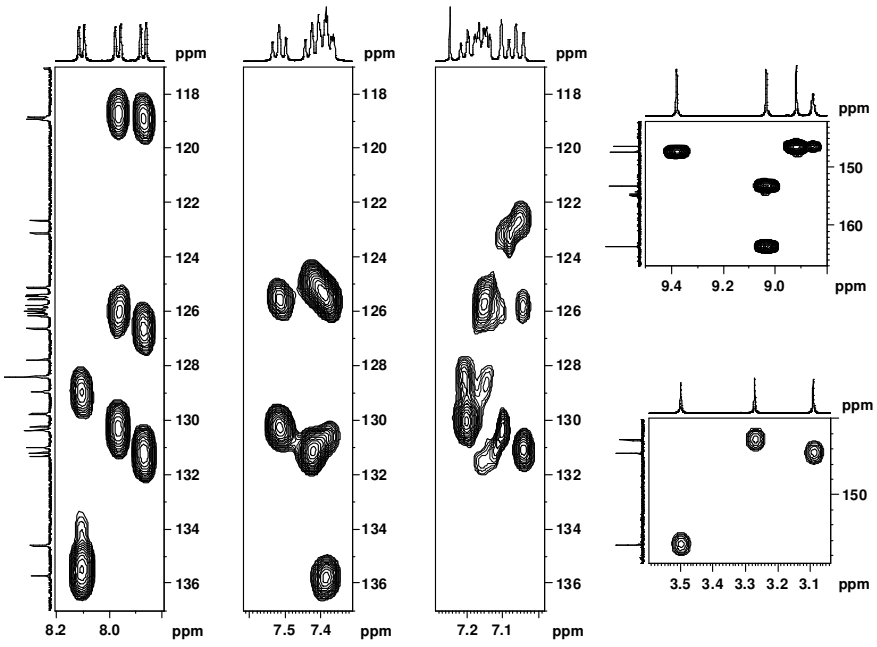

2D HMBC (^{1}H-^{13}C) spectrum of 1c, [*S*][*R*][*S*] (400 MHz, $CDCl_3$):

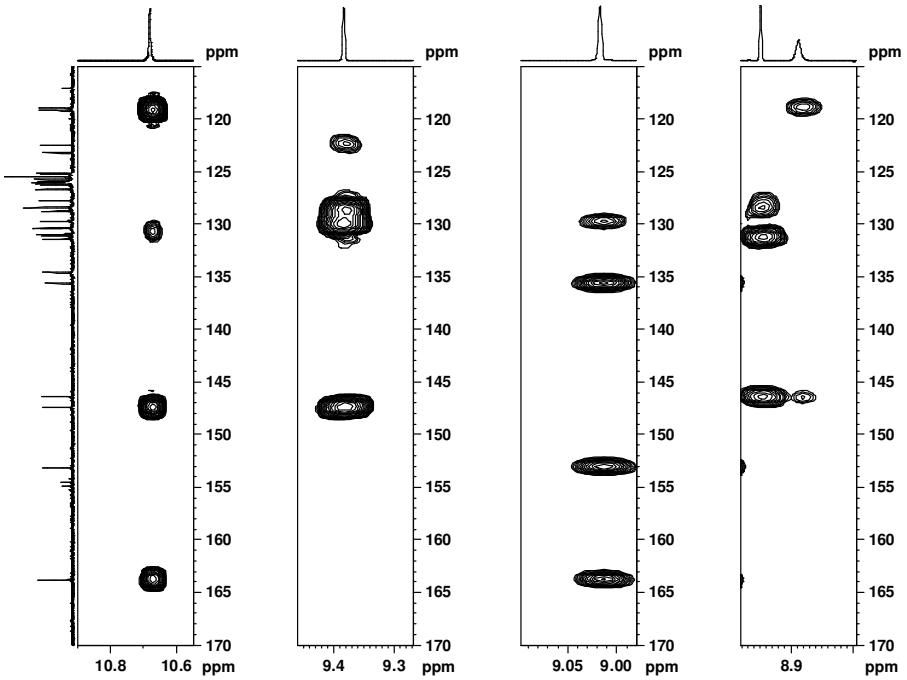

2D HMBC (1H-13C) spectrum of 1c, [S][R][S] (400 MHz, CDCl3):

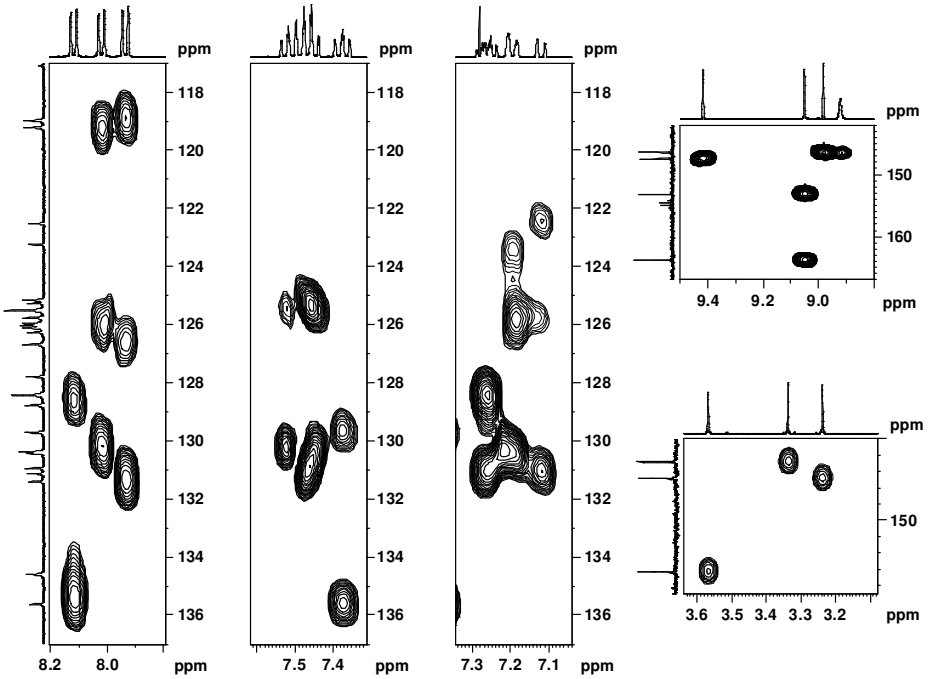

2D HMBC (^{1}H-^{13}C) spectrum of 2a, [*S*][*S*][*S*] (400 MHz, $CDCl_3$):

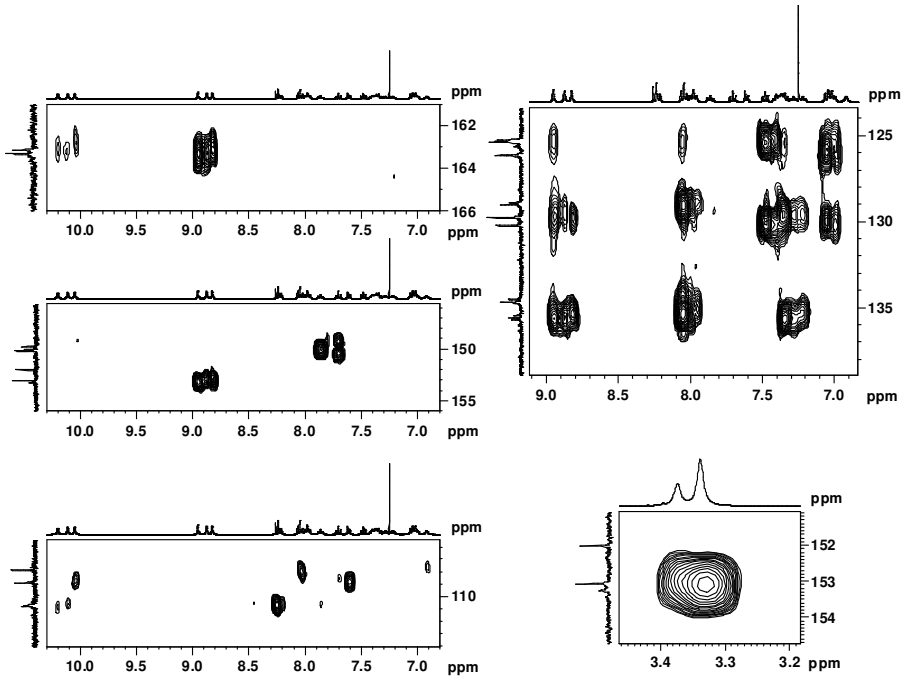

2D HMBC (^{1}H-^{13}C) spectrum of 2b, [*S*][*R*][*S*] (400 MHz, $CDCl_3$):

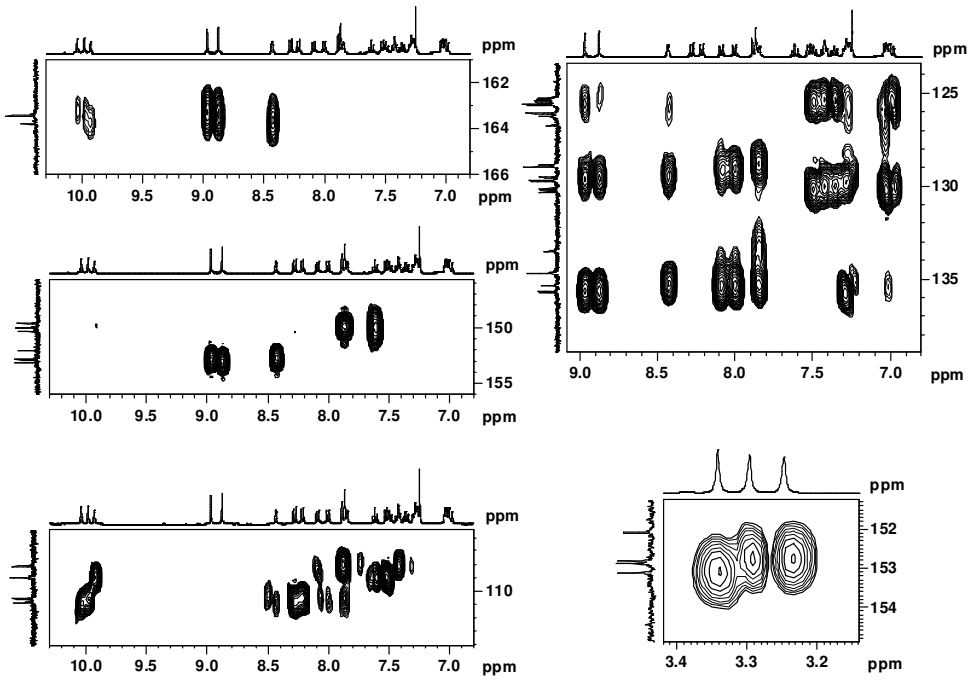

2D HSQC (^{1}H-^{15}N) and DEPT 45 (^{15}N) spectra of 1b, [*S*][*S*][*S*]:

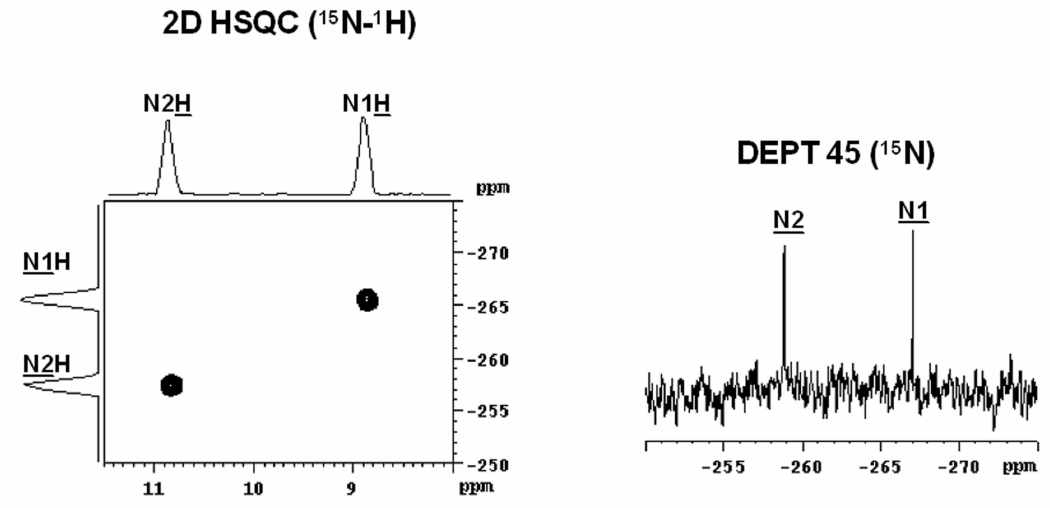

2D HSQC (^{1}H-^{15}N) and DEPT 45 (^{15}N) spectra of 1c, [*S*][*R*][*S*]:

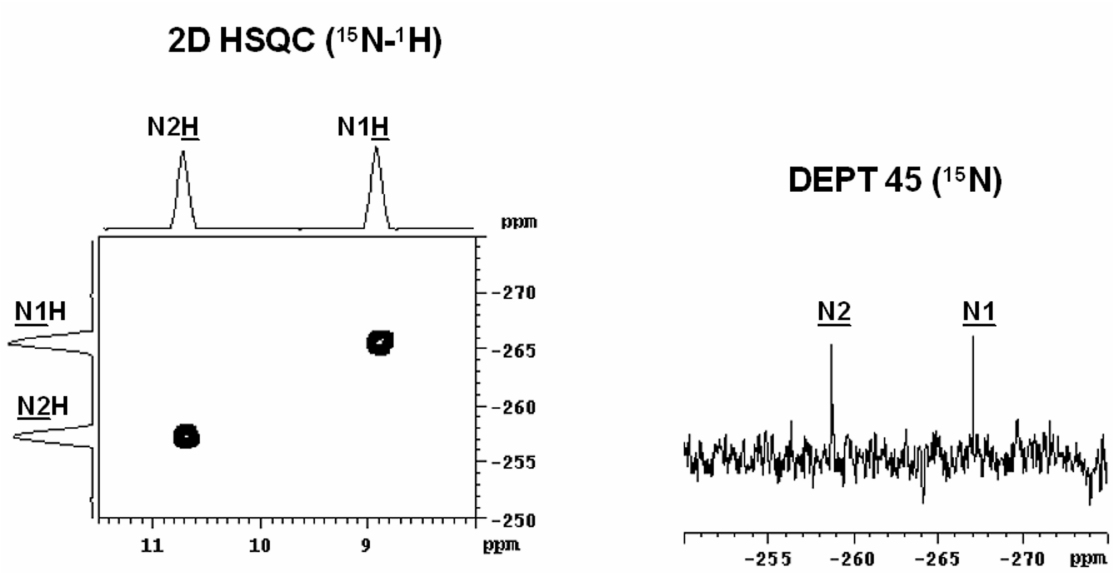

Table 1: ^{1}H, ^{13}C HSQC assignments for 1b

^{1}H (/ppm)	^{13}C (/ppm)
3.09	60.75
3.272	61.07
3.50	62.21
7.05	125.14
7.09	125.57
7.156	125.79
7.20	125.93
7.373	126.18
7.384	128.98
7.388	126.31
7.423	125.80
7.52	126.17
7.86	128.42
7.97	128.42
8.10	129.79
8.91	118.95
9.03	134.61
9.383	118.37

Table 2: ^{1}H, ^{13}C HSQC assignments for 1c

^{1}H (/ppm)	^{13}C (/ppm)
3.20	60.9
3.30	61.1
3.54	62.1
7.08	125.16
7.16	125.52
7.16	125.53
7.22	125.78
7.23	126.71
7.34	128.78
7.42	125.96
7.44	126.02
7.48	126.11
7.90	128.44
7.98	128.44
8.08	129.72
8.94	118.94
9.01	134.6
9.38	119.22

Table 3: ^{1}H, ^{13}C HSQC assignments for 2a

^{1}H (/ppm)	^{13}C (/ppm)
3.338	62.09
3.37	62.13
7.003	125.3
7.030	125.3
7.055	125.42
7.221	128.93
7.286	129.05
7.345	129.02
7.379	126.21
7.484	126.19
7.61	107.93
7.70	140.54
7.863	140.73
7.992	129.81
7.970	129.80
8.03	108.94
8.057	129.81
8.22	110.76
8.24	110.84
8.826	134.54
8.875	134.7
8.95	134.7

Table 4: ^{1}H, ^{13}C HSQC assignments for 2b

^{1}H (/ppm)	^{13}C (/ppm)
3.248	62.23
3.298	62.05
3.342	61.95
6.99	125.27
7.01	125.4
7.029	125.35
7.265	128.87
7.28	128.97
7.289	128.97
7.365	126.08
7.426	126.08
7.498	126.26
7.52	108.25
7.616	140.56
7.85	129.54
7.87	140.77
7.880	109.08
8.00	129.74
8.09	129.74
8.21	110.94
8.28	110.64
8.44	133.53
8.88	134.71
8.98	134.71

Table 5: ^{1}H, ^{13}C HMBC assignments for 1b

^{1}H (/ppm)	^{13}C (/ppm)
3.09	147.3
3.272	146.4
3.50	153.32
7.05	122.7, 125.80, 131.05
7.09	123.18, 126.18, 130.27
7.156	125.81, 126.17, 131.24, 128.98
7.20	128.42, 130.23
7.373	125.57
7.384	135.8,125.74
7.388	125.57, 131.35
7.423	125.14
7.52	125.79, 131.24
7.86	118.95, 126.31, 131.35
7.97	118.37, 125.93, 130.23
8.10	128.98, 134.61, 135.8
8.9	118.95, 146.4, 154.55
8.91	128.42, 131.35, 146.4, 123.18
9.03	129.79, 135.8, 153.32, 163.67
9.383	128.42, 130.23, 147.3, 122.7
10.82	118.37, 131.01, 147.3, 163.67

Table 6: ^{1}H, ^{13}C HMBC assignments for 1c

^{1}H (/ppm)	^{13}C (/ppm)
3.20	147.4
3.30	146.6
3.54	153.1
7.08	122.53, 126.02, 131.16
7.16	123.29, 125.96, 130.43
7.16	125.06,126.11, 130.45
7.22	128.44, 130.94
7.23	128.44, 131.13
7.34	129.72, 135.68
7.42	125.52
7.44	125.16
7.48	125.53, 130.45
7.90	118.94, 126.71, 131.13
7.98	119.22, 125.78, 130.94
8.08	128.78, 134.6, 135.68
8.9	118.94, 146.4
8.94	128.44, 131.13, 146.4
9.01	129.72, 135.68, 153.07, 163.8
9.38	128.44, 130.94, 147.4, 122.53
10.7	119.22, 131.13, 147.4, 163.8

Table 7: ^{1}H, ^{13}C HMBC assignments for 2a

^{1}H (/ppm)	^{13}C (/ppm)
3.338	
3.37	
6.91	107.93
7.003	126.21, 130.26
7.030	126.21, 130.28
7.055	126.19, 130.28
7.221	129.8, 135.48
7.286	129.81, 135.74
7.345	129.81, 135.64
7.379	125.3, 130.26
7.484	125.42, 130.28
7.61	108.94
7.70	149.78, 150.27
7.863	150.11, 150.4
7.992	129.05, 134.7
7.970	128.93, 134.54, 135.48
8.03	107.93
8.057	124.7, 129.02, 135.64
8.22	110.84

Table 8: ^{1}H, ^{13}C HMBC assignments for 2b

^{1}H (/ppm)	^{13}C (/ppm)
3.248	152.81
3.298	152.88
3.342	153.12
6.99	126.08, 126.27, 130.23
7.01	126.26 , 130.33, 135.68
7.029	126.02, 126.75, 130.12, 135.36
7.265	129.54, 135.36
7.28	129.74, , 135.68
7.289	129.74, 135.75
7.365	125.35, 130.12
7.426	125.27, 130.23
7.428	108.25, 150.05, 150.41
7.498	125.4, 130.33
7.52	109.08, 150.02
7.616	109.08, 149.69, 150.05
7.85	126.08, 130.12, 135.36
7.87	150.02, 150.05
7.880	108.25

Table 7: ^{1}H, ^{13}C HMBC assignments for 2a	
8.24	110.76
8.826	129.8, 135.48, 150.08, 163.12
8.875	129.8, 135.74, 153.08, 163.64
8.95	129.8, 135.64, 153.27, 163.34
10.05	108.94, 163.12
10.11	110.76, 163.34
10.2	110.84, 163.34

Table 8: ^{1}H, ^{13}C HMBC assignments for 2b	
8.00	128.97, 134.71, 135.75
8.09	128.97, 134.71, 135.68
8.21	110.64
8.28	110.94
8.44	129.54, 135.36, 152.81, 163.80
8.88	129.74, 135.75, 153.12, 163.46
8.98	129.74, 135.68, 152.877, 163.46
9.93	109.08, 163.80
9.98	110.64, 163.46
10.04	110.94, 163.46

Details of the ab initio MO studies

The conformation of all oligomers was investigated at the HF/6-31G* level of ab initio MO theory (all structures provided in pdb format). To consider correlation effects, the HF/6-31G* minimum structures were reoptimized at the B3LYP/6-31G* level of Density Functional Theory (DFT). Due to the extensive intramolecular hydrogen bonding, there are only conformational alternatives for the orientation of the methoxy groups, which were considered for the various oligomers. The most stable structures after geometry optimization are given. Their HF/6-31G* total energies are: **1a** = **1b** = -4319.951416 a.u.; **1c** = **1d** = -4319. 950143 a.u.; **2a** = -5764.147265 a.u.; **2b** = -5764.145866 a.u.

3.6 References and notes

(1) (a) Choi, S.; Clements, D. J.; Pophristic, V.; Ivanov, V.; Vemparala, S.; Bennett, J. S.; Klein, M. L.; Winkler, J. D.; DeGrado, D. F. *Angew. Chem. Int. Ed.* **2005**, *44*, 6685; (b) Porter, E. A.; Wang, X.; Lee, H.-S.; Weisblum, B.; Gellman, S. H. *Nature* **2000,** *404*, 565; (c) Hook, D. F.; Bindschädler, P.; Mahajan, Y. R.; Sebesta, R.; Kast, P.; Seebach, D. *Chem. Biodiv.* **2005**, *2*, 591; (d) Arvidsson, P. I.; Ryder, N. S.; Weiss, H. M.; Hook, D. F.; Escalante, J.; Seebach, D. *Chem. Biodiv.* **2005**, *2*, 401; (e) Steer, D. L.; Lew, R. A.; Perlmutter, P.; Smith; A. I.; Aguilar, M. I. *Curr. Med. Chem.* **2002**, *9*, 811; (f) Sagan, S.; Milcent, T.; Ponsinet, R.; Convert, O.; Tasseau, O.; Chassiang, G.; Lavielle, S.; Lequin, O. *Eur. J. Biochem.* **2003**, *270*, 939; (g) Gopi, H. N.; Ravindra, G.; Pal, P. P.; Pattanaik, P.; Balaram, H.; Balaram, P. *FEBS Lett.* **2003**, *535*, 175; (h) Arnold, U.; Hinderaker, M. P.; Nilsson, B. L.; Huck, B. R.; Gellman, S. H.; Raines, R. T. *J. Am. Chem. Soc.* **2002**, *124*, 8522; (i) Karlsson, A. J.; Pomerantz, W. C.; Weisblum, B.; Gellman, S. H.; Palecek, S. P. *J. Am. Chem. Soc*. **2006**, *128*, 12630; (j) Sadowsky, J. D.; Fairlie, W. D.; Hadley, E. B.; Lee, H. S.; Umezawa, U.; Nikolovska-Coleska, Z.; Wang, S. M.; Huang, D. C. S.; Tomita, Y.; Gellman, S. H. *J. Am. Chem. Soc.* **2007***, 129*, 139.

(2) Cornelissen, J. J. L. M.; Donners, J. J. J. M.; de Gelder, R.; Graswinckel, W. S.; Metselaar, G. A.; Rowan, A. E.; Sommerdijk, N. A. J. M.; Nolte, R. J. M. *Science* **2001**, *293*, 676.

(3) Estroff, L. A.; Incarvito, C. D.; Hamilton, A. D. *J. Am. Chem. Soc*. **2004**, *126*, 2.

(4) (a) Huc, I.; Maurizot, V.; Gornitzka, H.; Le´ger, J.-M. *Chem. Commun.* **2002**, 578; (b) Berl, V.; Huc, I.; Khoury, R. G.; Krische, M. J.; Lehn, J.-M. *Nature* **2000**, *407*, 720; (c) Berl, V.; Huc, I.; Khoury, R. G.; Lehn, J.-M. *Chem. Eur. J.* **2001**, *7*, 2810.

(5) (a) Hamuro, Y.; Geib, S. J.; Hamilton, A. D. *J. Am. Chem. Soc.* **1996**, *118*, 7529; (b) Hamuro, Y.; Geib, S. J.; Hamilton, A. D. *J. Am. Chem. Soc.* **1997**, *119*, 10587.

(6) Delnoye, D. A. P.; Sijbesma, R. P.; Vekemans, J. A. J. M.; Meijer, E. W. *J. Am. Chem. Soc.* **1996**, *118*, 8717.

(7) (a) Gong, B. *Chem. Eur. J.* **2001**, *7*, 4337; (b) Zhu, J.; Parra, R. D.; Zeng, H.; Skrzypczak-Jankun, E.; Zeng, X. C.; Gong, B. *J. Am. Chem. Soc.* **2000**, *122*, 4219.

(8) Hawryluk, N. A.; Murray, T. J. *J. Am. Chem. Soc.* **2001**, *123*, 10475.

(9) Garric, J.; Le´ger, J.-M.; Grelard, A.; Ohkita, M.; Huc, I. *Tetrahedron Lett.* **2003**, *44*, 1421.

(10) Prince, R. B.; Okada, T.; Moore, J. S. *Angew. Chem. Int. Ed.* **1999**, *38*, 233.

(11) (a) Ohkita, M.; Lehn, J.-M.; Baum, G.; Fenske, D. *Chem. Eur. J.* **1999**, *5*, 3471; (b) Ohkita, M.; Lehn, J.-M.; Baum, G.; Fenske, D. *Heterocycles* **2000**, *52*, 103.

(12) Cuccia, L. A.; Lehn, J.-M.; Homo, J.-C.; Schmutz, M. *Angew. Chem. Int. Ed.* **2000**, *39*, 233.

(13) Gardinier, K. M.; Khoury, R. G.; Lehn, J.-M. *Chem. Eur. J.* **2000**, *6*, 4124.

(14) Malone, J. F.; Murray, C. M.; Dolan, G. M.; Docherty, R.; Lavery, A. J. *Chem. Mater.* **1997**, *9*, 2983.

(15) Huc, I. *Eur. J. Org. Chem.* **2004**, 17.

(16) Jiang, H.; Lèger, J.-M.; Huc, I. *J. Am. Chem. Soc.* **2003**, *125*, 3448.

(17) Kanamori, D.; Okamura, T.; Yamamoto, H.; Ueyama, N. *Angew. Chem. Int. Ed.* **2005**, *44*, 969.

(18) Howard, H. A. K.; Hoy, V. J.; O'Hagan, D.; Smith, G. T. *Tetrahedron* **1996**, *52*, 12613.

(19) (a) Zhao, X.; Wang, X.-Z.; Jiang, X.-K.; Chen, Y.-Q.; Li, Z.-T.; Chen, G.-J. *J. Am. Chem. Soc.* **2003**, *125*, 15128; (b) Li, C.; Ren, S.-F.; Hou, J.-L.; Yi, H.-P.; Zhu, S.-Z.; Jiang, X.-K.; Li, Z.-T. *Angew. Chem. Int. Ed.* **2005**, *44*, 5725.

(20) Ernst, J. T.; Becerril, J.; Park, H. S.; Yin, H.; Hamilton, A. D. *Angew. Chem. Int. Ed.* **2003**, *42*, 535.

(21) (a) Hunter, C. A.; Purvis, D. H. *Angew. Chem. Int. Ed. Engl.* **1992**, *31*, 792; (b) Safarowsky, O.; Nieger, M.; Fröhlich, R.; Vögtle, F. *Angew. Chem. Int. Ed.* **2000**, *39*, 1616.

(22) Parra, R. D.; Zeng, H.; Zhu, J.; Zheng, C.; Zeng, X. C.; Gong, B. *Chem. Eur. J.* **2001**, *7*, 4352.

(23) Berl, V.; Huc, I.; Khoury, R. G.; Lehn, J.-M. *Chem. Eur. J.* **2001**, *7*, 2798.

(24) (a) Prince, R. B.; Barnes, S. A.; Moore, J. S. *J. Am. Chem. Soc.* **2000**, *122*, 2758; (b) Tanatani, A.; Moi, M. J.; Moore, J. S. *J. Am. Chem. Soc.* **2001**, *123*, 1792.

(25) Jiang, H.; Le´ger, J.-M.; Dolain, C.; Guionneau, P.; Huc, I. *Tetrahedron* **2003**, *59*, 8365.

(26) Eliel, E. L.; Wilen, S. H.; Mander, L. N. *Stereochemistry of Organic Compounds*; John Wiley & Sons: New York, **1994**; pp. 1142.

(27) Mislow, K. *Angew. Chem.* **1958**, *70*, 683.

(28) Akimoto, H.; Shioiri, T.; Iitaka, Y.; Yamada, S. *Tetrahedron Lett.* **1968**, *1*, 97.

(29) (a) Rosini, C.; Franzini, L.; Raffaelli, A.; Salvadori, P. *Synthesis* **1992**, 503; (b) Whitesell, J. K. *Chem. Rev.* **1989**, *89*, 1581; (c) Bringmann, G.; Walter, R.; Weirich, R. *Angew. Chem. Int. Ed.* **1990**, *29*, 977.

(30) (a) Kyba, E. B.; Koga, K.; Sousa, L. R.; Siegel, M. G.; Cram, D. J. *J. Am. Chem. Soc.* **1973**, *95*, 2692; (b) Cram, D. J.; Cram, J. M. *Science* **1974**, *183*, 803; (c) Peacock, S. S.; Walba, D. M.; Gaeta, F. C. A.; Helgeson, R. C.; Cram, D. J. *J. Am. Chem. Soc.* **1980**, *102*, 2043; (d) Lingenfelter, D.; Helgeson, R. C.; Cram, D. J. *J. Org. Chem.* **1981**, *46*, 393.

(31) (a) Dai, Y.; Katz. T. J.; Nichols, D. A. *Angew. Chem. Int. Ed.* **1996**, *35*, 2109; (b) Dai, Y.; Katz. T. J. *J. Org. Chem.* **1997**, *62*, 1274.

(32) Pu, L. *Chem. Rev.* **1998**, *98*, 2405.

(33) Tanaka, K.; Furuta, T.; Fuji, K.; Miwa, Y.; Taga, T. *Tetrahedron Asymmetry* **1996**, *7*, 2199.

(34) Tsubaki, K.; Miura, M.; Morikawa, H.; Tanaka, H.; Kawabata, T.; Furuta, T.; Tanaka, K.; Fuji, K. *J. Am. Chem. Soc.* **2003**, *125*, 16200.

(35) Kodama, H; Ito, J.; Hori, K.; Ohta, T, Furukawa, I. *J. Org. Chem.* **2000**, *603*, 6.

(36) Li, X.; Hewgley, J. B.; Mulrooney, C. A.; Yang, J.; Kozlowski, M. C. *J. Org. Chem.* **2003**, *68*, 5500.

(37) Cram, D. J.; Helgeson, R. C.; Peacock, S. C.; Kaplan, L. J.; Domeier, L. A.; Moreau, P.; Koga, K.; Mayer, J. M.; Chao, Y.; Siegel, M. G.; Hoffman, D. H.; Dotsevi, G.; Sogah, Y. *J. Org. Chem.* **1978,** *43*, 1930.

(38) Hungerhoff, B.; Metz, P. *Tetrahedron* **1999,** *55*, 14941.

(39) (a) Head-Gordon, T.; Head-Gordon, M.; Frisch, M. J.; Brooks, C. L.; Pople, J. A. *J. Am. Chem. Soc.* **1991**, *113*, 5989; (b) Ramek, M.; Cheng, V. K. W.; Frey, R. F.; Newton, S. Q.; Schäfer, L. *J. Mol. Struct. (Theochem)* **1991**, *231*, 1; (c) Böhm, H.-J.; Brode, S. *J. Am. Chem. Soc.* **1991**, *113*, 7129; (d) Frey, R. F.; Coffin, J.; Newton, S. Q.; Ramek, M.; Cheng, V. K. W.; Momany, F. A.; Schäfer, L. *J. Am. Chem. Soc.* **1992**, *114*, 5369; (e) Gould, I. R.; Kollmann, P. A. *J. Phys. Chem.* **1992**, *96*, 9255; (f) Rommel-Möhle, K.; Hofmann, H.-J. *J. Mol. Struct. (Theochem)* **1993**, *285*, 211; (g) Alemán, C.; Casanovas, J. *J. Chem. Soc., Perkin Trans. 2* **1994**, 563; (h) Endredi, G.; Perczel, A.; Farkas, O.; McAllister, M. A.; Csonka, G. I.; Ladik, J.; Csizmadia, I. G. *J. Mol. Struct. (Theochem)* **1997**, *391*, 15.

(40) (a) Wu, Y.-D.; Wang, D.-P. *J. Am. Chem. Soc.* **1998**, *120*, 13485; (b) Wu, Y.-D.; Wang, D.-P. *J. Am. Chem. Soc.* **1999**, *121*, 9352; (c) Zanuy, D.; Alemán, C.; Muñoz-Guerra, S. *Int. J. Biol. Macromolecules* **1998**, *23*, 175; (d) Möhle, K.; Hofmann, H.-J. *J. Pept. Res.* **1998**, *51*, 19; (e) Möhle, K.; Günther, R.; Thormann, M.; Sewald, N.; Hofmann, H.-J. *Biopolymers* **1999**, *50*, 167; (f) Gunther, R.; Hofmann, H.-J. *J. Am. Chem. Soc*. **2001**, *123*, 247; (g) Günther, R.; Hofmann, H.-J. *Helv. Chim. Acta* **2002**, *85*, 2149; (h) Baldauf, C.; Günther, R.; Hofmann, H.-J. *Helv. Chim. Acta* **2003**, *86*, 2573; (i) Baldauf, C.; Günther, R.; Hofmann, H.-J. *J. Org. Chem.* **2004**, *69*, 6214; (j) Baldauf, C.; Günther, R.; Hofmann, H. J. *J. Org. Chem.* **2005**, *70*, 5351; (k) Baldauf, C.; Günther, R.; Hofmann, H.-J. *Angew. Chem. Int. Ed.* **2004**, *43*, 1594; (l) Beke, T.; Csizmadia, I. G.; Perczel, A. *J. Comput. Chem.* **2004**, *25*, 285.

(41) Etter, M. C. *Acc. Chem. Res.* **1990**, *23*, 120.

(42) (a) Similar observation has been reported by Whitesides's group for the solubility of hydrogen-bonded aggregates: Mathias, J. P.; Simanek, E. E.; Whitesides, G. M. *J. Am. Chem. Soc.* **1994**, *116*, 4326; (b) For the use of hydrogen bonds to control molecular aggregation, see also: Simard, M.; Su, D.; Wuest, J. D. *J. Am. Chem. Soc.* **1991**, *113*, 4696.

(43) Sanford, A. R.; Yamato, K.; Yang, X.; Yuan, L.; Han, Y.; Gong, B. *Eur. J. Biochem*. **2004**, *271*, 1416.

(44) Buffeteau, T.; Ducasse, L.; Poniman, L.; Delsuc, N.; Huc, I. *Chem. Commun*., **2006**, 2714; (b) Woody, R. W. In *Circular Dichroism Principles and Applications;* Nakanishi, K., Berova, N., Woody, R. W., Eds.; VCH Publishers: New York, 1994; Chapter 17.

(45) *Circular Dichroism and the Conformational Analysis of Biopolymers;* Fasman, G. D., Ed.; Plenum Publishing: New York, **1996**.

(46) Hassan, J.; Se´vignon, M.; Gozzi, C.; Schulz, E.; Lemaire, M. *Chem. Rev.* **2002**, *102,* 1359.

(47) Molteni, V.; Rhodes, D.; Rubins, K.; Hansen, M.; Bushman, F. D.; Siegel, J. S. *J. Med. Chem.* **2000**, *43*, 2031.

(48) Ates, A.; Curran, D. P. *J. Am. Chem. Soc.* **2001**, *123,* 5130.

(49) (a) M. Noji, M. Nakajima, K. Koga, *Tetrahedron Lett.* **1994**, *35*, 7983; (b) C. R. H. I. de Jong, In *Organic Syntheses by Oxidation with Metal Compounds*; W. J. Mijs, C. R. H. I. de Jong, Eds.; Plenum Press Inc.: New York, **1986**, pp 423.